VOL. 653 NO. 2 NOVEMBER 5, 1993

# JOURNAL OF CHROMATOGRAPHY A

## INCLUDING ELECTROPHORESIS AND OTHER SEPARATION METHODS



ELSEVIER

# JOURNAL OF CHROMATOGRAPHY A

INCLUDING ELECTROPHORESIS AND OTHER SEPARATION METHODS

**Scope.** The *Journal of Chromatography A* publishes papers on all aspects of **chromatography, electrophoresis** and related methods. Contributions consist mainly of research papers dealing with chromatographic theory, instrumental developments and their applications. In the *Symposium volumes*, which are under separate editorship, proceedings of symposia on chromatography, electrophoresis and related methods are published. *Journal of Chromatography B: Biomedical Applications* —This journal, which is under separate editorship, deals with the following aspects: developments in and applications of chromatographic and electrophoretic techniques related to clinical diagnosis or alterations during medical treatment; screening and profiling of body fluids or tissues related to the analysis of active substances and to metabolic disorders; drug level monitoring and pharmacokinetic studies; clinical toxicology; forensic medicine; veterinary medicine; occupational medicine; results from basic medical research with direct consequences in clinical practice.

**Submission of Papers.** The preferred medium of submission is on disk with accompanying manuscript (see *Electronic manuscripts* in the Instructions to Authors, which can be obtained from the publisher, Elsevier Science Publishers B.V., P.O. Box 330, 1000 AH Amsterdam, Netherlands). Manuscripts (in English; *four* copies are required) should be submitted to: Editorial Office of *Journal of Chromatography A*, P.O. Box 681, 1000 AR Amsterdam, Netherlands, Telefax (+31-20) 5862 304, or to: The Editor of *Journal of Chromatography B: Biomedical Applications*, P.O. Box 681, 1000 AR Amsterdam, Netherlands. Review articles are invited or proposed in writing to the Editors who welcome suggestions for subjects. An outline of the proposed review should first be forwarded to the Editors for preliminary discussion prior to preparation. Submission of an article is understood to imply that the article is original and unpublished and is not being considered for publication elsewhere. For copyright regulations, see below.

**Publication information.** *Journal of Chromatography A* (ISSN 0021-9673): for 1994 Vols. 652–682 are scheduled for publication. *Journal of Chromatography B: Biomedical Applications* (ISSN 0378-4347): for 1994 Vols. 652–662 are scheduled for publication. Subscription prices for *Journal of Chromatography A*, *Journal of Chromatography B: Biomedical Applications* or a combined subscription are available upon request from the publisher. Subscriptions are accepted on a prepaid basis only and are entered on a calendar year basis. Issues are sent by surface mail except to the following countries where air delivery via SAL is ensured: Argentina, Australia, Brazil, Canada, China, Hong Kong, India, Israel, Japan, Malaysia, Mexico, New Zealand, Pakistan, Singapore, South Africa, South Korea, Taiwan, Thailand, USA. For all other countries airmail rates are available upon request. Claims for missing issues must be made within six months of our publication (mailing) date. Please address all your requests regarding orders and subscription queries to: Elsevier Science Publishers, Journal Department, P.O. Box 211, 1000 AE Amsterdam, Netherlands. Tel.: (+31-20) 5803 642; Fax: (+31-20) 5803 598. Customers in the USA and Canada wishing information on this and other Elsevier journals, please contact Journal Information Center, Elsevier Science Publishing Co. Inc., 655 Avenue of the Americas, New York, NY 10010, USA, Tel. (+1-212) 633 3750, Telefax (+1-212) 633 3764.

**Abstracts/Contents Lists** published in Analytical Abstracts, Biochemical Abstracts, Biological Abstracts, Chemical Abstracts, Chemical Titles, Chromatography Abstracts, Current Awareness in Biological Sciences (CABS), Current Contents/Life Sciences, Current Contents/Physical, Chemical & Earth Sciences, Deep-Sea Research/Part B: Oceanographic Literature Review, Excerpta Medica, Index Medicus, Mass Spectrometry Bulletin, PASCAL-CNRS, Referativnyi Zhurnal, Research Alert and Science Citation Index.

**US Mailing Notice.** *Journal of Chromatography A* (ISSN 0021-9673) is published weekly (total 52 issues) by Elsevier Science Publishers (Sara Burgerhartstraat 25, P.O. Box 211, 1000 AE Amsterdam, Netherlands). Annual subscription price in the USA US$ 5132.25 (US$ price valid in North, Central and South America only) including air speed delivery. Second class postage paid at Jamaica, NY 11431. **USA POSTMASTERS**: Send address changes to *Journal of Chromatography A*, Publications Expediting, Inc., 200 Meacham Avenue, Elmont, NY 11003. Airfreight and mailing in the USA by Publications Expediting.

**See inside back cover** for Publication Schedule, Information for Authors and information on Advertisements.



0021-9673/93/$06.00



Printed in the Netherlands

# CONTENTS

*(Abstracts/Contents Lists published in Analytical Abstracts, Biochemical Abstracts, Biological Abstracts, Chemical Abstracts, Chemical Titles, Chromatography Abstracts, Current Awareness in Biological Sciences (CABS), Current Contents/Life Sciences, Current Contents/Physical, Chemical & Earth Sciences, Deep-Sea Research/Part B: Oceanographic Literature Review, Excerpta Medica, Index Medicus, Mass Spectrometry Bulletin, PASCAL-CNRS, Referativnyi Zhurnal, Research Alert and Science Citation Index)*

## REGULAR PAPERS

*Column Liquid Chromatography*



*Gas Chromatography*



*(Continued overleaf)*

*Journal of Chromatography A*, 653 (1993) 189–198
Elsevier Science Publishers B.V., Amsterdam

CHROM. 25 396

# Peak resolution in linear chromatography

# Effects of intraparticle convection

A.E. Rodrigues*, Z.P. Lu and J.M. Loureiro

*Laboratory of Separation and Reaction Engineering, School of Engineering, University of Porto, 4099 Porto Codex (Portugal)*

G. Carta

*Center for Bioprocess/Product Development, Department of Chemical Engineering, University of Virginia, Charlottesville, VA 22903-2442 (USA)*

(First received April 15th, 1993; revised manuscript received July 1st, 1993)

ABSTRACT

The quantitative relationship between separation performance and intraparticle convection in large-pore, permeable supports for chromatography is examined. A model for linear chromatography is used in the analysis for particles that contain both throughpores where diffusive and convective transport occur and purely diffusive micropores. The key concept is that of a convection-augmented intraparticle diffusivity, which depends only on the intraparticle Peclet number, $\lambda$. The separation performance is expressed in terms of both resolution and peak profiles at the column outlet. It is shown that, for given operating conditions, the separation enhancement obtained for intraparticle convection is dependent on the relative importance of throughpore and micropore diffusion rates. In the absence of micropore resistances, the resolution is always increased by intraparticle convection. The latter, however, is shown to have no effect on the separation performance when micropore diffusional resistances are dominant. Relationships necessary to assess the importance of these effects for linear chromatography conditions are provided.

## INTRODUCTION

Permeable, large-pore materials are currently used as catalysts, adsorbents, supports for cell growth, membranes and HPLC packings [1]. Intraparticle transport of solutes in these materials is enhanced by pressure-driven intraparticle convection. As has been recognized since 1982, such an enhancement may be expressed in terms of a convection-augmented intraparticle diffusivity, $\tilde{D}_e$, defined as [2]

$$\tilde{D}_e = \frac{D_e}{f(\lambda)} = \frac{D_e}{\frac{3}{\lambda}\left(\frac{1}{\tanh\lambda} - \frac{1}{\lambda}\right)} \quad (1)$$

where $D_e$ is the intraparticle effective diffusion coefficient. The function $1/f(\lambda)$ represents the enhancement of intraparticle transport resulting from convection. It depends on the intraparticle Peclet number, which is defined as $\lambda = v_0 l/D_e$ for a slab-shaped pellet, where $\lambda$ is the ratio of the characteristic times for diffusion of a solute, $l^2/D_e$, and for convection, $l/v_0$, in the pellet.

When the pellets are packed in a fixed bed, the intraparticle convective velocity, $v_0$, appearing in these equations may be estimated from Darcy's law, by equating the pressure drop per particle, $\Delta p/2l$ to the pressure drop per unit length of bed, $\Delta P/L$ [2,3]. The expression $v_0 = (B_p/\mu)(\Delta p/2l)$ is obtained for slab-shaped particles of thickness $2l$ and permeability $B_p$.

* Corresponding author.

0021-9673/93/$06.00 

Applications of such large-pore materials in chromatography have recently been introduced by Afeyan and co-workers [4,5] for the separation of macromolecules. They showed experimentally that, for such materials, the curve relating the height equivalent to a theoretical plate (HETP) ($H$) to the mobile phase velocity, $u_0$, approaches a plateau at sufficiently high values of $u_0$. They also provided a semi-theoretical explanation of the enhanced chromatographic performance seen with these materials, by assuming that diffusion and convection provide additive contributions to the rate of intraparticle transport of solutes. A more rigorous theoretical treatment later led Rodrigues *et al.* [1] to the definition of an extended Van Deemter equation that incorporates intraparticle convection effects in terms of the convection-augmented diffusivity concept. For a slab-shaped particle, their result reduces to

$$h = \frac{H}{2l} = A + \frac{B}{u_0} + Cf(\lambda)u_0 \qquad (2)$$

where $A$, $B$ and $C$ are the constants in the classical Van Deemter equation [6] and $f(\lambda)$ is the same function used in eqn. 1. Fig. 1 shows the various effects of intraparticle convection that are predicted by this treatment. The function $1/f(\lambda)$, representing the ratio of the convection-augmented diffusivity and the effective molecular diffusivity, is shown in Fig. 1a. This function approaches unity at low values of $\lambda$, when intraparticle diffusion is dominant, and $\lambda/3$ at high values of $\lambda$, when intraparticle transport is dominated by convection. In this limit, the augmented diffusivity $\tilde{D}_e$ becomes equal to $v_0 l/3$ and depends only on the ratio of the particle and bed hydraulic permeabilities for given operating conditions. Fig. 1b shows qualitatively how intraparticle convection affects band broadening. For a given mobile phase flow-rate and particle size, a large-pore support gives a sharper band, as intraparticle transport limitations are reduced by the onset of intraparticle convection. Fig. 1c shows qualitatively the effect of the mobile phase velocity on the HETP for a conventional support containing only purely diffusive pores and for a support containing convective throughpores. We see that whereas with non-permeable supports

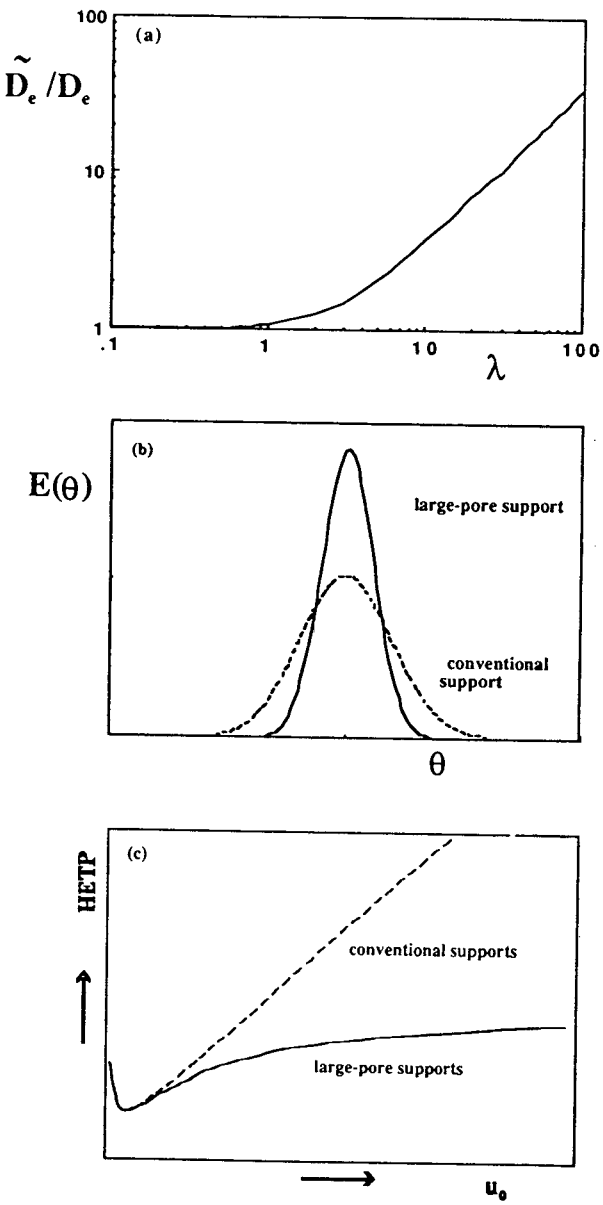


Fig. 1. Qualitative effects of intraparticle convection on (a) diffusivity, (b) peak sharpening and (c) HETP.

the HETP increases essentially linearly with increasing mobile phase velocity, a plateau is approached at high velocities with large-pore, permeable particles.

We should point out that intraparticle mass flux in permeable particles is the sum of diffusive and convective (viscous) fluxes, as both mass transport mechanisms act in parallel. This is in a

sense analogous to the coupling theory of Giddings [7] for the mobile phase contribution to the HETP. According to the coupling theory such contribution is $[(1/H_f) + (1/H_d)]^{-1}$ and comes from flow ($H_f$) and diffusional exchanges ($H_d$). At high flow-rates, diffusional exchanges are negligible and the contribution to the HETP is $H_f = 4\gamma R_p = A$ (eddy diffusivity term in the Van Deemter equation); at low velocities, flow exchanges become so slow that all velocity exchanges are caused by diffusion and the contribution to the HETP is $H_d = D_m/\omega R_p^2 u_0$. Therefore, one can say that convection and diffusion in the outer mobile phase also act in parallel to defeat concentration gradients outside particles; this was explained by Sie and Rijnders [8] in terms of the flow profile contribution for HETP. In the absence of intraparticle convection, eqn. 1 can be written as $H = (B/u_0) + A'u_0^n + Cu_0$ with $n = 1/3$ [9,10].

The analysis for slab-shaped particles of Rodrigues *et al.* [1] was extended to permeable spherical particles by Carta *et al.* [11]. These extensions, however, do not change the qualitative features predicted by the slab model, but only the magnitude of the effects. The effects of slow kinetics of adsorption and desorption and of diffusional limitations in non-convective micropores have also been addressed by Rodrigues *et al.* [12] and Carta and Rodrigues [13], respectively. Experimental evidence of these theoretically predicted effects has also been reported for different materials by Afeyan *et al.* [4], Lloyd and Warner [14], Frey *et al.* [15] and Carta *et al.* [11,16].

The objective of this paper is to explore through quantitative calculations the effects of intraparticle convection on peak resolution in linear chromatography. Models for particles containing both throughpores and purely diffusive micropores are considered in order to assess the relative importance of transport processes within the chromatographic particles.

## THEORY

Models describing diffusive transport in adsorbent particles have been reviewed, *e.g.*, by Ruthven [17]. Applications of such models to chromatography have recently been discussed by Golshan-Shirazi and Guiochon [18]. A model that is sufficiently general to describe diffusion within most porous particles is the "bidispersed pore model". In this model, the adsorbent particles are assumed to comprise an array of porous microparticles of radius $r_c$. These microparticles are, in turn, connected by a network of pores.

The bidispersed pore model was introduced by Carta and Rodrigues [13] for the analysis of intraparticle transport in permeable chromatographic media. In their analysis, intraparticle convection was assumed to occur only in the network of throughpores connecting the microparticles, while only diffusion was assumed to occur in the microparticle pores. The model equations are given in Table I for both spherical and slab-shaped pellets. The equations assume equilibrium between the fluid in the throughpores and the surface of the microparticles at each point in the pellet. The solution is obtained by means of the Laplace transform and the corresponding expressions for the transfer function of the chromatographic column, $G(s)$, the first moment, $\mu_i$, and variance, $\sigma_i^2$, of the response peak for a pulse injection are given in Table II. It should be noted that, although the spherical geometry is in most instances a more accurate representation of commercial media, the model for slab-shaped pellets is much simpler. The results of this model, in fact, can be rendered analogous to those of the model for spherical particles in most instances with appropriate numerical factors [11,13].

The model parameters for slab-shaped pellets are as follows:

(a) Adsorption equilibrium parameter:

$$b_i = 1 + \frac{1 - \varepsilon_p}{\varepsilon_p} m_i$$

(b) Mobile phase Peclet number:

$$P_e = \frac{Lu_0}{\varepsilon_b D_{ax}}$$

(c) Intraparticle Peclet number:

$$\lambda_i = \frac{v_0 l}{D_{ei}}$$

TABLE I

MODEL EQUATIONS FOR SPHERICAL AND SLAB-SHAPED PELLETS WITH BIDISPERSE POROUS STRUCTURE

| Structure | Spherical pellet | Slab-shaped pellet |
|---|---|---|
| Micropores | $D_c\left(\frac{\partial^2 q_i}{\partial r^2}+\frac{2}{r}\cdot\frac{\partial q_i}{\partial r}\right)=\frac{\partial q_i}{\partial t}$<br>$q_i(0,r)=0$<br>$\frac{\partial q_i}{\partial r}(t,0)=0$<br>$q_i(t,r_c)=m_i c_i'$ | Same as for spherical pellet |
| Throughpores | $D_e\left\{\frac{1}{R^2}\cdot\frac{\partial}{\partial R}\left(R^2\cdot\frac{\partial c_i'}{\partial R}\right)+\frac{1}{R^2}\cdot\frac{\partial}{\partial \mu}\left[(1-\mu^2)\frac{\partial c_i'}{\partial \mu}\right]\right\}$<br>$-v_0\left[\mu\cdot\frac{\partial c_i'}{\partial R}+\frac{1-\mu^2}{R}\cdot\frac{\partial c_i'}{\partial \mu}\right]$<br>$=\varepsilon_p\cdot\frac{\partial c_i'}{\partial t}+(1-\varepsilon_p)\frac{\partial\langle q_i\rangle}{\partial t}$<br>$c_i'(0,R)=0$<br>$c_i'(t,0)=\text{finite}$<br>$c_i'(t,R_p)=c_i$<br>$\langle q_i\rangle=\frac{3}{r_c^3}\int_0^{r_c} q_i r^2\,dr$ | $D_e\cdot\frac{\partial^2 c_i'}{\partial z'^2}-v_0\cdot\frac{\partial c_i'}{\partial z'}=\varepsilon_p\cdot\frac{\partial c_i'}{\partial t}+(1-\varepsilon_p)\frac{\partial\langle q_i\rangle}{\partial t}$<br>$c_i'(0,z')=0$<br>$c_i'(t,0)=c_i$<br>$c_i'(t,2l)=c_i$<br>$\langle q_i\rangle=\frac{3}{r_c^3}\int_0^{r_c} q_i r^2\,dr$ |
| Bed fluid | $\varepsilon_b D_{ax}\cdot\frac{\partial^2 c_i}{\partial z^2}-u_0\cdot\frac{\partial c_i}{\partial z}=\varepsilon_b\cdot\frac{\partial c_i}{\partial t}+(1-\varepsilon_b)\frac{\partial\langle\langle q_i\rangle\rangle}{\partial t}$<br>$c_i(0,z)=0$<br>$c_i(t,0)=M\delta(t)$<br>$c_i(t,\infty)=\text{finite}$<br>$\langle\langle q_i\rangle\rangle=\frac{3}{2R_p^3}\int_{-1}^{1}\int_0^{R_p} R^2[\varepsilon_p c_i'+(1-\varepsilon_p)\langle q_i\rangle]\,dR\,d\mu$ | Same as for spherical pellet with<br>$\langle\langle q_i\rangle\rangle=\frac{1}{2l}\int_0^{2l}[\varepsilon_p c_i'+(1-\varepsilon_p)\langle q_i\rangle]\,dz$ |

(d) Number of transfer units for diffusion in the throughpores:

$$n_{ti}=\frac{\varepsilon_b L/u_0}{\varepsilon_p l^2/D_{ei}}$$

(e) Number of transfer units for diffusion in the microparticles:

$$n_{mi}=\frac{\varepsilon_b L/u_0}{r_c^2/D_{ci}}$$

The numbers of transfer units for diffusion are introduced in a manner analogous to that of Golshan-Shirazi and Guiochon [18]. The reciprocals of the two quantities $n_t$ and $n_m$ give the contributions to band broadening resulting from diffusion limitations in the throughpores and in the microparticles, respectively. Their ratio, $T=n_m/n_t$, is introduced to quantify the relative importance of the two contributions. The same parameters apply to the model for spherical

TABLE II

TRANSFER FUNCTION AND MOMENTS OF THE RESPONSE PEAK

| Parameter | Spherical pellet | Slab-shaped pellet |
|---|---|---|
| Bed transfer function | $G(s) = \exp\left\{\frac{Pe}{2}\left[1 - \sqrt{1 + 4 \cdot \frac{N(s)}{Pe}}\right]\right\}$ | $G(s) = \exp\left\{\frac{Pe}{2}\left[1 - \sqrt{1 + 4 \cdot \frac{N(s)}{Pe}}\right]\right\}$ |
| | $N(s) = s\left[1 + \frac{1-\varepsilon_b}{\varepsilon_b} \cdot \varepsilon_p g_a(s)\right]$ | $N(s) = s\left[1 + \frac{1-\varepsilon_b}{\varepsilon_b} \cdot \varepsilon_p g_a(s)\right]$ |
| | $g_a(s) = \frac{3\pi}{4\lambda s/n_t} \sum_{m=0}^{\infty} (-1)^m (2m+1) I_{m+1/2}(\lambda)$ | $g_a(s) = \frac{r_1 - r_2}{2s/n_t} \cdot \frac{(1-e^{2r_2})(e^{2r_1}-1)}{e^{2r_1} - e^{2r_2}}$ |
| | $\left[\beta \cdot \frac{I_{m+3/2}(\beta)}{I_{m+1/2}(\beta)} - \lambda \cdot \frac{I_{m+3/2}(\lambda)}{I_{m+1/2}(\lambda)}\right]$ | $r_1, r_2 = \frac{\lambda}{2} \pm \sqrt{\frac{\lambda^2}{4} + s/n_t\left(1 + \frac{1-\varepsilon_p}{\varepsilon_p} \cdot m_i f(\sqrt{s/n_m})\right)}$ |
| | $\beta = \sqrt{\lambda^2 + s/n_t\left(1 + \frac{1-\varepsilon_p}{\varepsilon_p} \cdot m_i f(\sqrt{s/n_m})\right)}$ | $f(\sqrt{s/n_m}) = \frac{3}{\sqrt{s/n_m}}\left(\coth\sqrt{s/n_m} - \frac{1}{\sqrt{s/n_m}}\right)$ |
| | $f(\sqrt{s/n_m}) = \frac{3}{\sqrt{s/n_m}}\left(\coth\sqrt{s/n_m} - \frac{1}{\sqrt{s/n_m}}\right)$ | |
| First moment and variance of chromatographic peaks | $\mu_i = 1 + \frac{1-\varepsilon_b}{\varepsilon_b} \cdot \varepsilon_p b_i$ | $\mu_i = 1 + \frac{1-\varepsilon_b}{\varepsilon_b} \cdot \varepsilon_p b_i$ |
| | $\sigma_i^2 = \frac{2}{Pe} \cdot \mu_i^2 + \frac{2}{15} \cdot \varepsilon_p \cdot \frac{1-\varepsilon_b}{\varepsilon_b} \cdot \frac{b_i^2}{n_t}\left[f(\lambda/3) + \frac{b_i - 1}{b_i^2 T}\right]$ | $\sigma_i^2 = \frac{2}{Pe} \cdot \mu_i^2 + \frac{2}{3} \cdot \varepsilon_p \cdot \frac{1-\varepsilon_b}{\varepsilon_b} \cdot \frac{b_i^2}{n_t}\left[f(\lambda) + \frac{b_i - 1}{5 b_i^2 T}\right]$ |
| | $f(\lambda) = \frac{3}{\lambda}\left(\frac{1}{\tanh\lambda} - \frac{1}{\lambda}\right)$ | $f(\lambda) = \frac{3}{\lambda}\left(\frac{1}{\tanh\lambda} - \frac{1}{\lambda}\right)$ |

particles, simply by replacing the pellet half-thickness $l$ with the pellet radius $R_p$.

When micropore diffusional resistance is negligible ($T = \infty$), the bidispersed model reduces to a simpler model where only throughpores are considered [1].

## PEAK RESOLUTION AND BAND PROFILES

The resolution between the chromatographic peaks for two components 1 and 2 can be defined as [19]

$$R_s = \frac{\mu_2 - \mu_1}{2(\sigma_1 + \sigma_2)} \tag{14}$$

Following, for example, Giddings [19], unit resolution ($R_s = 1$) corresponds to an almost complete separation and is adequate for most analytical purposes.

The resolution is obtained directly from the expressions for the first moment and variance given in Table II for particles with a bidispersed pore structure. Calculated values of $R_s$ are given in Fig. 2 as a function of the intraparticle Peclet number, $\lambda$, for different values of the parameter $T$. These calculations were carried out with a value of $n_t = 100$. Such a value is representative of conditions that might be encountered in the HPLC of proteins. For a protein with an effective throughpore diffusivity $D_e = 1 \cdot 10^{-7}$ cm$^2$/s, using bed and particle porosities $\varepsilon_b = 0.3$ and $\varepsilon_p = 0.5$, respectively, and 10-$\mu$m particles in a 20-cm long chromatographic bed, the value $n_t = 100$ corresponds to a mobile phase velocity of *ca.*

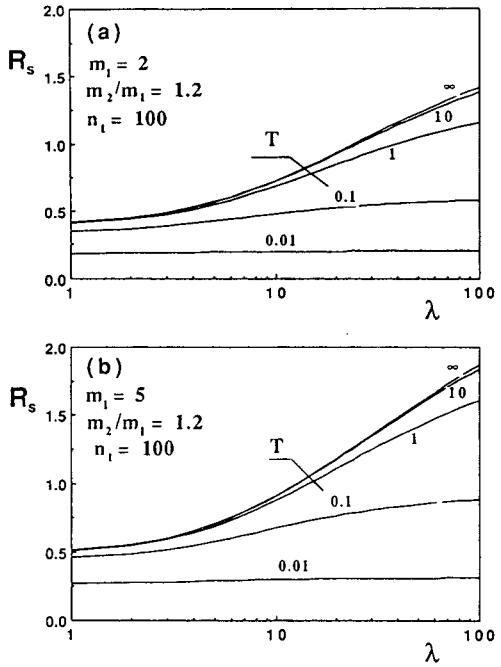


Fig. 2. Effect of the relative importance of micropore and throughpore diffusion rates, measured by $T$, on the $R_s$ *versus* $\lambda$ curves. (a) $m_1 = 2$, $m_2/m_1 = 1.2$, $n_t = 100$; (b) $m_1 = 5$, $m_2/m_1 = 1.2$, $n_t = 100$.

3 cm/min. The value of $T$ depends on the relative size of the protein and of the micropores. For small pores, when restricted or hindered diffusion occurs, values of $T$ much smaller than unity could be found. The selectivity value chosen for these calculations was $m_2/m_1 = 1.2$ while the distribution coefficient for the least retained species was $m_1 = 2$ in Fig. 2a and $m_1 = 5$ in Fig. 2b.

For simplicity, the calculations were carried out assuming that $\lambda_1 = \lambda_2 = \lambda$ and $n_{t1} = n_{t2} = n_t$. This is a reasonable assumption for the separation of two closely related species whose diffusivities are likely to be nearly the same. The values of the remaining model parameters were taken to be $Pe = 10\,000$, $\varepsilon_b = 0.3$ and $\varepsilon_p = 0.5$.

In both instances, when $T \leq 0.01$ the resolution is unaffected by the values of $\lambda$. In this instance, in fact, the separation performance is controlled by the micropore diffusional resistance. Conversely, for values of $T \geq 10$, the resistance to mass transfer in the micropores is unimportant, and the process is dominated by transport in the throughpores. For these conditions, as seen previously, at low $\lambda$ values diffusion in the throughpores is dominant, whereas at high $\lambda$ values intraparticle convection becomes dominant. Hence $R_s$ varies between two limits, one for low $\lambda$ where throughpore diffusion controls and the other for high $\lambda$ where intraparticle resistances are eliminated and equilibrium along with flow and geometric factors control the separation performance. When $T \rightarrow \infty$, in the limit of high $\lambda$ values, $R_s$ approaches a horizontal asymptote with a value given by

$$R_s = \sqrt{\frac{Pe}{2}} \cdot \frac{\frac{1-\varepsilon_b}{\varepsilon_b} \cdot \varepsilon_p (b_2 - b_1)}{2 + \frac{1-\varepsilon_b}{\varepsilon_b} \cdot \varepsilon_p (b_1 + b_2)}$$

A different asymptotic value is obtained, however, when $T$ is finite. Qualitatively similar results would be obtained for spherical particles, as shown by Carta and Rodrigues [13].

Fig. 3 shows the resolution as a function of $\lambda$

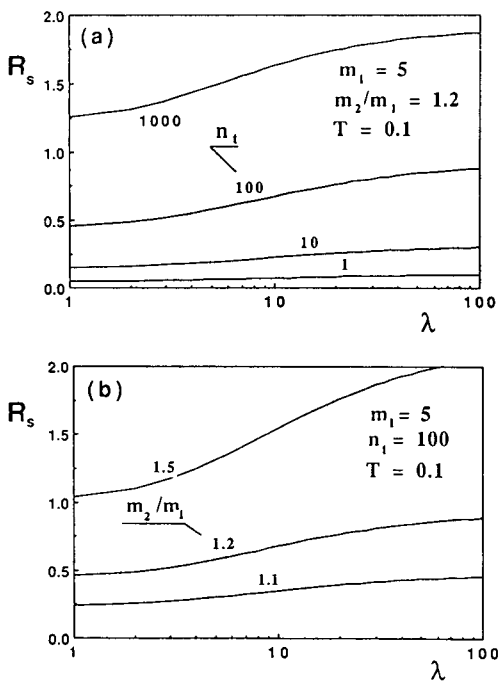


Fig. 3. Effect of (a) $n_t$, mass transfer units for diffusion in the throughpores (with $m_2/m_1 = 1.2$), and (b) $m_2/m_1$, the ratio of the adsorption equilibrium isotherm slopes of the two components (with $n_t = 100$), on the $R_s$ *versus* $\lambda$ curves. $m_1 = 5$, $T = 0.1$.

for an intermediate value of $T = 0.1$ with $m_1 = 5$. The effect of the number of transfer units for diffusion in the throughpores, $n_t$, is shown in Fig. 3a for $m_2/m_1 = 1.2$. It is seen that the enhancement of resolution by intraparticle convection is more significant when $n_t$ is high. This happens because in these calculations $T = n_m/n_t$ has been kept constant. Thus, as $n_t$ is reduced by a certain proportion, so is $n_m$ in the same proportion. Lower values of $n_m$ imply a greater contribution of the micropore diffusional resistance to the overall transport rate, thereby reducing the effects of convection in the throughpores. The effect of the equilibrium selectivity ratio, $m_2/m_1$, is shown in Fig. 3b for a constant value of $n_t = 100$. The resolution is increased as $m_2/m_1$ is increased. Similarly, $R_s$ becomes larger as $\lambda$ is increased, approaching a horizontal asymptote whose value is dependent on the ratio $m_2/m_1$ when $\lambda$ is very large.

The effects of intraparticle convection on the peak profiles at the exit of a chromatographic column are shown in Figs. 4–6 for slab-shaped pellets with a bidispersed pore structure. The

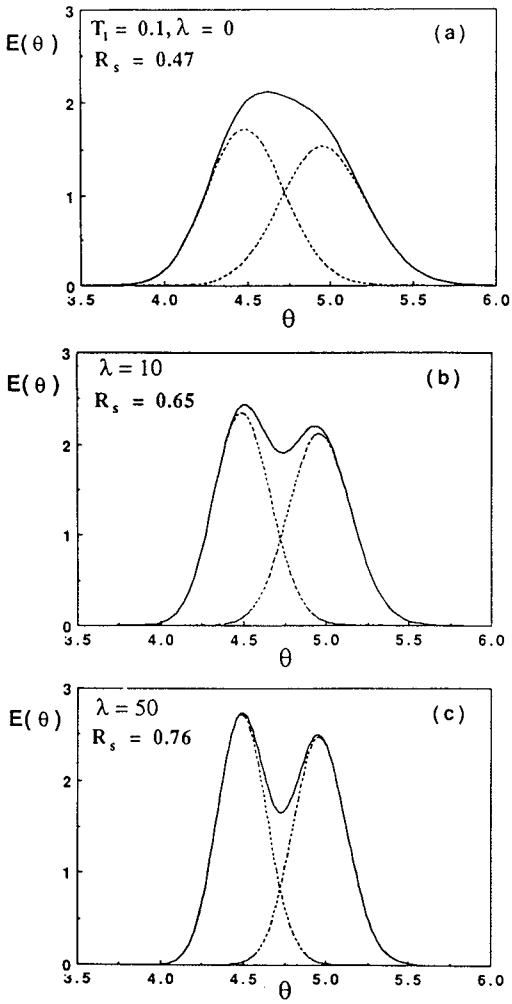


Fig. 4. Chromatographic response to a pulse input of two components. $Pe = 10\,000$; $m_1 = 2$; $m_2/m_1 = 1.2$; $n_t = 200$; bidisperse particles. Effect of intraparticle convection on peak resolution when micropore mass transfer resistances cannot be neglected ($T = 0.1$).

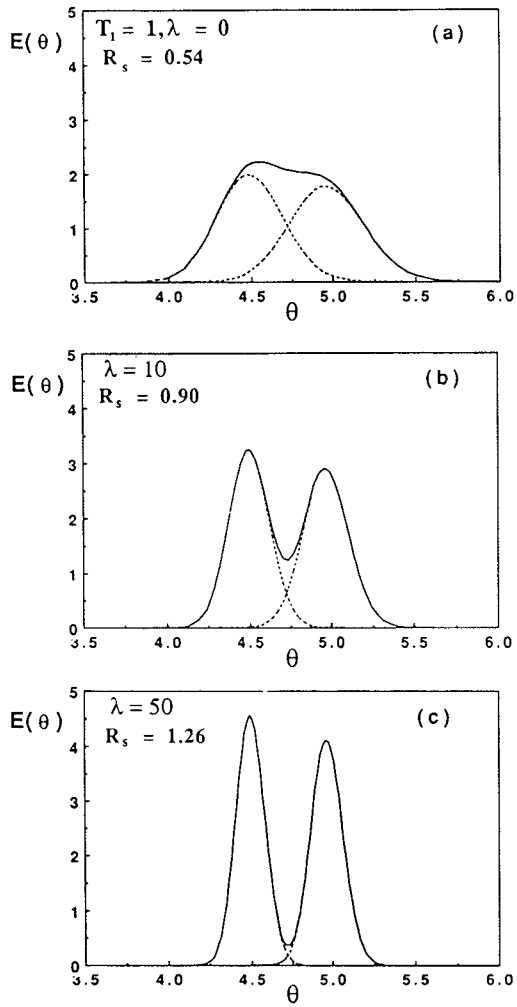


Fig. 5. Chromatographic response to a pulse input of two components. $Pe = 10\,000$; $m_1 = 2$; $m_2/m_1 = 1.2$; $n_t = 200$; bidisperse particles. Effect of intraparticle convection on peak resolution when micropore and throughpore resistances are comparable ($T = 1.0$).

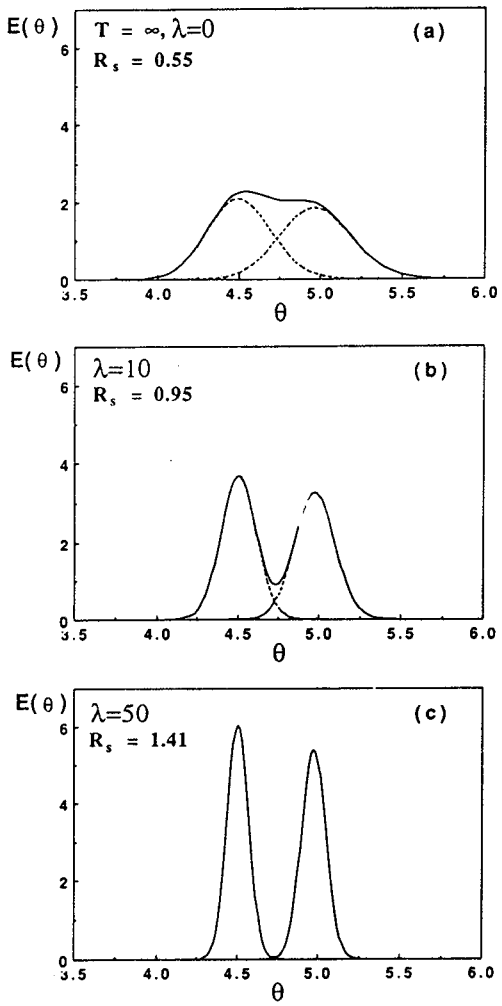


Fig. 6. Chromatographic response to a pulse input. $Pe = 10\,000$; $m_1 = 2$; $m_2/m_1 = 1.2$; $n_t = 200$; particles containing only throughpores ($T = \infty$). Effects of intraparticle convection.

peak profiles are obtained from the numerical inversion of the transfer function for the bed given in Table II. The numerical inversion was obtained with a fast Fourier transform algorithm. For all three cases considered, the values $Pe = 10\,000$, $m_1 = 2$, $m_2/m_1 = 1.2$ and $n_t = 200$ were used as representative of the HPLC of macromolecules such as proteins. Different levels of micropore diffusional resistance are, however, considered.

Fig. 4 shows the effect of $\lambda$ when $T = 0.1$, *i.e.*, $n_m = 20$. For these conditions, the micropore resistance is significant and only a small improvement in the resolution from $R_s = 0.47$ to 0.76 is obtained when $\lambda$ is increased from 0 to 50. However, when $T$ is increased to 1 ($n_m = 200$), as in Fig. 5, a much more pronounced effect of $\lambda$ is seen. In this instance, the micropore diffusional resistance becomes unimportant and $R_s$ increases from 0.54 to 1.26 when $\lambda$ is changed from 0 to 50, when an almost complete separation is obtained.

For comparison, Fig. 6 shows the calculated profiles obtained for different $\lambda$ values when micropore diffusion is neglected, *i.e.*, $T \rightarrow \infty$. The profiles in this instance were computed from the solution of Rodrigues *et al.* [1] for a pellet containing only throughpores. A greater resolution is obtained for each value of $\lambda$ and a baseline separation is realized when $\lambda = 50$.

## CONCLUSIONS

Large-pore, permeable supports have been shown to be promising in many applications, because in these materials intraparticle convection can reduce the overall transport resistance. The quantitative relationship between intraparticle flow and resolution in linear chromatography with such particles was examined in this paper. Two models were used: in the first, it is assumed that the particles contain only throughpores in which diffusion and convection occur simultaneously ($T = \infty$); in the second, the particles are assumed to compromise a bidispersed pore network with a microporous structure intercalated by throughpores. Only diffusion is assumed to occur in the micropores, while convection is accounted for in the throughpores.

When only the throughpores are considered, the onset of intraparticle convection improves the separation performance by enhancing the overall transport rate; accordingly, the resolution of two adjacent components is increased. For conditions which are representative of the HPLC of macromolecules, simulations carried out with this model show that starting with two non-separated peaks, for given equilibrium and flow characteristics, as the intraparticle convection is increased the separation is gradually improved and the two components become completely separated. This is also possible for conditions representative of gas chromatographic separa-

tions, but higher values of the intraparticle convection coefficient $\lambda$ would be required.

When the bidispersed model is used to simulate the chromatographic behaviour, two limiting situations can occur. In the first, the mass transfer resistance is dominated by transport within the throughpores, whereas in the second the mass transfer resistance is dominated by the micropores. In the former instance, the onset of intraparticle convection leads to an improved resolution, as mass transfer resistances are reduced. In the latter instance, intraparticle convection has no effect on resolution, which is entirely determined by the diffusional resistance in the micropores. In other situations between these two limits, intraparticle convection can increase the resolution to an extent that depends upon the relative magnitude of the $T$ ratio and the adsorption capacity.

The possibility of kinetic limitations resulting from a finite rate of adsorption at the microparticle surface should, of course, also be considered [12,20], especially when dealing with affinity chromatographic systems. However, when the rate of adsorption and desorption is not limiting, it is apparent that a key to the successful exploitation of intraparticle convection effects is that micropore transport resistances must be minimized. The equations given in this paper provide the quantitative relationship between chromatographic performance and intraparticle flow, and can be used in assessing the relative importance of diffusional resistances for the optimum design of permeable media for chromatography. Numerical inversion of the expressions provided for the bed transfer function in the Laplace domain can be used to obtain a prediction of peak histories for different values of the intraparticle convection velocity.

ACKNOWLEDGEMENTS

Financial support from JNICT is gratefully acknowledged.

SYMBOLS

| | |
|---|---|
| $b_i$ | parameter $[=1+(1-\varepsilon_p)m_i/\varepsilon_p]$ |
| $B_p$ | particle permeability, $cm^2$ |
| $c_i$ | species concentration in the bulk fluid phase, $mol/cm^3$ |
| $c_i'$ | species concentration in the macropore fluid, $mol/cm^3$ |
| $D_{ax}$ | axial dispersion coefficient, $cm^2/s$ |
| $D_{ei}$ | effective diffusivity of species $i$ in macropore, $cm^2/s$ |
| $D_{ci}$ | effective diffusivity in micropore, $cm^2/s$ |
| $D_m$ | molecular diffusivity, $cm^2/s$ |
| $\tilde{D}_e$ | "apparent" effective diffusivity in macropore, $cm^2/s$ |
| $E(\theta)$ | normalized response of the chromatographic column to a pulse input |
| $H_d$ | diffusion term in the mobile phase contribution to the HETP, cm |
| $H_f$ | flow term in the mobile phase contribution to the HETP, cm |
| $H$ | height equivalent to a theoretical plate (HETP), cm |
| $l$ | half-thickness of the slab, cm |
| $L$ | bed length, cm |
| $M$ | strength of the impulse, mol $s/cm^3$. |
| $m_i$ | slope of the adsorption isotherm of species $i$ |
| $n_m$ | mass transfer units for diffusion in micropores $\left(\frac{D_c}{r_c^2}\cdot\frac{\varepsilon_b L}{u_0}\right)$ |
| $n_t$ | mass transfer units for diffusion in throughpores $\left(\frac{D_e}{\varepsilon_p R_p^2}\cdot\frac{\varepsilon_b L}{u_0}\right.$ or $\left.\frac{D_e}{\varepsilon_p l^2}\cdot\frac{\varepsilon_b L}{u_0}\right)$ |
| $Pe$ | bed Peclet number $\left(\frac{Lu_0}{\varepsilon_b D_{ax}}\right)$ |
| $\Delta p$ | pressure drop across the particle, Pa |
| $\Delta P$ | pressure drop across the bed, Pa |
| $q_i$ | micropore concentration of species $i$ |
| $\langle q_i\rangle$ | average concentration in micropore of species $i$, $mol/cm^3$ |
| $\langle\langle q_i\rangle\rangle$ | average concentration inside the particle of species $i$, $mol/cm^3$ |
| $R$ | radius coordinate for the particle, cm |
| $R_p$ | particle radius, cm |
| $R_s$ | resolution |
| $r_c$ | micropore radius, cm |
| $s$ | Laplace variable |
| $T$ | parameter $(n_m/n_t)$ |
| $t$ | time, s |
| $u_0$ | bed superficial velocity, cm/s |
| $v_0$ | intraparticle convective velocity, cm/s |
| $z$ | axial coordinate for the bed, cm |
| $z'$ | axial coordinate for the particle, cm |

*Greek letters*

$\varepsilon_b$ bed porosity
$\varepsilon_p$ intraparticle porosity
$\gamma$ constant in the $A$ term of the Van Deemter equation
$\lambda_i$ intraparticle Peclet number ($v_0 R_p / D_{ei}$ or $v_0 l / D_{ei}$)
$\mu_i$ first moment of the impulse response for species $i$
$\sigma_i^2$ variance for species $i$
$\tau$ space time ($\varepsilon_b L / u_0$), s
$\theta$ reduced time ($t/\tau$)
$\omega$ constant in the $H_d$ contribution

*Subscript*

$i$ species

ACKNOWLEDGMENTS

Financial support from JNICT is gratefully acknowledged.

REFERENCES

1 A.E. Rodrigues, Z.P. Lu and J.M. Loureiro, *Chem. Eng. Sci.*, 46 (1991) 2765.
2 A.E. Rodrigues, B. Ahn and A. Zoulalian, *AIChE J.*, 28 (1982) 541.
3 H. Komiyama and H. Inoue, *J. Chem. Eng. Jpn.*, 7 (1974) 281.
4 N. Afeyan, N. Gordon, I. Mazsaroff, L. Varady, S. Fulton, Y. Yang and F. Regnier, *J. Chromatogr.*, 519 (1990) 1.
5 N. Afeyan, F. Regnier and R. Dean, *US Pat.*, 5 019 270 (1991).
6 J. van Deemter, F. Zuiderweg and A. Klinkenberg, *Chem. Eng. Sci.*, 5 (1956) 271.
7 J.C. Giddings, *Dynamics of Chromatography, Part I, Principles and Theory*, Marcel Dekker, New York, 1965.
8 S.T. Sie and G.W.A. Rijnders, *Anal. Chim. Acta*, 38 (1967) 3.
9 J.H. Knox and J.F. Parcher, *Anal. Chem.*, 41 (1969) 1599.
10 S.G. Weber and P.W. Carr, in P.R. Brown and R.A. Hartwick (Editors), *High Performance Liquid Chromatography*, Wiley, New York, 1989.
11 G. Carta, M. Gregory, D.J. Kirwan and H. Massadi, *Sep. Technol.*, 2 (1992) 62.
12 A.E. Rodrigues, A.M.D. Ramos, J.M. Loureiro, M. Diaz and Z.P. Lu, *Chem. Eng. Sci.*, 47 (1992) 4405.
13 G. Carta and A.E. Rodrigues, *Chem. Eng. Sci.*, in press.
14 L. Lloyd and F. Warner, *J. Chromatogr.*, 512 (1990) 365.
15 D. Frey, E. Schwesnheim and C. Horvath, *Biotech. Prog.*, 9 (1993) 273.
16 G. Carta, D.J. Kirwan and M.E. Gregory, in M. Perrut (Editor), *PREP'92*, Société Française de Chimie, Nancy, 1992, p. 333.
17 D.M. Ruthven, *Principles of Adsorption and Adsorption Processes*, Wiley, New York, 1984.
18 S. Golshan-Shirazi and G. Guiochon, *J. Chromatogr.*, 603 (1992) 1.
19 J.C. Giddings, *Unified Separation Science*, Wiley, New York, 1991.
20 A.I. Liapis and M.A. McCoy, *J. Chromatogr.*, 599 (1992) 87.

*Journal of Chromatography A*, 653 (1993) 199–206
Elsevier Science Publishers B.V., Amsterdam

CHROM. 25 402

# Polymer analysis using size-exclusion chromatography with coupled density and refractive index detection

# VI. Molecular mass dependence of preferential solvation of polyoxyethylenes in chloroform with different ethanol contents

B. Trathnigg* and X. Yan

*Institut für Organische Chemie, Universität Graz, Heinrichstrasse 28, A-8010 Graz (Austria)*

(First received May 4th, 1993; revised manuscript received June 14th, 1993)

ABSTRACT

It is shown that preferential solvation of polyoxyethylenes with hydroxy and methoxy end-groups in chloroform containing ethanol takes place mainly at the hydroxy end-groups, but also along the main chain. A method is described that allows a separate determination of the adsorbed ethanol molecules per repeating unit and per end-group.

## INTRODUCTION

It is well known that in a solution of a polymer in a mixed solvent, the composition of the latter within the polymer coils will be different from outside because of different interactions of the polymer chains with the components of the solvent. This effect, which is called preferential solvation [1–5], is often neglected in size-exclusion chromatography (SEC) because most chromatographers consider their mobile phase to be pure.

If one takes into account that HPLC solvents are, however, typically less than 99.9% pure, *e.g.*, some of them, such as tetrahydrofuran (THF), are hygroscopic [4] and others contain a stabilizer, such as chloroform, which contains up to 1% of ethanol (Aldrich, Fluka, Zinsser) or 2-methylbutene (Merck, Janssen, Riedel-de Haën), then the concentration of a second component can be considerably higher than the concentration of a sample. In the chromatographic column, the zone of "dialysed solvent" [1] is separated from the solute molecules and a "ghost" or vacant peak [1,2] appears (vacant peaks can, however, arise for other reasons also [2]).

If a non-specific detector, such as a refractive index (RI) detector, is used, its response will not only represent the concentration of the eluted polymer, but will also contain a contribution of the preferential solvation. Hence the response factor of the polymer will be only an apparent value. As long as the contribution of preferential solvation is the same over the entire peak, the accuracy of the molecular mass averages will not be affected.

As has already been shown [6], the response factors vary within a homologous series of poly-

* Corresponding author.

0021-9673/93/$06.00 

mers with molecular mass owing to different contributions of the repeating unit and end-groups. It is very likely that also the interaction of the repeating unit and the end-groups with the components of the solvent can differ considerably, hence the preferential solvation will also depend on molecular mass.

In this work, we tried to separate these effects in order to evaluate the influence of molecular mass on the true response factors and on the preferential solvation.

## RESPONSE FACTORS AND MOLECULAR MASS

Within a homologous series of polymers, specific properties, such as partial specific volume, refractive index and refractive index increment, vary with molecular mass because they are composed of the different contributions of the repeating unit and end-groups. This dependence can be described by the relationship

$$x_M = x_R + M_E(x_E - x_R)/M \quad (1)$$

where $x_M$, $x_R$ and $x_E$ are the properties of a polymer chain with the molecular mass $M$, of the repeating unit R and the end-groups E, and $M_E$ is the molecular mass of the end-groups [7–13]. With

$$M_E(x_E - x_R) = k \quad (2)$$

one may write

$$x_M = x_R + k/M \quad (3)$$

This equation has been demonstrated to describe the molecular mass dependence of specific properties of polymers [7–13].

As the response factors in density and RI detection are closely related to specific properties (apparent specific volume and refractive index increment, respectively), their variation with molecular mass can be described by

$$f_P = A_P/m_P = f_R + K/M_P \quad (4)$$

where $f_P$ is the response factor and $A_P$ is the area obtained for each interval of the peak, within which the mass $m_P$ is eluted [6] (the molecular mass $M_P$ of the fraction is obtained from the SEC calibration); $f_R$ is the response factor of the repeating unit and $K$ is a constant reflecting the difference between the repeating unit and end-groups.

For a sample with infinitely high molecular mass, the term $K/M_P$ disappears. Hence the response factor $f_\infty$ of such a sample equals the response factor $f_R$ of the repeating unit (in a plot of $f_P$ *vs.* $1/M_P$, $f_R$ is the intercept and $K$ the slope of the regression line).

In a previous paper [6], we described different approaches for the determination of the parameters $f_R$ and $K$ and the effect of compensation of response factors on the dependence of their molecular mass on the molecular mass averages, and the effect of compensating the molecular mass dependence of response factors on the molecular mass averages.

## PREFERENTIAL SOLVATION IN CHROMATOGRAPHY

When a polymer is dissolved in a mixed solvent, the polymer coils will be solvated preferentially as the components of the solvent have a different affinity for the polymer.

In chromatography, the absorbed solvent will move together with the polymer chain. Hence one has to consider two different situations. (a) If the solution passes the detector directly without separation, the detected area will reflect only the concentration of the polymer sample, whether preferential absorption occurs or not, and *true response factors* will be obtained. (b) On a chromatographic column the polymer peak will be separated from zone of "dialysed" solvent [1,2], hence the detected area will contain contributions from the polymer sample and the preferentially absorbed solvent. Hence *apparent response factors* will be found.

## MOLECULAR MASS DEPENDENCE OF PREFERENTIAL SOLVATION

If a polymer is separated on a chromatographic column, preferential solvation will have different effects on the parameters $f_R$ and $K$ in eqn. 4, whether it takes place at the end-groups or at the repeating units (or both): preferential solvation of the end-groups will only influence the slope $K$ without affecting the intercept $f_R$; preferential solvation of the repeating units will influence both the slope $K$ and the intercept $f_R$.

If a mass $m_P$ of a polymer is eluted together

with a mass $m_S$ of a preferentially adsorbed solvent, the apparent peak area $A_P^*$ of the polymer is given by

$$A_P^* = m_P f_P + m_S f_S \quad (5)$$

where $f_P$ and $f_S$ are the true response factors for the polymer and solvent, respectively. If other sources of ghost peaks (*e.g.*, evaporation) can be excluded, the sum of the apparent polymer peak area $A_P^*$ and the area of the solvent peak $A_S$ should equal the true peak area $A_P$, which is obtained when the polymer is injected into the bypass (without a column):

$$A_P^* + A_S = A_P \quad (6)$$

From the apparent peak area $A_P^*$, an apparent response factor $f_P^*$ will be obtained:

$$f_P^* = A_P^*/m_P = f_P + f_S m_S/m_P \quad (7)$$

Combination of eqns. 4 and 7 yields

$$f_P^* = f_R + K/M_P + f_S m_S/m_P \quad (8)$$

or, in terms of the numbers of polymer and solvent molecules ($n_P$ and $n_S$, respectively), and the corresponding molecular masses $M_P$ and $M_S$:

$$f_P^* = f_R + K/M_P + f_S n_S M_S/(n_P M_P) \quad (9)$$

If one considers the different possible sites of preferential solvation, the total number $n_S$ of preferentially adsorbed solvent molecules consists of the molecules adsorbed at the end-groups ($n_{S,E}$) and along repeating units of the chain ($n_{S,R}$):

$$n_S = n_{S,E} + n_{S,R} \quad (10)$$

Hence one may write

$$f_P^* = f_R + K/M_P + f_S M_S(n_{S,E} + n_{S,R})/n_P M_P \quad (11)$$

As the number of repeating units $n_R$ is given by their molecular mass $M_R$, the number of polymer molecules $n_P$, their molecular mass $M_P$ and the molecular mass $M_E$ of the end-groups, one may write

$$n_R = n_P(M_P - M_E)/M_R \quad (12)$$

and

$$f_P^* = f_R + K/M_P + (f_S M_S n_{S,E}/n_P M_P) + [f_S M_S n_{S,R}(M_P - M_E)/n_R M_R M_P] \quad (13)$$

It should be mentioned that $M_E$ is the sum of both end-groups: for polyethylene glycols it is 18 (H–OH), for polyoxyethylene monomethyl ethers 32 ($CH_3$–OH) and for dimethyl ethers 46 ($CH_3$–$OCH_3$).

Rearrangement of eqn. 13 yields

$$f_P^* = f_R + f_S M_S n_{S,R}/(n_R M_R) + \{K + f_S M_S[(n_{S,E}/n_P) - (n_{S,R} M_E)/(n_R M_R)]\}/M_P \quad (14)$$

In a linear polymer, the number of end-groups $n_E$ will equal the number of polymer chains $n_P$:

$$n_E = n_P \quad (15)$$

Introduction of the ratios $r_R$ and $r_E$ of the numbers of adsorbed solvent molecules to the numbers of repeating units and end-groups:

$$r_R = n_{S,R}/n_R \quad (16)$$

and

$$r_E = n_{S,E}/n_E = n_{S,E}/n_P \quad (17)$$

yields

$$f_P^* = f_R + r_R f_S M_S/M_R + \{K + f_S M_S[r_E - r_R M_E/M_R]\}/M_P \quad (18)$$

If one plots the response factors (from column and bypass measurements) *versus* $1/M_P$, $r_R$ can be calculated from the difference in the intercepts:

$$r_R = (f_P^* - f_P)M_R/f_S M_S \quad (19)$$

and $r_E$ from the difference in the slopes:

$$r_E = (K_{col.} - K_{byp.})/f_S M_S + r_R M_E/M_R \quad (20)$$

## EXPERIMENTAL

For these investigations, a DDS 70 density detection system (Paar, Graz, Austria) was used, which was developed in our group. It was combined with a Bischoff 8110 RI detector and connected to an MS-DOS computer for data

acquisition and processing. The entire system has been described in detail in previous papers [14–17]. Data acquisition and processing were performed using the software package CHROMA, which was developed for the DDS 70.

SEC measurements were performed on a set of four Phenogel 300 × 4.6 mm I.D. columns (2 × 500 + 2 × 100 Å) and in bypass. Columns could be selected using two Rheodyne Model 7660 switching valves. A flow-rate of 1.00 ml/min was maintained with a Gynkotek 300 C HPLC pump. A Sicon LCD 201 RI detector was coupled to the density detector for these measurements. Samples were injected using a VICI injection valve equipped with a 100-$\mu$l loop; the concentration range was 5–7 g/l. A measuring temperature of 25.0°C was maintained with a Lauda MS3 thermostat, which was coupled to the column box of the DDS 70. Each sample was injected into the SEC system twice at the bypass and connected columns.

Polyethylene glycol (PEG), polyethylene glycol monomethyl ether (MME-PEG) and polyethylene glycol dimethyl ether (DME-PEG) samples and the lower oligomers (DP 2–6) were purchased from Fluka and dried carefully *in vacuo* at 50°C for 40 h. The solvents used were of HPLC grade (Merck, LiChroSolv). Chloroform was dried over molecular sieve prior to use.

## RESULTS AND DISCUSSION

Before studying the preferential solvation of the samples in chloroform containing ethanol, we had to ensure that no other component (such as 2-methylbutene, which is added as a stabilizer, or moisture) in the solvent used for these investigations would also show preferential solvation. Hence we injected polyoxyethylenes with different end-groups (diols and mono- and dimethyl ethers) in dry, ethanol-free chloroform both on to the columns as also in bypass. Because the lowest oligomers of polyethylene glycols showed strong tailing in this mobile phase, they could not be analysed under these conditions. In the column measurements no solvent peak was observed, which proves the absence of any preferential solvation.

In Fig. 1 the response factors of polyoxyethylene monomethyl ethers as obtained from column and bypass measurements with RI detection are shown. The regression lines for column and bypass measurements agree very well, whether the polymer had been separated from the "dialysed" zone or not.

Fig. 2 shows a comparison of the regression lines for diols and mono- and dimethyl ethers. The corresponding intercepts, slopes and correlation coefficients are given in Table I. All

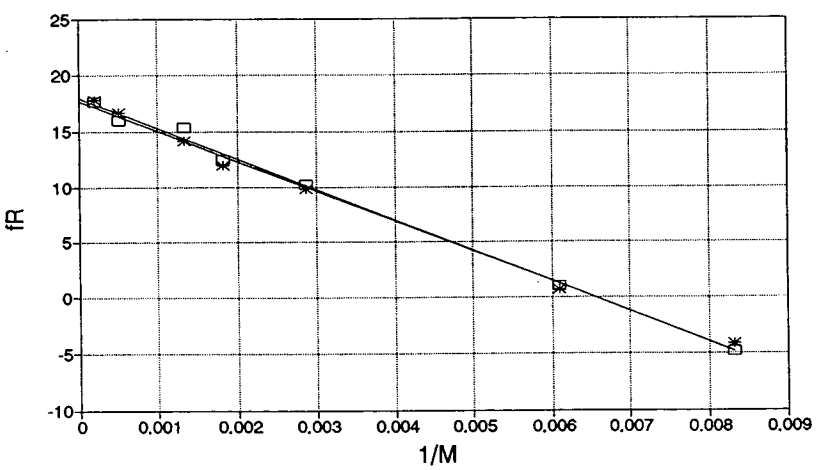


Fig. 1. Response factors of polyoxyethylene monomethyl ethers in dry, ethanol-free chloroform from (□) column and (*) bypass measurements with RI detection.

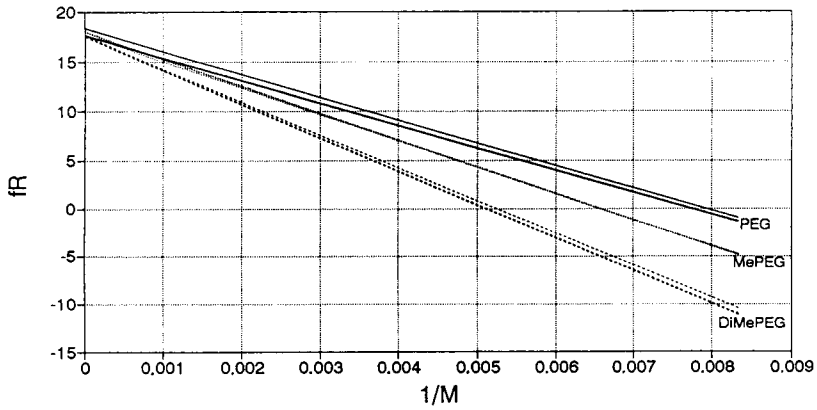


Fig. 2. Response factors of polyoxyethylenes with different end-groups in dry, ethanol-free chloroform from (thick lines) column and (thin lines) bypass measurements with RI detection.

regression lines had a similar intercept but a different slope, according to the different end-groups.

When 1.1% (v/v) of ethanol was added to the mobile phase, the chromatograms obtained on the column showed a vacancy peak (Fig. 3), the sign of which indicated that ethanol had been preferentially adsorbed by the polymer. As expected, the sum of the areas of polymer and solvent peaks on the column was equal to the area of the peak in bypass measurements.

In order to confirm the nature of the vacancy peak, the same analysis was performed without drying the chloroform. As can be seen from Fig. 4, the chromatogram obtained showed two vacancy peaks, which indicates that preferential solvation with both ethanol and water had occurred. (With density detection, the response factors of polyethylene oxide, ethanol, and water are negative, hence the polymer peak is negative and the vacancy peaks are positive. In Figs. 3 and 4 the sign of the density trace has been changed. With RI detection, the response factors of the polymer and solvents, ethanol and water, have opposite signs, hence all the peaks have the same sign.)

The results obtained in dry $CHCl_3$ containing 1.1% of EtOH are shown in Figs. 5 and 6 and the corresponding slopes, intercepts and correlation coefficients of the regression lines are given in Table II. For the dimethyl ethers, the intercepts obtained from bypass and column measurements were different, but the slopes were similar, which indicates that preferential solvation took place at the repeating units.

For monomethylethers and diols, both different slopes and intercepts were observed, which indicates that preferential solvation took place both at the end-groups and along the chain, but to different extents (depending on the nature of the end-groups). Using eqns. 19 and 20, we calculated $r_E$ and $r_R$ for different homologous series, as shown in Table III.

TABLE I

INTERCEPTS, SLOPES AND CORRELATION COEFFICIENTS OF THE REGRESSION LINES OBTAINED FROM BYPASS AND COLUMN MEASUREMENTS (WITH DENSITY AND RI DETECTION) OF MONO- AND DIMETHYL ETHERS OF POLYOXYETHYLENE IN DRY, ETHANOL-FREE CHLOROFORM

| Parameter | MePEG | | DiMePEG | |
|---|---|---|---|---|
| | Column | Bypass | Column | Bypass |
| $f_{D,\infty}$ | −17.73 | −17.08 | −17.11 | −16.69 |
| $K_D$ | −1600.3 | −1683.1 | −2635.8 | −2623.0 |
| $r$ | 0.9373 | 0.9979 | 0.9999 | 0.9991 |
| $f_{R,\infty}$ | 18.00 | 17.69 | 17.57 | 17.60 |
| $K_R$ | −2747.6 | −2694.5 | −3441.9 | −3371.1 |
| $r$ | 0.9978 | 0.9975 | 0.9984 | 0.9983 |

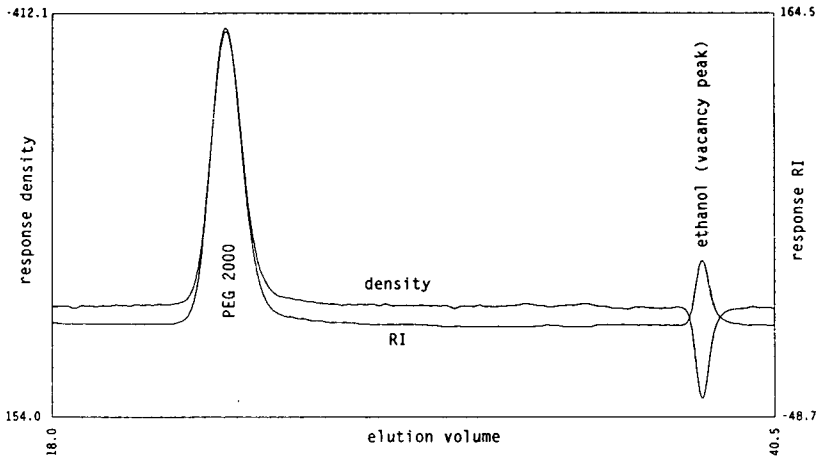


Fig. 3. Chromatogram of PEG 2000, as obtained with density and RI detection, in dry chloroform containing 1.1% (v/v) of ethanol.

From these data the following conclusions can be drawn:

(1) At a given ethanol content, all homologous series showed approximately the same value of $r_R$, as expected.

(2) For the dimethyl ethers, the slopes obtained in column and bypass measurements were almost the same, which indicates that the methoxy end-group behaves very much like the repeating unit.

(3) The preferential solvation of methoxy groups is small. Exchange of each methoxy group for a hydroxy group increased the $r_E$ value by roughly the same amount.

(4) The preferential solvation of the hydroxy groups was found to be much stronger than that of the repeating unit.

(5) Preferential solvation depends strongly on molecular mass for polyethylene glycols.

## CONCLUSIONS

In the liquid chromatography of polymers, preferential solvation has to be taken into account even in "pure" mobile phases, because even a very small amount of a second component in the mobile phase can be preferentially adsorbed, thus contributing to the detector signal.

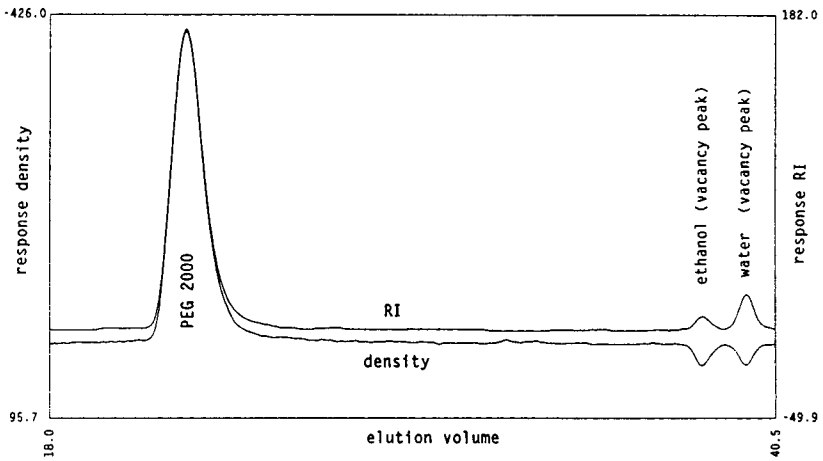


Fig. 4. Chromatogram of PEG 2000, as obtained with density and RI detection, in chloroform containing ethanol and water.

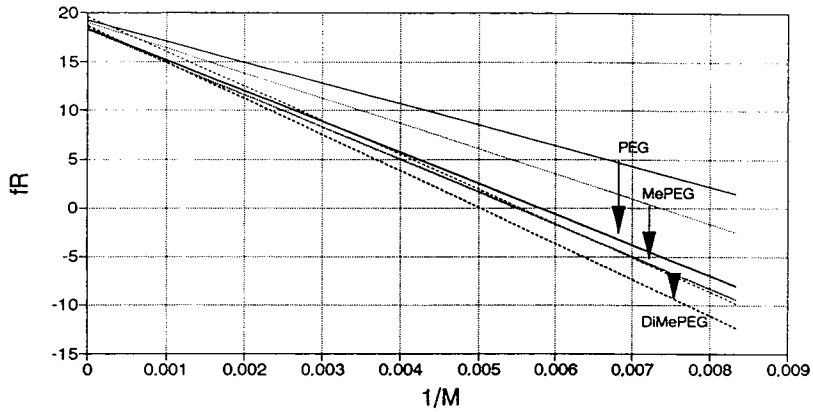


Fig. 5. Response factors of polyoxyethylenes with different end-groups in dry chloroform containing 1.1% (v/v) of ethanol from (thick lines) column and (thin lines) bypass measurements with RI detection.

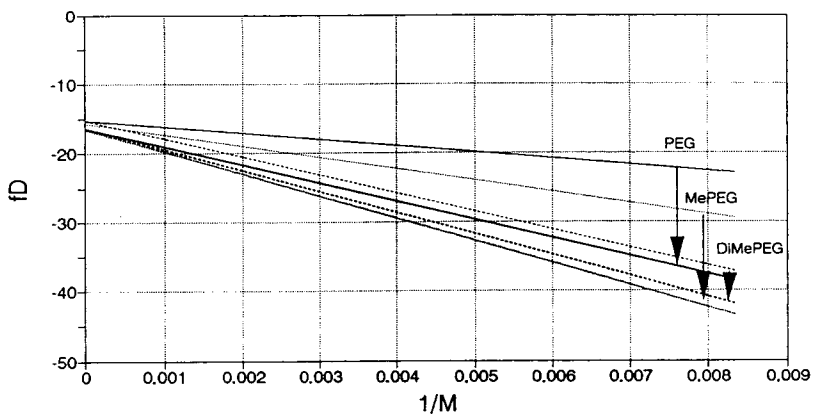


Fig. 6. Response factors of polyoxyethylenes with different end-groups in dry chloroform containing 1.1% (v/v) of ethanol from (thick lines) column and (thin lines) bypass measurements with density detection.

TABLE II

INTERCEPTS, SLOPES AND CORRELATION COEFFICIENTS OF THE REGRESSION LINES OBTAINED FROM BYPASS AND COLUMN MEASUREMENTS (WITH DENSITY AND RI DETECTION) OF POLYETHYLENE GLYCOLS AND THEIR MONO- AND DIMETHYL ETHERS IN DRY CHLOROFORM CONTAINING 1.1% (v/v) OF ETHANOL

| Parameter | PEG | | MePEG | | DiMePEG | |
|---|---|---|---|---|---|---|
| | Column | Bypass | Column | Bypass | Column | Bypass |
| $f_{D,\infty}$ | −16.36 | −15.27 | −16.46 | −15.59 | −16.12 | −15.29 |
| $K_D$ | −2658.7 | −912.4 | −3239.1 | −1653.4 | −3020.3 | −2627.5 |
| $r$ | 0.9926 | 0.9942 | 0.9937 | 0.9957 | 0.9984 | 0.9983 |
| $f_{R,\infty}$ | 18.32 | 19.21 | 18.27 | 18.95 | 18.85 | 19.64 |
| $K_R$ | −3165.9 | −2141.9 | −3334.7 | −2576.7 | −3740.3 | −3539.0 |
| $r$ | 0.9986 | 0.9993 | 0.9992 | 0.9983 | 0.9992 | 0.9995 |

TABLE III

AVERAGE NUMBERS OF ETHANOL MOLECULES ADSORBED PER REPEATING UNIT ($r_R$) AND PER END-GROUP ($r_E$) FOR DIFFERENT HOMOLOGOUS SERIES OF POLYOXYETHYLENES IN CHLOROFORM CONTAINING 1.1% (v/v) OF ETHANOL, AS OBTAINED WITH DENSITY AND RI DETECTION

| Derivative | $r_R$ | | $r_E$ | |
|---|---|---|---|---|
| | Density | RI | Density | RI |
| Diol | 0.0164 | 0.0200 | 0.603 | 0.531 |
| Monomethyl ether | 0.0131 | 0.0153 | 0.312 | 0.398 |
| Dimethyl ether | 0.0164 | 0.0200 | 0.167 | 0.113 |

If the end-groups of the polymer are considerably different from the repeating units, preferential solvation will depend on molecular mass, thus leading to errors in the molecular mass distributions determined by SEC if no compensation is performed. The response factors of non-specific detectors are apparent values, which will not affect the accuracy of the molecular mass averages as long as the composition of the mobile phase is kept constant.

ACKNOWLEDGEMENT

Financial support from the Austrian Fonds zur Förderung der wissenschaftlichen Forschung (Project-Nr. 8253 CHE) is gratefully acknowledged.

REFERENCES

1 D. Berek, T. Bleha and Z. Pevna, *J. Polym. Sci., Polym. Lett. Ed.*, 14 (1976) 323.
2 D. Berek, T. Bleha and Z. Pevna, *J. Chromatogr. Sci.*, 14 (1976) 560.
3 I. Katime and C. Strazielle, *Makromol. Chem.*, 178 (1977) 2295.
4 T. Spychaj, D. Lath and D. Berek, *Polymer*, 20 (1979) 437.
5 T. Spychaj and D. Berek, *Polymer*, 20 (1979) 1109.
6 B. Trathnigg and X. Yan, *J. Appl. Polym. Sci.*, 52 (1993), in press.
7 F. Candau, J. Francois and H. Benoit, *Polymer*, 15 (1974) 626.
8 G.V. Schulz and M. Hoffmann, *Makromol. Chem.*, 23 (1957) 220.
9 Y. Kobataka and H. Inagaki, *Makromol. Chem.*, 40 (1960) 118.
10 J. Francois, F. Candau and H. Benoit, *Polymer*, 15 (1974) 618.
11 R.-S. Cheng and X.-H. Yan, *Acta Polym. Sin.*, 12 (1989) 647.
12 I. Géczy, *Tenside Deterg.*, 9 (1972) 117.
13 I. Géczy, *Acta Chim. Acad. Sci. Hung.*, 79 (1973) 133.
14 B. Trathnigg and Ch. Jorde, *J. Liq. Chromatogr.*, 7 (1984) 1789.
15 B. Trathnigg and Ch. Jorde, *J. Chromatogr.*, 385 (1987) 17.
16 B. Trathnigg, Ch. Jorde and B. Maier, *Chromatogr. Anal.* (1989) 13.
17 B. Trathnigg, *GIT Fachz. Lab.*, 35 (1991) 35.

*Journal of Chromatography A*, 653 (1993) 207–218
Elsevier Science Publishers B.V., Amsterdam

CHROM. 25 458

# Anion-exchange chromatographic behavior of recombinant rat cytochrome $b_5$

# Thermodynamic driving forces and temperature dependence of the stoichiometric displacement parameter $Z$

David J. Roush, Davinder S. Gill and Richard C. Willson*

*Department of Chemical Engineering, University of Houston, 4800 Calhoun Avenue, Houston, TX 77204-4792 (USA)*

(First received May 24th, 1993; revised manuscript received July 27th, 1993)

ABSTRACT

The HPLC anion-exchange isocratic retention behavior of the recombinant soluble core of wild type rat cytochrome $b_5$ on Mono Q HR 5/5 was investigated as a function of temperature and sodium chloride concentration at fixed eluent flow-rates. Retention was measured over a range of eluent flow-rates at a specified temperature to determine if true adsorption equilibrium could be approximated by the HPLC method. Apparent Van 't Hoff enthalpies of adsorption obtained from the HPLC retention data were positive, indicating an entropically driven spontaneous adsorption process, and were found to decline with increasing ionic strength. The retention results were interpreted in terms of the stoichiometric displacement model to obtain the apparent number of binding sites in the contact region, $Z$, as a function of temperature and of protein concentration. $Z$ was found to depend significantly on temperature, even under conditions of nearly complete protein recovery, but did not depend on protein concentration at the low loadings studied.

## INTRODUCTION

Ion-exchange chromatography of proteins is based primarily on the coulombic interactions of oppositely charged groups on the protein and adsorbent surfaces. The ion-exchange adsorption of proteins has traditionally been assumed to be governed by the net charge of the protein resulting from ionizable groups on the protein surface, so that a protein will be retained on an anion exchange surface at a pH above the protein's isoelectric point. Several studies, however, have indicated that a protein may be retained on an ion-exchange surface of the *same* sign as the net charge of the protein [1,2] implying that the adsorption of a protein can be dominated by patches or clusters of charge on the protein's surface [1,3–6]. Another approach [7] has been to correlate retention data with the mean electrostatic potential as determined through electrostatic modeling of the protein surface.

The retention behavior of proteins on ion-exchange surfaces can often be successfully correlated using the non-mechanistic stoichiometric displacement model (SDM) originally proposed by Boardman and Partridge [8] and first applied to HPLC by Kopaciewicz *et al.* [1]. This model of protein adsorption is based on a mass-action

* Corresponding author.

0021-9673/93/$06.00 

description consisting of an exchange equilibrium between the counterions associated with the protein and displacing ions associated with the ion-exchange surface, and an equilibrium between the protein in the bound and free forms. The regression parameter $Z$, the apparent number of contacts between the protein and the ion-exchange surface participating in the adsorption–desorption process, can be determined by measuring the retention of the protein over a range of ionic strengths as described by these workers [1]. The SDM has been applied by other researchers to the ion-exchange adsorption of proteins in both batch [9,10] and HPLC [1,11–15] modes, and of nucleic acids [16]. Fractional $Z$ values have been obtained, and these have been observed to change as a function of loading [4,9,10]. Differences between values of $Z$ observed under isocratic and gradient elution conditions for the same system have been previously noted [17], and probably arise from incomplete equilibration of counterions and displacing ions during gradient elution. The difficulties associated with calculating isocratic elution parameters for proteins from gradient elution data have been documented by other researchers [17] and greatly impair the derivation of accurate thermodynamic quantities from such data [17–19]. Hence, isocratic elution is necessary to meet the requirements of counterion equilibrium for the SDM and to obtain thermodynamic information from the retention data. The completeness of equilibration of the protein between bound and free forms can be assessed by analyzing isocratic retention data over a range of eluent flow-rates. Careful control of temperature is also required for valid measurement of thermodynamic parameters.

In the analysis of experimental data from ion-exchange retention, it is important to establish that ion exchange is the dominant mechanism of adsorption. Other interactions, including Van der Waals and hydrophobic interactions can also influence retention [7,20–22] depending on the nature of the protein, eluent and ion exchanger. A combination of ion-exchange and other interactions ("mixed-mode adsorption" [23]) can occur for proteins such as lysozyme, which display both hydrophobic and charged patches. This phenomenon is generally believed to occur with most adsorbents [24], but has been best documented for polyethyleneimine-derivatized silica stationary phases with a range of hydrophobicities [11]. Hydrophobic interactions have been suggested to cause conformational changes in the protein upon adsorption [25,26] and are increased at elevated temperatures [27]. Minimization of these types of interactions is critical for characterization of ion-exchange adsorption alone, and to ensure that protein conformation is preserved during chromatography.

This study examines retention of the recombinant soluble core of wild type rat cytochrome $b_5$ on the strong anion exchanger Mono Q. This protein was chosen as an experimental model because of the wealth of related structural and biochemical data available and the existence of an efficient system for its expression in *Escherichia coli*, which will allow the future use of surface charge mutant forms of cytochrome $b_5$ to probe the potential existence of a favored "chromatographic contact region" in this protein–adsorbent system. The protein is well-suited for use in studies on anion-exchange adsorption of proteins because of its great stability in solution, strong chromopore (see below), moderate molecular mass ($M_r$ = 13 603) and negative net charge at pH values near neutrality; p$I$ 4.6 by isoelectric focusing (IEF); 23 negative charges (including the protoporphyrin) and 15 positive groups (allowing for partial titration of histidines) resulting in net charge −9.4 at pH 8.0. The effects of eluent flow-rate, temperature, protein concentration and ionic strength are examined in this work through application of the SDM and Van 't Hoff analyses. The goals of this investigation are to determine: (1) if a close approximation to equilibrium can be achieved in the HPLC system; (2) the apparent average number of interacting groups on the protein surface, "apparent $Z$"; (3) the apparent enthalpy of adsorption $\Delta H_{ads}$ as determined from Van 't Hoff analyses; and (4) any effects of temperature and eluent flow-rate on the apparent $Z$.

## EXPERIMENTAL

### *Chemicals and reagents*

The protein studied, recombinant soluble tryptic core of rat cytocrome $b_5$, was prepared in *E.*

*coli* using pUC plasmids containing a synthetic gene for this protein synthesized in the laboratory of Dr. Stephen Sligar at the University of Illinois [28]. The protein was purified from *E. coli* lysate using ion-exchange chromatography (Q Sepharose Fast Flow; Pharmacia, Uppsala, Sweden), ammonium sulfate fractionation and size exclusion chromatography (Sephacryl HR 100, Pharmacia). Protein purity was verified by silver stained 8–25% gradient sodium dodecyl sulfate–polyacrylamide gel electrophoresis (SDS-PAGE) analysis (PhastGel, Pharmacia), by ultraviolet–visible spectroscopy as described below, and by the fact that the protein ran as a single peak in the HPLC experiments.

Protein stock solutions were stored at −80°C at concentrations greater than 1.0 mg/ml in 10 m*M* Tris, pH 8.0 (pH adjusted at ambient temperature) and 0.1 m*M* EDTA. Protein stock solutions were assessed for purity and integrity after thawing by measuring the $R_Z$ (the ratio of the absorbances at 412 and 280 nm). All protein stock solutions used displayed an $R_Z$ greater than 5.6. Tris buffer salts of greater than 99.5% purity were obtained from ICN Biomedicals or Sigma.

*Protein solutions and buffers*

Eluents were prepared for each NaCl concentration by dilution of a 1.0 *M* Tris, pH 8.0 (at ambient temperature) stock solution and addition of the appropriate mass of NaCl. All solutions were prepared in volumetric flasks and adjusted to pH 8.0 with HCl and NaOH at the experimental temperature. Eluents were filtered through 0.2- or 0.45-$\mu$m cellulose acetate filters (Nalgene, Rochester, NY, USA) and degassed with high-purity helium (Linde, Houston, TX, USA).

Protein samples were prepared by dilution to approximately 0.25 mg/ml (0.50 mg/ml where specified) with 10 m*M* Tris, pH 8.0 and with 10 m*M* Tris, pH 8.0 + 2 *M* NaCl in a ratio such that the injected sample was in the same buffer concentration as the isocratic eluent. Protein samples were filtered using 0.22- or 0.45-$\mu$m cellulose acetate filters (Ultrafree-MC; Millipore, Marlborough, MA, USA) before injection. Protein concentrations were determined using a Beckman DU-64 spectrophotometer using the molar extinction coefficient of 130 m$M^{-1}$ cm$^{-1}$ at 412 nm for the strong Soret band of the oxidized protein.

*Equipment*

The entire HPLC system, with the exception of the computer (NEC 386/25 CUP; NEC Technologies, Boxborough, MA, USA), and the computer interface (System Interface Module; Waters, Milford, MA, USA) was located in a temperature-controlled environment room (Norlake, Hudson, WI, USA) regulated to within ±0.5°C. All chromatographic experiments were performed with a Waters HPLC system consisting of two Model 510 positive displacement pumps, a WISP 710B automated sample injection system and either a 441 ultraviolet–visible single-wavelength detector operating at 405 nm or a 481 variable-wavelength detector. The 405 nm wavelength was used for cytochrome $b_5$ retention measurements because it is located close to the oxidized protoporphyrin Soret band at 412 nm. For several experiments, the retention behavior of cytochrome $b_5$ was also monitored at 280 nm using the 481 detector in series to determine if the $R_Z$ changed during the chromatographic process. The Zn source of the 441 detector was employed to detect triglycine at 214 nm in column efficiency determinations.

Data were analyzed using Maxima 3.0 (Dynamic Solutions) software. Conductivity measurements were performed with an Amber Science Model 1054 (Eugene, OR, USA) digital conductivity meter and dip probe model 525. Calibration of the 525 probe was referenced to a nominal 10 000 $\mu$S conductivity standard (Fisher Scientific, Fair Lawn, NJ, USA). An in-line conductivity cell (Model 529, Amber Science) was employed to confirm column equilibration, which was defined as the inlet and exit conductivities being equal to within the measurement error of 0.9%. Conductivity was observed to be stable for at least five column volumes before each injection was made. Temperature measurements were made with an Omega (Stamford, CT, USA) DP41-TC display connected to an Omega hypodermic thermocouple probe (Model 3). Mono Q (Pharmacia) prepacked strong anion-exchange columns (HR 5/5, 50 mm × 5 mm I.D.) were used in all studies. The columns

were equilibrated according to the manufacturer's protocol (Pharmacia) as follows: washing with 5 ml of low-ionic-strength buffer (10 m*M* Tris, pH 8.0) followed by 10 ml of high-ionic-strength buffer (10 m*M* Tris, pH 8.0 + 2 *M* NaCl) and then by washing with low-ionic-strength buffer until the baseline stabilized. Additional column equilibration was performed as needed.

pH measurements were performed using an Orion (Cambridge, MA, USA) EA940 meter equipped with a Ross combination electrode, calibrated using pH 4.01, 7.00 and 10.01 standards (25°C, Orion), and pH adjustments made at the temperature at which the eluent was to be used.

Column performance (plate count) was verified using the retention behavior at 25°C of a 20-$\mu$l sample of 0.05 mg/ml triglycine [Sigma or United States Biochemicals (Cleveland, OH, USA)] in 10 m*M* Tris, pH 8.0 monitored at 214 nm. Each determination of the SDM parameter $Z$ was carried out entirely on a single column to avoid any effects of inter-column variations. Columns were retired when the plate count fell below the Pharmacia specification of 25 000 plates/m.

*Chromatography*

Protein samples were prepared in 10 m*M* Tris, pH 8.0 plus the appropriate NaCl concentration corresponding to the intended elution conditions. Protein samples of 50 $\mu$l were injected and eluted isocratically with eluents containing 10 m*M* Tris, pH 8.0 and NaCl in the range of NaCl concentration studied, 150 to 700 m*M*, matching the injection buffer. Protein sample concentrations were 0.25 ± 0.03 mg/m and 0.54 ± 0.01 mg/ml for the experiments designated 0.25 mg/ml and 0.50 mg/ml, respectively. The upper concentration range used was limited to approximately 0.60 mg/ml protein by the linearity of the 441 detector.

Retention was studied over the temperature range 4.7 to 36.2°C with a nominal eluent flow-rate of 0.5 ml/min. Retention behavior was also measured at 25°C over a range of eluent flow-rates between 0.1 and 1.0 ml/min. The evaluation of completeness of equilibration in these HPLC experiments is based on the independence of the capacity factor to changes in eluent flow-rate, as discussed below. For each eluent flow-rate, the protein was assigned a non-retained volume corresponding to the elution volume at 700 m*M* NaCl, corrected for non-column system volume, based on control experiments which showed that retention does not vary significantly in the range 600 to 700 m*M* NaCl.

Protein recovery calculations were based on detector calibration determined by direct injection into the absorbance detector of duplicate protein samples, separated by eluent blanks, for each retention measurement. Recoveries were determined using the same eluent and conditions as the protein retention experiment as it was observed that detector sensitivity [peak area (in $\mu$V·s) per $\mu$g protein] varied as a function of eluent flow-rate and temperature. The ratio of peak area to baseline noise integrated over a period equal to the peak width at baseline was typically *ca.* 80 under conditions of strong retention. The recoveries of cytochrome $b_5$ at temperatures below 37°C were 100% within experimental error, (±10%), except for the most strongly retained protein at 150 m*M* NaCl where recoveries were in excess of 85%. Protein recoveries for 37°C experiments at 175 and 150 m*M* NaCl were 70 and 35%, respectively, presumably due to structural rearrangements or denaturation which may occur under these conditions of strong retention (the retention time at 150 m*M* NaCl was 420 min). A gradient cleaning run, employing 10 m*M* Tris, pH 8.0 and 2 *M* NaCl, was performed after isocratic runs of less than 300 m*M* NaCl. The protein was not able to be quantitatively recovered from the most strongly retained conditions (150 m*M* and 175 m*M* NaCl at 37°C) during extensive cleaning runs, typically resulting in loss of separation efficiency of the column after experiments at 37°C. Values of $Z$ and Van 't Hoff enthalpies calculated without including the results of experiments showing recoveries of below 85%, were not significantly different from those calculated from the entire data set.

The accuracy and precision of the HPLC system were validated prior to acquisition of the experimental data, and control experiments were

performed to examine the effects of experimental parameters on retention. The conductivity detector and batch cell were found to give a linear response for sodium chloride concentrations of 100 to 1000 m*M*. The conductivity detector accuracy was 0.3% at 25°C and 1.0% at 4°C.

The eluent feed pumps were calibrated gravimetrically to 0.50 ml/min ± 2%. Eluent flow-rates ranged from 0.46 to 0.50 ml/min as determined gravimetrically for each chromatographic run, using the measured eluent density. Eluent flow-rates for the nominal 1.0 ml/min experiments ranged from 0.97 to 0.99 ml/min. The minimum flow-rate which can be commanded by software for the HPLC pumps is 0.1 ml/min, but accurate control is difficult at this low flow-rate, as the exit check valves do not close reliably at the low system pressure (less than 689 kPa). Experiments performed at a nominal flow-rate of 0.1 ml/min represent a range of flow rates from 0.083 to 0.105 ml/min. Given the strong dependence of $k'$ on ionic strength, the accuracy of the pumps was inadequate to allow for mixing of the two eluents to achieve a given sodium chloride concentration. Hence a separate eluent was prepared for each isocratic retention experiment as described under Materials.

As discussed previously by other authors [29], the $k'$ value can be a strong function of temperature, therefore the variation in the mean temperature of the system must be minimized in order to determine the effects of eluent flow-rate on retention. The protein samples and eluents were pre-equilibrated at the experimental temperature. Temperature measurements were conducted with the hypodermic thermocouple in the eluent reservoir, and also at the column outlet. The temperature at the column outlet was taken as that at which the reading stabilized to within 0.1°C, which occurred within several minutes. The average of the inlet and outlet temperatures is reported as the average temperature for a given run. The average difference in inlet and outlet temperatures for all experiments was 0.9 ± 0.7°C. Retention data were collected at mean system temperatures of 4.7 ± 0.2°C, 10.5 ± 0.2°C, 25.3 ± 0.2°C, 29.8 ± 0.1°C, and 36.2 ± 0.4°C at a nominal flow-rate of 0.50 ml/min, to assess the effect of temperature on retention and $Z$, and to allow for an approximate Van 't Hoff analysis.

In our studies of the effect of flow-rate on retention behavior, the mean system temperatures were 25 ± 0.4°C for the entire range of eluent flow-rates studied. As shown under Results, at 150 m*M*, 25°C, variations in temperature of this magnitude would produce a change in $k'$ and $Z$ of *ca.* 5% and 0.4%, respectively.

## DATA ANALYSIS

The capacity factor for each isocratic retention run was calculated from the following expression:

$$k' = (V_R - V_0)/V_0 \quad (1)$$

where $k'$ is the capacity factor, $V_R$ is the protein retention volume and $V_0$ is the protein non-retained volume. Retained and non-retained volumes were obtained from the retention time and the eluent volumetric flow-rate determined gravimetrically by eluent density for each run. The eluent flow-rate must be determined for each run as the pump delivery rate varied by up to 8% over the range of salt concentration used.

Thermodynamic information can be obtained from HPLC retention data if one can relate the measured parameter, $k'$, to the ratio of the protein concentration in the bound and the free phase. Once this relationship is defined, the application of an approximate Van 't Hoff analysis of the logarithm of $k'$ *versus* reciprocal absolute temperature is straightforward. The following description of the relationship of $k'$ to protein concentrations is adapted from Kopaciewicz *et al.* [1].

The capacity factor can be also defined as

$$k' = K_i y \quad (2)$$

where $K_i$ is the partition coefficient in liquid chromatography, $y$ is phase ratio equal to $A_s/V_m$, $A_s$ is the available surface area ($cm^2$) and $V_m$ is the mobile phase volume (ml). The partition coefficient can also be defined as

$$K_i = C_s/C_m \quad (3)$$

where $C_s$ is the protein concentration in the stationary phase (mol/cm$^2$) and $C_m$ is the protein concentration in the mobile phase (mol/ml).

The influence of temperature on chromatographic retention has been addressed for microcapillary chromatography for reversed- and normal-phase, and cation-exchange chromatography by Takeuchi *et al.* [29], and a relation between $k'$ and $\Delta H^0$ derived. In this derivation [29], it is assumed thermodynamic equilibrium is achieved in the column to allow for computation of thermodynamic parameters from a plot of ln $k'$ *versus* reciprocal absolute temperature, or an approximate Van 't Hoff analysis. A modified form of the derived expression is:

$$\ln k' = -\Delta H^0/RT + \Delta S^0/R + \ln(A_s/V_m) \qquad (4)$$

where $A_s$ = total area of the stationary phase (cm$^2$), $V_m$ = mobile phase volume of the column (ml), $\Delta H^0$ = enthalpy of transfer of a solute from the mobile phase to the stationary phase and $\Delta S^0$ = entropy of transfer of a solute from the mobile phase to the stationary phase.

For dilute solutions, the enthalpy of adsorption $\Delta H_{ads}$ can then be obtained by multiplying the slope of the plot of ln $k'$ *vs.* $1/T$ by the ideal gas constant, $R$ (1.978 cal/mol K).

Retention data can also be analyzed through application of the SDM [1] to yield the apparent number of protein–adsorbent contacts, $Z$. For the one-to-one electrolyte employed in this study, NaCl, the value of $Z$ equals half the slope of the plot of log $k'$ *versus* the log of the reciprocal ionic strength. Values of the capacity factor, $k'$, were calculated for representative runs from both the peak maximum and from the mean retention time and were in agreement within experimental error. The $k'$ data presented below were determined from the peak maxima.

The validity of several underlying assumptions must be confirmed to allow for a Van 't Hoff analysis of the HPLC data. One of these is the use of protein activity coefficients of unity, which is valid for the range of protein concentrations (15 to 45 $\mu M$) in sodium chloride concentrations (150 to 700 m$M$) used in this study [30]. Another assumption to be confirmed is that HPLC operation approximates adsorption equilibrium. As $Z$ appears to be essentially independent of eluent flow-rate for flow-rates between 0.2 and 1.0 ml/min (see Discussion section), the assumption of mass flux equilibrium appears to be justified for this experimental system under these operating conditions. It should be noted, however, that slow migration of protein molecules on the adsorbent surface and/or conformational changes of bound protein may only occur over time scales longer than typically sampled in column chromatographic experiments.

## RESULTS

A representative plot of $k'$ *vs.* [NaCl] for an average system temperature of 25.3°C, presented in Fig. 1, illustrates that the protein retention covers several orders of magnitude from completely unretained (700 m$M$ NaCl eluent, $k' = 0$) to very strongly retained (150 m$M$ NaCl, $k' = 177$). This broad sampling of the retention behavior was obtained for the entire temperature range studied using NaCl concentrations of 150 to 400 m$M$. Control experiments with 10 m$M$ Tris, pH 8.0 + 600 m$M$ NaCl eluents gave retention behavior statistically indistinguishable from the 700 m$M$ NaCl data. As is well known, the increased retention at the lower ionic strengths could be explained simply by increased competition by counterions and/or reduced electrostatic screening as compared with higher ionic strengths.

The application of the SDM to the data in Fig. 1 is illustrated in Fig. 2. For the salt employed in this study, a one-to-one electrolyte, the slope of the plot log $k'$ *vs.* log (1/[NaCl]) equals twice $Z$. For this example, a linear least squares regression of the data yields a value of $Z$ equal to 3.41.

The values for $Z$ obtained over the range of eluent flow-rate 0.1 to 1.0 ml/min are presented in Fig. 3. The values obtained for $Z$ are relatively independent of eluent flow-rate for flow-rates greater than 0.2 ml/min, and may be *ca.* 5% lower at the lowest flow-rate tested, 0.1 ml/min. The lowest eluent flow-rate may allow the protein to sample the ion-exchange medium for sufficient time to reach "true" adsorption equilibrium as would be determined by batch experiments. The average $Z$ value of 3.41 ± 0.09

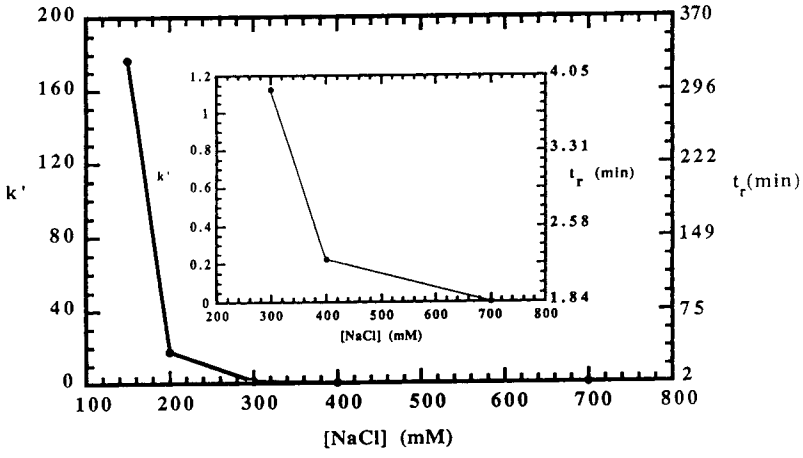


Fig. 1. Retention of cytochrome $b_5$ ($k'$) on Mono Q HR 5/5 as a function of ionic strength of NaCl at a mean system temperature of 25.3°C and an eluent flow-rate of 0.5 ml/min. The figure illustrates the wide range of $k'$ sampled during a representative set of retention experiments.

obtained over the range of flow-rates tested is in fair agreement with the value of $2.79 \pm 0.22$ obtained for batch equilibrium adsorption experiments [10] at 25°C with the value obtained at a flow-rate of 0.1 ml/min ($3.22 \pm 0.19$) being in closest agreement with the batch result. The results obtained at the lowest flow-rates used must be interpreted with caution, however, because of poor pump precision at these flow-rates. The remainder of the experimental data, therefore, were collected at nominal eluent flow-rates of 0.5 ml/min.

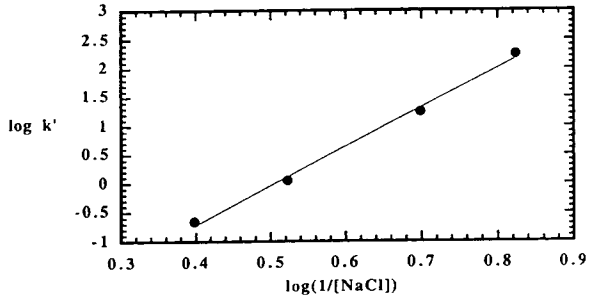


Fig. 2. Plot of log $k'$ *vs.* log (1/[NaCl]) or $Z$ plot of the data presented in Fig. 1. The value of $Z$ derived from the least squares linear analysis of the data equals one half the slope or 3.41. The data were acquired at a mean system temperature of 25.3°C and a nominal eluent flow-rate of 0.5 ml/min over the [NaCl] range 150 to 700 m$M$. The linear least squares fit is $y = -3.439 \pm 0.202 + 6.811 \pm 0.32x$ with $R = 0.998$.

The experimental data clearly indicate the strong dependence of $k'$ on temperature. Over the range of temperatures studied (4.7–36.2°C), $k'$ changes from 38.3 to 298 at 150 m$M$ NaCl, and from 0.100 to 0.267 at 400 m$M$ NaCl. As the ionic strength decreases, the sensitivity of $k'$ to temperature increases.

Another aspect of the influence of temperature on retention behavior is revealed by calculation of the SDM parameter $Z$, which is found to vary with temperature. Averaged $Z$ values as a function of mean system temperature from replicate experiments, with the exception of the single data point at 10.5°C, are presented in Table I; the individual measurements are displaced in Fig. 4, which clearly demonstrates a

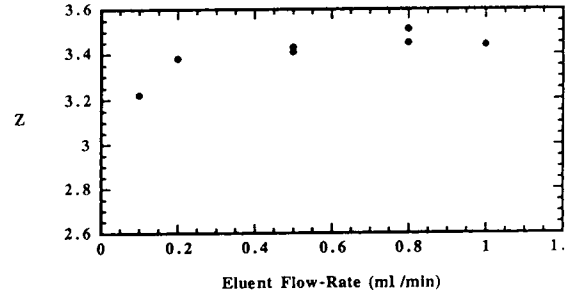


Fig. 3. Plot of $Z$ *vs.* eluent flow-rate at a mean system temperature of 25.2°C for the soluble tryptic core of rat cytochrome $b_5$. This figure illustrates the approximation to equilibrium for the flow-rate of 0.5 ml/min.

TABLE I

APPARENT NUMBER OF CONTACTS, $Z$, *VS.* TEMPERATURE

| System temperatures (°C) | | | $Z$ |
|---|---|---|---|
| Eluent | Column effluent | Mean | |
| 4.0 | 5.5 | 4.7 | 3.04 ± 0.05 |
| 9.9 | 11.2 | 10.5 | 3.19 ± 0.08 |
| 14.3 | 15.6 | 14.9 | 3.23 ± 0.10 |
| 24.8 | 25.8 | 25.3 | 3.42 ± 0.01 |
| 29.4 | 30.1 | 29.8 | 3.40 ± 0.07 |
| 36.1 | 36.4 | 36.2 | 3.58 ± 0.04 |

steady increase in $Z$ with increasing temperature. The change in $Z$ over the temperature range studied (0.54) is significantly larger than the maximum error associated with duplicate $Z$ measurements at a given temperature (0.20) and well above the standard deviation of replicate measurements (0.10).

Two other parameters, protein sample concentration and definition of the protein retention time, which could potentially affect the interpretation of the adsorption behavior were investigated through use of the SDM. For isocratic elution, the potential for peak asymmetry or skewness exists and would be expected to increase with increasing protein sample concentration or loading. The effect on $Z$ of calculating $k'$ based on mean retention time or peak maximum was explored at two temperatures at a

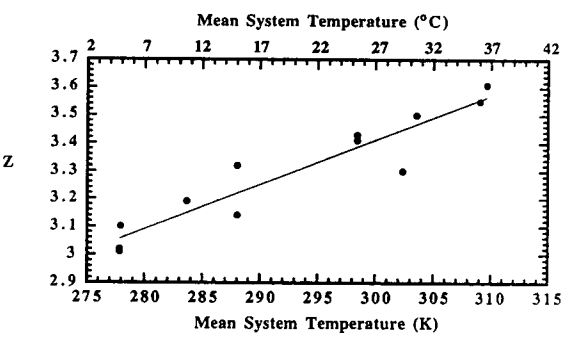


Fig. 4. A plot of $Z$ *vs.* mean system temperature for cytochrome $b_5$ for the range of temperatures 4.7 to 36.2°C and an eluent flow-rate of 0.5 ml/min. This plot demonstrates that $Z$ is a function of temperature for this protein–ion exchanger system. The linear least squares fit yields the equation with the standard deviation of the slope and intercept: $y = -1.41 \pm 0.52 + 1.61 \cdot 10^{-2} \pm 1.789 \cdot 10^{-3}\ T$.

nominal eluent flow-rate of 0.5 ml/min. Application of the two methods to data collected at a mean temperature of 30.4°C and an average protein concentration of 0.21 mg/ml yielded $Z$ values of 3.50 and 3.37 for peak maximum and mean retention time analyses, respectively, which compares favorably with the average value of $Z$ obtained from peak maxima for replicate experiments at a mean temperature of 29.8°C of 3.40.

The influence of protein loading was determined by comparison of $Z$ values obtained from retention data at 25.1°C and at a higher average protein concentration, 0.54 mg/ml, which yielded values of $Z$ of 3.45 (by peak maximum) and 3.44 (by mean retention time). The skewness would be expected to be even larger for this higher protein concentration. Little effect of skewness on calculated $Z$ values was observed, however, possibly because the amount of protein loaded even at the higher protein concentration is significantly less than the capacity of the Mono Q HR 5/5 column. As applied to the results of this study, the two methods of data analysis give indistinguishable results, independent of temperature and protein concentration. Therefore, the remainder of the data are presented based on peak maxima.

As described above, an estimate of the enthalpy of adsorption, $\Delta H_{ads}$, can be obtained from the approximate Van 't Hoff plot for each NaCl concentration. Representative analyses for given ionic strengths are presented in Fig. 5, which clearly indicate the strong dependence of $k'$ on temperature. Average values for $\Delta H_{ads}$ from duplicate experiments as a function of ionic strength are presented in Fig. 6.

## DISCUSSION

In this work the anion-exchange adsorption of cytochrome $b_5$ has been investigated by measuring the effects of temperature, eluent flow-rate and ionic strength on retention in isocratic HPLC. The extent of approximation of adsorption equilibria by HPLC in the system was defined, allowing for application of the SDM. The influence of temperature on the SDM parameter $Z$ could be observed, and an approxi-

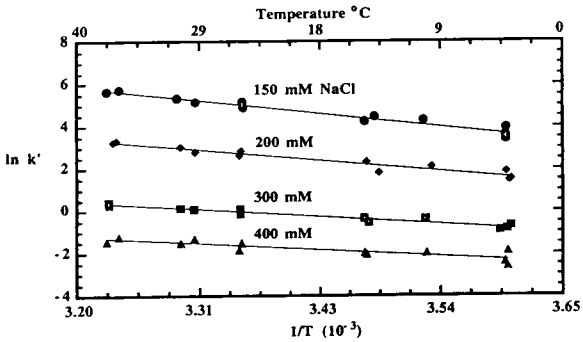


Fig. 5. Approximate Van 't Hoff plot of ln $k'$ *vs.* $1/T$ for the range of NaCl concentrations studied. The slope of the least squares linear fit for a given NaCl concentration is equal to $-\Delta H_{ads}/R$. Linear regression results are as follows:

| [NaCl] (m$M$) | $\Delta H_{ads}$ (kcal/mol) | Intercept | $R$ |
|---|---|---|---|
| 150 | 10.56 ± 0.36 | 23.56 ± 1.24 | 0.979 |
| 200 | 8.84 ± 0.36 | 17.96 ± 1.25 | 0.969 |
| 300 | 6.18 ± 0.25 | 10.57 ± 0.84 | 0.971 |
| 400 | 5.22 ± 0.44 | 7.46 ± 1.52 | 0.889 |

mate Van 't Hoff analysis allowed determination of $\Delta H_{ads}$ as a function of ionic strength.

Previous investigators have described the importance of satisfying the various requirements for a given chromatographic model. Several models [31–34] have been proposed to describe the criteria for equilibrium in HPLC ion-exchange and to account for the non-equilibrium behavior observed in some cases. The microscopic sub-processes involved in ion-exchange chromatography have been described by Norde [35]; the macroscopic effects of these sub-processes are most commonly manifested as variations in retention.

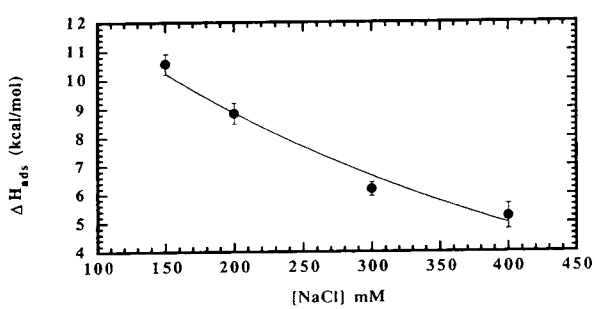


Fig. 6. Plot of the average $\Delta H_{ads}$ calculated from approximate Van 't Hoff analyses *versus* eluent NaCl concentration. The plot illustrates the decrease in enthalpy of adsorption with increasing NaCl concentration.

The best-characterized influence on the chromatographic capacity factor $k'$ is that of ionic strength, as presented in Fig. 1. Our results are in accord with those of previous investigators in that a plot of log $k'$ *vs.* log (1/[NaCl]) (Fig. 2) defined a straight line, supporting the application of the SDM to our data set.

Once the dominant effect of ionic strength on retention had been assessed, the influences of flow-rate and of temperature were considered. The value of $Z$ in this experimental system was found to be essentially independent of flow-rate between 0.2 to 1.0 ml/min, as presented in Fig. 3. The average value of $Z$ obtained over the flow-rates examined, $3.41 \pm 0.09$ is in close agreement with the value of $2.79 \pm 0.22$ obtained from batch equilibrium adsorption experiments [10]. The value obtained at 0.1 ml/min, the lowest flow-rate examined, was $3.22 \pm 0.19$ and was in even closer agreement with the equilibrium result.

The direct comparability of the batch and HPLC results may be reduced by differences in ionic strength and contact time. The batch experiments employ ionic strengths of 100 to 175 m$M$, and have been found to reach adsorption equilibrium in less than 60 min. In HPLC, the retention times for cytochrome $b_5$ at 0.5 ml/min ranged from approximately 2 min to greater than 300 min over the ionic strength range 400 to 150 m$M$, and extended to over 900 min at 0.1 ml/min. As discussed below, extended retention times may result in conformational changes in the protein, particularly at evaluated temperatures. The agreement of the HPLC data with the results of batch equilibrium adsorption experiments, along with the relative independence of $Z$ of flow-rate, indicates that equilibrium behavior could be approximated by the HPLC system.

The value of $Z$ was found to depend significantly on temperature, increasing from $3.04 \pm 0.05$ to $3.58 \pm 0.04$ as the temperature was varied from 4.7 to 36.2°C (Fig. 4). This increase in $Z$ suggests the creation of a larger number of contacts between the protein and the adsorbent surface at higher temperatures. This may arise from a more efficient optimization of the orienta-

tion and/or distribution of protein molecules on the adsorbent sites, from changes in the character of the polymeric adsorbent surface at higher temperatures, or from changes in protein structure as a function of temperature or time in the adsorbed state. The change with temperature of the activity coefficients of the counterions and coions and hydration waters on the ion exchange and protein surfaces could also be a potential explanation for the observed dependence of $Z$ on temperature. Any hydrophobic contributions to retention would also be expected to increase with temperature, possibly increasing the extent of any conformational rearrangements. The influence of these phenomena may be enhanced by the stronger retention, and hence longer contact times, observed at higher temperatures.

Previous investigators have ascribed abrupt changes in $Z$ as a function of ionic strength to changes in protein conformation [5,23], and nonlinear Van 't Hoff plots have been reported for reverse-phase chromatography [36], but there has been no previous report of a variation of $Z$ in a protein ion-exchange system with temperature.

Comparison of the $R_Z$ (ratio of absorbance at 405 nm to that at 280 nm) of the eluted protein with that of the loaded protein ($R_Z = 5.6$) revealed no significant change after chromatography at 25°C, but $R_Z$ changed and multiple peaks were observed at 280 nm at 37°C, providing further evidence for a possible conformational change of the eluted protein. This result was in accord with the reduced recoveries observed at 37°C at 150 and 175 m$M$ NaCl, which could be a result of changes in conformation as a function of time in the adsorbed state. Additional evidence for a contact time-dependent change in protein conformation is provided by the fact that doubling the eluent flow-rate at 37°C at 150 and 175 m$M$ NaCl, resulting in reduced contact times, improved recovery with similar values of $k'$.

While cytochrome $b_5$ is stable in solution to temperatures well above those studied here [37], adsorption is known to reduce protein stability in some cases. These previous examples involved mixed-mode adsorption of lysozyme on silica [26], and the adsorption of $\gamma$-crystallins on surfaces of increasing hydrophobicity [25]; such a result has not previously been reported for an ion-exchange system.

The study of adsorption thermodynamics through HPLC has previously been investigated [29,36,38,39], although results for protein and peptide systems are scarce. Hancock *et al.* [36] observed a linear dependence of ln $k'$ on reciprocal absolute temperature in reversed-phase chromatography of a lipid associating peptide, but a non-linear dependence for insulin, and other authors have noted a strong dependence of $k'$ on temperature in modes other than ion-exchange [38–41]. Takeuchi *et al.* [29] noted a linear dependence of ln $k'$ on reciprocal temperature for cation-exchange HPLC of adenosine and cytidine in derivatized microcapillary columns at pH 3.5.

The present work involved the determination of the enthalpy of adsorption of the protein in an isocratic anion-exchange system which had been verified to approximate equilibrium at the flow-rates employed. An entropic driving force for adsorption is implied by the fact that protein adsorption is a spontaneous process (negative $\Delta G_{ads}$), and the Van 't Hoff enthalpy of adsorption $\Delta H_{ads}$ is positive for all NaCl concentrations tested. The same conclusion has been reached from the results of batch adsorption experiments on this system [10].

Enthalpies of adsorption were observed to decrease significantly with increasing ionic strength. There are several possible explanations for this behavior, and it is not possible to select among the potential explanations with the limited data available. The possible explanations include changes in the nature of the adsorbent surface, protein conformational changes, and activity effects. The mobility, packing and flexibility of the adsorbent's charged polymer chains would be expected to vary with ionic strength, perhaps changing the nature of their interactions with adsorbed protein molecules. Slight conformational change may be induced in protein molecules strongly bound at low ionic strengths, resulting in larger enthalpies of adsorption. The activity effect arises from the fact that counterions and waters of hydration can have different activity coefficients in the bulk solution than

when associated with the charged surfaces of the protein and ion exchanger [24]. Changes in counterion activities (and in the activities of the associated waters of hydration) upon protein adsorption results from a dilution effect associated with the release of the counterions from the surface into the bulk [42]. The observed decrease in the enthalpy of adsorption with increasing NaCl concentration is potentially consistent with a decrease in the dilution effect at higher ionic strength, potentially resulting in a reduced contribution to $\Delta H_{ads}$ with increased ionic strength.

While there are no directly comparable thermodynamic results for protein ion exchange available in the literature, data on related protein/polyelectrolyte systems may aid in interpretation of the present results. Koutsoukos *et al.* [43] inferred an entropic driving force from data on adsorption of human serum albumin to hematite. The hematite surface is relatively hydrophilic, but adsorption on hematite is not mediated solely by ion exchange, particularly near the protein's isoelectric point.

Record *et al.* [42] have reviewed the extensive literature on the involvement of counterions and waters of hydration in the association of proteins with nucleic acids. In cases of sequence-independent binding, in which the primary interactions of the protein with the nucleic acid are mediated by the backbone charges, this phenomenon which may well be comparable to ion exchange adsorption of proteins. In these systems, the release of counterions and waters of hydration upon protein binding provides a significant entropic driving force. Based on the arguments summarized by Record *et al.*, the release of counterions and waters of hydration upon the binding of cytochrome $b_5$ to Mono Q could be the primary mechanistic driving force for adsorption. The discussion by Fraaije and Lyklema [44] of the binding of ions by proteins suggests that the electrolyte binds preferentially in the double layer associated with the protein surface. In the double layer formulation, overlap of the double layers associated with the charged ion exchange surface and the protein surface upon binding would result in release of counterions, further supporting the arguments of Record *et al.* [42]. The thermodynamic manifestation of these subprocesses would be an entropic driving force arising from the increased degrees of freedom associated with the liberated ions and water molecules, in agreement with our observations.

## ACKNOWLEDGEMENTS

*E. coli* strain TB1 expressing recombinant soluble core of rat cytochrome $b_5$ was the generous gift of Dr. Stephen Sligar of the University of Illinois. We would like to thank Dr. Sligar and Dr. Karla Rodgers for helpful discussions. Support was provided by NSF under CTS-8910087, and by an NSF Presidential Young Investigator Award to R.C.W. Additional support was provided by Pharmacia and by the Waters Chromatography Division of Millipore Corporation.

## REFERENCES

1 W. Kopaciewicz, M.A. Rounds, J. Fausnaugh and F.E. Regnier, *J. Chromatogr.*, 266 (1983) 3.
2 V. Lesins and E. Ruckenstein, *Colloid Polym. Sci.*, 266 (1988) 1187.
3 J. Fausnaugh-Pollitt, G. Thevenson, L. Janis and F.E. Regnier, *J. Chromatogr.*, 443 (1988) 221.
4 I. Mazsaroff, S. Cook and F.E. Regnier, *J. Chromatogr.*, 443 (1988) 119.
5 R. Chicz and F.E. Regnier, *J. Chromatogr.*, 443 (1988) 193.
6 R. Chicz and F.E. Regnier, *Anal. Chem.*, 61 (1989) 2059.
7 L. Haggerty and A.M. Lenhoff, *J. Phys. Chem.*, 95 (1991) 1472.
8 N.K. Boardman and S.M. Partridge, *Biochem. J.*, 59 (1955) 543.
9 R.D. Whitley, R. Wachter, F. Liu and N.-H.L. Wang, *J. Chromatogr.*, 465 (1989) 137.
10 D.S. Gill, D.J. Roush and R.C. Willson, in preparation.
11 W. Kopaciewicz, M.A. Rounds and F.E. Regnier, *J. Chromatogr.*, 318 (1985) 157.
12 M.A. Rounds and F.E. Regnier, *J. Chromatogr.*, 283 (1984) 37.
13 R.P. Drager and F.E. Regnier, *J. Chromatogr.*, 406 (1987) 237.
14 A. Velayudhan and Cs. Horváth, *J. Chromatogr.*, 443 (1988) 13.
15 A. Velayudhan and Cs. Horváth, *J. Chromatogr.*, 367 (1986) 160.
16 R.P. Drager and F.E. Regnier, *J. Chromatogr.*, 359 (1986) 147.
17 M.T.W. Hearn, A.N. Hodder and M.I. Aguilar, *J. Chromatogr.*, 458 (1988) 27.

18 E. Parente and D. Wetlaufer, *J. Chromatogr.*, 355 (1986) 29.
19 M.A. Quarry, R.L. Grob and L.R. Snyder, *J. Chromatogr.*, 285 (1984) 1.
20 W. Norde and J. Lyklema, *J. Colloid Interface Sci.*, 71 (1979) 350.
21 J.N. Israelachvilli and R.M. Pashley, *J. Colloid Interface Sci.*, 98 (1984) 500.
22 M.T.W. Hearn, A.N. Hodder and M.I. Aguilar, *J. Chromatogr.*, 458 (1988) 45.
23 A.N. Hodder, K.J. Machin, M.I. Aguilar and M.T.W. Hearn, *J. Chromatogr.*, 517 (1990) 317.
24 W. Norde, in J.D. Andrade (Editor), *Surface and Interfactial Aspects of Biomedical Polymers*, Plenum Press, New York, Vol. 2, Ch. 8, p. 280.
25 K. Matsuno, R. Lewis and C. Middaugh, *Arch. Biochem. Biophys.*, 292 (1991) 349.
26 B.L. Steadman, K.C. Thompson, C.R. Middaugh, K. Matsuno, S. Vrona, E.Q. Lawson and R.V. Lewis, *Biotechnol. Bioeng.*, 40 (1992) 8.
27 A.W. Purcell, M.I. Aguilar and M.T.W. Hearn, *J. Chromatogr.*, 476 (1989) 125.
28 S. Beck von Bodman, M. Schuler, D. Jollie and S. Sligar, *Proc. Natl. Acad. Sci. U.S.A.*, 83 (1986) 9443.
29 T. Takeuchi, M. Masayoshi and D. Ishii, *J. Chromatogr.*, 235 (1982) 309.
30 G. Weber, *Protein Interactions*, Routledge, Chapman and Hall, London, 1992, p. 8.
31 S. Yamamoto, K. Nakanishi and R. Matsuno, *Ion-Exchange Chromatography of Proteins* (Chromatographic Science Series, Vol. 43), Marcel Dekker, New York, 1988.
32 H. Hethcote and C. DeLisi, *J. Chromatogr.*, 260 (1982) 269.
33 S. Yamamoto, K. Nakanishi, R. Matsuno and T. Kamikubo, *Biotechnol. Bioeng.*, 25 (1983) 1373.
34 A.M. Lenhoff, *J. Chromatogr.*, 384 (1987) 285.
35 W. Norde, *Adv. Colloid Interface Sci.*, 25 (1986) 267.
36 W.S. Hancock, D.R. Knighton, J.R. Napier, R.K. Harding and R. Venable, *J. Chromatogr.*, 367 (1986) 1.
37 D.S. Gill, unpublished results.
38 R. Dybcsynski, *J. Chromatogr.*, 31 (1967) 155.
39 S. Abbott, P. Achener, R. Simpson and F. Klink, *J. Chromatogr.*, 218 (1981) 123.
40 H. Poppe and J.C. Kraak, *J. Chromatogr.*, 282 (1983) 399.
41 H. Schrenker, *J. Chromatogr.*, 213 (1981) 243.
42 M.T. Record Jr., C.F. Anderson and T.M. Lohman, *Q. Rev. Biophys. 11*, 2 (1978) 103.
43 P.G. Koutsoukos, W. Norde and J. Lyklema, *J. Colloid Interface Sci.*, 95 (1983) 385.
44 J.G.E.M. Fraaije and J. Lyklema, *Biophys. Chem.*, 39 (1991) 31.

*Journal of Chromatography A*, 653 (1993) 219–228
Elsevier Science Publishers B.V., Amsterdam

CHROM. 25 470

# Effects of compound structure and temperature on the resolution of enantiomers of cyclopentenones by liquid chromatography on derivatized cellulose chiral stationary phases

Larry Miller* and Cara Weyker

*Chemical Sciences Department, Searle, 4901 Searle Parkway, Skokie, IL 60077 (USA)*

(First received April 6th, 1993; revised manuscript received July 30th, 1993)

ABSTRACT

Analytical HPLC methods using derivatized cellulose chiral stationary phases were developed for the separation of the enantiomers of eight cyclopentenone derivatives. The mobile phase and the chiral stationary phase were varied to achieve the best resolution. It was shown that the chemical environment distant from the chiral center had large effects on the separation obtained. The effect of subambient and elevated temperature on the retention, separation and the resolution of the enantiomers was also investigated. Maximum resolution was obtained at elevated temperatures. Three of the compounds were scaled up to preparative loadings to determine the correlation between analytical resolution and preparative resolution. In addition, an example of the sample self-displacement effect observed during the preparative resolution of one of these compounds will be discussed.

## INTRODUCTION

Cyclopentenones are important intermediates for numerous natural products including prostaglandins [1,2]. They contain a chiral carbon and exist as enantiomers. There are two approaches to obtaining enantiomerically pure chemicals. These are (1) asymmetric synthesis of the desired isomer and (2) resolution of a racemic mixture into individual isomers. Various synthetic methods to produce optically pure cyclopentenones have been developed [3–5]. In addition, enzymatic methods have been developed to resolve the enantiomers of cyclopentenones [6]. Methods for the resolution of a racemic mixture include recrystallization of diastereomeric salts, formation of diastereomeric derivatives followed by chromatographic resolution on an achiral stationary phase, or direct chromatographic resolution of enantiomers using a chiral stationary phase or a chiral mobile phase additive. Only a limited amount of work using liquid chromatography for the analytical or preparative resolution of cyclopentenone precursors of prostaglandins has been published [2,7–9].

The use of temperature has become an increasingly useful parameter to achieve chiral separations. The effect of temperature on chiral separations using cellulose [10–12], cyclodextrins [13–17], Pirkle type [19,20], and cellulose tris-3,5-dimethylphenyl carbamate (Chiralcel OD) [20–23] chiral stationary phases (CSPs) has been reported. For cellulose triacetate CSP, separation factor $\alpha$ and resolution increase with increasing temperature. For cyclodextrin CSPs, decreasing temperature increases $\alpha$ and can either decrease or increase resolution based on

* Corresponding author.

0021-9673/93/$06.00 

the compound being separated. For separations with adequate $\alpha$ values at room temperature, elevated temperatures have been used to increase resolution. For Pirkle type CSPs, $\alpha$ increases with decreasing temperature while resolution again decreases due to poorer mass transfer rates. For Chiralcel OD CSPs, $\alpha$ is relatively unaffected by column temperature, while maximum resolution was obtained at either ambient or subambient temperatures.

Sample self-displacement is a phenomenon that is observed during the preparative purification of a binary mixture under sample overload conditions. Sample self-displacement causes a sharpening of the elution band of the first eluting component of the mixture. This results in a larger yield of pure chemical than would be expected based on the separation seen at analytical loadings. For sample self-displacement to occur, the second eluting component of the binary mixture must be present in equal or greater amounts relative to the first eluting component. The phenomenon of sample self-displacement has been shown to occur for numerous types of chemicals and can be used to increase the throughput of any separation involving a binary mixture [24–26].

## EXPERIMENTAL

### *Materials*

The chiral stationary phases used for these studies were obtained from Daicel (Tokyo, Japan) through Baker (Phillipsburgh, NJ, USA) or Regis (Morton Grove, IL, USA) as prepacked analytical (250 mm × 4.6 mm I.D.) and preparative columns (500 mm × 10 mm I.D. and 500 mm × 20 mm I.D.). The prostaglandin precursors were synthesized in the Chemical Development laboratories of Searle (Skokie, IL, USA). The solvents were reagent grade or better and obtained from a variety of sources.

### *Equipment*

The analytical chromatograph consisted of a Waters Assoc. Model 590 solvent delivery system and a U6K injector of Waters Intelligent Sample Processor Model 712 (Milford, MA, USA), a Kratos Model 783 variable wavelength detector (Ramsey, NJ, USA), a Linear Model 585 recorder (Hackensack, NJ, USA), and Digital Equipment Corporation VAX 11/785 computer with Searle chromatography data system. Elevated column temperatures were achieved using a Fiatron CH-30 column heater equipped with a TC-50 temperature controller (Oconomowoc, WI, USA). Subambient column temperatures were achieved either with tap water flowing through a column jacket or by immersing the column in an ice bath. For column temperatures of 0°C, the mobile phase was stored in a refrigerator overnight prior to use and kept in an ice bath during use. For all other temperatures studied the mobile phase was kept at room temperature.

The preparative chromatograph consisted of two Beckman Model 101 pumps with preparative heads, a Model 165 variable wavelength detector with a 5-mm semi-preparative flowcell, a Model 450 data system/controller (Berkeley, CA, USA) and a Kipp and Zonen Model BD41 two channel recorder (Delft, Netherlands). A Rheodyne Model 7125 syringe loading sample injector (Cotati, CA, USA) equipped with a 10-ml loop (Valco, Houston, TX, USA). The column effluent was fractionated using a Gilson Model FC220 fraction collector (Middleton, WI, USA).

## RESULTS AND DISCUSSION

### *Analytical HPLC*

Recently in our laboratories, the use of enzymes to resolve racemic mixtures of various cyclopentenones has been explored [6]. In order to monitor the extent of these resolutions, analytical HPLC methods were needed that could be used to determine low levels of the undesired enantiomer. Analytical HPLC methods for the enantiomeric separation of the eight cyclopentenones shown in Figs. 1 and 2 were developed using Chiralcel columns. Chiralcel chiral stationary phases are derivatives of cellulose which are adsorbed on silica gel. For this work Chiralcel OA (acetate derivative), OC (phenylcarbamate derivative), OD (dimethyl phenylcarbamate derivative), OJ (p-methylbenzoate derivative) and OK (tricinnamate derivative) were used (Fig. 3).

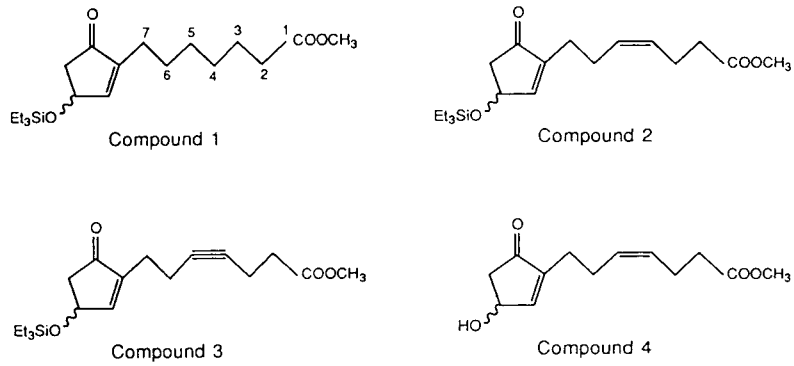


Fig. 1. Structures of cyclopentenone precursors; compounds 1 to 4.

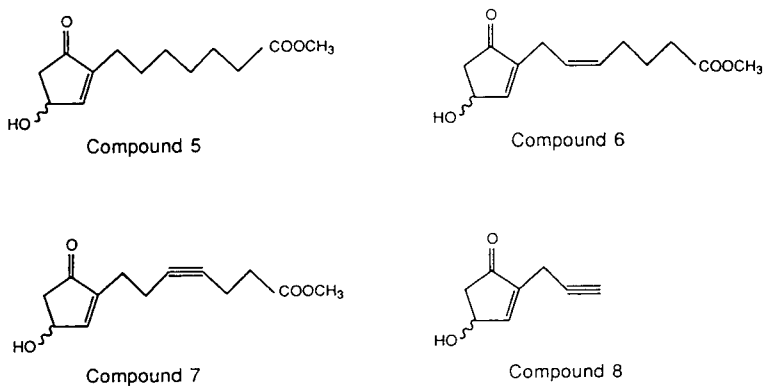


Fig. 2. Structures of cyclopentenone precursors; compounds 5 to 8.

The analytical HPLC separations for compounds 1 to 8 are shown in Figs. 4 and 5. Table I summarizes the capacity factors ($k'$), separation factor ($\alpha$), and resolution ($R_s$) for the enantiomer separation of these eight compounds.

Since the eight cyclopentenone compounds

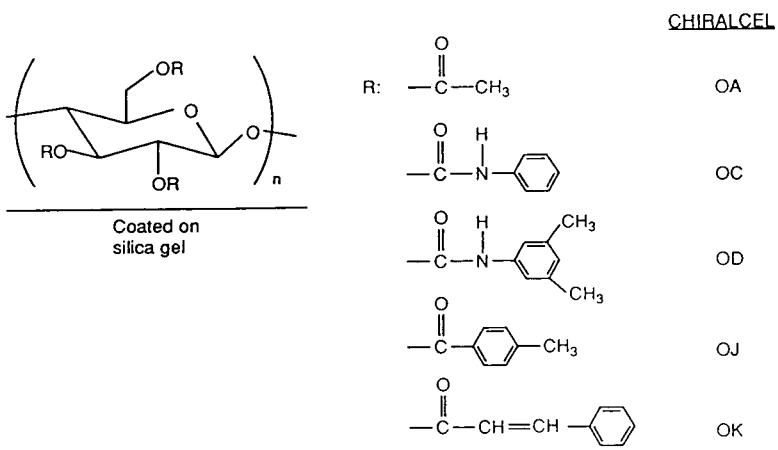


Fig. 3. Structures of various Chiralcel packings.

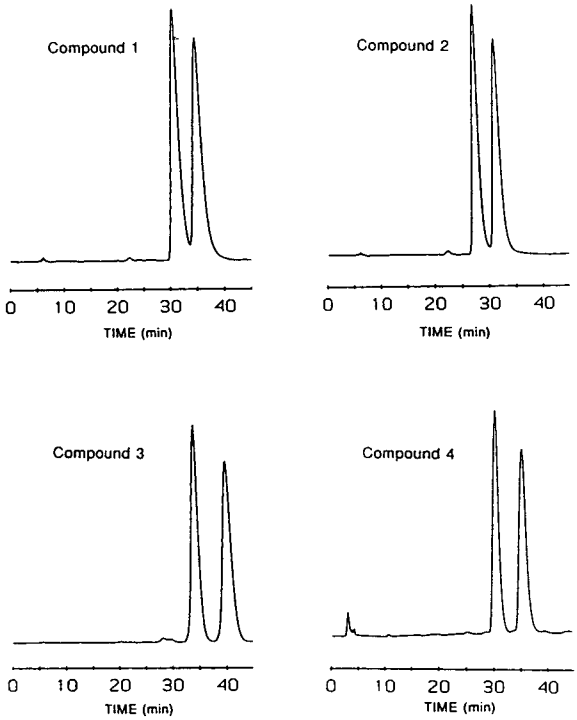


Fig. 4. Analytical HPLC separation of compounds 1 to 4. Analysis conducted on Chiralcel OC (compounds 1 to 3) or Chiralcel OD (compound 4) (250 mm × 4.6 mm I.D.), detection at 215 nm, 0.2 AUFS. Mobile phase, flow-rate: compound 1, 2 and 3 hexane–isopropanol (98:2), 0.5 ml/min; compound 4 hexane–isopropanol (93:7), 0.7 ml/min. All analyses performed at room temperature.

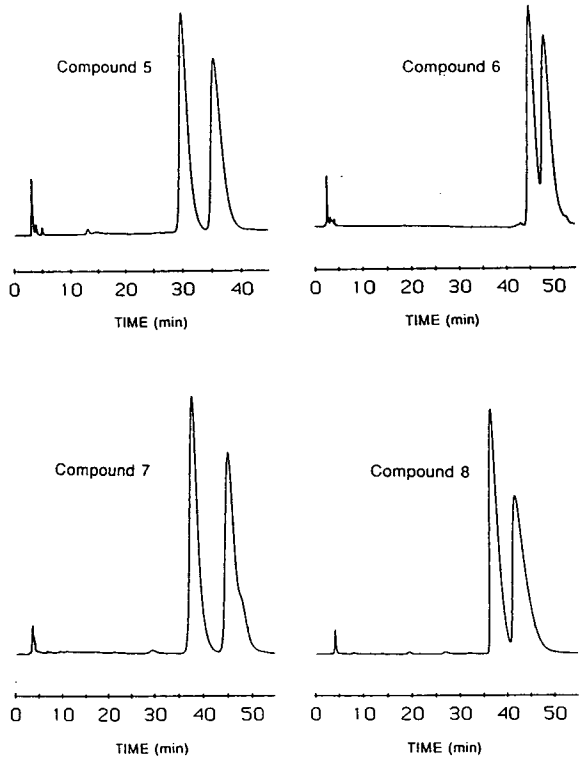


Fig. 5. Analytical HPLC separation of compounds 5 to 8. Detection at 215 nm, 0.2 AUFS. Column, mobile phase, flow-rate: compound 5 Chiralcel OC, hexane–isopropanol (90:10), 1 ml/min; compound 6 Chiralcel OD, hexane–isopropanol (97:3), 1.2 ml/min; compound 7 Chiralcel OC hexane–isopropanol (90:10), 1.0 ml/min; compound 8 Chiralcel OA hexane–isopropanol (96:4), 1.0 ml/min. All analyses performed at room temperature except for compound 5 and 7 which were performed at 50°C.

that were studied are structurally similar, having their chiral center on the same position on the cyclopentenone ring, it is possible to study the effect structural changes distant from the chiral center have on the enantiomeric separation. For example, compounds 1 to 3 all have a triethylsilyl protected group on the chiral center. The only difference between these three compounds is the degree of saturation in the 4,5 position of the upper side chain. Reviewing the data in Table I shows that the degree of saturation in the upper side chain has little effect on retention, but has an effect on $\alpha$ and $R_s$. From compound 1 (single bond) to compound 3 (triple bond) we see an increase in $\alpha$ of 0.05 (1.16 to 1.21) and an increase in $R_s$ of 1.0 (1.51 to 2.51). The plate number for the separation of compounds 1, 2 and 3 is 2076, 2583 and 3161, respectively. It is apparent that both $\alpha$ and plate number have an effect on resolution.

Another example is the results obtained with compounds 5 and 7, the unprotected analogues of compounds 1 and 3. When a triple bond is present at the 4,5 position (compound 7) $\alpha$ is unchanged, retention is increased (30%) and resolution is increased (2.02 to 2.25).

Other examples of the effect structural changes distant from the chiral center can have on the enantiomeric separation were realized during the method development to produce the analytical HPLC methods shown in Figs. 4 and 5. Compounds 4, 5 and 7 are the unprotected analogues of compounds 2, 1 and 3, respectively.

TABLE I

VALUES FOR ANALYTICAL SEPARATION OF ENANTIOMERS FOR COMPOUNDS 1 TO 8

See Figs. 4 and 5 for HPLC conditions.

| Compound | $k_1'$ [a] | $k_2'$ [b] | $\alpha$ | $R_s$ |
|---|---|---|---|---|
| 1[c] | 4.14 | 4.83 | 1.16 | 1.51 |
| 2[c] | 3.59 | 4.23 | 1.18 | 1.85 |
| 3[c] | 4.68 | 5.68 | 1.21 | 2.51 |
| 4[d] | 6.06 | 7.20 | 1.19 | 2.42 |
| 5[e] | 9.08 | 10.89 | 1.20 | 2.02 |
| 6[f] | 18.50 | 21.46 | 1.16 | 1.02 |
| 7[e] | 11.72 | 14.15 | 1.21 | 2.25 |
| 8[g] | 11.33 | 13.00 | 1.15 | 1.16 |

[a] Capacity factor for first eluting enantiomer.
[b] Capacity factor for second eluting enantiomer.
[c] Chiralcel OC, hexane–isopropanol (98:2).
[d] Chiralcel OD, hexane–isopropanol (93:7).
[e] Chiralcel OC, hexane–isopropanol (90:10).
[f] Chiralcel OD, hexane–isopropanol (97:3).
[g] Chiralcel OA, hexane–isopropanol (96:4).

TABLE II

VALUES FOR ANALYTICAL SEPARATION

| Compound | $k_1'$ [a] | $k_2'$ [b] | $\alpha$ | $R_s$ |
|---|---|---|---|---|
| 4[c] | 6.07 | 7.19 | 1.19 | 2.00 |
| 5[c] | 6.16 | 6.77 | 1.10 | 1.32 |
| 7[c] | 8.40 | 8.40 | 1.00 | 0.00 |
| 4[d] | 7.07 | 8.53 | 1.21 | 1.31 |
| 5[d] | 6.47 | 7.53 | 1.16 | 1.23 |
| 7[d] | 9.27 | 10.80 | 1.17 | 1.28 |
| 4[e] | 8.32 | 10.15 | 1.22 | 3.49 |
| 6[e] | 9.14 | 9.79 | 1.07 | 0.89 |

[a] Capacity factor for first eluting enantiomer.
[b] Capacity factor for second eluting enantiomer.
[c] Conditions: Chiralcel OD, hexane–isopropanol (93:7).
[d] Conditions: Chiralcel OC, hexane–isopropanol (85:15).
[e] Conditions: Chiralcel OD, hexane–isopropanol (94:6).

When the unprotected compounds (compounds 4, 5 and 7) were analyzed using a Chiralcel OC column different results are seen compared to the triethylsilyl (TES) protected compounds (compounds 1, 2 and 3). The protected compounds showed a drastic difference in resolution (Table I), while only slight differences were seen with the unprotected compounds (Table II). In addition, different trends for $\alpha$ *vs.* degree of saturation at the 4,5 position are observed. For the TES protected compounds, $\alpha$ increases as saturation decreases (single bond to triple bond). With the unprotected compounds, the single bond also results in the lowest separation, but the maximum separation is seen for the compound with a double bond in the 4,5 position. This is different from the protected compounds which exhibit the largest separation for the compound with a triple bond in the 4,5 position. An interesting observation is seen when compounds 4, 5 and 7 are analyzed on two different CSPs (Chiralcel OC and Chiralcel OD). These results are summarized in Table II. On the Chiralcel OC column, all three compounds are separated. Only minor differences in $\alpha$ and $R_s$ are observed. An increase in $\alpha$ and resolution is seen from the single bond compound to the triple bond compound, with maximum separation seen for the double bond compound. When the compounds are analyzed on a Chiralcel OD column, the double bond compound again has increased $\alpha$ and $R_s$ relative to the single bond compound, but all separation is lost for the triple bond compound.

The final effect is seen when compounds 4 and 6 are analyzed using a Chiralcel OD column with a mobile phase of isopropanol–hexane (6:94). The only difference between these two compounds is the location of the *trans* double bond in the upper side chain. With compound 4 the double bond is located in the 4,5 position. With compound 6 it is located in the 5,6 position. Evaluation of the data in Table II shows that moving the double bond from the 4,5 position to the 5,6 position results in a pronounced decrease in both $\alpha$ and $R_s$.

*Temperature effects*

During HPLC method development it was found that elevated temperature improved the separation of compounds 5 and 7. A review of literature showed that both subambient and elevated temperatures had been used in other laboratories to improve chiral separations [10–23]. To better understand the effects of tempera-

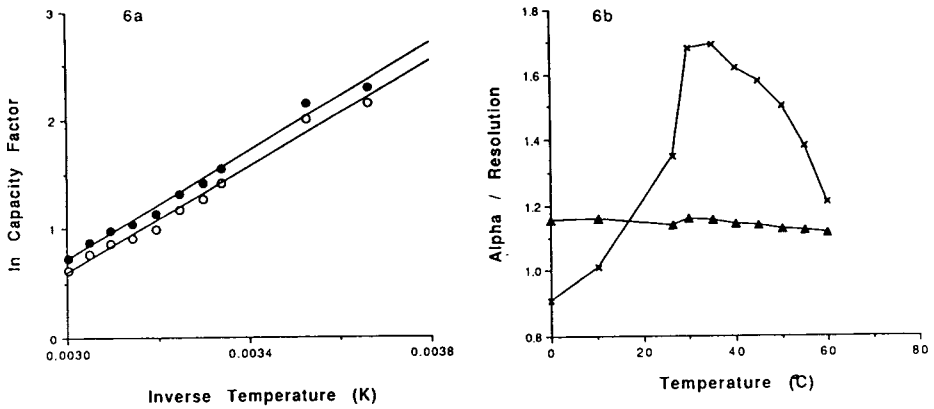


Fig. 6. Effect of temperature on analytical HPLC separation of compound 1. See Fig. 4 for chromatographic conditions. ● = $k'$ for first eluting enantiomer; ○ = $k'$ for second eluting enantiomer; ▲ = $\alpha$; × = $R_s$.

ture on the separations of cyclopentenones using derivatized cellulose CSPs, the separation of compounds 1, 2 and 5 were investigated at column temperatures between 0°C and 60°C.

The results of the temperature experiments for compounds 1, 2 and 5 are shown in Figs. 6, 7 and 8, respectively. The effect of temperature on plate number for the three compounds is shown in Fig. 9. For all three compounds, retention decreases with increasing temperature. Good linear correlation is obtained between ln $k'$ and $1/T$. Enantioselectivity ($\alpha$) is relatively unchanged for all compounds at all temperatures explored. The effect of temperature on enantiomeric resolution is more drastic. For all three compounds, subambient temperatures decrease enantiomeric resolution. Different effects are seen with elevated temperatures for the three compounds studied. For the TES-protected compounds (compounds 1 and 2, Figs. 6 and 7) maximum enantiomeric resolution is obtained at slightly elevated temperatures (30–35°C). Above 35°C resolution decreases for both compounds. For compound 5, no maximum in resolution was seen with increasing temperature. Resolution increased up to 60°C, the maximum temperature explored. Review of the plate numbers obtained at the various temperatures (Fig. 9) shows plate number increasing with temperature for all three compounds studied. The drastic results of this elevation in temperature is shown in Fig. 10. Much sharper peaks are obtained at 60°C, relative to 25°C and 45°C. The effect is not only a faster analysis, but also a lower detection limit

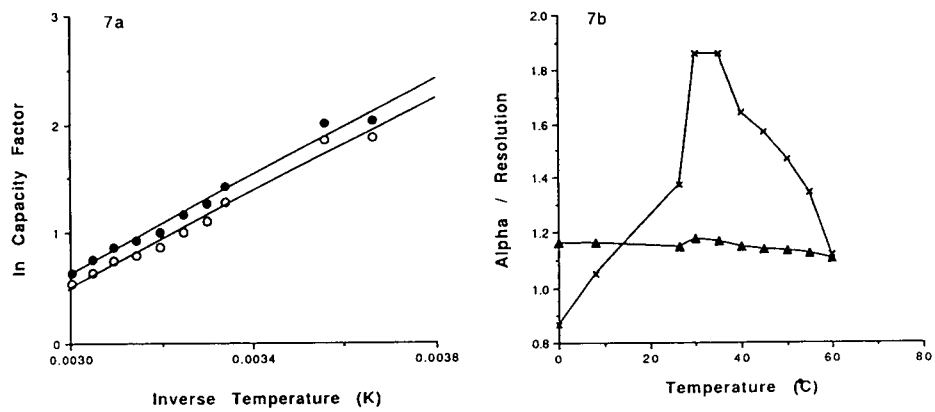


Fig. 7. Effect of temperature on analytical HPLC separation of compound 2. See Fig. 4 for chromatographic conditions. ● = $k'$ for first eluting enantiomer; ○ = $k'$ for second eluting enantiomer; ▲ = $\alpha$; × = $R_s$.

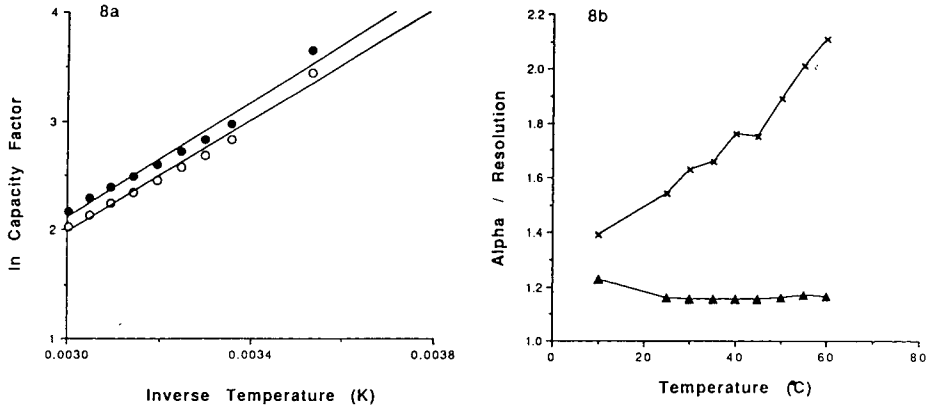


Fig. 8. Effect of temperature on analytical HPLC separation of compound 5. See Fig. 5 for chromatographic conditions. ● = $k'$ for first eluting enantiomer; ○ = $k'$ for second eluting enantiomer; ▲ = $\alpha$; × = $R_s$.

for either enantiomer. It must be noted that the manufacturer of Chiralcel columns recommends a maximum temperature of 40°C.

Why is it that temperature has this effect with cellulose based CSPs? The answer lies in the microscopic structure of the stationary phase. The cellulose derivatives are adsorbed onto silica gel, resulting in a coating which is approximately 100 Å thick. This results in poor mass transfer between the solute and the stationary phase. Elevated temperatures improve mass transfer and result in increased resolution. Subambient temperatures have the opposite effect, reducing mass transfer and decreasing resolution. While this explains the trends seen with temperature, it does not explain the difference increasing temperature has on the three compounds studied. Fig. 9 shows that theoretical plates increase with temperature for all three compounds, so it does not appear this is responsible for the differences observed between the compounds. There are two possible reasons why maximum resolution with increasing temperature was seen for compounds 1 and 2, but not for compound 5. The first possibility is the different viscosities of the mobile phases used for the separations. The HPLC conditions for compounds 1 and 2 has a mobile phase of 2% isopropanol in hexane, while compound 5 has a mobile phase of 10% isopropanol in hexane. The mobile phase for

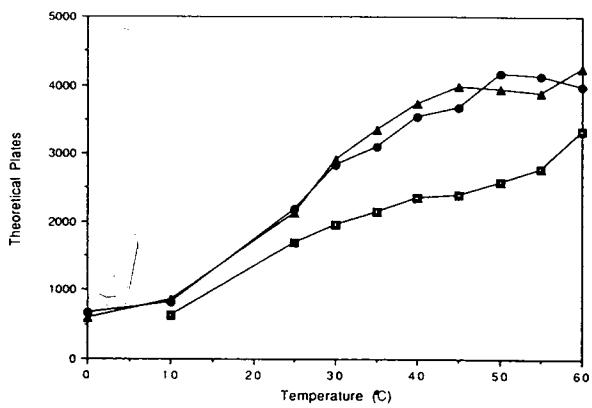


Fig. 9. Effect of temperature on theoretical plates for the analytical separation of compounds 1, 2 and 5. See Figs. 4 and 5 for chromatographic conditions. ● = compound 1; ▲ = compound 2; ■ = compound 5.

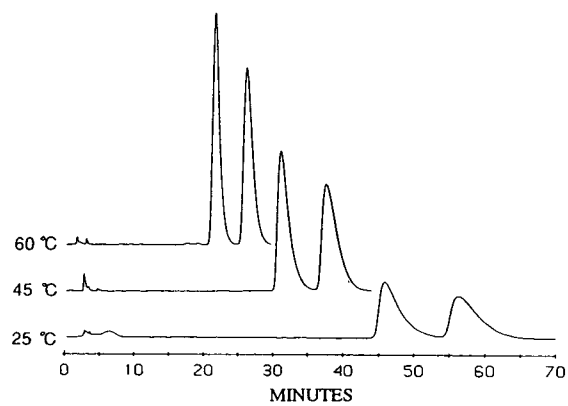


Fig. 10. Analytical HPLC separation of compound 5 at 25, 45 and 60°C. Analysis conducted on Chiralcel OC, isopropanol–hexane (90:10); flow-rate, 1 ml/min; detection at 215 nm, 0.2 AUFS.

compound 5 is more viscous than that for compounds 1 and 2. Since elevated temperature improves chromatographic efficiency by decreasing the viscosity of the mobile phase [27], it follows that a larger temperature effect would be expected for a mobile phase with increased viscosity (compound 5) relative to a lower viscosity mobile phase (compounds 1 and 2). Another possibility is the increased retention seen for compound 5 relative to compounds 1 and 2. The retention of compound 5 at room temperature is approximately 60% longer than those of compounds 1 and 2. At elevated temperatures (above 40°C), the retention for compounds 1 and 2 is small enough ($k' < 3$) that the $[k'/(k'+1)]$ component of the resolution equation causes a drop in resolution. Since the retention of compound 5 is larger, $k'$ never becomes the limiting factor in the resolution and therefore a maximum is never reached. Additional experiments are presently being conducted in our laboratories to determine if either of these two theories are correct.

*Preparative chromatography*

The preparative resolution of compound 2 has been previously investigated in our laboratories [7]. This work showed that while an isopropanol–hexane mobile phase gave better analytical separation, a mobile phase of ethanol–hexane gave superior results at preparative loadings. The preparative resolution of compounds 1 and 3 were investigated using the method developed for compound 2. [Chiralcel OC (500 mm × 22 mm I.D.), flow-rate, 20 ml/min; mobile phase, ethanol–hexane (1:99); loading 4 mg sample per gram of packing]. Due to the limited separation seen on the preparative UV chromatogram, HPLC analysis of the individual fractions was necessary to determine enantiomeric content. The results from these analyses for compound 2 are shown in Fig. 11. The isolated yields for the preparative resolution of compounds 1, 2 and 3 are summarized in Table III. A good correlation between analytical separation (see Table I) and preparative resolution was obtained. With compound 1 ($\alpha = 1.16$), 37% of the available first eluting enantiomer was isolated. With compound 2 ($\alpha = 1.18$), 54% was isolated, and with compound 3 ($\alpha = 1.21$), 71% of the first eluting enantiomer was isolated. This demonstrates the benefit of developing the best separation prior to scale-up to preparative loadings. An increase in $\alpha$ of only 0.05 resulted in a near doubling of isolated yield for the first eluting enantiomer. In addition, the increased separation allowed the isolation of the second eluting enantiomer of compounds 2 and 3, which was not possible for compound 1.

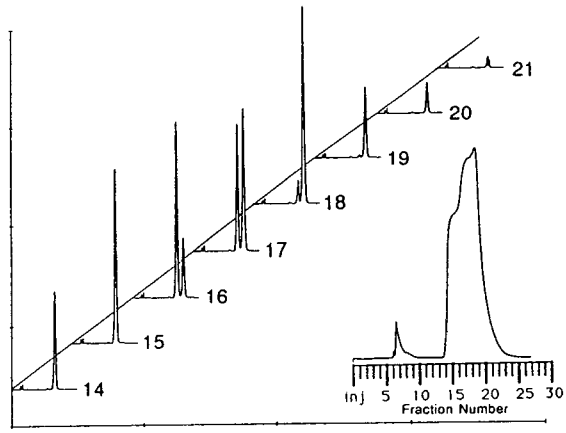


Fig. 11. Analytical HPLC analysis of wet fractions generated during preparative purification of compound 2. See text for preparative conditions. See Fig. 4 for analytical HPLC conditions.

TABLE III

RESULTS OF PREPARATIVE RESOLUTION OF COMPOUNDS 1 TO 3

Chiralcel OC (500 mm × 22 mm I.D.) containing approximately 125 g of packing; flow-rate 20 ml/min; mobile phase, ethanol–hexane (1:99); loading, 4 mg sample per gram of packing.

| Compound | First eluting enantiomer | |
|---|---|---|
| | %[a] | Mass (mg) |
| 1 | 37 | 92 |
| 2 | 54 | 137 |
| 3 | 71 | 177 |

[a] Enantiomeric purity >99.5%.

*Sample self displacement effect*

The observation of the sample self-displacement effect during the preparative resolution of compound 2 has been previously reported by our laboratories [28]. Since that time, additional investigations into the sample self-displacement effect in chiral separations have been conducted. The results shown in Fig. 12 verified that a sample self-displacement effect was occurring. Individual preparative injections of the *R* and *S* enantiomers of compound 2 show overlapping elution profiles. Based on these profiles, one would except little *R* enantiomer to be isolated from a mixture of the enantiomers. When this mixture is injected onto the column, drastically different elution profiles are obtained. The elution band of the first eluting enantiomer is moved forward and compressed by the large amount of the second eluting enantiomer. The end result is a better recovery of *R* enantiomer than predicted based on the individual elution profiles. The isolated yield of the *R* enantiomer was 54%. This improved yield is consistent with that expected if sample self-displacement is occurring.

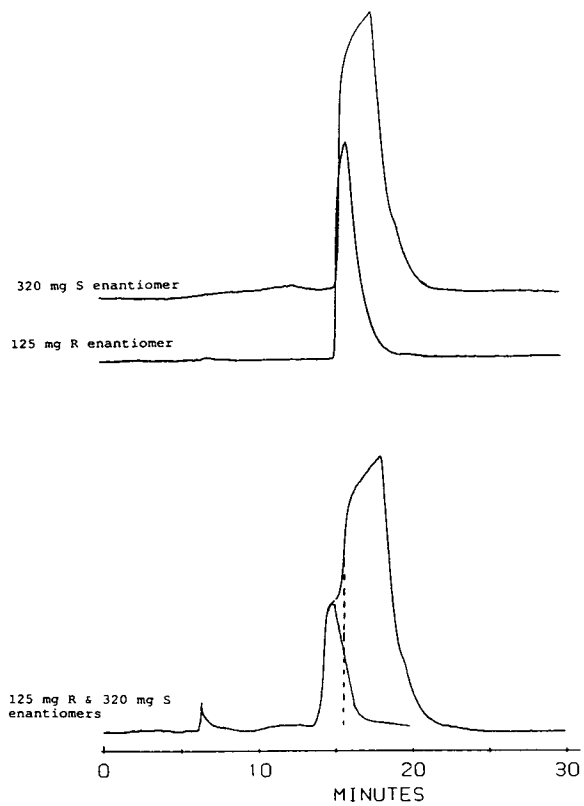


Fig. 12. Elution profiles for individual injections of *R* and *S* enantiomer of compound 2 and elution profile for mixture of *R* and *S* enantiomers.

The effect of differing enantiomeric ratio on the resolution of compound 2 was also investigated. A racemic mixture along with mixtures enriched in both the first eluting and the second eluting enantiomer were explored. The loading (500 mg on a 500 mm × 20 mm I.D. column) was kept constant for all three mixtures. The isolated recoveries of the *R* and *S* enantiomers are summarized in Table IV. The preparative UV traces along with the elution patterns of the enantiomers are shown in Fig. 13. For a racemic mixture, we see a sharpening of the elution band for the first eluting enantiomer. This is caused by the elution of the second enantiomer. The isolated yield of the first eluting *R* enantiomer is 54%. The isolated yield of the second eluting *S* enantiomer is only 17% due to tailing of the first enantiomer into a large portion of the elution band of the second enantiomer. When a mixture that is enriched in the first eluting *R* enantiomer (85/15) is purified, we see a larger, broader elution profile for the *R* enantiomer. This is due to the lack of a large amount of second eluting enantiomer to compress the elution band of the first eluting enantiomer. This results in increased overlap with the *S* enantiomer and an isolated

TABLE IV

RECOVERY AS A FUNCTION OF ENANTIOMER RATIO FOR COMPOUND 2

See text for chromatographic conditions.

| Enantiomer ratio (*R*/*S*)[a] | Percent *R* isolated | Percent *S* isolated |
|---|---|---|
| 50/50 | 54 | 17 |
| 85/15 | 50 | none |
| 22/78 | 31 | 14 |

[a] Elution order for compound 2 is *R*, *S*.

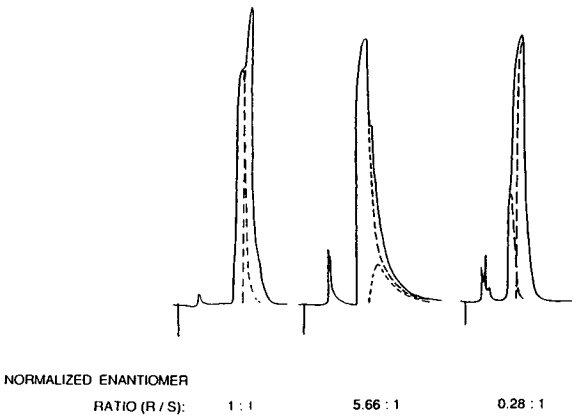


Fig. 13. Elution profiles for mixtures of varying enantiomer ratios for compound 2. See text for discussion.

yield of the *R* enantiomer of only 50%. No pure *S* enantiomer was produced with this sample. Drastic differences are seen when an excess of *S* enantiomer is present in the mixture (22/78). The large amount of the second eluting *S* enantiomer compresses the elution band of the first eluting *R* enantiomer. The isolated yield of the *R* enantiomer is 31%. The isolated yield of the second eluting *S* enantiomer is still poor due to tailing of the *R* enantiomer.

## CONCLUSIONS

Analytical and preparative HPLC can be used for the direct resolution of cyclopentenone precursors to prostaglandins. The chemical environment far removed from the chiral center can have some effect on the enantiomeric separation obtained. The use of elevated temperature can be used to increase the enantiomeric separation obtained with cellulose based chiral stationary phases due to increased mass transfer between the solute and the stationary phase. The resolution obtained at preparative loadings is directly related to the analytical separation and small increases in $\alpha$ can cause large increases in isolated yields. Sample self-displacement occurs during the preparative resolution of cyclopentenones. An excess of the second elution enantiomer is required for sample self-displacement to occur.

## ACKNOWLEDGEMENTS

The authors thank Helga Bush, John Ng and Kevin Babiak for their technical support. The compounds were provided by chemists in the Synthesis Development group at Searle.

## REFERENCES

1 A.J.H. Klunder, W.B. Huizinga, P.J.M. Sessink and B. Zwanenburg, *Tetrahedron. Lett.*, 28 (1987) 357.
2 Y. Okamoto, R. Aburatani, M. Kawashima, K. Hatada and N. Okamura, *Chem. Lett.*, (1986) 1767.
3 R. Noyori and M. Suzuki, *Angew. Chem. Int. Ed. Engl.*, 23 (1984) 847.
4 G. Stork and M. Isobe, *J. Am. Chem. Soc.*, 97 (1975) 6260.
5 M. Asami, *Tetrahedaron Lett.*, 26 (1985) 5803.
6 K. Babiak, J. Ng, J. Dygos and C. Weyker, *J. Org. Chem.*, 55 (1990) 3377.
7 L. Miller and H. Bush, *J. Chromatogr.*, 484 (1989) 337–345.
8 L. Miller and C. Weyker, *J. Chromatogr.*, 511 (1990) 97–107.
9 D. Roston and R. Wijayaratne, *Anal. Chem.*, 60 (1988) 948–950.
10 A.M. Rizzi, *J. Chromatogr.*, 478 (1989) 101–119.
11 R. Isaksson, P. Erlandsson, L. Hansson, A. Holmberg and S. Berner, *J. Chromatogr.*, 498 (1990) 257–280.
12 A.M. Rizzi, *J. Chromatogr.*, 478 (1989) 87–99.
13 K.G. Feitsma, J. Bosman, B.F.H. Drenth and R.A. de Zeeuw, *J. Chromatogr.*, 333 (1985) 59–68.
14 W.L. Hinze, T.E. Riehl, D.W. Armstrong, W. Demond, A. Alak and T. Ward, *Anal. Chem.*, 57 (1985) 237–242.
15 M. Gasdag, G. Szepesi and K. Mihalyfi, *J. Chromatogr.*, 450 (1988) 145–155.
16 I.M. Merino, E.B. Gonzalez and A. Sanz-Medel, *Anal. Chim. Acta*, 234 (1990) 127.
17 H.Y. Aboul-Enein, M.R. Islam and S.A. Bakr, *J. Liq. Chromatogr.*, 11 (1988) 1485.
18 W.H. Pirkle and A. Tsipouras, *J. Chromatogr.*, 291 (1984) 291–298.
19 L.E. Weaner and D.C. Hoerr, *J. Chromatogr.*, 437 (1988) 109–119.
20 M. Rudolph, *J. Chromatogr.*, 525 (1990) 161–168.
21 H.Y. Aboul-Enein and M. Rafiqul Islam, *Anal. Lett.*, 23 (1990) 83–91.
22 H.Y. Aboul-Enein and M. Rafiqul Islam, *J. Chromatogr. Sci.*, 28 (1990) 307–310.
23 H.Y. Aboul-Enein and M. Rafiqul Islam, *J. Chromatogr.*, 511 (1990) 109–114.
24 J. Newburger, L. Liebes, H. Colin and G. Guiochon, *Sep. Sci. Technol.*, 22 (1987) 1933–1952.
25 J. Newburger and G. Guiochon, *J. Chromatogr.*, 484 (1989) 153–166.
26 J. Newburger and G. Guiochon, *J. Chromatogr.*, 523 (1990) 63–80.
27 Y. Hirata and E. Sumiya, *J. Chromatogr.*, 267 (1983) 125–131.
28 L. Miller and H. Bush, *Prep-89*, May, 1989, Washington D.C.

*Journal of Chromatography A*, 653 (1993) 229–234
Elsevier Science Publishers B.V., Amsterdam

CHROM. 25 393

# Two-dimensional high-performance liquid chromatographic system for the determination of enantiomeric excess in complex amino acid mixtures

## Single amino acid analysis

Arnaldo Dossena, Gianni Galaverna, Roberto Corradini and Rosangela Marchelli*

*Dipartimento di Chimica Organica e Industriale dell' Università, Viale delle Scienze, I-43100 Parma (Italy)*

(First received May 6th, 1993; revised manuscript received June 29th, 1993)

ABSTRACT

An HPLC system that allows the determination of the enantiomeric composition of complex mixtures of amino acids such as those occurring in biological fluids (*e.g.*, serum, cerebrospinal fluid) and foods is described. D- and L-amino acids (including proline) can be determined. First, amino acid separation is achieved by means of an ion-exchange column by elution with a lithium chloride–lithium citrate buffer. Each peak corresponding to an individual amino acid can be switched to a reversed-phase column ($C_{18}$) and eluted with an aqueous solution containing chiral copper(II) complexes which perform chiral discrimination by a ligand-exchange mechanism. The method is very flexible as several chiral selectors and different types of detection (*e.g.*, UV, fluorescence) can be used. Moreover, it avoids unnecessary overrunning of the chiral system with the whole mixture, by switching only the peaks under investigation. It is possible to evaluate D-amino acids up to a 0.1% D to D + L ratio in the nanomolar range. Postcolumn derivatization with 7-chloro-4-nitrobenzo-2-oxa-1,3-diazole and fluorimetric detection were utilized for proline and hydroxyproline and with *o*-phthaldehyde for the other amino acids.

## INTRODUCTION

The presence of D-amino acids in nature has become an increasingly fascinating subject. The biological role of such unusual "oddities", not only in prokariotes and in eukariotes [1], but also in higher organisms such as insects, sharks, guinea pigs and marine invertebrates [2,3], is not known.

Recently, chiral separations of modified and unmodified amino acids have been achieved by HPLC, utilizing either chiral derivatizing agents [4–7] or chiral complexes added to the mobile phase [8,9]. Unfortunately, the methods are not readily applicable to complex mixtures, such as those present in natural systems, biological fluids, foods and beverages, because both chemoselectivity and stereoselectivity have to be taken into consideration. Moreover, although the biological matrices are in most instances extracted with ethereal solvents and eluted through ion-exchange resins before the analysis, nevertheless, amino alcohols, biogenic amines, dipeptides and oligopeptides are often present together with the desired amino acids, giving rise to unknown peaks that interfere in the chromatograms.

Despite the possibility of cross-checking the results by using different methods (GC, pre- and post-column derivatization in HPLC) [10,11], it is difficult to obtain very reliable and reproducible determinations of the enantiomeric ratio of

* Corresponding author.

0021-9673/93/$06.00 

amino acids in very complex and diluted mixtures, such as serum or cerebrospinal fluid (CSF). This may lead to undesirable controversies such as that concerning the racemization of proline in connection with microwave heating [12–15].

In the past, we developed a good method for the separation of D,L-dansylamino (Dns-amino) acids in HPLC by using either copper(II) complexes of L-amino acid amides [16] or of diaminodiamido-type ligands [17]. With the former complexes we were able to separate a mixture of fifteen D,L-Dns-amino acids by utilizing a gradient system in 1.5 h.

However, when trying to determine the D/L ratio with the same system, we realized that D- and L-enantiomers of all Dns-amino acids give different fluorescent responses. The phenomenon was thoroughly investigated by fluorescence experiments in aqueous solution [18], which led to the discovery of the enantioselective fluorescence quenching of D- and L-Dns-amino acids by L-amino acid amidate copper(II) complexes. This, on the one hand, allowed several clues to be obtained on the mechanism of chiral discrimination by a ligand-exchange mechanism, and on the other it caused concern regarding the use of the method for the determination of the D/L ratio. Subsequently, we advised caution when using copper(II) complexes in the eluent for the determination of Dns-amino acids.

A system proposed by Tapuhi *et al.* [19] involved the separation of Dns-amino acids on an achiral $C_{18}$ column, switching of a single peak to another $C_8$ column eluted with an Ni(II) complex of L-prolyl-*n*-octylamide. Ni(II) is also known to be a fluorescence quencher of Dns-amino acids and peptides [20]. Hence also in this case enantioselective fluorescence quenching could be possible, impairing the determination of the D/L ratio.

For all these reasons, we decided to develop a method for the separation of unmodified amino acids in complex mixtures, avoiding prederivatization procedures and work-up of the biological samples.

We report here a method that allows the problem to be addressed in a sound and reliable way, a two-dimensional HPLC procedure that utilizes two different separation methods: first the achiral separation of unmodified amino acids on a cation-exchange column, switching of the amino acid under investigation to a reversed-phase column and chiral discrimination by elution with a chiral copper(II) complex. Several copper(II) complexes can be used according to the amino acid to be separated.

The advantage over the reported methods, which operated "in series", is that in this way we measure only the single amino acid under investigation, avoiding overusage and spoilage of expensive chiral columns, thus obtaining a "clean" separation and saving time. By using the present method, we were able to demonstrate that, under normal microwave heating conditions, racemization does not occur in either proteins or the free amino acid pool [21].

## EXPERIMENTAL

### *Reagents*

*o*-Phthalaldehyde (OPA) and 7-chloro-4-nitrobenzo-2-oxa-1,3-diazole (NBD-Cl) were obtained from Fluka (Buchs, Switzerland) and Pierce (Rockford, IL, USA). D,L and D- and L-amino acids were obtained from Sigma (St. Louis, MO, USA) and Pierce. Acetonitrile (LC grade), methanol (LC grade), copper(II) acetate and sodium acetate were obtained from Carlo Erba (Milan, Italy). Lithium hydroxide, lithium chloride, citric acid, phenol, boric acid, 2-mercaptoethanol, sodium hypochlorite and hydrochloric acid were obtained from Fluka. Water (HPLC grade) was produced in our laboratory utilizing an Alpha-Q system (Millipore).

The chiral selectors used ($N^2$,$N^2$-dimethyl-L-phenylalaninamide ($Me_2$Phe-A) [22], $N^2$-methyl-L-phenylalaninamide (MePhe-A) [23] and bis (L,L-N,N′-dimethylphenylalanyl)ethane ($Me_2$-Phe-NN-2) [21,24]) were synthesized in our laboratory. Their copper(II) complexes were characterized [22–25] and their ability to perform chiral discrimination in reversed-phase HPLC [23] was examined.

### *Equipment*

The chromatographic system utilized is shown in Fig. 1. It is composed of two parts: a common

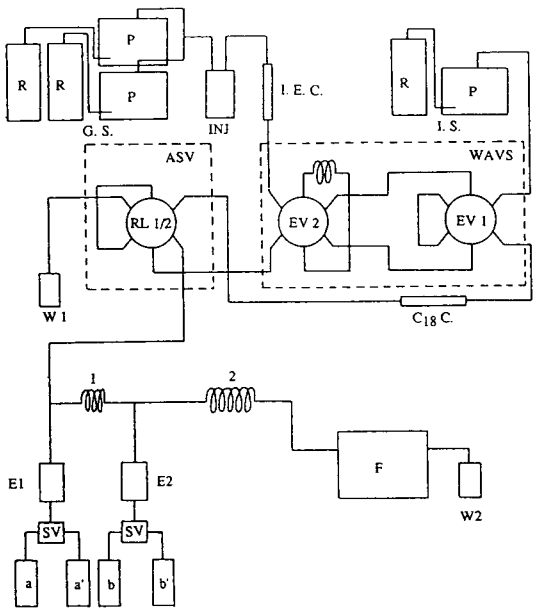


Fig. 1. Scheme of the chromatographic system for single amino acid analysis. G.S. = gradient system; I.S. = isocratic system; I.E.C. = ion-exchange column; $C_{18}C.$ = $C_{18}$ reversed-phase column, EV 1 and EV 2 = events 1 and 2; F = fluorescence detector; 1 and 2 = reaction coils 1 and 2, E 1 and E 2 = Eldex pumps 1 and 2; ASV = automated switching valve; WAVS = Waters automated valve system; R = reservoir; P = pump; SV = switching valve; a and b = derivatizing reagents for ion-exchange analysis; a′ and b′ = derivatizing reagents for enantiomeric separation.

ion-exchange apparatus for the separation of amino acids and a reversed-phase column for the chiral separation. The two chromatographic systems are interconnected through a Waters WAVS valve and a Waters automated switching valve. The system is controlled by a Maxima 820 chromatography workstation. The gradient system (G.S.) for the ion-exchange separation of amino acids consists of two Waters Model 510 pumps. The samples are injected utilizing a WISP 712 automatic sample processor (Waters). The mobile phase for the isocratic system, responsible for the enantiomeric separations, is delivered using another Waters Model 510 pump. The eluate is mixed, in two different T-pieces, with the derivatizing agents necessary for the analysis.

The postcolumn derivatization differs according to the analyte: a single treatment, using OPA, for all amino acids and a two-stage treatment for proline and hydroxyproline. The derivatizing agents are delivered using one or two (in series) single plunger pumps (Eldex, E1 and E2). For proline, two manual switching valves are utilized to change the derivatizing eluents necessary to effect detection during the ion-exchange separation (reagent a, borate buffer containing sodium hypochlorite; reagent b, borate buffer containing OPA) and during the reversed-phase enantiodiscrimination (reagent a′, borate buffer containing EDTA; reagent b′, NBD-Cl in ethanol). Both the reaction coil 1 (stainless steel, $1000 \times 0.5$ mm I.D.) and the reaction coil 2 (stainless steel, $4000 \times 0.5$ mm I.D.) are kept at 55°C. The fluorescence intensity of the effluent is measured using a Waters Model 470 spectrofluorimeter (for OPA derivatives, $\lambda_{exc.} = 330$ nm, $\lambda_{em.} = 440$ nm; for NBD-Cl derivatives, $\lambda_{exc.} = 465$ nm, $\lambda_{em.} = 525$ nm).

*Columns*

Amino acids are separated on an Interaction amino acid analysis column ($12 \times 0.46$ cm I.D.), a sulphonated polystyrene–divinylbenzene copolymer in the lithium form, spherical particles with a diameter of $6 \pm 0.5$ $\mu$m. The reversed-phase column used for the enantiomeric separation is a Spherisorb ODS-2, 3 $\mu$m ($15 \times 0.46$ cm I.D.). The ion-exchange column is maintained at 45°C and the reversed-phase column at 25 or 35°C depending on the amino acid to be measured.

*Eluents for ion exchange (flow-rate 0.4 ml/min)*

Eluent A is $LiOH \cdot H_2O$ (2.1 g), LiCl (6.0 g), citric acid (9.6 g) and phenol (1.0 g), diluted to 1 l and adjusted to pH 2.87 with HCl.

Eluent B is $LiOH \cdot H_2O$ (2.1 g), LiCl (65.7 g), phenol (1.0 g) and boric acid (1.0 g), diluted to 1 l and adjusted to pH 9.20 with LiOH.

*Eluents for enantiomeric separation (flow-rate 0.3–2.0 ml/min)*

Eluent C is $Me_2$Phe-A or MePhe-A. The ligand (2 m*M*) and copper(II) acetate (1 m*M*) are added to 1 l of water containing 0.3 *M* sodium acetate and adjusted to pH 6.35 with acetic acid.

Eluent D is $Me_2$Phe-NN-2 (0.45 m*M*) and copper(II) acetate (0.45 m*M*) added to 1 l of water containing sodium acetate (4.2 g), LiCl (1.8 g) and $LiOH \cdot H_2O$ (0.63 g) and adjusted to pH 6.5 with acetic acid. For apolar amino acids 5% $CH_3CN$ is added.

*Post-column derivatization with OPA (for ion exchange and for enantiomeric separation): one Eldex pump*

EDTA (2.0 g) is dissolved in 1 l of 0.3 *M* borate buffer (pH 10, adjusted with KOH) and mixed with OPA (0.8 g) dissolved in 2-mercaptoethanol (4 ml) (flow-rate 0.6 ml/min).

*Derivatization of D,L-proline*

The derivatization of D,L-proline is achieved by the following procedure. For ion-exchange analysis (two Eldex pumps), (1) the first reagent (a) is 0.1% sodium hypochlorite (chlorine concentration 10%) dissolved in 1 l of 0.4 *M* borate buffer (pH 10, adjusted with KOH) (flow-rate 0.6 ml/min) and (2) the second reagent (b) is OPA (0.8 g) dissolved in 2-mercaptoethanol (4 ml), added to 1 l of 0.3 *M* borate buffer (pH 10, adjusted with KOH) (flow-rate 0.6 ml/min).

For enantiomeric separation (two Eldex pumps), (1) the first reagent (a′) is EDTA (2 g) dissolved in 1 l of a mixture (1:1) of ethanol and 0.05 *M* borate buffer (pH 9.5, adjusted with KOH) (flow-rate 0.6 ml/min) and (2) the second reagent (b′) is NBD-Cl (1 g) dissolved in ethanol (500 ml) (flow-rate 0.6 ml/min).

## RESULTS AND DISCUSSION

In order to achieve the enantiomeric analysis of each individual amino acid in complex biological mixtures, we modified our HPLC system according to the scheme shown in Fig. 1. The aim was to avoid cross-interference with dipeptides, oligopeptides, amino alcohols and biogenic amines.

The system is based on a preliminary ion-exchange achiral separation of the mixture with a gradient system and a subsequent chiral separation on an achiral reversed-phase column and elution with chiral copper(II) complexes added to the eluent. The selectors utilized are mainly chosen among the series described elsewhere [23], in particular the copper(II) complexes of MePhe-A, $Me_2$Phe-A and $Me_2$Phe-NN-2. When the peak corresponding to the amino acid to be investigated, during the ion exchange run, arrives at the loop present in EV2, the configuration of Event 2 (EV2) is changed in order to block the unmodified amino acid in the loop. Immediately afterwards, the CSV valve is turned to the eluent containing the chiral selector with the derivatizing agent, thus discharging the ion-exchange buffered eluents into waste 1 and simultaneously allowing the reaction coils to be washed with the new mixture. When the system is equilibrated, by switching Event 1 (EV1), the amino acid blocked in the loop (EV2) is injected into the reversed-phase column responsible for the enantiomeric separations (Fig. 2). The same derivatizing agent is used for the two different analyses (borate buffer, containing OPA and EDTA).

In order to detect the enantiomers of imino acids such as proline or hydroxyproline, a different derivatization agent is used. As described under Experimental, two different single-plunger pumps are necessary: the first is used to detect proline in the ion-exchange analysis and the second to derivatize, after the enantiomeric separation, the same amino acid with a fluorescent reagent able to react with secondary amines.

On the basis of the considerations reported elsewhere [23], it is reasonable to assume that enantiomeric recognition occurs on the column where the initial complexes are adsorbed. Therefore, it is necessary to allow the eluent containing the copper complex to flow through the column for several minutes (120 min at 1 ml/min, 30 column volumes).

The elution order of the enantiomers is L < D for polar and D < L for apolar amino acids when using copper(II) complexes of $Me_2$Phe-NN-2, MePhe-A and $Me_2$Phe-A as chiral selectors. Further control can be effectively performed if one wishes, as is advisable, to have the less abundant enantiomer eluted before the more abundant enantiomer, by using the selector with opposite configuration (*e.g.*, D-MePhe-A). In this event D-Asp and D-Glu are eluted first. How-

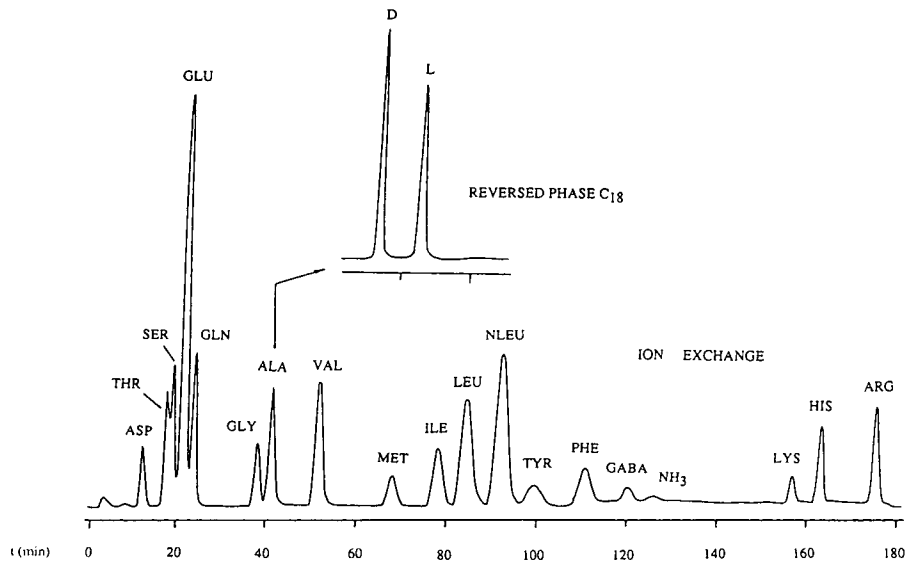


Fig. 2. Example of a single amino acid analysis. Lower trace: Separation of amino acids by ion exchange. Column, Interaction, lithium form (6 $\mu$m) (12 × 0.46 cm I.D.); temperature, 45°C; eluents A and B, see Experimental; flow-rate, 0.4 ml/min. Inset: Enantiomeric separation on a Spherisorb ODS-2 column (3 $\mu$m) (15 × 0.46 cm I.D.); temperature, 25°C; eluent, MePhe-A (2 m*M*)–copper acetate (1 m*M*)–sodium acetate (0.3 *M*) (pH 6.35); flow-rate, 0.5 ml/min.

ever, in most instances examined so far this was not necessary, because the separation factors ($\alpha$) are sufficiently high to cause no concern about the latter enantiomer being "carried along" by the former. $Me_2$Phe-A is preferentially used to perform chiral discrimination of proline (Fig. 3) and $Me_2$Phe-NN-2 for polar and apolar amino acids (Fig. 4).

After the enantiomeric analysis, the chiral eluent can be recovered in the following way. Copper is precipitated as sulphide with gaseous hydrogen sulphide in acidic solution and then,

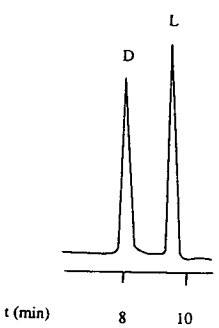


Fig. 3. Enantiomeric separation of D,L-Pro. Eluent, $Me_2$-Phe-A (2 m*M*)–copper acetate (1 m*M*)–sodium acetate (0.3 *M*) (pH 6.35); column, Spherisorb ODS-2 (3 $\mu$m) (15 × 0.46 cm I.D.); room temperature; flow-rate, 0.5 ml/min; fluorescence detection (postcolumn derivatization with NBD-Cl).

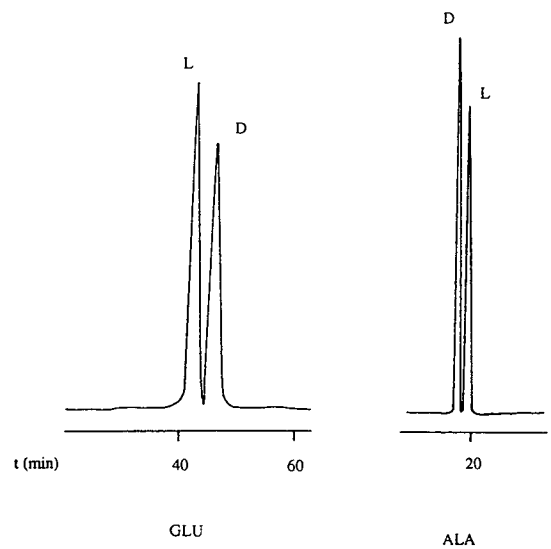


Fig. 4. Enantiomeric discrimination of polar and apolar amino acids. Eluent, $Me_2$-Phe-NN-2 (0.5 m*M*)–copper acetate (0.5 m*M*)–sodium acetate (0.05 *M*) (pH 6.5); column, Spherisorb ODS-2 (3 $\mu$m) (15 × 0.46 cm I.D.); room temperature; flow-rate, 0.5 ml/min; fluorescence detection (postcolumn derivatization with OPA).

after filtration, the aqueous solution is extracted with chloroform; sodium hydroxide is added to give basic conditions and the ligand is extracted with chloroform. The chloroform extracts are dried and the ligand is recrystallized twice from chloroform–diethyl ether. The recovered chiral ligand (90% of the total used) can be reutilized without loss of its discriminating ability.

## CONCLUSIONS

Using the chromatographic method described here, it is possible to obtain optimum enantiomeric discrimination of amino and imino acids in complex mixtures, avoiding the occurrence of the pitfalls that often arise with biological matrices. The described apparatus can be totally automated and computer assisted to perform automated on-line determinations of D- and L-amino acids.

## ACKNOWLEDGEMENTS

We are grateful to Waters-Millipore, Italy, for assistance provided during the assembly of the chromatographic system. This work was supported by the Consiglio Nazionale delle Ricerche (CNR), Rome, Progetto Finalizzato Chimica Fine e Secondaria II.

## REFERENCES

1 J.S. Davies, in B. Weinstein (Editor), *Chemistry and Biochemistry of Amino Acids, Peptides and Proteins*, Vol. 4, Marcel Dekker, New York, 1977, p. 1.
2 J.J. Corrigan, *Science*, 164 (1969) 142.
3 R.L. Preston, *Comp. Biochem. Physiol. B*, 87 (1987) 55.
4 W. Lindner, in M. Zief and L.J. Crane (Editors), *Chromatographic Separation*, Marcel Dekker, New York, Basle, 1988, p. 91.
5 S. Einarsson, B. Josefsson, P. Moeller and D. Sanchez, *Anal. Biochem.*, 59 (1987) 1191.
6 M. Marfey, *Carlsberg Res. Commun.*, 49 (1984) 591.
7 H. Brückner, R. Wittner and H. Godel, *Chromatographia*, 32 (1991) 383, and references cited therein.
8 V.A. Davankov, J.D. Navratil and H.F. Walton, *Ligand Exchange Chromatography*, CRC Press, Boca Raton, FL, 1988, p. 67.
9 V.A. Davankov, *Handbook of HPLC for the Separation of Amino Acids, Peptides and Proteins*, Vol. 1, CRC Press, Boca Raton, FL, 1986, p. 393.
10 G. Palla, R. Marchelli, A. Dossena and G. Casnati, *J. Chromatogr.*, 475 (1989) 45.
11 I. Gandolfi, G. Palla, L. Delprato, F. De Nisco, R. Marchelli and C. Salvadori, *J. Food Sci.*, 57 (1992) 377.
12 G. Lubec, C. Wolf and B. Bartosch, *Lancet*, 334 (1989) 1392.
13 D. Kampel, R. Kupfersmidt and G. Lubec, in G. Lubec and G.A. Rosenthal (Editors), *Amino Acids*, Escom, Leiden, 1990, p. 1164.
14 W. Segal, *Lancet*, 335 (1990) 470.
15 W. Segal, *Lancet*, 336 (1990) 49.
16 E. Armani, L. Barazzoni, A. Dossena and R. Marchelli, *J. Chromatogr.*, 441 (1988) 287.
17 E. Armani, A. Dossena, R. Marchelli and R. Virgili, *J. Chromatogr.*, 441 (1988) 275.
18 R. Corradini, G. Sartor, R. Marchelli, A. Dossena and A. Spisni, *J. Chem. Soc., Perkin Trans. 2*, 11 (1992) 1979.
19 Y. Tapuhi, N. Miller and B.L. Karger, *J. Chromatogr.*, 205 (1981) 325.
20 W.Y. Lin and H. Van Want, *J. Inorg. Biochem.*, 32 (1988) 21.
21 R. Marchelli, A. Dossena, G. Palla, M. Audhuy-Peaudecerf, S. Lefeuvre, P. Carnevali and M. Freddi, *J. Sci. Food Agric.*, 59 (1992) 217.
22 F. Dallavalle, E. Fisicaro, R. Corradini and R. Marchelli, *Helv. Chim. Acta*, 72 (1989) 1479.
23 G. Galaverna, R. Corradini, E. De Munari, A. Dossena and R. Marchelli, *J. Chromatogr.*, in press.
24 E. Armani, R. Marchelli, A. Dossena, G. Casnati and F. Dallavalle, *Helv. Chim. Acta*, 69 (1986) 1916.
25 R. Corradini, G. Gasparri Fava, M. Belicchi Ferrari, A. Dossena, R. Marchelli and G. Pelosi, *Tetrahedron: Asymmetry*, 3 (1992) 387.

*Journal of Chromatography A*, 653 (1993) 235–240
Elsevier Science Publishers B.V., Amsterdam

CHROM. 25 450

# High-performance liquid chromatography of N-terminal tryptophan-containing peptides with precolumn fluorescence derivatization with glyoxal

Masaaki Kai, Eijiro Kojima and Yosuke Ohkura*

*Faculty of Pharmaceutical Sciences, Kyushu University 62, Maidashi, Higashi-ku, Fukuoka 812 (Japan)*

Masatake Iwasaki

*Daiichi College of Pharmaceutical Sciences, Tamagawa-cho, Minami-ku, Fukuoka 815 (Japan)*

(First received April 26th, 1993; revised manuscript received June 29th, 1993)

ABSTRACT

A precolumn fluorescence derivatization method combined with high-performance liquid chromatography is described for the sensitive and selective determination of N-terminal tryptophan-containing peptides. The peptides and tryptophan were converted into fluorescent derivatives with glyoxal in a moderately acidic medium (pH 4.5). The derivatives were separated on a reversed-phase column with isocratic elution with an aqueous mobile phase composed of acetonitrile, methanol and phosphate buffer (pH 6.0), and subsequently detected by fluorimetry. The derivatization technique provided the respective N-terminal tryptophan-containing oligopeptides with single fluorescent peaks in chromatography. The detection limits for the peptides were 55–382 fmol per 100-$\mu$l injection volume at a signal-to-noise ratio of 3. The method also allowed the facile detection of an N-terminal tryptophyl fragment in the enzyme reaction mixture of dynorphin A with trypin.

## INTRODUCTION

High-performance liquid chromatography (HPLC) is advantageous for the separation of various peptides. Many detection techniques in HPLC have been proposed for the determination of peptides, including radioimmunoassay, mass spectrometric, ultraviolet (UV) absorption, electrochemical activity and fluorescence measurements.

Radioimmunoassay [1] as an off-line detection method in HPLC generally offers high sensitivity and selectivity for peptides, but it is difficult to obtain specific antibodies, especially for oligopeptides. Mass spectrometric detection [2] coupled with off-line HPLC needs expensive instrumentation and refined operation, although the method shows satisfactory structural specificity for peptides. UV detection [3] at wavelengths between 200 and 280 nm and electrochemical detection [4] are frequently influenced by either various UV-absorbing components or oxidizing components in biological samples and in the mobile phase, although these techniques are convenient for the detection of peptides without derivatization. Fluorescence detection utilizing fluorescamine [5] or *o*-phthalaldehyde [6] as fluorogenic reagents selective for primary amines shows insufficient selectivity for the target peptides.

On the other hand, fluorogenic reagents that can recognize an amino acid residue of peptides are available for the facile detection of particular

* Corresponding author.

0021-9673/93/$06.00 

peptides in complex samples such as enzymatic digests [7]. In this respect, we have developed fluorescence derivatization methods in HPLC for the selective determination of arginine-containing peptides with benzoin reagent [8,9] and of N-terminal tyrosine-containing peptides with hydroxylamine–cobalt(II)–borate reagent [10–13].

We previously reported [14] that phenylglyoxal reacted selectively with tryptophan (Trp) in a strongly acidic medium to give three fluorescent compounds, of which the major product was 1-(1-hydroxybenzyl)-$\beta$-carboline. In a further study [15] on a survey of more suitable fluorogenic reagents for Trp and/or Trp-containing peptides, using glyoxal, methylglyoxal and four synthesized analogues of phenylglyoxal substituted with electron-donating group(s) as the reagent, we found that glyoxal could offer intense fluorescence for N-terminal Trp-containing peptides in a weakly acidic solution under relatively mild reaction conditions.

We therefore considered that the glyoxal reaction may be useful for converting N-terminal Trp-containing peptides into the corresponding fluorescent derivatives that can be separated by HPLC; the expected structure on the basis of the reaction product of Trp with phenylglyoxal is shown here. In this work, we studied the con-

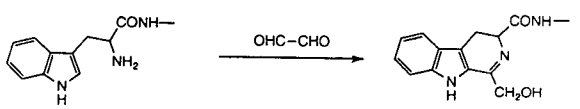


N-terminal Trp-containing peptide possible fluorophore

ditions of precolumn fluorescence derivatization and HPLC separation that give single fluorescent peaks in chromatography. The efficiencies of the HPLC method were also evaluated with respect to the determination of the synthetic peptides and the simple detection of peptide fragments produced by enzymatic digestion of a heptadecapeptide, dynorphin A, with trypsin.

## EXPERIMENTAL

### *Materials and solutions*

The N-Terminal Trp-containing peptides listed in Table I (six species), Ala–Trp, Lys–Trp–Lys and dynorphin A were obtained from Sigma (St. Louis, MO, USA). Stock solutions of these synthetic peptides (1.0 $\mu$mol/ml each) were prepared in methyl Cellosolve, then diluted to 100 nmol/ml with water and stored at −80°C. The stock solutions were diluted with water to appropriate concentrations before use and used within 1 day. Glyoxal as an aqueous solution (21.9 *M*) from Sigma was diluted with water to obtain a 0.2 *M* solution, which was usable as a reagent solution for at least 1 month when stored at 4°C. Other chemicals were of the highest purity available.

### *Derivatization procedure*

A portion (100 $\mu$l) of peptide solution was mixed with 100 $\mu$l each of 0.2 *M* succinate buffer (pH 4.5) and 0.2 *M* glyoxal solution. The mixture was heated at 100°C for 30 min. A portion (100 $\mu$l) of the final reactions mixture was used for HPLC.

### *Apparatus and HPLC conditions*

The HPLC system consisted of a Tosoh (Tokyo, Japan) HLC-803D high-performance liquid chromatograph, a Rheodyne Model 7125 syringe-loading sample injector (100-$\mu$l loop) and a Hitachi F-1000 spectrofluorimeter fitted with a 12-$\mu$l flowcell. A reversed-phase column of TSKgel ODS-80T$_M$ (150 × 4.6 mm I.D., particle size 5 $\mu$m) (Tosoh) was used. The column temperature was ambient (25 ± 4°C). For the separation of the fluorescent derivatives of peptides on the column, isocratic elution with an aqueous mobile phase of acetonitrile–methanol–20 m*M* phosphate buffer (pH 6.0) (23:17:60, v/v/v) was carried out at a constant flow-rate of 0.8 ml/min. The fluorescence intensity of the column eluate was monitored at 465 nm (emission) with excitation at 275 nm.

Uncorrected fluorescence excitation and emission spectra of the eluates from the fluorescent peaks were measured with a Hitachi F-2000 spectrofluorimeter in 10 × 10 cm quartz cells; spectral band widths of 10 nm were used in both the excitation and emission monochromators.

## RESULTS AND DISCUSSION

### *HPLC separation*

The three N-terminal Trp-containing peptides, Trp–Leu, Trp–Gly–Gly and Trp–Met–Asp–Phe–$NH_2$, and Trp were converted into the corresponding fluorescent derivatives under the recommended reaction conditions.

When the derivatization mixture of the peptides and Trp was subjected to reversed-phase HPLC on an ODS column (TSKgel ODS-80$T_M$), single fluorescent peaks were observed for the respective compounds. Their peaks were mutually separated within 22 min by isocratic elution with the above mobile phase (Fig. 1).

The elution of the peaks for the peptides was delayed when the pH of the phosphate buffer in the mobile phase was <5.5, although no effect of pH on the retention time of the Trp peak was detected (Fig. 2). The peptide derivatives in the reaction mixture fluoresced most intensely at pH 6.0, although the derivative of Trp fluoresced intensely at pH >9.0 (Fig. 3). Therefore, the maximum peak heights for the respective peptides were observed at pH 6.0 and phosphate

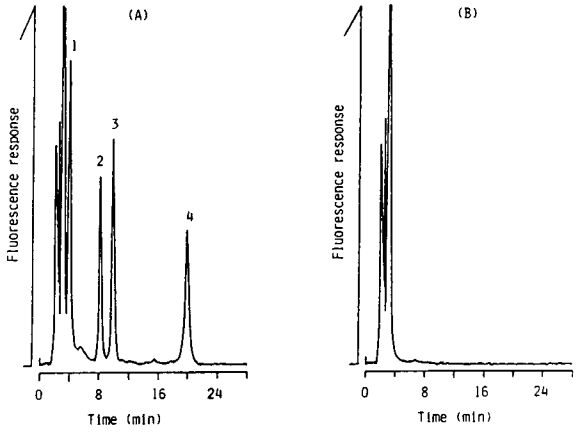


Fig. 1. Chromatograms of (A) the fluorescent derivatives of three N-terminal Trp-containing peptides and Trp and (B) the reagent blank. A portion (100 $\mu$l) of a mixture of the peptides and Trp (250 pmol/ml for Trp–Gly–Gly and 500 pmol/ml for the others) was treated under the recommended conditions for derivatization and HPLC. Peaks: 1 = Trp–Gly–Gly; 2 = Trp; 3 = Trp–Leu; 4 = Trp–Met–Asp–Phe–$NH_2$.

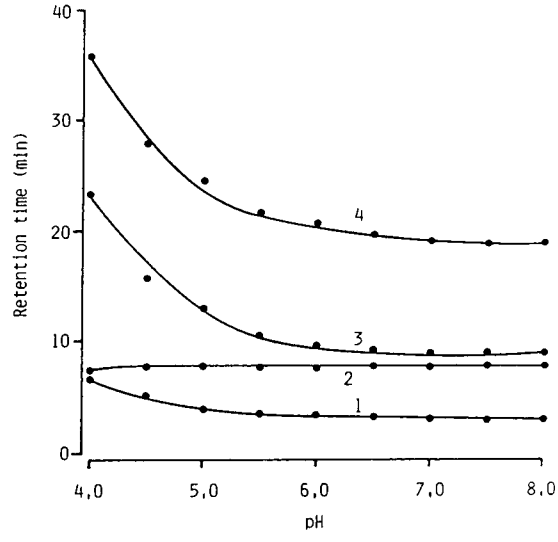


Fig. 2. Effect of pH of 20 m$M$ phosphate buffer in the mobile phase on the separation. Portions (100 $\mu$l) of the mixture of the peptides and Trp were treated as in Fig. 1 except that buffers of various pH were used in the mobile phase. Numbers on curves as for peaks in Fig. 1.

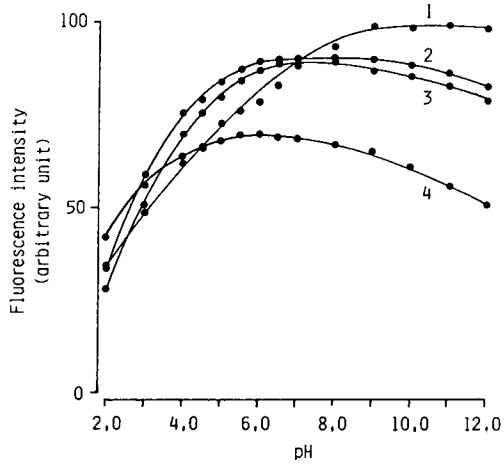


Fig. 3. Effect of pH of the reaction mixture on the fluorescence intensity after the derivatization. Portions (100 $\mu$l) of the final derivatization mixture (500 pmol of each compound per tube) were diluted with 1.0 ml of 40 m$M$ Britton–Robinson buffer (pH 2–12) and the fluorescence intensities of the resulting solutions were measured manually with emission at 465 nm and excitation at 275 nm. 1 = Trp; 2 = Trp–Gly–Gly; 3 = Trp–Leu; 4 = Trp–Met–Asp–Phe–$NH_2$.

buffer of pH 6.0 was selected for use in the mobile phase.

The fluorescence excitation and emission maxima of the peptide derivatives in the column eluates were all around 275 and 465 nm, respectively, although the Trp peak showed the respective maxima at 286 and 455 nm. At the former wavelengths the peak height of Trp was approximately 72% of that at the latter wavelengths.

*Derivatization and determination*

The fluorescence derivatization of the three N-terminal Trp-containing peptides with glyoxal occurred most effectively with succinate buffer of pH 4.5. Buffer concentrations, >0.15 *M* resulted in constant peak heights for the peptides and Trp with; 0.2 *M* succinate buffer of pH 4.5 was adopted in the procedure.

Higher temperatures in the range 40–100°C allowed the derivatization of the peptides and Trp to proceed more rapidly, and at 100°C nearly maximum peak heights were achieved on heating for 30 min (Fig. 4). With heating at 140°C for 5 min, the peak heights were also maximum and almost the same as those obtained at 100°C for 30 min. In these instances, no by-product peaks due to the degradation of the peptides were found in the chromatograms.

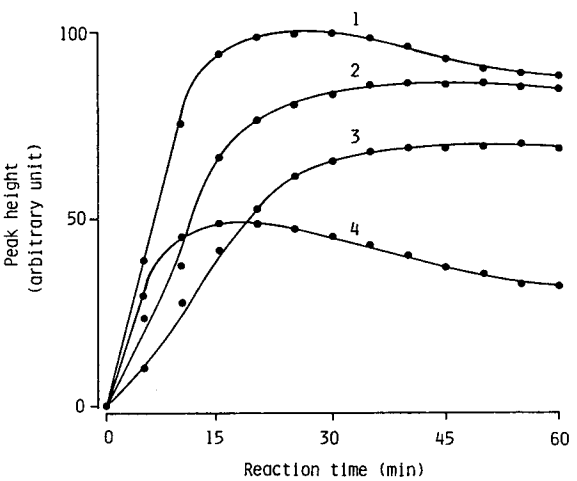


Fig. 4. Effect of reaction time at 100°C on the fluorescence derivatization. Portions (100 μl) of the mixture of the peptides and Trp were treated as in Fig. 1 except that the reaction mixtures were heated for various periods in the derivatization. Numbers on curves as on peaks in Fig. 1.

Maximum and constant peak heights from the peptides were attained at glyoxal concentrations >0.1*M*; 0.2*M* was adopted for the fluroescence derivatization.

The fluorescent derivatives of the peptides were fairly stable; the corresponding peak heights did not change when the derivatization mixture after the reaction was allowed to stand in an ice–water bath for 2 h and no peaks due to by-products were detected in the chromatograms.

Under the established conditions for the fluorescence derivatization, the peptides without an N-terminal Trp residue (Ala–Trp and Lys–Trp–Lys), Trp-related compounds (5-hydroxytryptophan, serotonin, melatonin, kynurenine and 3-hydroxykynurenine), amines (histamine, epinephrine, norepinephrine, spermidine, spermine), nineteen L-α-amino acids, amino sugars (galactosamine and N-acetylgalactosamine) and nucleic acid bases (adenine, guanine, thymine, cytosine and uracil) did not form any fluorescent derivatives.

Table I gives the detection limits and the retention times of various N-terminal Trp-containing oligopeptides, Trp, tryptamine and tryptophamide (Trp-$NH_2$) obtained by the proposed precolumn fluorescence derivatization HPLC method. These compounds gave single

TABLE I

RETENTION TIMES AND DETECTION LIMITS OF N-TERMINAL TRP-CONTAINING PEPTIDES AND TRP-RELATED COMPOUNDS

| Compound | Retention time (min) | Detection limit[a] (fmol) |
|---|---|---|
| Trp–Gly–Gly | 3.7 | 55 |
| Trp–Gly | 4.0 | 97 |
| Trp–Ala | 4.8 | 79 |
| Trp–$NH_2$ | 7.4 | 143 |
| Trp | 7.8 | 314 |
| Tryptamine | 7.8 | 311 |
| Trp–Trp | 8.0 | 4166 |
| Trp–Leu | 9.2 | 192 |
| Trp–Met–Asp–Phe–$NH_2$ | 18.2 | 382 |

[a] Defined as the amount per 100-μl injection volume giving a signal-to-noise ratio of 3.

peaks in the chromatograms. The detection limits for the compounds other than Trp–Trp were in the range 55–382 fmol in a 100-$\mu$l injection volume at a signal-to-noise ratio of 3. The peak height due to the fluorescent derivative of Trp–Trp was unexpectedly low, being *ca.* 1% of that for Trp–Gly–Gly at an equimolar concentration (500 pmol/ml). This weak fluorescence may be caused by a low derivatization yield for Trp–Trp and/or internal molecular quenching of fluorescence due to the absorption of excitation energy with its C-terminal Trp. The Trp residue in peptide molecules exhibits its native fluorescence, the excitation and emission maxima of which are around 290 and 350 nm, respectively.

The native fluorescence of the Trp-containing peptides was not detected with the present detector, because they have different emission wavelengths to those of the peptide derivatives, although the native fluorescence intensities of the peptides at equimolar concentrations were *ca.* 20% of the intensities given by the glyoxal reaction when the optimum wavelengths for emission and excitation were used in each instance.

The calibration graphs for the peptides Trp–Gly–Gly, Trp–Leu and Trp–Met–Asp–Phe–$NH_2$ of the peak height *versus* concentration (0.25–500 pmol per derivatization mixture) were all linear with correlation coefficients of 0.998–0.999. In within-day assays, the relative standard deviations ($n = 10$) of the peak heights were 3.0, 1.3 and 4.2% for Trp–Gly–Gly, Trp–Leu and Trp–Met–Asp–Phe–$NH_2$, respectively, at the concentrations used for Fig. 1.

Fig. 5 shows the application of the present method to the detection of the tryptic digest of dynorphin A (Tyr–Gly–Gly–Phe–Leu–Arg–Arg–Ile–Arg–Pro–Lys–Leu–Lys–Trp–Asp–Asn–Gln; 5 nmol used for the enzyme reaction). In the sample, Trp–Asp–Asn–Gln and many other C-terminal Lys- or Arg-containing peptides are produced in the course of the enzyme reaction, as trypsin mediates the hydrolysis of peptide bonds at the carboxyl sides of lysyl and arginyl residues. In the chromatograms obtained with the present fluorescence detection and conventional UV detection, the fluorescent derivative due to the N-terminal Trp-containing fragment was readily detected with fluorescence detection. With UV detection, however, it was difficult to identify the fragment because many other peaks were detected.

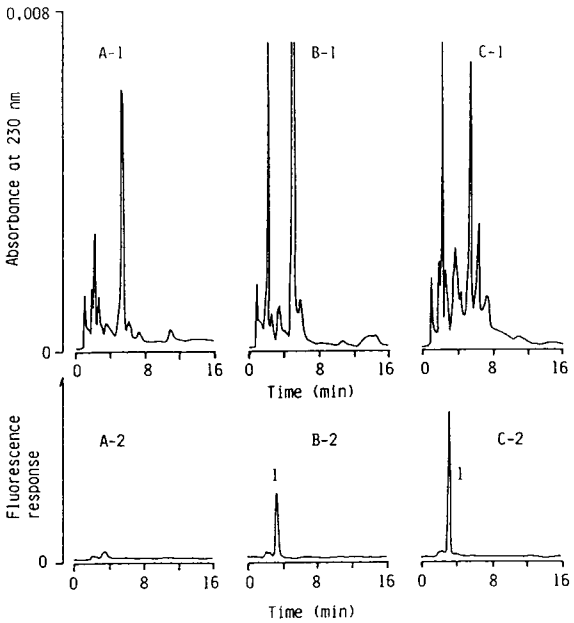


Fig. 5. Chromatograms of the peptide fragments produced by tryptic digestion of dynorphin A. A 50-$\mu$l portion of 100 nmol/ml dynorphin A was mixed with 100 $\mu$l of 50 m*M* sodium phosphate buffer (pH 8.0) and 50 $\mu$l of 1.0 mg (122 000 units)/ml trypsin and the mixture was incubated at 37°C for (A) 0, (B) 5 and (C) 30 min. A 20-$\mu$l portion of the enzyme reaction mixture was chromatographed for UV detection (A-1, B-1, C-1). Another 100-$\mu$l portion of the mixture was used for the fluorescence derivatization, and a 100-$\mu$l portion of the final reaction mixture was chromatographed for fluorescence detection (A-2, B-2, C-2). HPLC conditions: mobile phase, acetonitrile–methanol–20 m*M* phosphate buffer (pH 6.0)–water (14:14:60:12, v/v); other conditions as under Experimental. Peak 1 = fluorescent derivative of Trp–Asp–Asn–Gln.

## CONCLUSION

This is the first method for the selective fluorescence derivatization HPLC of N-terminal Trp-containing peptides. It permits the sensitive determination of the peptides at the sub-picomole level. The sensitivity of the method is nearly three and two orders of magnitude higher

than those of the manual fluorimetric method [15] and conventional HPLC–UV detection method, respectively. The proposed method is probably useful for the simple identification of Trp-containing fragments of high-molecular-mass peptides in various enzymatic digests. The specificity of the method may also be an aid for the quantitative or qualitative determination of biogenic N-terminal Trp-containing peptides such as delta-sleep-inducing peptides (Trp–Ala–Gly–Gly–Asp–Ser–Gly–Glu) [16], a metabolic fragment peptide of cholecystokinin (Trp–Met–Asp–Phe–$NH_2$) [17] or unknown bioactive peptides in the complex matrices of mammalian tissues and fluids. Studies on these aspects are in progress.

## REFERENCES

1 J.F. Rehfeld, *J. Biol. Chem.*, 253 (1978) 4016.
2 J.J. Kusmierz, R. Sumrada and D.M. Desiderio, *Anal. Chem.*, 62 (1990) 2395.
3 J. River, R. McClintock, R. Galyean and H. Anderson, *J. Chromatogr.*, 288 (1984) 303.
4 S. Mousa and D. Couri, *J. Chromatogr.*, 267 (1983) 191.
5 M. Rubinstein, S.C. Kiang, S. Stein and S. Udenfriend, *Anal. Biochem.*, 95 (1979) 117.
6 H. Nakamura, C.L. Zimmerman and J.J. Pisano, *Anal. Biochem.*, 93 (1979) 423.
7 K.A. Cobb and M.V. Novotny, *Anal. Biochem.*, 200 (1992) 149.
8 M. Kai, T. Miyazaki, Y. Sakamoto and Y. Ohkura, *J. Chromatogr.*, 322 (1985) 473.
9 M. Ohno, M. Kai and Y. Ohkura, *J. Chromatogr.*, 490 (1989) 301.
10 M. Kai and Y. Ohkura, *Anal. Chim. Acta*, 182 (1986) 177.
11 M. Nakano, M. Kai, M. Ohno and Y. Ohkura, *J. Chromatogr.*, 411 (1987) 305.
12 G.-Q. Zhang, M. Kai and Y. Ohkura, *Anal. Sci.*, 6 (1990) 671.
13 G.-Q. Zhang, M. Kai, M. Nakano and Y. Ohkura, *Chem. Pharm. Bull.*, 39 (1991) 126.
14 E. Kojima, M. Kai and Y. Ohkura, *Anal. Chim. Acta*, 248 (1991) 213.
15 E. Kojima, M. Kai and Y. Ohkura, *Anal. Chim. Acta*, 280 (1993) 157.
16 G.A. Schoenenberger and M. Monnier, *Proc. Natl. Acad. Sci. U.S.A.*, 74 (1977) 1282.
17 J.F. Rehfeld, L.I. Larsson, N.R. Goltermann, T.W. Schwartz, J.J. Holst, S.L. Jensen and J.S. Morley, *Nature*, 384 (1980) 33.

*Journal of Chromatography A*, 653 (1993) 241–246
Elsevier Science Publishers B.V., Amsterdam

CHROM. 25 445

# Characterization of further association of the trimeric membrane protein porin by low-angle laser-light scattering photometry coupled with high-performance gel chromatography

Yasushi Watanabe and Toshio Takagi*

*Institute for Protein Research, Osaka University, Yamadaoka 3-2, Suita, Osaka 565 (Japan)*

(First received April 19th, 1993; revised manuscript received July 20th, 1993)

ABSTRACT

Porin (OmpF), a trimeric membrane protein, in an extract of the outer membrane of *Escherichia coli* gave a twin-peaked elution pattern on Sephacryl S-300HR gel chromatography in the presence of sodium dodecyl sulphate. The species eluting earlier and later were found to be the hexamer and trimer, respectively, from molecular mass determination by low-angle laser-light scattering photometry coupled with TSK-G3000SWXL gel chromatography. As the hexamer was dissociated into the trimer under the conditions of sodium dodecyl sulphate polyacrylamide gel electrophoresis, its presence had been overlooked. The addition of lipopolysaccharide, another component of the outer membrane, and subsequent dialysis induced association of the trimer, the product containing an appreciable amount of the hexamer.

## INTRODUCTION

Pores formed by the outer membrane protein of *Escherichia coli*, porin (OmpF), allow the restricted passage of hydrophilic substances with molecular masses of less than about 600 [1]. Porin is a trimeric integral membrane protein and is highly resistant to proteases and surfactants such as sodium dodecyl sulphate (SDS). Recent X-ray analysis revealed that the porin subunit with a molecular mass of 37 000 [2,3] has a sixteen-stranded $\beta$-barrel structure [4]. Lipopolysaccharide (LPS) is another predominant component of the outer membrane, and binds tightly to porin [1]. The formation of a channel requires the presence of both LPS and further association of the trimer [5]. The product of such an association has not been well characterized with respect to the molecular mass.

In the course of the isolation of porin, we extracted it from the outer membrane of *Escherichia coli* and found that the preparation gave a twin-peaked elution curve on Sephacryl S-300HR gel chromatography. Yamada and Mizushima [6] observed a similar mode of elution from a Sephadex G-200 column. These observations suggested that the extract contains two species of porin differing in the degree of association. The latter group, however, could only detect trimeric porin for both the peaks on SDS polyacrylamide gel electrophoresis (PAGE) [6]. In this study, the molecular masses of the protein species giving the peaks were determined in the same medium as that for the Sephacryl gel chromatography by low-angle laser-light scattering photometry coupled with high-performance gel chromatography. This technique is suitable for the molecular mass determination of the

* Corresponding author.

0021-9673/93/$06.00 

protein moiety of a membrane protein solubilized by a surfactant [7].

The first and second peaks could be assigned to the hexamer and trimer of porin, respectively, by the light scattering technique. The hexamer was found to dissociate into the trimer under the conditions of SDS-PAGE. The addition of LPS to the purified trimer was found to give a further associated species comprising the hexamer.

## EXPERIMENTAL

SDS was purchased from BDH (Poole, UK) and LPS (type B055) from Sigma (St. Louis, MO, USA). Other chemicals were of analytical-reagent grade.

Porin was isolated from *Escherichia coli* B specifically producing porin of the OmpF type by the following modification of the method reported previously [8]. Wet bacterial cells (80 g) were suspended in 240 ml of 50 m*M* Tris–HCl buffer (pH 7.6) containing 0.1% mercaptoethanol. The suspension was then sonicated twice for 10 min with an interval of 5 min at below −10°C. The cell wall debris was collected by centrifugation at 27 000 *g* for 110 min, dispersed in 0.01 *M* Tris–HCl buffer (pH 7.5) and re-collected by centrifugation at 80 000 *g* for 60 min. The cell envelope obtained as a pellet was stored at −80°C until used.

The cell envelope (15 g) was washed with 320 ml of 2% SDS at 30°C for 30 min to remove peripheral proteins and then collected by centrifugation at 80 000 *g* for 30 min at 20°C. The pellet was washed three times by suspension in water and subsequently collected by centrifugation at 80 000 *g* for 30 min at room temperature. The pellet was suspended in 320 ml of 50 m*M* Tris–HCl buffer (pH 7.6) containing 1% SDS, 5 m*M* EDTA and 0.03% sodium azide and then left overnight at 37°C. The porin thus obtained is in the form of a complex with the peptidoglycan matrix. The complex was collected by centrifugation at 80 000 *g* for 60 min at 20°C and then washed twice by centrifugation as a suspension in water at 80 000 *g* for 60 min at 20°C.

Porin was removed from the matrix by suspending the complex in 100 ml of 15 m*M* Tris–HCl buffer (pH 7.6) containing 0.5 *M* NaCl, 5 m*M* EDTA and 1% SDS. The insoluble material was removed by centrifugation at 80 000 *g* for 90 min after allowing the extract to stand overnight with stirring, and the supernatant was concentrated about tenfold using a PM-30 Amicon ultrafilter at room temperature. The concentrate was applied to a Sephacryl S-300HR (Pharmacia, Uppsala, Sweden) column (details are given in the legend to Fig. 1).

The fraction rich in trimeric porin obtained by the above-mentioned gel chromatography was further purified as follows, and used as the starting material in experiments carried out to examine the potential of the trimer for further association. The trimer-rich fraction was further purified by hydroxyapatite chromatography in the presence of SDS according to the procedure described previously [9]. A tandem array of a guard column (type A-4001) and a main column (HCA column type A-7610; 100 mm × 4.0 mm I.D.), both from Mitsui-Toatsu Chemicals (Tokyo, Japan) (now distributed by Koken, Tokyo, Japan), was used. The columns were equilibrated with 50 m*M* sodium phosphate buffer (pH 6.9) containing 0.1% SDS and 0.01% sodium azide. The sample solution (15 ml) was applied to the columns after dialysis against the above buffer. After passage of the starting buffer for 15 min, the concentration of phosphate in the buffer was increased linearly to 500 m*M* over 25 min at a flow-rate of 1.0 ml/min, the concentrations of other components being kept constant. Fractions containing porin were collected and concentrated about fivefold with a PM-30 Amicon ultrafilter and then applied to a TSK-G3000SW column (600 mm × 21.6 mm I.D.) (Tosoh, Tokyo, Japan) equipped with a guard column of TSK-GCSW (50 mm × 21.6 mm; I.D.) (Tosoh) equilibrated with 50 m*M* sodium phosphate buffer (pH 6.9) containing 0.1% SDS and 0.01% sodium azide. The temperature and flow-rate were 25°C and 2.0 ml/min, respectively. Porin was eluted as a single peak and the peak fraction was used as the stock solution of trimeric porin. The concentration of porin was determined spectrophotometrically assuming the absorbance value of a 1% solution at 278 nm for a 1-cm light path to be 14.1 [10].

The molecular mass was determined by moni-

toring elution from high-performance gel chromatographic columns using a measuring system for molecular mass determination. The solvent delivery system was the same as that described previously [7], and equipped with a sample loop with an internal volume of 500 $\mu$l. The columns and detectors were products of Tosoh and were arranged along the flow-line in the following sequence: guard column of TSK-GEL GCSWXL (40 mm × 6.0 mm I.D.), two tandem-linked TSK-GEL G3000SWXL columns (300 mm × 7.8 mm I.D.), low-angle laser-light scattering photometer (LS-8000), UV spectrophotometer (UV-8000) and differential refractometer (RI-8000). The temperature of the columns and the flow-through cell in the low-angle laser-light scattering photometer was kept constant at 25°C using a column jacket and a metallic cell holder through which water of constant temperature was circulated.

The molecular mass of the protein moiety of a surfactant–protein complex, $M_r$, is related to the signal intensities from the three detectors mentioned above according to the following equation [7]:

$$M_r = kE^{-1}(\text{Output})_{LS}(\text{Output})_{UV}(\text{Output})_{RI}^{-2} \quad (1)$$

where $k$ is an instrumental constant, $E$ the specific absorptivity at 280 nm (ml/mg, for a 1-cm light path) and (Output) the output of the respective detectors specified by the subscripts LS (low-angle laser-light scattering photometer), UV (spectrophotometer) and RI (differential refractometer). The retention times refer to those observed for the light scattering photometer. The actual retention times observed for the other detectors were corrected for the time lag due to their sequential arrangement.

The constant $k$ was determined by using the following proteins of known molecular masses and absorptivities: bovine carbonic anhydrase ($M_r = 29\,000$, $E = 1.9$ [11]), bovine serum albumin ($M_r = 66\,300$, $E = 0.678$ [11]) and heat-treated porin monomer and purified trimer {$M_r = 37\,000$ (monomer), 111 000 (trimer) [2,3] $E = 1.38$ [10]}.

SDS-PAGE was performed with a mini-sized apparatus (12.5% gel; 60 mm long and 1 mm thick) at 6°C according to the method of Laemmli [12].

LPS was determined through the determination of 2-keto-3-deoxyoctonic acid by the thiobarbituric acid method described by Osborn *et al.* [13].

## RESULTS

For the purification of porin, it was extracted from the complex between the protein and the peptidoglycan matrix with a buffer solution containing 0.5 *M* sodium chloride, 5 m*M* EDTA and 1% SDS. As shown in Fig. 1, when the crude extract was applied to a Sephacryl S-300HR

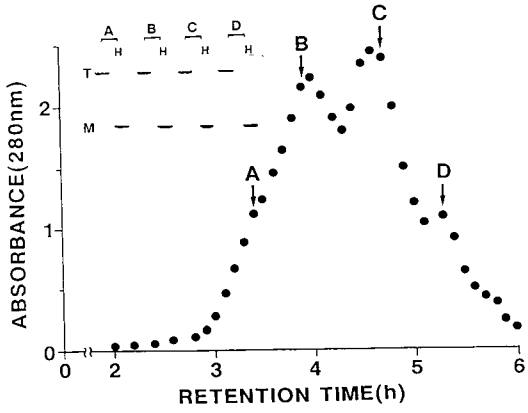


Fig. 1. Typical elution pattern of the crude extract of porin in the presence of SDS. A 10-ml aliquot of the extract from 15 g of wet cell envelope fraction was applied to a Sephacryl S-300HR column (85 cm × 2.6 cm I.D.) equilibrated with 50 m*M* sodium phosphate buffer (pH 6.9) containing 0.1% SDS, 5 m*M* EDTA and 0.03% sodium azide at a flow-rate of 1.1 ml/min. The eluate was collected in 7-ml fractions and monitored for absorbance at 280 nm with a cell of 1-cm light path. The fractions designated A, B, C and D were analysed by SDS-PAGE as described below, and the electrophoretic patterns obtained are shown in the inset. Each of the fractions was diluted with the elution buffer to give an absorbance of 0.3 at 280 nm for a 1-cm light path. A 60-$\mu$l volume of each of the diluted solutions was mixed with 20 $\mu$l of an aqueous solution with the composition 8% SDS, 20 m*M* EDTA and 40% glycerol. A 10-$\mu$l volume of each of the solutions was applied to the unmarked lanes. Each of the lanes marked H was loaded with 10 $\mu$l of the respective sample heated at 95°C for 5 min. The protein was stained with Coomassie Brilliant Blue R-250. T and M are the positions of the bands expected for the intact trimer and denatured monomer of porin, respectively.

column after concentration, a twin-peaked elution profile was observed in the frontal region.

Four fractions were chosen from those from the Sephacryl column, and designated A, B, C and D, as shown in Fig. 1. They were analysed by SDS-PAGE for the detection of porin and possible contaminating proteins. The electrophoretic patterns obtained are included as an inset in Fig. 1. For fractions A, B and C, only a single protein band was observed. Only for fraction D, another protein band with a faster electrophoretic mobility was detected in addition to the band described above (not shown). The mobilities of the commonly observed bands were significantly enhanced on heating. This heat sensitivity is the so-called heat modifiability characteristic of porin. The results obtained by electrophoresis indicate that fractions A, B and C contain only the porin trimer.

To examine further the molecular assembly in the fractions A, B and C, they were analysed by the light scattering technique coupled with a tandem array of two TSK-G3000SWXL columns in the same medium. Elution from the columns was monitored with a low-angle laser-light scattering photometer, a UV spectrophotometer and a differential refractometer. The three sets of elution curves are shown in Fig. 2, together with the change in the molecular mass of porin with retention time in the peak region. In contrast to the conclusion obtained from SDS-PAGE, none of the fractions was dominated by the porin trimer. Moreover, they differed significantly with regard to the profile of the change in molecular mass. The molecular mass observed for fraction A was found to start from more than 400 000 and to decrease rapidly.

Fraction A is clearly rich in a highly associated species. The molecular mass profiles for both fractions B and C show plateaux at about 200 000–210 000 and about 110 000, respectively. These values correspond roughly to molecular masses of six and three times that for the subunit molecular mass ($M_r = 37\,000$) [2,3] of porin, respectively. Clearly, porin in the extract from the outer membrane matrix is highly heterogeneous as to the degree of association. To summarize, a highly associated species is eluted in the frontal region and the porin hexamer and trimer

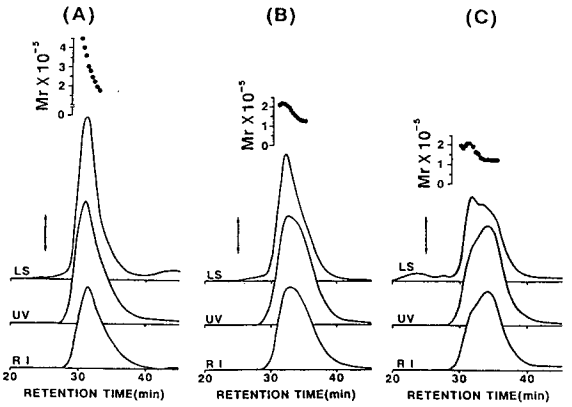


Fig. 2. Characterization of the fractions obtained on Sephacryl gel chromatography (Fig. 1) with respect to molecular mass. (A), (B) and (C) show the sets of elution patterns obtained with the measuring system for molecular mass determination described under Experimental and the molecular masses (O) determined according to eqn. 1. LS, UV and RI are as in eqn. 1. The gain settings of the detectors were 32, 0.16 and 32, in the order given above. A 500-$\mu$l volume of each of the solutions with an absorbance of 0.3 prepared as described in Fig. 1 was applied to TSK-G3000SWXL columns in the system. The same buffer solution as described in Fig. 1 was used for equilibration and elution (0.4 ml/min). The length of the vertical bar with arrowheads corresponds to one tenth of the full scale for the respective detector.

are dominant in the first and second peaks, respectively. Rechromatography of the trimer fraction gave only the trimer peak, but that of the hexamer fraction gave a trimer peak corresponding to a few per cent of the total area.

In addition, the amounts of LPS bound to porin were estimated to be 0.6, 8 and 18 mg/g protein for fractions A, B and C, respectively. Assuming the molecular mass of LPS to be 4300 [6] and that all proteins in the fractions are porin, the molar ratios of LPS to the porin trimer were calculated to be 0.02, 0.2 and 0.5 mol/mol of the trimer, respectively.

Fraction B was subjected to harsh conditions and then analysed with the measuring system for molecular mass to examine the stability of the hexamer. Incubation with 8 *M* urea for 24 h at room temperature failed to dissociate the hexamer. Neither 10 m*M* EDTA nor 0.5 *M* sodium chloride was effective. Conversion to the trimer was only observed when the fraction was heated at 55°C for 30 min in the presence of 1% SDS.

These results indicate that the hexamer is fairly stable.

Starting from the porin trimer purified by hydroxyapatite chromatography, we tried to convert the trimer into the hexamer. As LPS has been suggested to play a crucial role in the oligomerization of the porin trimer [1,5], it was incubated with LPS in the presence of SDS. As shown in Fig. 3A, incubation with LPS for 120 h induced association of the trimer only slightly, as is suggested by the small shoulder peak in the light scattering trace and the upward shift of the molecular mass profile in the frontal region. It should be noted, however, that the retention time of the sample prepared with LPS was significantly shorter than that of the purified trimer used as the starting material (Fig. 3A). This result suggests that the porin trimer binds with LPS, and consequently its molecular size increases.

The presence of SDS was presumed to be responsible for the inefficient conversion to the hexamer. SDS was, therefore, removed from the sample solution by dialysis (for details, see the legend to Fig. 3). As shown in Fig. 3B, extensive aggregation of the trimer was observed. A shoulder was observed in the molecular mass profile, indicating that the trimer could be partially converted into the hexamer.

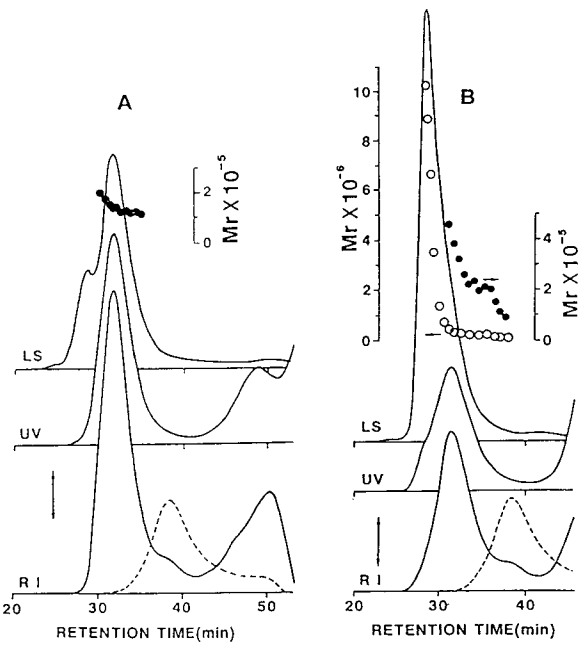


Fig. 3. Elution patterns obtained on TSK-G3000SWXL gel chromatography carried out for examination of the effectiveness of attempts at the preparation of the hexamer from the purified trimer. Two sets of elution patterns and molecular masses (circles), like those in Fig. 2, were obtained for samples prepared as follows. (A) A 600-$\mu$l volume of the purified trimer solution (0.4 mg/ml) in 50 m*M* sodium phosphate buffer (pH 6.9) containing 0.1% SDS and 0.01% sodium azide was mixed with an equal volume of an LPS solution (1.2 mg/ml) in the same buffer as above. After standing for 120 h at 25°C, 500 $\mu$l of the mixture were applied to the same measuring system as in Fig. 2, except for the absence of EDTA. The elution conditions were the same as those in Fig. 2. The gain settings of the detectors were 16 for LS, 0.16 for UV and 32 for RI. (B) A mixture was prepared in the same manner as described above and then dialysed against 10 m*M* sodium phosphate buffer (pH 7.0) for 24 h. As the solution became turbid, 50 $\mu$l of 2% SDS in the 50 m*M* buffer mentioned above were added to 450 $\mu$l of the suspension to clarify it. After standing overnight at room temperature, the solution obtained was applied to the same system. The gain settings of the detectors were 8 for LS, 0.16 for UV and 32 for RI. Note that the scale for the molecular masses shown by the open circles is different from that for the closed circles. Other conditions were the same as in (A). In both (A) and (B), the broken line in the refractive index (RI) trace indicates the elution pattern obtained for the purified porin trimer used as the starting material.

## DISCUSSION

Yamada and Mizushima [6] obtained a twin-peaked elution curve similar to that in Fig. 1 on Sephadex G-200 chromatography of a crude preparation of porin. They collected the eluate in the frontal region and used it in reconstruction of the membrane with a lattice structure in which LPS is involved. The porin used in their study was assumed to exist as a trimer. They presumed that a difference in the amount of LPS produced the twin-peaked elution curve. In this study, however, the species in the frontal region on Sephacryl chromatography was found by light scattering photometry coupled with high-performance gel chromatography to be an associated form of the porin trimer, as shown in Fig. 2. Our results for the amounts of LPS bound are in agreement with those obtained by Yamada and Mizushima. As the amounts of LPS bound are very small (see Results), the observation of the associated species suggests that the trimers are

directly assembled with each other in such an associated species.

The results obtained with the light scattering technique contradict the observation that the hexamer is not detected on SDS-PAGE. SDS-PAGE according to the method of Weber and Osborn [14], in which a sodium phosphate buffer is used, also reportedly failed to detect the hexamer [6], and we found this to be reproducible (not shown). There are significant differences in the conditions between the two separation techniques with regard to both the medium conditions and the mechanism of separation. We have no immediate explanation for the discrepancy, however. In any case, the present results indicate that the porin trimer can associate to form the hexamer, and the stability of the product is comparable to but slightly lower than that of the trimer. The trimer could be converted into the hexamer in a low yield, as shown in Fig. 3.

Schindler and Rosenbusch [5] reported that the presence of LPS and the association of the porin trimer are necessary for the formation of stable channels in a lipid bilayer. Our results together with theirs strongly suggest that porin exists not as a trimer but as a further associated form in the outer membrane. In this study, a major product of such an associated species was found to be the porin hexamer even in the presence of SDS. This finding was only possible using the measuring system for molecular mass determination in which a light scattering photometer plays a pivotal role. The technique allows the unique determination of the molecular mass of a protein moiety without reference to the retention time of a sample, as shown in Fig. 3A. Further studies on the relationship between the channel activity and the well characterized associated state of porin trimers will lead to a better understanding of the molecular organization and functions of the bacterial outer membrane.

## REFERENCES

1 H. Nikaido, *Mol. Microbiol.*, 6 (1992) 435–442.
2 R. Chen, C. Krämer, W. Schmidmayr and U. Henning, *Proc. Natl. Acad. Sci. U.S.A.*, 76 (1979) 5014–5017.
3 K. Inokuchi, N. Mutoh, S. Matsuyama and S. Mizushima, *Nucleic Acids Res.*, 10 (1982) 6957–6968.
4 S.W. Cowan, T. Schirmer, G. Rummel, M. Steiert, R. Ghosh, R.A. Pauptit, J.N. Jansonius and J.P. Rosenbusch, *Nature*, 358 (1992) 727–733.
5 H. Schindler and J.P. Rosenbusch, *Proc. Natl. Acad. Sci. U.S.A.*, 78 (1981) 2302–2306.
6 H. Yamada and S. Mizushima, *Eur. J. Biochem.*, 103 (1980) 209–218.
7 T. Takagi, *J. Chromatogr.*, 506 (1990) 409–416.
8 K. Kameyama, T. Nakae and T. Takagi, *Biochim. Biophys. Acta*, 706 (1982) 19–26.
9 Y. Watanabe, T. Okuno, K. Ishigaki and T. Takagi, *Anal. Biochem.*, 202 (1992) 268–274.
10 J.P. Rosenbusch, *J. Biol. Chem.*, 249 (1974) 8019–8029.
11 G.D. Fasman (Editor), *Handbook of Biochemistry and Molecular Biology*, Vol. II, CRC Press, Cleveland, OH, 1976.
12 U.K. Laemmli, *Nature*, 227 (1970) 680–685.
13 M.J. Osborn, J.E. Gander, E. Parisi and J. Carson, *J. Biol. Chem.*, 247 (1972) 3962–3972.
14 K. Weber and M. Osborn, *J. Biol. Chem.*, 244 (1969) 4406–4412.

*Journal of Chromatography A*, 653 (1993) 247–251
Elsevier Science Publishers B.V., Amsterdam

CHROM. 25 441

# Separation of chlorophyll $c_1$ and $c_2$ by reversed-phase high-performance liquid chromatography

Koichi Saitoh*, Izumi Awaka and Nobuo Suzuki

*Department of Chemistry, Faculty of Science, Tohoku University, Sendai 980 (Japan)*

(First received December 10th, 1992; revised manuscript received July 15th, 1993)

ABSTRACT

The separation of chlorophyll $c_1$ and $c_2$ was performed using an octadecyl-bonded polymer column with an aqueous methanolic mobile phase, *e.g.* a 90:10 (v/v) mixture of methanol and pH 3 buffer. The retention of both types of chlorophyll *c* increases with decreasing methanol content and also with decreasing pH (particularly lower than about pH 6) of the aqueous component of the mobile phase. Chlorophyll $c_1$ is eluted from the column in preference to chlorophyll $c_2$. UV–visible spectral data were obtained for the chlorophylls.

## INTRODUCTION

Chlorophylls are the photosynthetic pigments contained in certain plant tissues. Every plant contains chlorophyll *a* (CHL-*a*) and, in addition, chlorophyll *b* (CHL-*b*) is contained in green plants and chlorophyll *c* (CHL-*c*) in brown algae. CHL-*c* occurs in two different forms [1,2], chlorophyll $c_1$ (CHL-$c_1$) and chlorophyll $c_2$ (CHL-$c_2$), which are magnesium complexes of tetra- and hexahydropheoporphyrin $a_5$ monomethyl esters, respectively (Fig. 1) [3].

The determination of chlorophylls and their degradation products in natural samples from the sea, lakes, rivers and other sources gives valuable information about the biological activity in different environments. In oceanography, the determination of particulate chlorophylls is an important measurement to estimate biomass. Traditional and popular analytical methods for chlorophylls are based on spectrophotometry or fluorimetry. Neither of these methods can cope with the difference in form of CHL-*c*, results being obtained only for the total of CHL-$c_1$ and CHL-$c_2$.

High-performance liquid chromatography (HPLC) is a promising technique for chlorophyll determination [4–6]. The separation of CHL-*a*

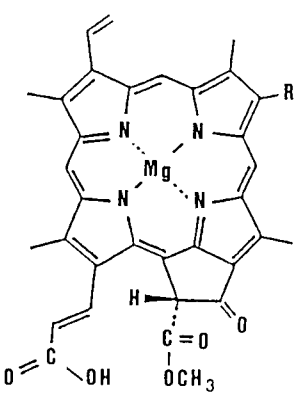


Fig. 1. Structure of CHL-$c_1$ (R = ethyl) and -$c_2$ (R = vinyl).

* Corresponding author.

0021-9673/93/$06.00 

and CHL-*b* is possible by reversed-phase HPLC [7]. However, no clear evidence has been reported on the feasibility of HPLC for the resolution of CHL-*c* into its different forms, except for particular instances of thin-layer chromatography [1,2] and column liquid chromatography [8] developed by Jeffrey using a specially prepared polyethylene power as an adsorbent.

In our previous studies on the HPLC of chlorophylls and related compounds, the retention characteristics of CHL-*a* and CHL-*b* [7] and also various metal complexes of pheophorbide-*a* and -*b* [9] were investigated. In preference to the extension of such studies to CHL-*c*s and their derivatives, it was urgently required to develop a reliable HPLC method for separation of CHL-$c_1$ and -$c_2$. This paper describes the successful resolution of CHL-*c* into the $c_1$ and $c_2$ forms by reversed-phase HPLC with a commercially available octadecyl-bonded vinyl alcohol copolymer gel (polymer) column.

## EXPERIMENTAL

### *HPLC*

A Twincle liquid chromatograph (JASCO, Tokyo, Japan) was equipped with a UV–visible photodiode-array detector (Shimadzu Model SPD-M6A) for real-time recording of the spectra of the eluate. An octadecyl-bonded silica gel (ODS) column (particle diameter 5 $\mu$m; 15 cm × 4.6 mm I.D.) (Inertsil ODS-2; GL Science, Tokyo, Japan) and an octadecyl-bonded polymer (ODP) column (particle size 5 $\mu$m; 15 cm × 6.0 mm I.D.) (Asahipak ODP-50; Asahi Kasei, Kawasaki, Japan) were tested. The mobile phase was a 90:10 (v/v) mixture of methanol and pH 3 phosphate buffer (containing 1.24 m*M* phosphoric acid and 8.76 m*M* sodium dihydrogenphosphate). The flow-rates were 1.0 and 1.7 ml min$^{-1}$ with the ODS and the ODP column, respectively. All chromatographic experiments were carried out in a thermostated room at 25°C.

### *Mass spectrometry*

A JEOL Model JMS-HX2100 mass spectrometer was equipped with a fast atom bombardment (FAB) ionization system (JEOL, Tokyo, Japan). Nitrobenzyl alcohol was used as a matrix.

### *Preparation of CHL-c*

Algal pigments were extracted with acetone from the fresh brown alga *Undaria pinnatifida* obtained at Onagawa Bay, Miyagi, Japan. The acetone extract was agitated with both light petroleum (b.p. 30–60°C) and a saturated aqueous solution of NaCl in order to remove the majority of co-extracted pigments, such as CHL-*a* and carotenoids. The resulting aqueous acetone phase was shaken with ethyl acetate. The ethyl acetate solution was then passed through a cellulose column, followed by concentration under a stream of nitrogen. The pigments in the concentrated ethyl acetate solution were resolved by preparative liquid chromatography using an octadecyl-bonded silica gel column (36 cm × 2.4 cm I.D.) (Fuji Gel RQ-2; Fuji, Tokyo, Japan) with methanol–water (90:10, v/v). The desired pigment passed easily through the column, whereas co-existing pigments, such as CHL-*a* and pheophytin *a* (demetallated form of CHL-*a*), were strongly retained.

## RESULTS

The UV–visible spectral characteristics, such as the shape and the absorption maximum wavelengths, of the pigment separated from the alga agreed closely with that of CHL-*c* [1,2,10]. In the mass spectrum of the pigment, significant signals were detected around $m/z$ 608–610, which matched the molecular ion peaks of CHL-$c_1$ and -$c_2$ (the molecular masses of CHL-$c_1$ and -$c_2$ are 610 and 608, respectively).

The feasibility of HPLC and high-performance TLC (HPTLC) was examined for resolving this pigment into CHL-$c_1$ and -$c_2$ by using various stationary phase substances, such as cellulose, silica gel and chemically bonded silica gels possessing cyano, amino, octyl and octadecyl groups, in the normal- or reversed-phase separation mode. No successful resolution was obtained, but all results implied that the pigment was a pure substance. The pigment, after being treated with 0.1 *M* hydrochloric acid for demetallation, gave two resolved peaks in the chromatogram obtained with an ODS column, as shown in Fig. 2. The early- and late-eluted peaks were assigned to pheoporphyric $c_1$ (PHEO-$c_1$)

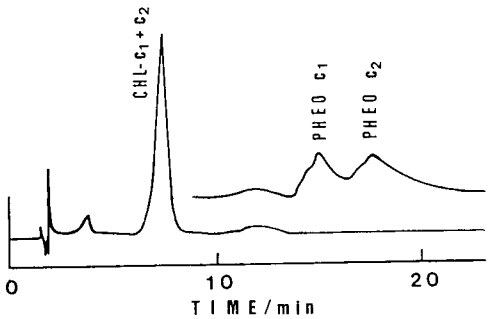


Fig. 2. Resolution of CHL-*c* and PHEO-*c* on an ODS column. Column: Inertsil ODS-2 (5 μm) (15 cm × 4.6 mm I.D.). Mobile phase: methanol–pH 3 buffer (90:10, v/v); flow-rate, 1.0 ml $min^{-1}$. Detection at 440 nm.

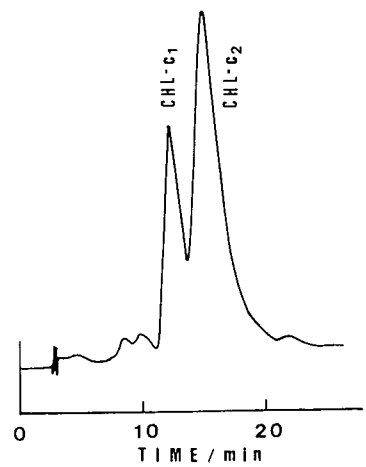


Fig. 3. Separation of CHL-$c_1$ and CHL-$c_2$ on an ODP column. Column: Asahipak ODP-50 (5 μm) (15 cm × 6.0 mm I.D.). Mobile phase: methanol–pH 3 buffer (90:10, v/v); flow rate, 1.7 ml $min^{-1}$. Detection at 440 nm.

and pheoporphyrin $c_2$ (PHEO-$c_2$), respectively, by comparing the UV–visible spectra of the peak fractions of the eluate with those of the pure substances [7].

According to the above results, the pigment of interest was regarded as a mixture of CHL-$c_1$ and CHL-$c_2$ at this stage. The pigment is hereafter denoted CHL-*c* for convenience.

*Resolution of CHL-c*

It was found that CHL-*c* could be resolved into two species by use of an ODP column with aqueous methanolic mobile phase, as shown in Fig. 3. The resolved CHL-*c* species were crystallized from corresponding fractions of the eluate. The early- and the late-eluted fractions of CHL-*c* gave intense mass spectral signals at *ca.* *m/z* 610 and 608, respectively (see Fig. 4), which matched the molecular ion peaks of CHL-$c_1$ and CHL-$c_2$. Accordingly, the early- and late-eluted species from the ODP column were identified as CHL-$c_1$ and CHL-$c_2$, respectively.

The UV–visible absorption spectral data for CHL-$c_1$ and -$c_2$ in methanol and 1% pyridine–methanol are given in Table I.

*Effect of mobile phase solvent*

Fig. 5 shows the effect of the methanol content of the mobile phase on the capacity factors ($k'$) of CHL-$c_1$ and -$c_2$. For calculation of $k'$, the column void volume was determined by injection of a nearly saturated solution of sodium nitrate. The plots of log $k'$ *versus* methanol content for CHL-$c_1$ and -$c_2$ are almost parallel to

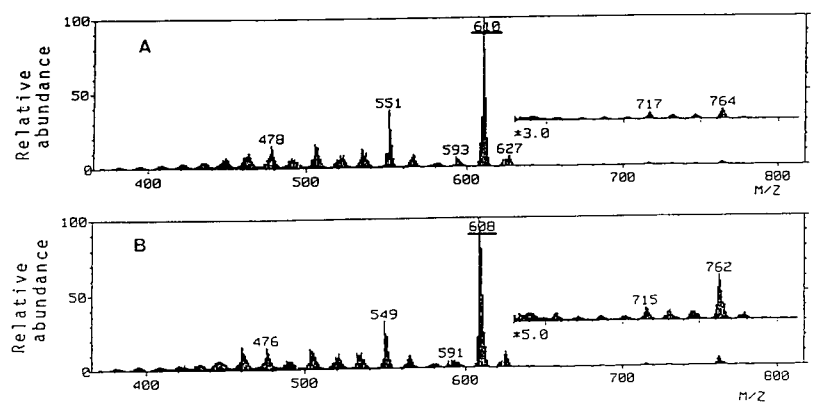


Fig. 4. Mass spectra of (A) CHL-$c_1$ and (B) CHL-$c_2$.

TABLE I

ABSORPTION MAXIMUM WAVELENGTHS ($\lambda_{max}$) AND MOLAR ABSORPTION COEFFICIENTS ($\varepsilon$) AT $\lambda_{max}$ OF CHL-$c_1$ AND -$c_2$

| Compound | In methanol | | In 1% pyridine in methanol | | |
|---|---|---|---|---|---|
| | $\lambda_{max}$ (nm) | $\varepsilon(10^3\,l\,mol^{-1}\,cm^{-1})$ | $\lambda_{max}$ (nm) | $\varepsilon(10^3\,l\,mol^{-1}\,cm^{-1})$ | Literature $\lambda_{max}$ (nm) [2] |
| CHL-$c_1$ | 631 | 8.6 | 634 | 13 | 634 |
| | 588 | 4.9 | 584 | 7.6 | 584 |
| | 451 | 85 | 449 | 94 | 445 |
| CHL-$c_2$ | 635 | 6.1 | 635 | 7.9 | 635 |
| | 588 | 5.8 | 587 | 6.6 | 587 |
| | 454 | 58 | 452 | 74 | 452 |

each other, and CHL-$c_1$ always gives a smaller $k'$ than CHL-$c_2$ within the range of methanol contents tested.

It was found that both PHEO-$c_1$ and -$c_2$, which are the magnesium-free forms of CHL-$c_1$ and -$c_2$, were more strongly retained on the column than the respective chlorophylls, as shown in Fig. 5. A mobile phase containing 90% (v/v) of methanol was effective for the separation of CHL-$c_1$ and -$c_2$. Such a methanol content, however, was not practical if PHEO-$c_1$ and -$c_2$ were also present in the same HPLC run because of their much higher retentions. The plots for PHEO-$c_1$ and -$c_2$ at methanol contents 90% and 92% are not given in Fig. 5 owing to their large retentions.

*Effect of pH of aqueous mobile phase component*

The effect of the pH of the aqueous component of the mobile phase on the capacity factors of CHL-$c_1$ and -$c_2$ was examined using methanol–buffer (90:10, v/v). The buffers (about 10 m*M* solutions) were prepared at pH 3 as described under Experimental, at pH 4–6 with acetic acid and sodium acetate and at pH 8 with Tris and hydrochloric acid. The results are shown in Fig. 6, in which the results for PHEO-

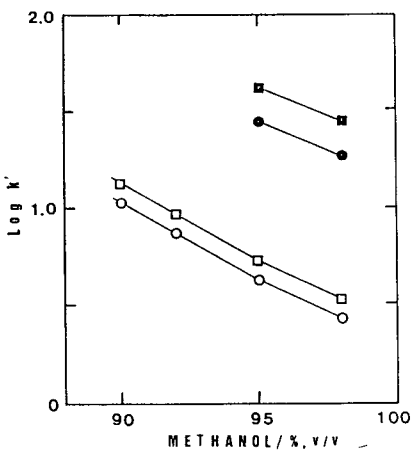


Fig. 5. Effect of the methanol content of the mobile phase on the capacity factors. Column: Asahipak ODP-50. Mobile phase: methanol–buffer (pH 3). Compounds: ○ = CHL-$c_1$; □ = CHL-$c_2$; ● = PHEO-$c_1$; ■ = PHEO-$c_2$.

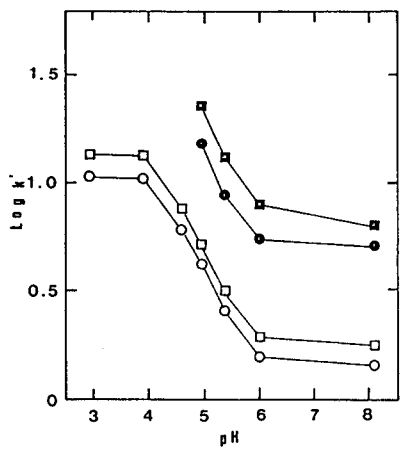


Fig. 6. Effect of the pH of the aqueous component of the mobile phase on the capacity factors. Column: Asahipak ODP-50. Mobile phase: methanol–buffer (90:10, v/v). Symbols as in Fig. 5.

$c_1$ and -$c_2$ are also plotted for comparison. A significant change in the retention of CHL-$c_1$ and -$c_2$ occurs in the pH range *ca.* 4–6, and a similar tendency is shown also for the corresponding metal-free forms, *i.e.*, PHEO-$c_1$ and -$c_2$. When the pH is lower than 5, both PHEO-$c_1$ and -$c_2$ are retained so strongly that they cannot be eluted in a short separation time. Such a pH dependence of the retention is attributable to the weakly acidic characteristics of the carboxylic groups possessed by these compounds. A pH lower than 4 is recommended for the separation of CHL-$c_1$ and -$c_2$ with a high reproducibility of the retention time, because their capacity factors are almost independent of pH.

ODP appears to be a promising reversed-phase column packing for chlorophyll analysis, particularly for the separation of CHL-$c_1$ and -$c_2$, because these pigments could not be resolved by the use of popular reversed-phase columns such as ODS. A 90:10 (v/v) mixture of methanol and a buffer solution of pH 3 is recommended as the mobile phase for this purpose. Application of ODP column to the determination of chlorophylls in real algal samples will be dealt with elsewhere.

ACKNOWLEDGEMENT

This work was supported by a Grant-in-Aid for Scientific Research from the Ministry of Education, Science and Culture.

REFERENCES

1 S.W. Jeffrey, *Biochim. Biophys. Acta*, 162 (1968) 271.
2 S.W. Jeffrey, *Biochim. Biophys. Acta*, 177 (1969) 456.
3 H.H. Strain, B.T. Core, Jr., G.N. McDonald, W.A. Svec and J.J. Katz, *Phytochemistry*, 10 (1971) 1109.
4 R.F. Montoura and C.A. Llewellyn, *Anal. Chim. Acta*, 151 (1983) 297.
5 A.P. Murray, C.F. Gibbs, A.R. Longmore and D.J. Elett, *Mar. Chem.*, 19 (1986) 211.
6 I.D. Gilaudiere, P. Laborde and J.-C. Romano, *Mar. Chem.*, 26 (1989) 189.
7 N. Suzuki, K. Saitoh and K. Adachi, *J. Chromatogr.*, 408 (1987) 181.
8 S.W. Jeffrey, *Biochim. Biophys. Acta*, 279 (1972) 15.
9 K. Adachi, K. Saitoh and N. Suzuki, *J. Chromatogr.*, 457 (1988) 99.
10 M.W. Fawley, *Plant Physiol.*, 91 (1989) 727.

*Journal of Chromatography A*, 653 (1993) 253–259
Elsevier Science Publishers B.V., Amsterdam

CHROM. 25 483

# Automated derivatization and high-performance liquid chromatographic analysis of ibuprofen enantiomers

D. Nicoll-Griffith*, M. Scartozzi and N. Chiem

*Merck Frosst Centre for Therapeutic Research, P.O. Box 1005, Pointe Claire-Dorval, Québec H9R 4P8 (Canada)*

(First received February 5th, 1993; revised manuscript received July 22nd, 1993)

ABSTRACT

The automated pre-column derivatization and HPLC analysis of ibuprofen enantiomers was accomplished using a Gilson–Advanced Automated Sample Processor combination similar to the Bio-Fully Automated Sample Treatment system, and an (*R*)-N-(3,5-dinitrobenzoyl)phenylglycine-derived Pirkle chiral column. In the derivatization reaction excess ethylchloroformate and anisidine were used to form the amide derivative of ibuprofen. After injection of the crude derivatized mixture through the AASP, strong cation-exchange cartridges efficiently trapped the excess anisidine and the enantiomeric ibuprofen amides passed directly into the analytical column where baseline separation was achieved. UV detection was accomplished at 254 nm. Linear standard curves were obtained for each enantiomer of ibuprofen in the range of 7.5–200 $\mu$g per derivatization with coefficients of correlation of 0.994 or greater. The quality control samples gave relative standard deviations of 17% for the low quality control (QC) samples (8.0 $\mu$g/enantiomer) and 7% for the middle and high QCs (60 $\mu$g and 160 $\mu$g/enantiomer respectively).

## INTRODUCTION

Ibuprofen, [2-4-isobutylphenyl)propionic acid], is a non-steroidal anti-inflammatory drug which exists in two enantiomeric forms due to the presence of an asymmetric carbon atom $\alpha$ to the carbonyl function. Ibuprofen is frequently sold as a racemic mixture of (*R*)- and (*S*)-enantiomers, although it has been demonstrated that the anti-inflammatory activity resides predominantly in the (*S*)-enantiomer. Furthermore, it has been reported that this drug undergoes an *in vivo* uni-directional inversion from the inactive (*R*)-enantiomer to the active (*S*)-enantiomer [1–3]. This finding has sparked considerable research aiming to understand the mechanism of this inversion [4–7] and the organs responsible [8,9] for this conversion *in vivo*.

Three approaches have been used for the separation and quantification of ibuprofen enantiomers. The simplest method was direct resolution on a chiral column such as the $\alpha_1$-glycoprotein column [10]. With this method it was necessary to develop a delicate compromise giving sufficient resolution, and short retention times using conditions which guaranteed an acceptable column lifetime [10]. A second approach was the derivatization of ibuprofen with a chiral reagent, resulting in two diastereomers, which were subsequently separated on a non-chiral column by gas chromatography [3,4] or HPLC [11–14]. The possible disadvantages of this approach were: (i) the rates of reaction for the formation of the two diastereomers could be different, resulting in an incorrect ratio of the two diastereomers, and (ii) impurity of the chiral reagent could result in four diasteromers instead of only two. A third approach was to prepare a non-chiral derivative of ibuprofen and separate the resulting enantiomers on a chiral column [15]. While analytical methods utilizing a derivatization are frequently quite efficient and

* Corresponding author.

0021-9673/93/$06.00 

sensitive, the derivatization adds a time consuming step. The objective of this report is to describe the development of an approach for automating pre-column derivatizations using the analysis of ibuprofen enantiomers as a model system.

In a previous study ibuprofen was manually derivatized using ethyl chloroformate and *p*-anisidine to yield enantiomeric amides which were then resolved on a (3,5-dinitrobenzoyl)-phenylglycine (DNBPG) chiral column [15]. It was critical to do a liquid–liquid extraction with aqueous acid in order to remove excess anisidine prior to chromatography since it co-eluted with the ibuprofen amides. The liquid–liquid extraction of anisidine was very effective, however, this step was very time consuming and severely limited the number of samples which could be processed each day. An automated method involving on-line extraction of the anisidine would be more appropriate for the derivatization and analysis of large numbers of samples.

This paper describes the successful automation of this method using an autosampler to mix the reagents, on-line solid phase extraction to trap excess anisidine and the DNBPG column to separate the enantiomers. The instrumentation used is an adaption of the Bio-Fully Automated Sample Treatment (Bio-FAST) system [16,17]. The Bio-FAST is a sophisticated column switching system in which a fresh pre-column is used for each sample. In this application, the pre-columns were used to retain the excess anisidine from each derivatization while the ibuprofen amides passed directly onto the analytical column.

## EXPERIMENTAL

### *Apparatus*

A diagram of the Bio-FAST type HPLC system used is given in Fig. 1. The system is comprised of a Vista 5500 LC (Pump A) (Varian, Walnut Creek, CA, USA), a Gilson 323-401 sample processor and injector with a 25-$\mu$l loop (Gilson Medical Electronics, Middleton, WI, USA), an Advanced Automated Sample Processor (AASP) (Varian) and an AASP injector valve (Valve 2 in Fig. 1) (Varian), a Model 510 pump (Pump B) (Waters Assoc., Milford, MA, USA), a UV 200 detector (Varian) and an HP 3396 Series II Integrator (Hewlett-Packard, Palo Alto, CA, USA). For manual injections, a Valco 6CW Valve (Valco, Houston, TX, USA), fitted with a 25-$\mu$l sample loop, was installed between the AASP injector valve and the HPLC column.

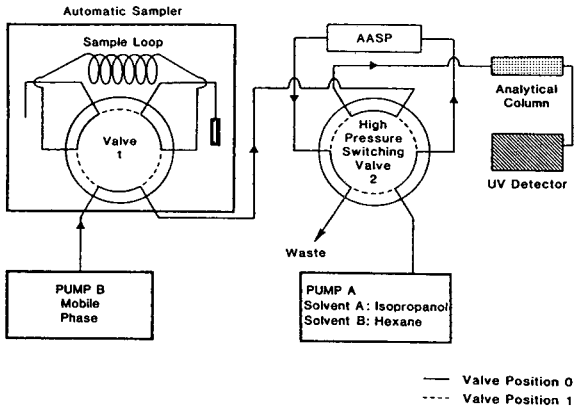


Fig. 1. Bio-FAST type HPLC system flow diagram.

### *Reagents*

Racemic ibuprofen, 2-phenylpropionic acid (internal standard), ethylchloroformate and *p*-anisidine were all purchased from Aldrich (St. Louis, MO, USA). The ibuprofen was recrystallized from heptane [18] and the *p*-anisidine was recrystallized from water–ethanol before use. Heptane, hexane, 2-propanol, methylene chloride and triethylamine (stored over KOH) were purchased from BDH (Montreal, Canada). The amide standard of racemic ibuprofen was prepared as previously described [19].

### *Derivatization procedures*

The derivatization procedures were based on the method previously described [15], with minor modifications. All the reagents were prepared as solutions in methylene chloride.

For the manual derivatizations each sample consisted of a mixture of 100 $\mu$l of ibuprofen stock solution and 100 $\mu$l of internal standard stock solution (500 $\mu$g/ml of 2-phenylpropionic acid). After the addition of 200 $\mu$l of 100 m*M*

triethylamine and 100 μl of 60 m*M* ethylchloroformate the sample was vortexed for 15 s. After a 15-min interval (T1), 100 μl of 0.5 *M* *p*-anisidine were added to the sample mixture, which was then vortexed for 15 s. After a 5-min interval (T2) the sample was diluted with 600 μl of isopropanol–hexane (10:90, v/v) to give a total volume of 1200 μl. The sample was vortexed for 15 s, and a 25-μl aliquot was injected.

The automated derivatization was performed by the Gilson sample processor and injector. The procedure was identical to the manual procedure described above, except for sample mixing. After the addition of each reagent, half the sample was aspirated and dispensed back into the vial three times.

*Bio-FAST HPLC procedure*

The time programming of valves and pumps is shown in Table I. AASP cartridges were purchased from Analytichem (Harbor City, CA, USA) and the AASP washing and conditioning solvents were 2-propanol and hexane. The analytical column was a Rexchrom Regis Pirkle D-phenylglycine column (25 cm × 4.6 mm I.D., 5 μm particle size) (Regis, Morton Grove, IL, USA). The mobile phase consisted of 2-propanol–hexane (10:90, v/v) at a flow-rate of 2.0

TABLE I

SEQUENCE OF VALVE SWITCHING AND PUMP OPERATION

| Time (min) | Operation | Effect |
|---|---|---|
| 0.0 | Valve 1: position 0<br>Valve 2: position 0 | Load fresh AASP cartridge |
| 0.05 | Gilson automatic sample processor and injector is started | Derivatization procedure is started |
| 15.05 | Pump A: isopropanol (4.0 ml/min) | Isopropanol wash of AASP cartridges |
| 16.56 | Pump A: isopropanol–hexane (10:90) (4.0 ml/min) | Conditioning of AASP cartridges with mobile phase |
| 18.56 | Pump A is stopped | AASP cartridges are prepared |
| 25.0 | Valve 2: position 1 | Mobile phase goes through AASP to effect final conditioning of cartridges |
| 25.45 | Sample is injected into loop filler port | Sample is loaded onto sample loop |
| 25.57 | Valve 1: position 1 | Integrator is started and sample is carried through the AASP cartridges where excess anisidine is trapped and mobile phase elutes the derivatized ibuprofen on to column |
| 25.60–29.30 | | Rinsing of injection needle and loop filler port |
| 28.0 | Valve 2: position 0 | End of on line time for AASP cartridge with column |
| 29.30 | Valve 1: position 0 | Sample loop ready for next sample |
| 29.9–30.0 | Automated advance to next AASP cartridge | Re-initiate cycle |

ml/min and was pumped continuously by Pump B. UV detection was at 254 nm.

*Anisidine trapping by AASP cartridges*

Solutions of ibuprofen amide standard and anisidine were prepared in 2-propanol–hexane (25:75, v/v). These were injected using the Gilson autosampler through the AASP when it was connected directly on-line with the HPLC column. Silica (SI), phenylboronic acid (PBA), carboxylic acid (CBA), propylbenzenesulfonic acid (SCX) and propylsulfonic acid (PRS) cartridges were evaluated for their efficiency in trapping the anisidine.

*Dilution of derivatization mixture with mobile phase*

Solutions of ibuprofen amide standards were prepared with varying ratios of methylene chloride and mobile phase. These were injected directly onto the analytical column and the resolution determined according to the formula $R_s = 1.18\Delta t_R/(w_1 + w_2)$ where $t_R$ indicates retention time and $w_1$ and $w_2$ are the peak widths at half height.

*Derivatization time study*

To optimize the derivatization times, T1 and T2 (see *Derivatization Procedures*) were evaluated. With T2 kept constant at 8 min, T1 was varied from 0.5 to 48 min. With T1 kept at 15 min, T2 was varied from 0.5 to 100 min. The total peak areas of the ibuprofen amides in triplicate analyses were used to evaluate the derivatization as a function of time.

*Determination of percent derivatization*

A standard curve from 40 to 170 $\mu$g/ml was prepared with synthetic ibuprofen amide standards. A quantity of ibuprofen was derivatized so that a 100% theoretical yield would have given a final derivative concentration of 100 $\mu$g/ml. These experiments were conducted using both the manual and automated procedures. From the calibration curve the true concentrations of derivatized product were determined. The percent yield was calculated as the ratio of experimental to theoretical concentrations of the amide derivatives.

*Validation study; standard curves*

Stock solutions of ibuprofen were prepared in methylene chloride at concentrations of 150, 300, 500, 1000, 2000 and 4000 $\mu$g/ml. Quality control (QC) solutions were prepared at concentrations of 160, 1200 and 3200 $\mu$g/ml. A 100-$\mu$l aliquot of each stock solution (see *Derivatization Procedures*) was processed through the fully automated procedure.

Standard curves were plotted using peak area ratios (each ibuprofen peak over the first internal standard peak) as a function of the amount of ibuprofen derivatized. Standard curves were generated on three different days, as well as on the same day, so as to give an indication of inter-day and intra-day reproducibility. Duplicate samples of three QC samples were run with each standard curve and were then back calculated using the best-fit linear regression of the standard curve for further statistical analysis.

## RESULTS AND DISCUSSION

The research was conducted to determine whether an HPLC system such as the Bio-FAST [16] could be used to effect a fully automated pre-column derivatization requiring solid phase work-up prior to analysis. The analysis of ibuprofen amides on the DNBPG column was chosen as a model system to develop this approach. The previously described manual derivatization procedure required a liquid–liquid extraction of excess anisidine since this reagent masked the ibuprofen peaks during chromatography [15]. Two approaches for the Bio-FAST method were envisaged. The first was to operate the column-switching so that the ibuprofen amides were retained on the pre-column and the anisidine transferred to waste. Unfortunately, none of the AASP cartridges selectively retained the ibuprofen amides. The second approach was to trap the excess anisidine on the cartridge while the ibuprofen amides passed directly onto the analytical column. Solutions of the ibuprofen amide standards injected directly onto the column compared with injections which passed through the AASP first, demonstrated that the retention times were retarded by about 0.5 min but the resolution did not deteriorate (data not

shown). This suggested that this approach would be viable, providing an appropriate cartridge could be found to retain the anisidine.

It was anticipated that anisidine could be trapped by an acidic solid phase. This was tested by injecting a mixture of the ibuprofen amide standards and anisidine through the AASP prior to chromatography. SI and PBA cartridges caused increased retention time of the anisidine but did not trap it. The addition of acetic acid to the injection solution did not increase the retention of anisidine. CBA cartridges had no apparent effect on the anisidine. SCX and PRS cartridges both effectively retained the anisidine. The extraction mechanisms for the SCX and PRS cartridges, proposed in Fig. 2, suggest that the interaction is ionic. The effect of a $\pi-\pi$ interaction between the aromatic ring of the anisidine and the sorbent group of the SCX cartridge is probably minimal since the PRS and SCX cartridges were equally efficient. Since the Bio-FAST HPLC uses a new cartridge for each sample the extraction efficiency for anisidine will be constant for a batch of samples. Fig. 3A and B compare a blank manual derivatization injected directly onto the analytical column with an automated blank derivatization processed through the PRS AASP cartridge. This demonstrates the effectiveness of the extraction.

Methylene chloride is used as the solvent for derivatization. A standard solution of ibuprofen amides in methylene chloride injected directly onto the analytical column gave broad peaks. The addition of mobile phase to the injection solution improved the peak shape and resolution (Fig. 4). Although the graph suggests that even 10% added mobile phase gave adequate resolution, fronting was observed on the peaks and baseline separation of the enantiomers was not achieved. It was concluded that a 1:1 ratio of methylene chloride and mobile phase gave good

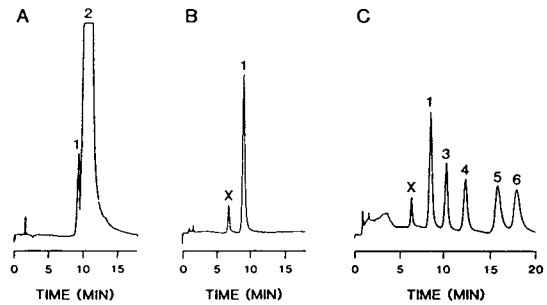


Fig. 3. Typical chromatograms. (A) Manual blank derivatization mixture (diluted 1:1 with mobile phase) injected directly onto the analytical column. (B) Automated blank derivatization (diluted as above) processed through PRS AASP cartridge. (C) Automated derivatization, dilution, extraction and analysis of racemic ibuprofen and internal standard (50 $\mu$g of each). Peaks: X = unknown impurity seen in automated derivatization procedure; 1 = urethane by-product [19]; 2 = anisidine; 3 = (*S*)-ibuprofen amide derivative; 4 = (*R*)-ibuprofen amide derivative; 5 = (*S*)-internal standard amide derivative; 6 = (*R*)-internal standard amide derivative. See Experimental section for HPLC conditions.

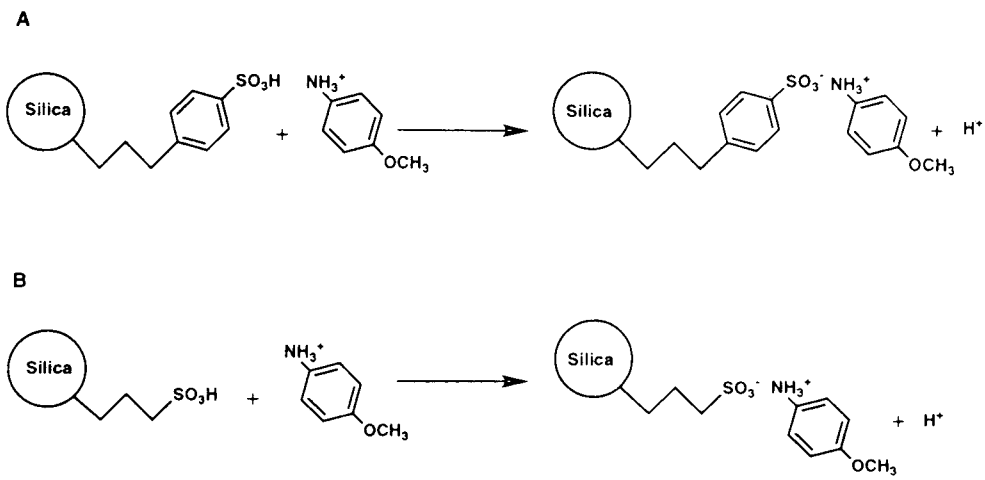


Fig. 2. Proposed extraction mechanisms for (A) SCX and (B) PRS cartridges.

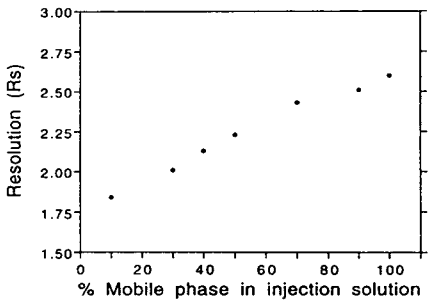


Fig. 4. Graph showing determination of optimal dilution of the methylene chloride solution with mobile phase. Chromatographic resolution of the racemic ibuprofen amide standard peaks is plotted against the percent mobile phase present in the injection solution.

compromise between maximum peak area and adequate peak shape. Therefore, before injection of the automated derivatizations, each crude mixture was diluted with an equal volume of mobile phase.

The Gilson sample processor and injector has been used in combination with the AASP for several bioanalytical applications [20,21]. In this application for ibuprofen derivatization the Gilson injector was preferred since flexible programming allowed for the optimization of some important parameters, including: (i) the rate of aspirating and dispensing the reagents, (ii) proper mixing of the samples and (iii) rinsing of the needle and injection port to avoid cross contamination. A study of the timing for T1 and T2 (see methods) indicated that each step of the derivatization could be as short as 5 min and longer periods of T1 or T2 did not increase the amount of derivatized product (data not shown). The percentage yields for the derivatization were $61.4 \pm 0.7\%$, $n = 2$ and $61.2 \pm 3.4$, $n = 3$ for the manual and automated derivatizations, respectively. Fig. 3C shows a typical chromatogram of ibuprofen and the internal standard processed through the entire automated derivatization, dilution, extraction and analysis procedure.

A validation study of the automated method was done in order to evaluate the accuracy and reproducibility of the assay. Intra-day reproducibility was assessed by using back-calculated QC samples as seen in Table II. These results indicate acceptable reproducibility and accuracy.

TABLE II

INTRA-DAY PRECISION (USING BACK-CALCULATED QC SAMPLES)

| | Nominal amount ($\mu$g/derivatization) | | |
|---|---|---|---|
| | 8.0 | 60.0 | 160.0 |
| *(S)-Ibuprofen* | | | |
| Mean observed | 7.8 | 55.9 | 168.3 |
| ±S.D. | 1.32 | 3.89 | 11.15 |
| R.S.D. (%) | 16.9 | 6.96 | 6.62 |
| % Nominal amount | 97.5 | 93.2 | 105.2 |
| *n* | 6 | 6 | 6 |
| *(R)-Ibuprofen* | | | |
| Mean observed | 7.2 | 54.4 | 167.8 |
| ±S.D. | 1.22 | 3.55 | 11.40 |
| R.S.D. (%) | 17.1 | 6.53 | 6.79 |
| % Nominal amount | 90.0 | 90.7 | 104.9 |
| *n* | 6 | 6 | 6 |

Linearity and inter-day reproducibility were assessed by comparing the six point standard curves obtained using racemic ibuprofen (15 $\mu$g–400 $\mu$g/derivatization) on three different days. The coefficients of correlation exceeded 0.994 for each enantiomer (*i.e.* 7.5 $\mu$g–200 $\mu$g range for each enantiomer). Average equations of the lines were: (*S*)-enantiomer $y = 0.029763x - 0.043725$ (slope relative standard deviation, R.S.D. = 4.72%, $n = 3$). (*R*)-Enantiomer $y = 0.031372x - 0.057435$ (slope R.S.D. = 6.54%, $n = 3$). The linearity range, reproducibility and accuracy were comparable to results obtained with the manual derivatization [15]. The limit of detection was 0.5 $\mu$g/ml ($S/N$ ratio = 2) for a racemic ibuprofen amide derivative standard solution injected directly onto the analytical column. For biological applications, a sample would need to be extracted and dried down before derivatization [15]. The limit of an assay would be governed by the volume of the biological fluid extracted and the presence of interfering peaks at the retention times of interest.

As seen in Table I, the derivatization process, the washing and conditioning of the AASP cartridges, and the HPLC analysis were all synchronized. Thus, as one sample was being

chromatographed, the next was undergoing the derivatization. During a 24-h run, up to 48 samples could be processed completely unattended. It would be difficult to do this many samples per day by the original manual method [15].

## CONCLUSIONS

The automated derivatization and HPLC analysis of ibuprofen enantiomers was achieved on a HPLC system similar to the Bio-FAST. The process was optimized by trapping the excess anisidine using either SCX or PRS solid-phase extraction cartridges prior to chromatography. Linear standard curves were obtained, with a detection range of 7.5–200 $\mu$g per derivatization for each enantiomer. Statistical analysis proved that the accuracy, intra-day and inter-day reproducibility of the assay were within acceptable limits.

This method demonstrates an application of a Gilson-AASP combination similar to the Bio-FAST wherein AASP cartridges are used for the efficient trapping of excess derivatizing reagent. It could be applied to the analysis of ibuprofen enantiomers in drug samples or in biological samples such as urine [15]. It could also be adapted for the normal-phase analysis of other drugs requiring pre-column derivatization and extraction of excess basic reagents, such as amines, prior to chromatography.

## REFERENCES

1 W.J. Wechter, D.G. Loughhead, R.J. Reischer, G.J. VanGiessen and D.G. Kaiser, *Biochem. Biophys. Res. Commun.*, 61 (1974) 833.
2 S.S. Adams, P. Bresloff and C.G. Mason, *J. Pharm. Pharmacol.*, 28 (1976) 256.
3 D.G. Kaiser, G.J. VanGiessen, R.J. Reischer and W.J. Wechter, *J. Pharm. Sci.*, 65 (1976) 269.
4 S.M. Sanins, W.J. Adams, D.G. Kaiser, G.W. Haltead, J. Hosley, H. Barnes and T.A. Baillie, *Drug Met. Dispos.*, 19 (1991) 405.
5 M.P. Knadler and S.D. Hall, *Chirality*, 2 (1990) 67.
6 R.D. Knihinicki, K.M. Williams and R.O. Day, *Biochem. Pharmacol.*, 38 (1989) 4389–4395.
7 Y. Nakamura, T. Yamaguchi, S. Takahashi, S. Hashimoto, K. Iwatari and Y. Nakagawa, *J. Pharm. Dyn.*, 4 (1981) S-1.
8 T. Yamaguchi and Y. Nakamura, *Drug Met. Dispos.*, 15 (1987) 535.
9 F. Jamali, N.N. Singh, F.M. Pasutto, A.S. Russell and R.T. Coutts, *Pharmaceutical Res.*, 5 (1988) 40.
10 S. Menzel-Soglowek, G. Gleisslinger and K. Brune, *J. Chromatogr.*, 532 (1990) 295.
11 E.J.D. Lee, K.M. Williams, G.G. Graham, R.O. Day and G.D. Champion, *J. Pharm. Sci.*, 73 (1984) 1984.
12 S. Fournel and J. Caldwell, *Biochem. Pharm.*, 35 (1986) 4153.
13 J.M. Maître, G. Boss and B. Testa, *J. Chromatogr.*, 299 (1984) 397.
14 A.C. Rudy, K.S. Anliker and S.D. Hall, *J. Chromatogr.*, 528 (1990) 395.
15 D.A. Nicoll-Griffith, T. Inaba, B.K. Tang and W. Kalow, *J. Chromatogr.*, 428 (1988) 103–112.
16 D. Lessard, D. Nicoll-Griffith and H.M. Hill, *Am Lab.*, October (1990) 42.
17 D. Nicoll-Griffith, R. Zamboni, J.B. Rasmussen, D. Ethier, S. Charleson and P. Tagari, *J. Chromatogr.*, 526 (1990) 341.
18 V.J. Capponi, G.W. Halstead and D.L. Theis, *J. Labelled Compd. Radiopharm.*, 23 (1986) 192–193.
19 D. Nicoll-Griffith, *J. Chromatogr.*, 402 (1987) 179.
20 E. Doyle, R.D. McDowall, G.S. Murkitt, V.S. Picot and S.J. Rogers, *J. Chromatogr.*, 527 (1990) 67–77.
21 D. Nicoll-Griffith and R. Zamboni, *Prostaglandins*, 43 (1992) 523–532.

*Journal of Chromatography A*, 653 (1993) 261–265
Elsevier Science Publishers B.V., Amsterdam

CHROM. 25 435

# Direct stereochemical resolution of SM-11044, a novel anti-asthmatic drug, and its stereoisomers using a chiral immobilized protein stationary phase

Masahiko Okamoto*, Yasutaka Ohgami and Hiroshi Nakazawa☆

*Environmental Health Science Laboratory, Sumitomo Chemical Co., Ltd., 1-98, 3-chome, Kasugade-naka, Konohana-ku, Osaka 554 (Japan)*

(First received March 15th, 1993; revised manuscript received July 6th, 1993)

ABSTRACT

A high-performance liquid chromatographic separation of SM-11044, a novel anti-asthmatic drug, and its antipode and stereoisomers was achieved using a chiral protein column that permits low levels of the antipode to be measured in the SM-11044. The influence of replacing $H_2O$ with $^2H_2O$ as the mobile phase and the effect of buffer ionic strength, pH, organic modifiers and temperature on the retention times and enantiomeric resolution are discussed.

## INTRODUCTION

SM-11044, L-*threo*-3-(3, 4-dihydroxyphenyl)-N-[3-(4-fluorophenyl)propyl]serine pyrrolidine amide hydrogen bromide (Fig. 1), is a newly synthesized anti-asthmatic drug that has potent anti-leukotriene $D_4$ ($LTD_4$) and anti-neurokinin A (NKA) activity and an inhibitory effect on the late asthmatic response in guinea pigs [1]. Bearing in mind the current importance of the optical purity of new drugs [2,3], we have been working with several chiral HPLC columns on the chiral separation of a variety of molecules [4–10].

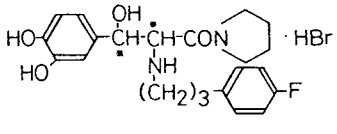


Fig. 1. Structure of SM-11044.

In this paper, we describe the direct separation of SM-11044 and its enantiomer on an ovomucoid column (Ultron ES-OVM). We also examine in detail the influence of replacing $H_2O$ with $^2H_2O$ as the mobile phase, and the effect of pH, buffer strength, temperature and organic modifier on retention time and resolution of SM-11044 and its enantiomer in order to gather information about the possible mechanisms of chiral recognition [11,12].

## EXPERIMENTAL

### *High-performance liquid chromatography*

A Shimadzu LC-5A instrument equipped with an SPD-2A variable-wavelength UV monitor was used. The eluent was pumped at 1.0 ml/min. The column was an Ultron ES-OVM (Shinwakako, Kyoto, Japan; 150 × 4.6 mm). The column temperature was controlled by an Eyela Uni Cool UC-65 circulating water bath (Tokyo Rikakikai, Tokyo, Japan).

* Corresponding author.
☆ Present address: Biotechnology Laboratory, Takarazuka Research Center, Sumitomo Chemical Co., Ltd., 4-chome, Takatsukasa, Takarazuka, Hyogo 665, Japan.

0021-9673/93/$06.00 

*Chemicals*

SM-11044, its enantiomer and its *erythro* forms were supplied by Research Laboratories, Sumotomo Pharmaceuticals (Osaka, Japan). Deuterium oxide ($^2H_2O$) was obtained from Wako (Osaka, Japan). Aqueous buffer solutions were prepared from potassium phosphate purchased from Wako. All other chemicals were of analytical-reagent grade.

*The acidity of $^2H_2O$ solutions*

The acidity ($p^2H$) of $^2H_2O$ solutions was measured with an ordinary glass electrode by adding 0.40 to the observed reading of the pH meter, which was calibrated with standard buffers in aqueous solution [13].

## RESULTS AND DISCUSSION

Experiments with the ovomucoid chiral column (Ultron ES-OVM) were immediately successful. The chromatographic conditions for the resolution of SM-11044, its enantiomer and stereoisomers with Ultron ES-OVM were optimized by changing mobile phase conditions such as buffer strength, pH and organic modifiers, and temperature. The optimal conditions shown in Fig. 2a allowed for the complete baseline separation of SM-11044 and its enantiomer. Under these conditions four possible stereoisomers of SM-11044 could be separated, as shown in Fig. 2b. The total HPLC run time was less than 20 min. It was determined by chromatography of each individual isomer of SM-11044 that the elution order was SM-11044 first (retention time, $t_R = 7$ min), the *erythro* forms of SM-11044 second and third ($t_R = 9$ and 11 min) and the antipode of SM-11044 fourth ($t_R = 17$ min).

The precision of this method was addressed by performing a recovery test. The antipode of SM-11044 was added to SM-11044 to give a concentration of 0.5 or 1.0%. The added antipode of SM-11044 was recovered quantitatively at both concentrations using this procedure (Table I), demonstrating the chromatographic method to be precise and repeatable.

To gather information on the mechanism of interaction between ovomucoid and SM-11044 and its enantiomer, we examined the influence on the enantiomeric separation of replacing water ($H_2O$) with deuterium oxide ($^2H_2O$) as

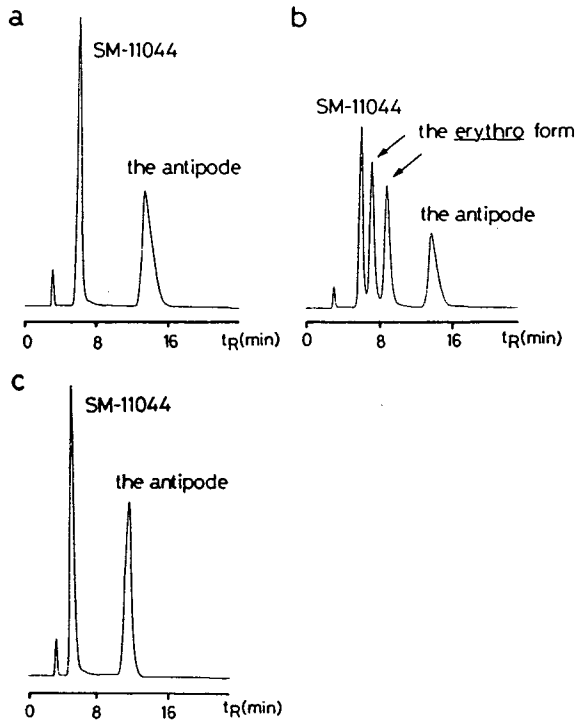


Fig. 2. (a) Resolution of SM-11044 and its enantiomer on an Ultron ES-OVM column. Mobile phase, 20 m*M* phosphate buffer (pH 5.2)–acetonitrile (94:6); flow-rate, 1.0 ml $min^{-1}$; temperature, 25°C; UV detection at 280 nm; injection volume, 5 $\mu$l (1 $\mu$g each). (b) Resolution of SM-11044 and its stereoisomers. Other conditions as in (a). (c) Chromatogram of separation of SM-11044 and its enantiomer at $p^2H$ around 5.2. Other conditions as in (a).

TABLE I

RESULTS OF TESTS ON THE RECOVERY OF THE ANTIPODE OF SM-11044 FROM SM-11044

| Calculated (%) | Found (%) | Recovery (%) | Standard deviation |
|---|---|---|---|
| 1.00 | 1.00 | 100.0 | $8.9 \cdot 10^{-3}$ ($n = 5$) |
| 0.50 | 0.49 | 98.0 | $7.5 \cdot 10^{-3}$ ($n = 5$) |

the mobile phase. The viscosity, dipole moment, dielectric constant and ionization of $^2H_2O$ are significantly different from those of $H_2O$ [14,15]. We could not observe any apparent effect on the resolution, although the retention of the solutes was slightly decreased (Fig. 2c). Camilleri and Dyke [16] have reported that for atenolol there is no significant increase in resolution of the enantiomer on an $\alpha_1$-acid glycoprotein ($\alpha_1$-AGP) column using $^2H_2O$ as the mobile phase, whereas the effect of $^2H_2O$ on the enantiomeric separation of ibuprofen is drastic. We suppose that such an effect is not universal with all compounds.

The retention and resolution of SM-11044 can be regulated in four ways: by varying the buffer ionic strength or the pH of the mobile phase, by addition of an organic modifier to the mobile phase or by changing the column temperature.

The effects of buffer ionic strength were examined at pH 5.2 using three phosphate buffer concentrations ranging from 5 to 50 m*M*. All the mobile phases contained 6% acetonitrile as the organic modifier. The data are shown in Table II. At higher buffer strength, the capacity factors ($k'$) were increased, the separation factors ($\alpha$) were slightly decreased and the peaks were broadened. This indicates that hydrophobic interactions are involved in the retention of SM-11044.

The effect of mobile phase pH was studied in the range between 4.5 and 7.3 while maintaining a 20 m*M* phosphate concentration and buffer–acetonitrile (9:1, v/v) composition. The results, as shown in Table III indicate increased resolution with decreasing pH. Retention of SM-11044 became stronger with increasing pH. Ovomucoid has an isoelectric point of 4.1 and has a net negative charge at higher pH. Our preliminary experiment shows that SM-11044 has a $pK_a$ of 8.6. At pH 5.2 the protein has a negative charge, and the solute is positively charged. Hence Coulombic interaction is important for the chiral recognition of SM-11044 as well as for its retention.

The retention and selectivity were greatly influenced by the content and type of organic modifier in the mobile phase. Increasing the concentration of the organic modifier reduces the

TABLE II

INFLUENCE OF BUFFER IONIC STRENGTH (m*M*) ON THE CAPACITY FACTOR ($k_1'$), SEPARATION FACTORS ($\alpha$), RESOLUTION ($R_s$), THEORETICAL PLATE NUMBER ($N$) AND BAND ASYMMETRY FACTOR (*asf*)

Mobile phase: phosphate buffer (pH 5.2)–acetonitrile (94:6); column temperature: 25°C.

| Ionic strength (m*M*) | $k_1'$[a] | $\alpha$[b] | $R_s$[c] | $N$[d] | *asf*[e] |
|---|---|---|---|---|---|
| 5 | 1.43 | 4.20 | 2.81 | 1350 | 1.20 |
| 20 | 1.80 | 4.70 | 3.56 | 1300 | 1.20 |
| 50 | 2.09 | 3.33 | 5.01 | 1150 | 1.21 |

[a] The capacity factors, $k_1'$ (of the first-eluted enantiomer) and $k_2'$ (of the second-eluted enantiomer), were calculated as follows: $k_1' = (t_{R1} - t_0)/t_0$. $k_2' = (t_{R2} - t_0)/t_0$.

[b] The separation factor $\alpha = k_2'/k_1'$.

[c] $R_s$ (resolution factor) = 2 × (distance of the two enantiomer peak positions/sum of the band widths of the two peaks at their bases); $R_s = 2\ (t_{R2} - t_{R1})/(w_1 + w_2)$.

[d] $N$ (theoretical plate number) = 5.54 × ($t_{R1}$/the peak width at half-height)$^2$. The peak of SM-11044 was used for calculation.

[e] ASF (band asymmetry factor) = $(a + b)/2a$ where $a$ and $b$ are the peak width of SM-11044, as shown below.

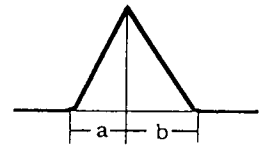


TABLE III

INFLUENCE OF pH ON THE CAPACITY FACTORS ($k_1'$), SEPARATION FACTORS ($\alpha$), RESOLUTION ($R_s$), THEORETICAL PLATE NUMBER ($N$) AND BAND ASYMMETRY FACTOR (*asf*)

Mobile phase: 20 m*M* phosphate buffer–acetonitrile (90:10); column temperature: 25°C. Footnotes as in Table II.

| pH | $k_1'$[a] | $\alpha$[b] | $R_s$[c] | $N$[d] | *asf*[e] |
|---|---|---|---|---|---|
| 4.5 | 0.76 | 1.55 | 3.55 | 980 | 1.18 |
| 5.2 | 1.80 | 3.56 | 4.70 | 1300 | 1.20 |
| 6.5 | 4.79 | 1.38 | 3.72 | 550 | 1.43 |
| 7.3 | 9.87 | 1.32 | 2.75 | 270 | 1.72 |

TABLE IV

INFLUENCE OF MONOVALENT ALCOHOLS AND ACETONITRILE ON THE RESOLUTION OF SM-11044 AND ITS ANTIPODE

Mobile phase: modifier + 20 m*M* phosphate buffer (pH 5.2); column temperature: 25°C. Footnotes as in Table II.

| Modifier | $k'^a$ | $\alpha^b$ | $R_s^c$ | $N^d$ | $asf^e$ | Elution order |
|---|---|---|---|---|---|---|
| Acetonitrile (6%) | 1.80 | 3.56 | 4.70 | 1300 | 1.20 | L/D |
| Methanol (15%) | 1.96 | 4.86 | 3.58 | 700 | 1.29 | L/D |
| Ethanol (10%) | 1.10 | 3.18 | 2.79 | 1030 | 1.25 | L/D |
| 1-Propanol (2%) | 2.13 | 6.29 | 4.37 | 700 | 1.29 | L/D |
| 2-Propanol (3%) | 1.97 | 7.70 | 4.58 | 700 | 1.25 | L/D |

capacity factor. Table IV gives some results obtained using monovalent alcohol and acetonitrile as an organic modifier. Acetonitrile was found to be the best modifier for SM-11044. Although 1- and 2-propanol gave good separation factors for SM-11044 (6.29 and 7.70 respectively), the peaks were broadened in both cases. The elution order was not changed by changing the organic modifier used. These results show that the organic modifiers are involved in the hydrophobic interactions required for the chiral recognition process.

The chromatography was evaluated at temperatures from 5 to 45°C. These data are shown in Table V. As expected, the resolution increased at the expense of longer retention times as well as broadened peak shape when the column temperature was decreased. No significant column degradation was observed upon operation at higher temperatures. Around 25°C chromatography was not affected by slight changes in temperature.

TABLE V

EFFECT OF TEMPERATURE ON THE CAPACITY FACTORS ($k'_1$), SEPARATION FACTORS ($\alpha$), RESOLUTION ($R_s$), THEORETICAL PLATE NUMBER ($N$) AND BAND ASYMMETRY FACTOR ($asf$)

Mobile phase: 20 m*M* phosphate buffer (pH 5.2)–acetonitrile (94:6). Footnotes as in Table II.

| Temperature (°C) | $k'^a_1$ | $\alpha^b$ | $R_s^c$ | $N^d$ | $asf^e$ |
|---|---|---|---|---|---|
| 5 | 3.15 | 4.16 | 5.86 | 1820 | 1.20 |
| 15 | 2.35 | 3.80 | 5.04 | 1390 | 1.23 |
| 25 | 1.80 | 3.56 | 4.70 | 1300 | 1.20 |
| 35 | 1.36 | 3.20 | 3.15 | 1410 | 1.21 |
| 45 | 1.06 | 2.81 | 1.41 | 780 | 1.22 |

In conclusion, excellent resolution can be obtained for SM-11044, its antipode and stereoisomers by using ovomucoid as the chiral stationary phase. The enantiomeric purity of SM-11044 can be also evaluated directly, rapidly and accurately by this HPLC method.

REFERENCES

1 T. Sugasawa, M. Uchida and S. Morooka, *XIII World Congress of Asthmology, Maebashi, Japan, October 1990*, abstracts, p. 203.
2 A.M. Krstulovic (Editor), *Chiral Separations by HPLC*, Ellis Horwood, Chichester, 1989.
3 M.N. Cayen, *Chirality*, 3 (1991) 94.
4 M. Okamoto and H. Nakazawa, *J. Chromatogr.*, 504 (1990) 445.
5 M. Okamoto and H. Nakazawa, *J. Chromatogr.*, 508 (1990) 217.
6 M. Okamoto and H. Nakazawa, *J. Chromatogr.*, 588 (1991) 177.
7 M. Okamoto and H. Nakazawa, *Anal. Sci.*, 7 (Suppl.) (1991) 147.
8 M. Okamoto, R. Sato, E. Nagano and H. Nakazawa, *Agric. Biol. Chem.*, 55 (1991) 3151.
9 M. Okamoto and H. Nakazawa, *Biosci. Biotech. Biochem.*, 56 (1992) 1172.
10 M. Okamoto and H. Nakazawa, *Biosci. Biotech. Biochem.*, 57 (1993) 1768.
11 T. Miwa, M. Ichikawa, M. Tsuno, T. Hattori, T. Miyakawa, M. Kawano and Y. Miyake, *Chem. Pharm. Bull.*, 35 (1987) 682.

12 T. Miwa, T. Miyakawa and M. Kawano, *J. Chromatogr.*, 408 (1987) 316.
13 P.K. Glasoe and F.A. Long, *J. Phys. Chem.*, 64 (1960) 188.
14 T.A. Baillie, *Stable Isotopes*, Macmillan, London, 1978.
15 K.B. Wiberg, *Chem. Rev.*, 55 (1955) 713.
16 P. Camilleri and C. Dyke, *J. Chromatogr.*, 518 (1987) 277.

*Journal of Chromatography A*, 653 (1993) 267–273
Elsevier Science Publishers B.V., Amsterdam

CHROM. 25 419

# Evaluation of the capability of different chromatographic systems for the monitoring of thimerosal and its degradation products by high-performance liquid chromatography with amperometric detection

M. del Pilar da Silva, Jesús R. Procopio* and Lucas Hernández

*Department of Analytical Chemistry and Instrumental Analysis, Science Faculty, Autonoma University of Madrid, Cantoblanco, E-28049 Madrid (Spain)*

(First received October 27th, 1992; revised manuscript received June 22nd, 1993)

ABSTRACT

Several liquid chromatographic systems using electrochemical detection on carbon electrodes were compared for the analysis of thimerosal and its degradation products, thiosalicylic acid and dithiodibenzoic acid. The studied separation systems included reversed-phase ion-suppressed chromatography, reversed-phase ion-pair chromatography and ion chromatography. Amperometry and coulometry were evaluated as electrochemical detection techniques. The best method for thimerosal determination in ophthalmic solutions in terms of selectivity and sensitivity was ion-pair chromatography.

## INTRODUCTION

Thimerosal (sodium ethylmercury thiosalicylate, TMS) is an organomercurial compound widely employed as a topical antiseptic and antimicrobial preservative for ophthalmic use and, in particular, is routinely employed in the formulation of hard and soft contact lens antiseptic solutions. Stability studies have revealed that this compound is unstable to light in aqueous solutions [1,2], mainly in glass bottles, and can be adsorbed by plastic [3,4], both of which factors influence the potential shelf-life of pharmaceutical products. It has also been reported that the presence of halides can have an adverse influence on the stability of thimerosal [5].

The decomposition of thimerosal in aqueous solution has been reported [2,4], and it has been shown that the major degradation products are thiosalicylic acid, (TSA) and 2,2′-dithiodibenzoic acid (DTDBA). In studies of degradation, and for routine analytical purposes, a number of analytical methods have been developed, including colorimetry [3,5,6], atomic absorption spectrometry [7–9] and polarography [10–11]. These techniques, based on total mercury or total organic mercury assay, do not indicate accurately the amount of intact thimerosal present in solution. Liquid chromatography has been suggested as a simple, specific method for analysis of intact thimerosal and its degradation compounds [3,4,7,12–17]. In all these methods, UV detection was used, except one [16] in which coulometric detection was applied for TMS determination, but no information regarding degradation products was given.

In our laboratory, we are developing different

* Corresponding author.

0021-9673/93/$06.00 

chromatographic methods for the determination of TMS and its degradation products in manufactured samples. In order to obtain more sensitive and selective detection of these samples, and considering the easy oxidation of these compounds on carbon electrodes, electrochemical detection was chosen as the most appropriate technique. Two electrochemical detection modes, amperometric and coulometric, were evaluated.

Related to these studies, in a previous paper [18] we described the use of amperometric detection on a glassy carbon electrode for determination of TMS, TSA and DTDBA by reversed-phase ion-suppressed chromatography. The method was applied to the determination of these compounds in ophthalmic formulations and, although detectability was adequate, high limits of detection were obtained, of the same order of magnitude as with UV detection. The present work improves previous results by increasing the sensitivity obtained using coulometric detection compared with amperometric ion-suppression chromatography (ISC).

Another problem associated with using ISC with real samples is the significant decrease in the retention time of TMS observed as a result of the presence of polymers in the samples. To resolve this problem, we propose the use of reversed-phase ion-pair chromatography (IPC) and ion-exchange chromatography (IEC) as separation techniques.

## EXPERIMENTAL

### *Reagents and samples*

Thimerosal (Alcon Iberhis, Madrid, Spain), thiosalicylic and 2,2′-dithiodibenzoic acids (Sigma, St. Louis, MO, USA) were used without further purification. Methanol, acetonitrile, 85% phosphoric acid, 99% acetic acid, 30% ammonium hydroxide, sodium perchlorate, potassium hydrogenphthalate, potassium nitrate (Carlo Erba, Milan, Italy), tetrabutylammonium perchlorate (TBAP) and tetraethylammonium perchlorate (TEAP; Sigma) were analytical reagent grade. Stock solution of thimerosal was made up in water, whereas stock solutions of TSA and DTDBA were made up in methanol, in a concentration of about 100 $\mu$g/ml. These solutions were stable for a week when stored at 4°C and protected from light.

Soft lens care products were obtained from Alcon Iberhis. These samples contain TMS in a concentration of 0.01 mg/ml. Other ingredients were disodium edetate, sodium chloride, phosphate buffer and a catalase.

### *Apparatus*

For reversed-phase chromatography, the HPLC system consisted of a Gilson Model 302C pumping system, equipped with a membrane damper, a Rheodyne Model 7125 injector equipped with a 20-$\mu$l loop, and a Spectra Physics SP 4290 integrator. When ion chromatography was used, the HPLC system consisted of a Shimadzu Model LC9A pumping system and a CTO-6A column oven and the injector was equipped with a 100-$\mu$l loop. A Shimadzu CR4A Cromatopac was used in this case. As a detector we used a Metrohm Model 461 amperometric detector equipped with a Metrohm Model 656 flow cell, of less than 1 $\mu$l volume, or an ESA Model 5010 coulometric cell of 2 $\mu$l volume. A glassy carbon electrode (Metrohm 6.0805.010) or a carbon paste electrode (Metrohm 6.0807.000) with an area of 7 $mm^2$ was used as the amperometric working electrode. The detector was operated in amperometric mode at a sensitivity of 10 nA full scale. When coulometric mode was used, the detector was operated at a sensitivity of 0.1 $\mu$A full scale.

### *Chromatographic conditions*

For reversed-phase chromatography the column used was a 150 × 4 mm stainless-steel prepacked column containing 5-$\mu$m Spherisorb $C_{18}$ particles (Tracer, Madrid, Spain). In IPC, the mobile phase was methanol–water (55:45, v/v) containing 2 mmol of TBAP or methanol–water (50:50, v/v) containing 2 mmol of TEAP, both adjusted to pH 4.8 with $HClO_4$. For ISC with coulometric detection, the mobile phase was methanol–water (60:40, v/v) containing 0.005 mol/l phosphoric acid. The flow-rate was 1.0 ml/min. For IEC the column was a 50 × 4.6 mm plastic column prepacked with 10-$\mu$m ammonium quaternary polymeric resin of low capacity

(30 μequiv./g) (TR-anion; Tracer). The mobile phase was 7.5 m*M* potassium perchlorate, and the flow-rate was adjusted in this case to 1.5 ml/min.

Mobile phase solutions were filtered through a Millipore Durapore filter (0.45 μm pore size) and deaerated by stirring under vacuum for at least 15 min. Standard solutions of all compounds were prepared in mobile phase and filtered through a similar filter before injection into the chromatograph.

The aqueous manufactured samples of TMS were injected without modification or after extraction with a $C_{18}$ Sep-Pak cartridge (Millipore). The extraction procedure was as follows. A 0.1-ml aliquot of concentrated phosphoric acid was added to 10 ml of soft lens care solution. The mixture was pumped with a syringe through a Sep-Pak cartridge preconditioned with methanol and water. The cartridge was washed with 5 ml of water and 2 ml of 20% of methanol solution and then TMS, TSA and DTDBA were eluted with 2 ml of methanol. The extract was diluted to 10 ml with eluent and injected into the chromatograph.

*Electrode pretreatment procedure*

The pretreatment procedure for LC working electrodes was as follows. Before each set of measurements (every day), the amperometric glassy carbon electrode surface was polished with the polishing cloth for 60 s and rinsed with water before being attached to the detector. The coulometric cell was cleaned by flushing the cell with 5 ml each of water, 3 *M* nitric acid and water again before attaching the cell to the chromatograph. A suitable working potential was applied to the electrode while the mobile phase was passed through the system until a stable baseline was obtained.

## RESULTS AND DISCUSSION

*Chromatographic studies*

Chromatographic conditions for TMS, TSA and DTDBA in reversed-phase ion-suppression chromatography have been reported elsewhere [18]. In IPC, the effect of the counter-ion concentration on separation and signal-to-noise ratio was studied for both TEAP and TBAP, varing the concentration between 0.01 and 0.001 *M*. Adequate resolutions and analytical signals were obtained at concentrations of 0.002 *M* for both types of counter-ions studied. Mobile phases containing 55 and 50% methanol for TBAP and TEAP, respectively, were chosen in order to obtain a similar retention of the products for both types of counter-ions. The pH value of the eluent does not affect the retention times of TMS and TSA, as long as it is higher than 4 ($pK_a$ values are lower than 4); in this case the retention time of TSA is lower than that of TMS. For DTDBA, which contains two acidic groups, the pH value of mobile phase must be kept between 4 and 5 in order to obtain an adequate resolution. Under these conditions, DTDBA appears at retention times higher than TMS.

When IEC was employed, potassium hydrogenphthalate, potassium nitrate and potassium perchlorate were evaluated as eluents. The most efficient compound was potassium perchlorate as determined by both adequate separation and low noise in the detector. Appropriate resolutions for TMS and TSA were obtained using eluent concentrations of 0.0075 *M* at a flow-rate of 1.5 ml/min. Under these conditions, DTDBA presented retention times higher than 30 min, and no peak was observed at concentrations lower than 20 μg/ml. Under these conditions, peaks were broad and not baseline resolved ($R_s$ = 0.95). No improvement in the resolution was obtained by including small amounts of methanol or acetonitrile in the eluent. Therefore IEC was not further considered.

*Electrochemical studies*

Fig. 1 shows the hydrodynamic curves obtained for the three compounds studied using ion-pair chromatography in amperometric mode. It was observed that TMS and TSA reached a maximum and almost constant signal at potentials higher than 0.8 V. For DTDBA, however, the higher signal was obtained at a potential of 1.2 V. In addition to these results, lower backgrounds and noises were obtained at potentials lower than 1.0 V. At higher potentials a significant increase in background and noise was ob-

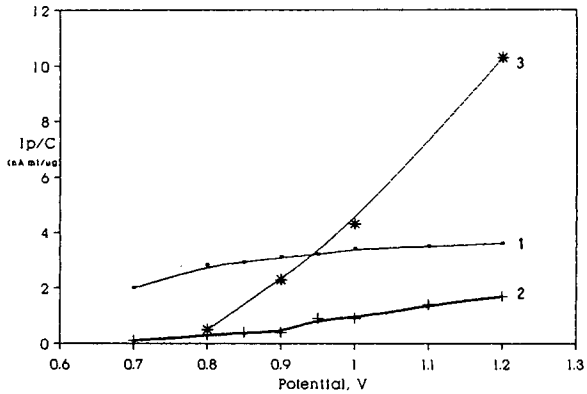


Fig. 1. Hydrodynamic voltammograms of compounds studied with amperometric detection. Eluent: 50% (v/v) methanol in water, containing 0.0020 *M* TEAP adjusted to pH 4.8 with perchloric acid. Concentrations: (2) TMS 11.1 μg/ml, (1) TSA 9.1 μg/ml and (3) DTDBA 9.6 μg/ml. Background (···).

served when the potential increased. Because of these results, a potential of 0.9 V for the simultaneous quantitation of TMS and TSA and a potential of 1.2 V for the quantitation of DTDBA were chosen in order to obtain the highest sensitivity for each compound.

The hydrodynamic curves obtained in the coulometric detection mode for IPC (Fig. 2) showed a higher signal at a potential value of 0.8 V for all studied compounds. Therefore, a potential of 0.8 V was chosen for simultaneous detection of TMS, TSA and DTDBA.

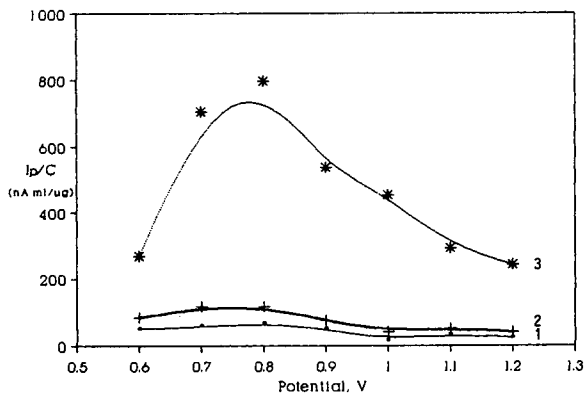


Fig. 2. Hydrodynamic voltammograms of compounds studied with coulometric detection. Concentrations: (1) TSA 1.00 μg/ml, (2) TMS 1.22 μg/ml and (3) DTDBA 1.06 μg/ml. Eluent as Fig. 1.

As in IPC, in ISC the efficiency of the coulometric detector observed allowed the detection of DTDBA, together with TMS and TSA, at potentials lower than 1.2 V with a better sensitivity. From coulometric hydrodynamic voltammograms, a potential of 0.9 V was chosen for simultaneous detection and quantitation of all compounds studied. The variation of signal-to-noise ratio with phosphoric acid concentration in the eluent, ranging from 0.01 to 0.001 *M*, was evaluated for this detector type. An eluent with a lower concentration of phosphoric acid, 5 m*M*, than in amperometric detection was chosen in order to obtain an optimum signal-to-noise ratio without a significant increase in the retention time.

*Calibration graphs, sensitivity and precision*

The linearity of the calibration graphs was checked up to 100 μg/ml in the amperometric detection mode and up to 5 μg/ml in the coulometric mode. For amperometric detection, linearity was observed at all concentration ranges assayed, whereas in coulometric detection no linearity was observed at concentrations higher than 2 μg/ml. The statistical treatment of the calibration graphs and limits of detection obtained for all compounds are reported in Table I for the ion-pair chromatographic method. As can be observed, the detection limits found in amperometric mode when TBAP was used as counter-ion were two orders of magnitude higher than when TEAP was used. In coulometric detection the results obtained were of the same order of magnitude for both counter-ions when the working electrode was treated daily with 3.0 *M* nitric acid. When no pretreatment was applied, the analytical signal decreased with increasing number of injections, especially when TBAP was used as counter-ion, obtaining under these conditions limits of detection higher than 0.1 μg/ml and poorer linearity. This could be due to adsorption of counter-ion on the electrode surface. This effect is less important for TEAP. Periodic cleaning of the glassy carbon electrode surface with 3.0 *M* nitric acid removes impurities and regenerates the analytical signal. This electrode pretreatment must be carried out very frequently when TBAP is used, whereas

TABLE I

STATISTICAL TREATMENT OF CALIBRATION GRAPHS AND DETECTION LIMITS (LD) ON CARBON ELECTRODES IN ION-PAIR CHROMATOGRAPHY

Working potential: amperometry, TSA and TMS 0.9 V and DTDBA 1.2 V; coulometry, 0.8 V (signal-to-noise ratio = 3:1). GCE = Glassy carbon electrode; CPE = carbon paste electrode.

| Counter-ion | Detection technique | Compound | Sensitivity ($\mu$A ml/$\mu$g) | LD ($\mu$g/ml) | $r$ |
|---|---|---|---|---|---|
| TBAP | Amperometry GCE | TSA | 225 | 0.2 | 0.9967 |
| | | TMS | 11 | 2.0 | 0.9990 |
| | | DTDBA | 11 | 2.0 | 0.9996 |
| | Coulometry | TSA | 29.33 | 0.002 | 0.9998 |
| | | TMS | 3.86 | 0.02 | 0.9997 |
| | | DTDBA | 30.76 | 0.002 | 0.9993 |
| | Amperometry CPE | TSA | 0.049 | 0.04 | 0.9987 |
| | | TMS | 0.022 | 0.09 | 0.9994 |
| | | DTDBA | 0.011 | 0.2 | 0.9997 |
| TEAP | Amperometry GCE | TSA | 0.017 | 0.07 | 0.9994 |
| | | TMS | 0.002 | 0.7 | 0.9950 |
| | | DTDBA | 0.012 | 0.4 | 0.9997 |
| | Coulometry | TSA | 29.5 | 0.004 | 0.9995 |
| | | TMS | 29.8 | 0.006 | 0.9997 |
| | | DTDBA | 55.2 | 0.003 | 0.9995 |
| | Amperometry CPE | TSA | 0.089 | 0.03 | 0.9990 |
| | | TMS | 0.045 | 0.09 | 0.9994 |
| | | DTDBA | 0.023 | 0.1 | 0.9993 |

when TEAP was used the pretreatment was carried out weekly. These problems can be easily solved in amperometric detection using a carbon paste electrode. This electrode presents lower passivation effects, and lower detection limits were obtained without changing the electrode surface (see Table I). It is more advantageous to use TEAP as counter-ion because of its superior electrochemical behaviour. Fig. 3 shows typical chromatograms of mixtures of TSA, TMS and DTDBA obtained with eluents and potential values optimum for simultaneous detection.

In ion-suppressed chromatography, the limits of detection found for coulometric detection mode ranged between 1 and 12 $\mu$g/ml, and were only one order of magnitude lower than those obtained in amperometric mode [18], but three orders of magnitude higher than IPC (Table I). From these results it can be deduced that IPC is a more suitable separation method than ISC when electrochemical detection is used.

Replicate samples of the three compounds were injected at approximately 1.0 $\mu$g/ml concentration in amperometric detection and 0.1 $\mu$g/ml in coulometric detection for IPC, in order to obtain a measure of method reproducibility. For amperometric detection using carbon paste electrodes, the methods exhibited a relative standard deviation ranging between 1.0 and 3.0% when TEAP was used as counter ion. When TBAP was used, higher relative standard deviation values (up to 7.0%) were obtained. In coulometric detection, relative standard deviation values ranging from 0.0 to 4.0% for both counter ions were obtained.

*Determination of TMS in ophthalmic solutions*

Several soft lens products containing non-degraded 0.001% TMS were assayed using the proposed methods. Contaminants present in the sample did not interfere with the IPC method, but a small decrease in the retention time for TMS was observed when successive sample solutions were injected owing to the presence of

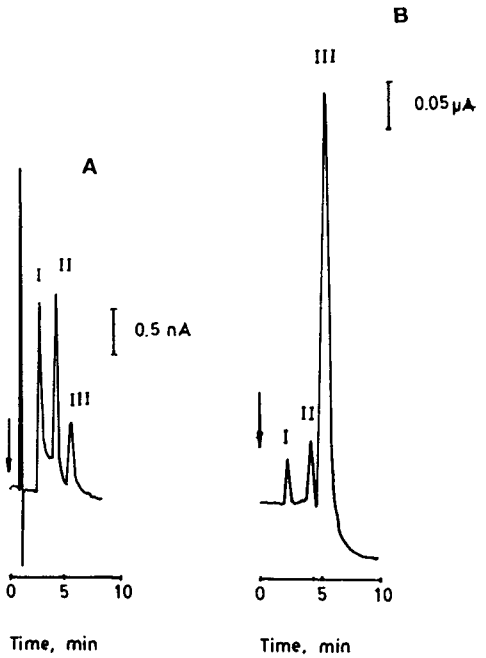


Fig. 3. Chromatogram obtained in ion-pair chromatography. (A) Carbon paste amperometric detection at 1.2 V. Concentrations: TSA (I) 5.05 μg/ml, TMS (II) 6.50 μg/ml and DTDBA (III) 5.00 μg/ml. (B) Coulometric detection at 0.8 V. Concentrations: TSA (I) 1.00 μg/ml, TMS (II) 1.22 μg/ml and DTDBA (III) 1.06 μg/ml. Eluent as Fig. 1.

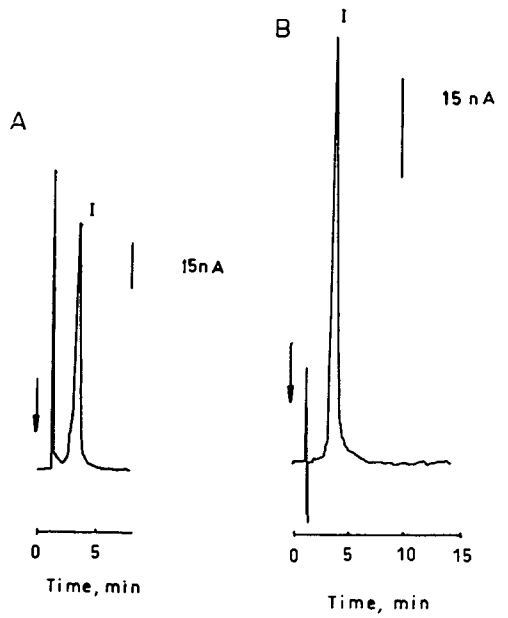


Fig. 4. Chromatogram of a manufactured sample containing 10 μg/ml thimerosal (I) in ion-pair chromatography using carbon paste electrodes and amperometric detection. (A) Mobile phase containing 20 n*M* TEAP as counter-ion concentration without extraction. (B) Mobile phase containing 2 m*M* TEAP, after Sep-Pak extraction.

polymers that can coat the column packing. This small decrease in the retention time of TMS did not affect the peak area evaluation. In ISC this effect was more important [18]. The changes in retention times can be almost removed by increasing the concentration of counter-ion in eluent up to 20 m*M* (Fig. 4A). In order to overcome this problem, a $C_{18}$ Sep-Pak cartridge was used for quantitative extraction of TMS and degradation products. Using this method of separation, retention time and peak shape of TMS do not change and the external standard method can be used for quantitation (Fig. 4B). Recoveries higher than 95% were obtained in the extraction step for TMS, in concentrations ranging from 1.0 to 10 μg/ml.

The results obtained for TMS concentration by IPC methods are compared with those obtained by standard cold-vapour atomic absorption spectrometry (CVAAS) (Table II). The good agreement between these data and the absence of changes in the retention times when the IPC method was used indicate that this method is more useful for the determination of TMS and its degradation products in ophthalmic solutions than other methods described previously. The sensitivity of the coulometric detection mode is sufficient to detect small amounts of TSA and DTDBA in low degraded samples.

TABLE II

THIMEROSAL CONCENTRATION (μg/ml) IN SOFT CONTACT LENS PRODUCTS BY IPC ($n = 3$)

| Sample | I | II | III |
|---|---|---|---|
| 1 | 10.7 ± 0.7 | 10.3 ± 0.3 | 10.6 ± 0.4 |
| 2 | 10.5 ± 0.4 | 10.1 ± 0.7 | 10.7 ± 0.7 |
| 3 | 9.3 ± 0.6 | 10.1 ± 0.6 | 10.7 ± 0.3 |

REFERENCES


1 K. Tsuji, Y. Yamawaki and Y. Miyazaki, *Arch. Pract. Pharm.*, 24 (1951) 110.
2 E.O. Davisson, H.M. Powell, J.O. MacFarlane, R. Hodson, R.L. Stone and D.G. Culbertson, *J. Lab. Clin. Med.*, 47 (1956) 8.
3 N.E. Richardson, D.J.G. Davies, V.J. Meakin and D.A. Norton, *J. Pharm. Pharmacol.*, 29 (1977) 717.
4 M.J. Reader and C.D. Lines, *J. Pharm. Sci.*, 72 (1983) 1406.
5 E. Lüdtke, J. Darsow and R. Pohloudek-Fabini, *Pharmazie*, 32 (1977) 99.
6 J. Viska and A. Okac, *Cesk. Farm.*, 16 (1967) 29.
7 S.N. Ibrahim, N. Stroud and V.J. Meakin, *J. Pharm. Pharmacol.*, 30 (1978) 52.
8 B.J. Meakin and Z.M. Khammas, *J. Pharm. Pharmacol.*, 31 (1979) 653.
9 P.G. Takla and V. Valajanian, *Analyst*, 107 (1982) 378.
10 W. Hollk, *J. Assoc. Off. Anal. Chem.*, 66 (1983) 1203.
11 S. Pinzauti and M. Casini, *Il Farmaco, Ed. Pr.*, 2 (1980) 92.
12 C. Fu and M.J. Sibley, *J. Pharm Sci.*, 66 (1977) 738.
13 R.C. Meyer and L.D. Cohn, *J. Pharm. Sci.*, 67 (1978) 1636.
14 S.W. Lam, R.C. Meyer and L.T. Takahashi, *J. Parent. Sci. Tech.*, 35 (1981) 262.
15 D.S. Bushee, *Analyst*, 133 (1988) 1167.
16 G.C. Visor, R.A. Kenley, J.S. Fleitman, D.A. Neu and I.W. Partridge, *Pharm. Res.*, 2 (1985) 73.
17 J.E. Parkin, *J. Chromatogr.*, 542 (1991) 137.
18 J.R. Procopio, M.P. da Silva, M.C. Asensio, M.T. Sevilla and L. Hernández, *Talanta*, 49 (1992) 1619.

*Journal of Chromatography A*, 653 (1993) 275–282
Elsevier Science Publishers B.V., Amsterdam

CHROM. 25 300

# Prediction of gas chromatographic retention indices of alkenes from the total solubility parameters

Zhide Hu* and Hongwei Zhang

*Department of Chemistry, Lanzhou University, Lanzhou, Gansu 730000 (China)*

(First received September 24th, 1992; revised manuscript received March 24th, 1993)

ABSTRACT

Gas chromatographic retention indices ($I$) for a large number of $C_5$–$C_{10}$ alkenes on different stationary phases at various temperatures were correlated with total solubility parameters ($\delta_T$), molar volumes ($V$) and the number ($N$) of carbon atoms in the solute molecules. The correlation is a new three-parameter equation $I = aN + b\Delta(V\delta_T) + c\Delta V + d$, which is based on the expanded solubility parameter model. Two new parameters, $\Delta(V\delta_T)$ and $\Delta V$, are introduced, accounting for the deviations of the $V\delta_T$ and the $V$ values of the solutes from those of $n$-alkanes which have the same carbon number as the solutes. The empirically introduced constants $a$, $b$, $c$ and $d$ depend on the phase characteristics and column temperature. High correlation coefficients and low standard deviations were found in all instances. Especially for isomeric alkenes, the correlation between the $I$ and $\delta_T$ and $V$ values of the solutes, which is $I = bV\delta_T + cV + e$, is excellent. The above two equations could be used to predict retention indices of alkenes successfully.

## INTRODUCTION

There have been many studies on the establishment of retention–structure relationships for alkene analysis [1–10]. Takács *et al.* [1] separated the retention index ($I$) into two additive components which represented molecular and interaction contributions. Sanz *et al.* [2] utilized the contributions of the different structural units of molecules. Bermejo and Guillen [3] studied the relationships between parameters related to electronic polarizability, such as molar refraction, refractive index, Van der Waals volume and molar volume, and the retention indices of alkenes. Papazova and Dimov [4,5] predicted $I$ values with the help of a physico-chemical index and a structural number correction. Sojsk *et al.* [6] obtained the correlations between the structure and retention increments considering the position of the double bond and the geometrical arrangement. Chrétien and Dubois [7,8] extensively analysed experimental retention indices of alkenes using the DARC topological system. Considering the influence of molecular parameters such as total energy and binding energy, Garcia-Raso *et al.* [9] studied the retention of $n$-alkenes with molecular orbital calculations. Rohrbaugh and Jurs [10] studied the relationships between $I$ and different structure-based descriptors of alkenes and the correlation coefficient was 0.998.

A very different and simple approach to calculating retention indices of alkenes is proposed in this paper. The approach is more theoretical than pure empirical correlations because the equation is derived from Karger's expanded solubility model [11]. It is, however, empirical and practicable because the fundamental parameters employed are easily obtained and the relationship between the parameters in question and the retention is empirical.

In a recent study [12], we investigated the theoretical aspects of the solubility parameter

* Corresponding author.

0021-9673/93/$06.00 

model and found two equations for predicting retention indices of alkylbenzenes. We applied these equations to a large number of alkylbenzenes on different stationary phases at various temperatures and obtained satisfactory results.

The aim of this study was twofold: first, to establish whether the proposed method [12] could be used to calculate the retention data of alkenes, or in other words to support the usefulness of the model [12], and second, to obtain general expressions for alkenes that are analytically useful for the prediction of retention indices on different stationary phases at various temperatures.

## DATA HANDLING

In a previous study [12], we applied the solubility parameter model to gas–liquid chromatography (GLC) and obtained the equation

$$I = aN + b\Delta(V\delta_T) + c\Delta V + d \quad (1)$$

where $N$ refers to number of carbons atoms in the compound of interest, $\Delta(V\delta_T)$ is the difference between the product of $V^i$ and $\delta_T^i$, and that of $V^{al}$ and $\delta_T^{al}$:

$$\Delta(V\delta_T) = V^i\delta_T^i - V^{al}\delta_T^{al} \quad (2)$$

$\Delta V$ is the difference between $V^i$ and $V^{al}$:

$$\Delta V = V^i - V^{al} \quad (3)$$

where the superscript $i$ refers to the solute and the superscript al refers to the $n$-alkane with the same carbon atom number as the solute, and $a$, $b$, $c$ and $d$ are constants.

For isomers, $N$, $V^{al}\delta_T^{al}$ and $V^{al}$ are constants, so rearranging eqn. 1 one obtains

$$I = bV\delta_T + cV + e \quad (4)$$

where $i$ in $V^i\delta_T^i$ and $V^i$ has been omitted, and $b$, $c$ and $e$ are constants for a given phase. Constants $b$ and $c$ stem from eqn. 1, so for the same system, $b$ and $c$ in eqn. 1 should be identical with $b$ and $c$ in eqn. 4. Constant $e$ is given by

$$e = aN - bV^{al}\delta_T^{al} - cV^{al} + d \quad (5)$$

Eqns. 1 and 4 represent the basic equations of the retention indices in terms of solubility parameters. Constants $a$, $b$, $c$, $d$ and $e$ are dependent on the stationary phase characteristics and the column temperature; $d$ and $e$ are also related to specific interactions of the solute and stationary phase. In this paper, no further attention is paid to this phenomenon. These two equations can be formulated and statistically evaluated from regression analysis of experimental retention indices, total solubility parameters and molar volume data for a sufficient large set of compounds. The best correlations were found for alkenes on a series of non-polar and moderately polar stationary phases at several temperatures.

## EXPERIMENTAL

### *Calculation of total solubility parameter*

The total solubility parameter, $\delta_T$, is the sum of a series of specific solubility parameters related to each other by the equation [13–15]

$$\delta_T^2 = \delta_d^2 + 2\delta_{in}\delta_d + \delta_0^2 + 2\delta_a\delta_b \quad (6)$$

where the specific solubility parameters $\delta_d$, $\delta_0$, $\delta_{in}$, $\delta_a$ and $\delta_b$ are measures of the ability of the substance to enter into selective interactions of the type dispersive, dipole orientation, dipole inductive and hydrogen bonding, respectively.

Sufficiently accurate data for the total solubility parameter are obtained from readily available and simple physical parameters, such as the molar volume, the heat of vaporization and the boiling point [13,14,16,17]. In this paper, total solubility parameters were calculated according to Sun *et al.*'s expression [18] from boiling points and densities of substances:

$$\delta_T^2 = -0.02085 \cdot \frac{T_b^2}{V} + 58.93 \cdot \frac{T_b}{V} - 6892.14 \cdot \frac{1}{V} - 26.76 \quad (7)$$

where $T_b$ is the boiling point and $V$ the molar volume of the solute. The equation was derived by regression analysis based on the systematic analysis of the relevant factors and had been employed to calculate total solubility parameters of more than 300 compounds with satisfactory results. Boiling points and densities were taken

from handbooks [19,20]. The molar volume is the ratio between molecular mass and density.

*Data set*

Retention indices of alkenes in different phases at several temperatures were taken from the literature [7,21–23]. The alkenes ranged from $C_5$ to $C_{10}$ compounds and included straight-chain and branched compounds. The 86 compounds are listed in Table I. The stationary phases and column temperatures used are given in Table II.

*Regression analysis*

Regression coefficients and statistics were calculated by a multiple regression linear program on a personal computer.

## RESULTS

Regression coefficients $a$, $b$, $c$ and $d$, correlation coefficients $R$ and standard deviations $S$ for eqn. 1 are given in Table II. The correlation coefficients are better than 0.9988 and the standard deviations are better than 3.9 i.u. Obviously, the proposed method has good accuracy.

Comparing constants $a$, $b$, $c$ and $d$ in Table II for the same stationary phases but different temperatures, such as SQ and OV-101, we found that a difference exists between each group of constants. For instance, for the stationary phase SQ at 80, 50 and 70°C, the corresponding constant $a = 97.21$, 96.56, 97.13, respectively, $b =$ 1.19, 1.19 and 1.17, $c = -3.44$, $-3.33$ and $-3.23$ and $d = 12.63$, 16.45 and 13.55. This shows that $a$, $b$, $c$ and $d$ depend slightly on temperature. This can be explained by the expressions for constants $a$, $b$, $c$ and $d$ [12]. The expressions for $b$, $c$ and $d$ contain the term $(\Delta E^s)^{m/j}$, which is the solution energy of solute $i$ in liquid stationary phase $j$. Further, the term is related to temperature, so $b$, $c$ and $d$ are dependent on temperature. The adjustable constant $a$ should be related to $b$, $c$ and $d$, so $a$ also depends on temperature. Evidently, the model [12] is in agreement with the regression results.

One can expect the coefficient ($a$) of carbon atom number ($N$), which was proposed to be an adjustable constant in the original paper [12] instead of 100, will be close to 100. The results in Table II confirm this, with $a$ values ranging from 95.79 to 98.17.

Isomeric alkenes having the same molecular mass provide nearly the same molar refraction, molar volume or connectivity indices but widely different retention data. This always worsens the correlation, so it is necessary to propose a method for predicting the retention of isomers. Fortunately, eqn. 4 is good enough to distinguish the isomers. This is confirmed by the results for eqn. 4 in Table III. The best quantitative correlation is obtained within a series of isomeric compounds when we apply eqn. 4 to alkenes. We only list representatives of each kind of stationary phase in Table III as examples. The correlation coefficients are not as good as those from eqn. 1, but it is notable that the deviations are much smaller than those from eqn. 1 except for DB-1 and HP-PONA. The accuracy is good.

Further, in order to illustrate the predictive ability of eqn. 4, we used it to estimate the retention indices of solutes not included in the original regression analysis. First, we selected some alkenes at random and, using their experimental retention index values, we could obtain the regression coefficient of eqn. 4. Then we used the regression equation to calculate the retention indices of other alkenes. Finally, we compared the calculated retention indices with the experimental values. Here we only list a representative group of results as an example. For the stationary phase 1-octadecene (25°C), there are sixteen isomeric alkenes whose carbon number is 6. We selected eight of the alkenes at random. To illustrate the random selection, we selected three times, in other words, there are three different group selections for the same system. For the first group, the serial numbers (No.) of the selected alkenes, for which the names are given in Table I, are 6, 9, 10, 14, 16, 17, 19 and 20. The following regression equation is obtained:

$$I = 1.0776V\delta_T - 4.4725V + 116.01 \quad (8)$$

$$R = 0.999, S = 1.4$$

For the second group, the selected alkenes are Nos. 7, 9, 13, 14, 16, 18, 20 and 21. The following regression equation is obtained:

TABLE I

VALUES OF PARAMETERS UTILIZED IN THIS STUDY

| No. | Compound | $V$ | $\delta_T$ | $\Delta(V\delta_T)$ | $\Delta V$ |
|---|---|---|---|---|---|
| 1 | 1-Pentene | 109.51 | 7.48 | −30.04 | −5.71 |
| 2 | *cis*-2-Pentene | 106.99 | 7.80 | −14.65 | −8.23 |
| 3 | *trans*-2-Pentene | 109.05 | 7.68 | −11.67 | −6.17 |
| 4 | 2-Methyl-1-butene | 107.84 | 7.60 | −29.59 | −7.38 |
| 5 | 2-Methyl-2-butene | 105.90 | 7.91 | −11.50 | −9.32 |
| 6 | 1-Hexene | 125.03 | 7.61 | −27.42 | −5.49 |
| 7 | *cis*-2-Hexene | 122.52 | 7.85 | −17.12 | −8.00 |
| 8 | *trans*-2-Hexene | 124.06 | 7.76 | −16.19 | −6.46 |
| 9 | *cis*-3-Hexene | 123.84 | 7.73 | −21.62 | −6.68 |
| 10 | *trans*-3-Hexene | 124.28 | 7.73 | −18.22 | −6.24 |
| 11 | 3-Methyl-1-pentene | 126.08 | 7.34 | −53.47 | −4.44 |
| 12 | 2-Methyl-1-pentene | 123.78 | 7.63 | −34.46 | −6.74 |
| 13 | 4-Methyl-1-pentene | 126.71 | 7.31 | −52.65 | −3.81 |
| 14 | 2-Methyl-2-pentene | 122.63 | 7.81 | −21.16 | −7.89 |
| 15 | *cis*-3-Methyl-2-pentene | 120.47 | 7.91 | −25.18 | −10.05 |
| 16 | *cis*-4-Methyl-2-pentene | 125.80 | 7.40 | −47.98 | −4.72 |
| 17 | *trans*-4-Methyl-2-pentene | 125.88 | 7.45 | −41.09 | −4.64 |
| 18 | 2-Ethyl-1-butene | 122.08 | 7.77 | −30.34 | −8.44 |
| 19 | 2,3-Dimethyl-1-butene | 123.71 | 7.48 | −53.55 | −6.81 |
| 20 | 2,3-Dimethyl-2-butene | 118.87 | 8.12 | −13.68 | −11.65 |
| 21 | 3,3-Dimethyl-1-butene | 128.90 | 6.98 | −79.18 | −1.62 |
| 22 | *trans*-3-Methyl-2-pentene | 121.44 | 7.93 | −15.88 | −9.08 |
| 23 | 1-Heptene | 140.88 | 7.61 | −24.17 | −5.68 |
| 24 | *cis*-2-Heptene | 138.69 | 7.79 | −15.87 | −7.87 |
| 25 | *trans*-2-Methyl-3-hexene | 143.28 | 7.35 | −43.16 | −3.28 |
| 26 | *trans*-2-Heptene | 140.03 | 7.73 | −13.84 | −6.53 |
| 27 | *cis*-3-Heptene | 138.82 | 7.73 | −23.19 | −7.74 |
| 28 | 5-Methyl-1-hexene | 142.78 | 7.36 | −45.41 | −3.78 |
| 29 | *trans*-3-Heptene | 140.65 | 7.66 | −18.89 | −5.91 |
| 30 | 4-Methyl-1-hexene | 141.44 | 7.44 | −43.96 | −5.12 |
| 31 | *trans*-5-Methyl-2-hexene | 142.66 | 7.42 | −37.73 | −3.90 |
| 32 | 2,3-Dimethyl-1-pentene | 139.26 | 7.48 | −54.60 | −7.30 |
| 33 | *cis*-5-Methyl-2-hexene | 140.88 | 7.52 | −36.85 | −5.68 |
| 34 | 2,4-Dimethyl-1-pentene | 141.42 | 7.33 | −59.66 | −5.14 |
| 35 | 4,4-Dimethyl-1-pentene | 143.83 | 7.05 | −82.27 | −2.73 |
| 36 | 2-Ethyl-1-pentene | 138.71 | 7.70 | −28.20 | −7.85 |
| 37 | 2,3-Dimethyl-2-pentene | 134.93 | 7.93 | −26.27 | −11.63 |
| 38 | 3-Ethyl-1-pentene | 141.95 | 7.37 | −50.10 | −4.61 |
| 39 | 3-Ethyl-2-pentene | 136.30 | 7.84 | −27.68 | −10.26 |
| 40 | *trans*-3,4-Dimethyl-2-pentene | 137.83 | 7.68 | −37.73 | −8.73 |
| 41 | *cis*-4,4-Dimethyl-2-pentene | 141.26 | 7.31 | −63.66 | −5.30 |
| 42 | 2,3,3-Trimethyl-1-butene | 139.28 | 7.34 | −73.95 | −7.28 |
| 43 | 2-Ethyl-3-methyl-1-butene | 137.33 | 7.65 | −45.69 | −9.23 |
| 44 | 3,3-Dimethyl-1-pentene | 140.79 | 7.27 | −72.73 | −5.77 |
| 45 | 3,4-Dimethyl-1-pentene | 141.61 | 7.31 | −61.10 | −4.95 |
| 46 | 2,4-Dimethyl-2-pentene | 141.20 | 7.38 | −54.21 | −5.36 |
| 47 | *trans*-4,4-Dimethyl-2-pentene | 142.53 | 7.19 | −71.48 | −4.03 |
| 48 | *cis*-4-Methyl-2-hexene | 141.24 | 7.44 | −45.44 | −5.32 |
| 49 | *trans*-4-Methyl-2-hexene | 141.79 | 7.45 | −39.93 | −4.77 |
| 50 | *trans*-3-Methyl-3-hexene | 139.28 | 7.67 | −27.99 | −7.28 |
| 51 | *trans*-3-Methyl-2-hexene | 138.30 | 7.74 | −25.83 | −8.26 |
| 52 | *cis*-3,4-Dimethyl-2-pentene | 138.45 | 7.61 | −42.66 | −8.11 |

TABLE I (*continued*)

| No. | Compound | $V$ | $\delta_T$ | $\Delta(V\delta_T)$ | $\Delta V$ |
|---|---|---|---|---|---|
| 53 | 2-Methyl-1-hexene | 140.27 | 7.58 | −33.02 | −6.29 |
| 54 | 2-Methyl-2-hexene | 139.51 | 7.70 | −22.04 | −7.05 |
| 55 | 3-Methyl-1-hexene | 142.91 | 7.33 | −48.74 | −3.65 |
| 56 | *cis*-3-Methyl-2-hexene | 130.68 | 8.10 | −37.76 | −15.88 |
| 57 | *cis*-3-Methyl-3-hexene | 138.71 | 7.73 | −24.04 | −7.85 |
| 58 | 1-Octene | 156.97 | 7.53 | −24.58 | −5.64 |
| 59 | *cis*-2-Octene | 154.94 | 7.68 | −16.63 | −7.67 |
| 60 | *trans*-2-Octene | 155.88 | 7.64 | −15.64 | −6.73 |
| 61 | *trans*-4-Octene | 157.15 | 7.55 | −20.08 | −5.46 |
| 62 | 2,3,4-Trimethyl-2-pentene | 150.96 | 7.66 | −50.21 | −11.65 |
| 63 | 2,4,4-Trimethyl-2-pentene | 155.47 | 7.28 | −74.74 | −7.14 |
| 64 | 2,4,4-Trimethyl-1-pentene | 156.95 | 7.16 | −82.80 | −5.66 |
| 65 | 2,5-Dimethyl-2-hexene | 156.24 | 7.40 | −50.39 | −6.37 |
| 66 | 2,3-Dimethyl-2-hexene | 151.53 | 7.75 | −32.21 | −11.08 |
| 67 | *cis*-2,2-Dimethyl-3-hexene | 158.37 | 7.19 | −67.89 | −4.24 |
| 68 | 2,3-Dimethyl-1-hexene | 156.47 | 7.35 | −56.51 | −6.14 |
| 69 | *trans*-2-Methyl-3-heptene | 159.86 | 7.26 | −45.98 | −2.75 |
| 70 | *trans*-4-Methyl-2-heptene | 157.61 | 7.38 | −43.40 | −5.00 |
| 71 | 2-Methyl-1-heptene | 157.97 | 7.46 | −28.11 | −4.64 |
| 72 | 2-Methyl-2-heptene | 155.86 | 7.60 | −22.03 | −6.75 |
| 73 | *cis*-4-Octene | 155.60 | 7.60 | −24.01 | −7.01 |
| 74 | *trans*-3-Octene | 156.91 | 7.57 | −18.76 | −5.70 |
| 75 | *cis*-3-Octene | 156.10 | 7.59 | −21.77 | −6.51 |
| 76 | *trans*-4-Methyl-2-heptene | 157.61 | 7.38 | −43.40 | −5.00 |
| 77 | 2-Methyl-1-Octene | 171.92 | 6.92 | −30.94 | −6.81 |
| 78 | 1-Nonene | 172.93 | 7.42 | −25.16 | −5.80 |
| 79 | *trans*-3-Nonene | 172.46 | 7.46 | −21.75 | −6.27 |
| 80 | 2-Methyl-1-nonene | 189.25 | 7.27 | −25.41 | −5.64 |
| 81 | 2,3-Dimethyl-2-heptene | 172.69 | 7.41 | −28.67 | −6.04 |
| 82 | 1-Decene | 189.35 | 7.30 | −19.00 | −5.54 |
| 83 | *cis*-5-Decene | 188.41 | 7.32 | −22.10 | −6.48 |
| 84 | *trans*-4-Decene | 189.45 | 7.30 | −18.27 | −5.44 |
| 85 | *cis*-4-Decene | 189.45 | 7.30 | −18.27 | −5.44 |
| 86 | *trans*-5-Decene | 189.53 | 7.29 | −19.59 | −5.36 |

$$I = 1.0780V\delta_T - 4.5465V + 125.09 \quad (9)$$

$$R = 0.999, S = 1.6$$

For the third group, the selected alkenes are Nos. 6, 8, 10, 13, 15, 17, 19 and 21. The following regression equation is obtained:

$$I = 1.1120V\delta_T - 4.2073V + 50.51 \quad (10)$$

$$R = 0.999, S = 1.9$$

Using the above equations, we calculated the retention indices of the remaining eight alkenes for each group. Comparisons of the predicted and measured $I$ values are given in Table IV. There is good agreement between the experimental and predicted retention data.

The good results suggest that $V\delta_T$ is a promising parameter for describing the retention behaviour of alkenes. As we have already noted in Table I, the difference between the $\delta_T$ values of a group isomers is small and also $V$ does not change significantly from compound to compound in isomers, but the difference between the $V\delta_T$ values of isomers obtained by multiplying $V$ and $\delta_T$ becomes large, so $V\delta_T$ may be an important parameter for distinguishing the isomers in eqn. 4.

Comparing the regression coefficients $b$ and $c$

TABLE II

REGRESSION COEFFICIENTS AND STANDARD DEVIATIONS IN VARIOUS PHASES FOR THE EQUATION $I = aN + b\Delta(V\delta_T) + c\Delta V + d$

$n$ = number of the alkene (see Table I); R = regression coefficient; S = standard deviation; SQ = squalane; DB-1 is a cross-linked and bonded methylsilicone phase; DB-5 is similar to DB-1 with 5% phenyl substitution; HP-PONA is a cross-linked methylsilioxane phase.

| No. | Phase | Temperature (°C) | $a$ | $b$ | $c$ | $d$ | $n$ | $R$ | $S$ |
|---|---|---|---|---|---|---|---|---|---|
| 1 | SQ | 80 | 97.21 | 1.19 | −3.44 | 12.63 | 39 | 0.9990 | 3.9 |
| 2 | 1-Octadecene | 25 | 95.79 | 1.21 | −3.77 | 20.10 | 35 | 0.9991 | 2.7 |
| 3 | OV-101 | 50 | 96.84 | 1.19 | −3.19 | 23.23 | 46 | 0.9989 | 3.5 |
| 4 | SQ | 50 | 96.56 | 1.19 | −3.33 | 16.45 | 46 | 0.9990 | 3.3 |
| 5 | OV-101 | 70 | 96.97 | 1.17 | −3.26 | 21.74 | 46 | 0.9988 | 3.7 |
| 6 | SQ | 70 | 97.13 | 1.17 | −3.23 | 13.55 | 46 | 0.9988 | 3.6 |
| 7 | OV-101 | 40 | 97.71 | 1.24 | −3.61 | 16.16 | 61 | 0.9996 | 3.8 |
| 8 | OV-101 | 60 | 97.87 | 1.21 | −3.74 | 13.75 | 61 | 0.9996 | 3.7 |
| 9 | OV-101 | 80 | 98.05 | 1.18 | −3.91 | 10.91 | 61 | 0.9996 | 3.8 |
| 10 | DB-1 | 40 | 98.11 | 1.26 | −3.27 | 18.13 | 69 | 0.9991 | 3.7 |
| 11 | HP-PONA | 40 | 98.10 | 1.26 | −3.27 | 18.27 | 69 | 0.9991 | 3.7 |
| 12 | DB-5 | 40 | 98.17 | 1.29 | −3.33 | 20.90 | 67 | 0.9990 | 3.8 |

TABLE III

REGRESSION COEFFICIENTS AND STANDARD DEVIATIONS OF ALKENES ISOMERS FOR THE EQUATION $I = bV\delta_T + cV + e$

See Table II for $n$, $R$ and $S$. $N$ = No. of carbon atoms in the molecule.

| No.[a] | $N$ | $b$ | $c$ | $e$ | $n$ | $R$ | $S$ |
|---|---|---|---|---|---|---|---|
| 2 | 6 | 1.09 | −4.45 | 97.47 | 16 | 0.999 | 1.5 |
| | 7 | 1.26 | −3.38 | −192.64 | 15 | 0.999 | 1.9 |
| 3 | 6 | 1.12 | −4.23 | 53.73 | 12 | 0.998 | 1.5 |
| | 7 | 1.19 | −3.16 | −139.45 | 23 | 0.993 | 3.6 |
| | 8 | 1.33 | −3.27 | −273.97 | 8 | 0.998 | 1.9 |
| 4 | 6 | 1.04 | −4.80 | 194.90 | 12 | 0.998 | 1.6 |
| | 7 | 1.20 | −3.20 | −155.06 | 23 | 0.995 | 3.0 |
| | 8 | 1.33 | −3.46 | −249.07 | 8 | 0.999 | 1.2 |
| 10 | 6 | 1.10 | −4.30 | 80.18 | 17 | 0.999 | 1.7 |
| | 7 | 1.28 | −3.13 | −243.37 | 35 | 0.991 | 3.8 |
| | 8 | 1.32 | −4.61 | −41.79 | 11 | 0.994 | 2.4 |
| 11 | 6 | 1.10 | −4.30 | 81.15 | 17 | 0.999 | 1.7 |
| | 7 | 1.29 | −3.14 | −243.59 | 35 | 0.991 | 3.8 |
| | 8 | 1.32 | −4.56 | −48.71 | 11 | 0.993 | 2.4 |
| 12 | 6 | 1.12 | −4.39 | 74.15 | 17 | 0.999 | 1.7 |
| | 7 | 1.31 | −3.2 | −255.70 | 35 | 0.992 | 3.8 |
| | 8 | 1.36 | −4.45 | −110.57 | 10 | 0.993 | 2.5 |

[a] See stationary phases and column temperatures in Table II.

TABLE IV

COMPARISONS OF $I_{exp.}$ WITH $I_{calc.}$ ACCORDING TO EQNS. 8, 9 AND 10

| No.[a] | Eqn. 8 | | Eqn. 9 | | Eqn. 10 | |
|---|---|---|---|---|---|---|
| | Standard [b] | $\Delta I$ [c] | Standard [b] | $\Delta I$ [c] | Standard [b] | $\Delta I$ [c] |
| 6 | * | | | −2.0 | * | |
| 7 | | 0.5 | * | | | 0.6 |
| 8 | | −0.3 | | −0.1 | * | |
| 9 | * | | * | | | 0.4 |
| 10 | * | | | 1.9 | * | |
| 12 | | −1.6 | | −1.3 | | −1.7 |
| 13 | | −2.7 | * | | * | |
| 14 | * | | * | | | 0.4 |
| 15 | | 0.8 | | 1.3 | * | |
| 16 | * | | * | | | −0.8 |
| 17 | * | | | 0.3 | * | |
| 18 | | −1.1 | * | | | −1.6 |
| 19 | * | | | 1.2 | * | |
| 20 | * | | * | | | −1.4 |
| 21 | | 1.9 | * | | * | |
| 22 | | −2.5 | | −2.0 | | −2.6 |

[a] For compound numbers see Table I.
[b] Standard = alkenes used to obtain the regression coefficients (constants $b$, $c$ and $e$ in eqn. 4).
[c] $\Delta I = I_{calc.} - I_{exp.}$.

in Tables II and III for the same system, it can be seen that the values of $b$ and $c$ obtained by regressing $I$ in eqn. 1 are approximately equal to the values obtained in eqn. 4 for a given system. Evidently, the results are in agreement with our model. The small disagreement is probably due to the fact that some small approximations were involved in formulating eqns. 1 and 4 [12].

The model is based on a non-polar and weakly polarizable system [12], so for more polar stationary phases and more polar solutes, such as organic compounds containing nitrogen, oxygen and halogen atoms, the regression results for eqns. 1 and 4 are not so good. Further investigations on the relationship between the chromatographic behaviour of more polar solutes on the more polar stationary phases and solubility parameters are being carried out.

ACKNOWLEDGEMENT

We thank the National Science Foundation of China for financial support.

REFERENCES

1 J. Takács, Zs. Tálas, I. Bernáth, Gy. Czakó and A. Fisher, *J. Chromatogr.*, 67 (1972) 203.
2 J. Sanz, J. Calderon and M.V. Dabrio, *An. Quim.*, 75 (1979) 408.
3 J. Bermejo and M.D. Guillen, *Int. J. Environ. Anal. Chem.*, 23 (1985) 77.
4 D. Papazova and N. Dimov, *J. Chromatogr.*, 137 (1977) 259.
5 N. Dimov and D. Papazova, *Chromatographia*, 12 (1979) 720.
6 L. Sojsk, J. Krupzik and J. Jansk, *J. Chromatogr.*, 195 (1980) 43.
7 J.R. Chrétien and J.E. Dubois, *Anal. Chem.* 49 (1977) 747.
8 J.R. Chrétien and J.E. Dubois, *J. Chromatogr.*, 158 (1978) 43.
9 A. Garcia-Raso, F. Saura-Calixto and M.A. Raso, *J. Chromatogr.*, 302 (1984) 107.
10 R.H. Rohrbaugh and P.C. Jurs, *Anal. Chem.* 57 (1985) 2770.
11 B.L. Karger, L.R. Snyder and C. Eon, *Anal. Chem.* 50 (1978) 2126.
12 H. Zhang and Z. Hu, *Chromatographia*, 33 (1992) 575.
13 B.L. Karger, L.R. Snyder and C. Eon, *J. Chromatogr.*, 125 (1976) 71.

14 P.H. Shetty, P.J. Youngberg, B.R. Kersten and C.F. Poole, *J. Chromatogr.*, 411 (1987) 61.
15 P. Laffort and F. Patte, *J. Chromatogr.*, 126 (1976) 625.
16 D.D. Lawson and J.D. Ingham, *Nature*, 223 (1969) 614.
17 A. Munafo, M. Buchmane, H. Nam-Tram and U.W. Kesselring, *J. Pharm. Sci.*, 77 (1988) 169.
18 Z. Sun, M. Lui and Z. Hu, *Fenxi Ceshi Tongbao*, 7 (1988) 15.
19 R.C. Weast and M.J. Astle (Editors), *CRC Handbook of Chemistry and Physics*, CRC Press, Boca Raton, FL, 63rd ed., 1982–83.
20 R.C. Weast and M.J. Astle (Editors), *CRC Handbook of Chemistry and Physics*, CRC Press, Boca Raton, FL, 69th ed., 1988–89.
21 S. Boneva and N. Dimov, *Chromatographia*, 21 (1986) 149.
22 R.J. Laub and J.H. Purnell, *J. High Resolut. Chromatogr. Chromatogr. Commun.*, 11 (1988) 649.
23 A.J. Lubeck and D.L. Sutton, *J. High Resolut. Chromatogr. Chromatogr. Commun.*, 7 (1984) 542.

*Journal of Chromatography A*, 653 (1993) 283–291
Elsevier Science Publishers B.V., Amsterdam

CHROM. 25 439

# Sensitive determination of alkyl hydroperoxides by high-resolution gas chromatography–mass spectrometry and high-resolution gas chromatography with flame ionization detection

J. Polzer and K. Bächmann*

*Technische Hochschule Darmstadt, Fachbereich Chemie, Hochschulstrasse 10, W-6100 Darmstadt (Germany)*

(First received January 21st, 1993; revised manuscript received July 15th, 1993)

ABSTRACT

A method for the determination of alkyl-hydroperoxides by high-resolution GC was developed. Alkyl hydroperoxides were synthesized in the gaseous phase and identified in the chromatograms of the reaction mixture using a GC–MS system. Electron impact mass spectra of $C_1$–$C_6$ alkyl hydroperoxides were recorded. The hydroperoxides were determined using flame ionization detection (FID). FID response factors of these compounds were calculated using the concept of the effective carbon number. Detection limits of the hydroperoxides ranged from 91 to 127 pg absolute. The system is also useful for the qualitative identification of labile hydroperoxides as, *e.g.*, 1,2-dichloroethyl hydroperoxide.

## INTRODUCTION

The identification and determination of hydroperoxides are important owing to their use as oxidants in industrial processes. Further, they play an important role as intermediates in the oxidation of organic compounds in both the liquid and gaseous phases. Hydroperoxides are also atmospheric oxidation products of natural and anthropogenic hydrocarbons. They are considered to damage plants in conjunction with hydrogen peroxide and contribute significantly to the oxidation potential of the atmosphere [1].

The sensitive determination of hydroperoxides is difficult owing to their thermolability and their tendency to undergo heterogeneous catalysed decay. Therefore, only a few sensitive chromatographic methods for the determination of these species exist.

Liquid chromatography was applied by Deelder *et al.* [2] and Kok *et al.* [3]. Kok *et al.* developed a method for the determination of hydrogen methyl and ethyl hydroperoxide and a few hydroxyhydroperoxides using HPLC and postcolumn reaction for the production of fluorescent derivatives. The detection limit was $5 \cdot 10^{-9}$ *M* for hydrogen peroxide.

There have been only a few applications of gas chromatography (GC) for the determination of hydroperoxides. The determination of selected relatively stable species in large amounts has been described by several workers [4–7]. For example, cumene hydroperoxide, ethylbenzene hydroperoxide, *tert.*-butyl hydroperoxide, ethyl hydroperoxide and cyclohexyl hydroperoxide could be determined using packed columns and flame ionization detection (FID). Disadvantages were the low resolution and the low sensitivity achieved with the packed columns and a varying extent of heterogeneous decomposition of the analytes depending on the stationary phase.

* Corresponding author.

0021-9673/93/$06.00 

In this paper, we present a sensitive method for the identification and determination even of complex mixtures of hydroperoxides in the gaseous phase by capillary GC–MS and GC–FID.

## EXPERIMENTAL

Fig. 1 gives a schematic diagram of the analytical system. It consists of a glass vessel for the synthesis of hydroperoxides and GC systems for the qualitative and quantitative analysis of the gaseous mixture.

### *Synthesis of hydroperoxides*

Hydroperoxides were synthesized in the gaseous phase using a method according to Warneck and Bächmann [8]. Hydrocarbons are oxidized by hydroxyl radicals produced from photolysis of hydrogen peroxide by UV radiation. The UV source was a mercury lamp (Oriel, Type 6035). The main reaction pathway is as follows [8,9]:

$$H_2O_2 + h\nu \rightarrow 2^{\bullet}OH$$

$$(H_2O_2 + {}^{\bullet}OH \rightarrow {}^{\bullet}O_2H + H_2O)$$

$$RH + {}^{\bullet}OH \rightarrow R^{\bullet} + H_2O$$

$$R^{\bullet} + O_2 \rightarrow ROO^{\bullet}$$

$$ROO^{\bullet} + {}^{\bullet}O_2H \rightarrow ROOH + O_2$$

$$ROO^{\bullet} + ROO^{\bullet} \rightarrow \text{further oxidation products (ketones, aldehydes, alcohols, . . .)}$$

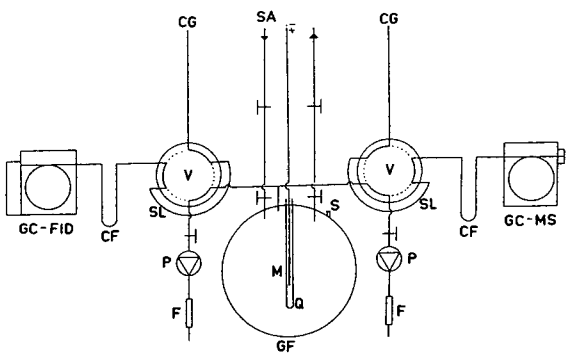


Fig. 1. Schematic diagram of the analytical system. CG = carrier gas; SA = synthetic air; V = six-port valve; F = flowmeter; P = pump; CF = cryofocusing; SL = sample loop; GF = glass flask; Q = quartz glass finger; M = mercury lamp; S = sample injection.

Analytical-reagent grade liquid hydrocarbons and unstabilized 34% hydrogen peroxide were purchased from Merck (Darmstadt, Germany). Gases were obtained from Messer Griesheim at purities of 99.5% or better.

A few micromoles of a single hydrocarbon or a hydrocarbon mixture were injected into a 10-l glass flask (deactivated by treatment with trimethylchlorosilane) followed by unstabilized 34% hydrogen peroxide (molar ratio about 1:1). After a short time for vaporization of the compounds the reaction was started by inserting the mercury lamp into the quartz finger of the reaction vessel.

### *Gas chromatographic system*

The analytical system consisted of two gas chromatographs: a Siemens Sichromat I GC–FID system for quantitative analysis and a Hewlett-Packard GC–MS system (Model 5890/5970 + UNIX chemstation for data analysis) for qualitative analysis. Both gas chromatographs were equipped with 25 m × 0.2 mm I.D. columns with a 0.5-$\mu$m Ultra I coating (Hewlett-Packard). The carrier gas was helium at a linear velocity of 45 cm/s (100°C).

The sample was introduced by a six-port valve switching with a sample loop for vapour-phase compounds. In order to avoid hydroperoxide losses due to heterogeneous decay, all connections were made of inert material: the reaction vessel was connected to the valve with a PTFE line and the sample loop was made of Silcosteel (Amchro, Sulzbach, Germany), a stainless-steel tube coated with deactivated fused silica [38 cm × $\frac{1}{8}$ in. I.D. (1 in. = 2.54 cm)]. The analytical column was connected to a precolumn (methylsilyl-deactivated uncoated fused-silica retention gap, 2 m × 0.32 mm I.D.), which was directly connected to the six-port valve through a reduction unit.

### *Analytical procedure*

Vapour-phase samples were taken directly from the reaction mixture in the sample loop (1.4 ml) by a pump, then the transfer of the analytes on to the column was started. The precolumn was cooled to −196°C with liquid nitrogen during transfer of the analytes from the

sample loop to the analytical column in order to provide sharp peaks even of very volatile components (external cryofocusing). Analysis was started by removing the cooling of the pre-column. The separation was carried out with temperature programming, starting at −40°C for 2 min, then increased at 4°C/min to 150°C and maintained at 150°C until all compounds had eluted.

Reproducibility of the sample introduction was tested with mixtures of alkanes, alcohols and ketones. The relative standard deviation of the peak areas was less than 3.2% for all species (five repetitions and FID).

*Mass spectrometer analysis*

For qualitative analysis, mass spectra were acquired on a Hewlett-Packard Model 5970 quadrupole mass spectrometer with electron impact ionization (electron energy 70 eV). The mass range scanned was 19–200 u at a scan cycle time of 400 ms. Ion abundances of the mass spectrometer were calibrated using perfluorotri-*n*-butylamine (PFTBA). The column was coupled directly to the ion source, the transfer line being kept at 150°C.

*Identification*

For compound identification a commercially available reference library of mass spectra (NBS–Wiley Library) adopted for the HP 5890/5970 system was used. As only few hydroperoxides were included in the spectral library and the library search for these compounds often failed, the identification was carried out by classical mass spectra interpretation techniques.

*Quantification*

Owing to the lack of commercially available standards for the hydroperoxides, we used the effective carbon number (ECN) concept for the calculation of response factors. The ECN of a compound was calculated by using the contributions of different molecular structures as determined by Sternberg *et al.* [10]. Using this method, Scanlon and Willis [11] and Jorgenson *et al.* [12] predicted FID response factors with good accuracy (typical relative standard deviations of *ca.* 2–3%) for a wide variety of compounds. As no recommendations for the calculation of the ECN of alkyl hydroperoxides exist, we treated these compounds like the corresponding alcohols.

TABLE I

CONTRIBUTIONS TO THE EFFECTIVE CARBON NUMBER

Data from ref. 11.

| Atom | Type of atom | ECN contribution |
|---|---|---|
| C | Aliphatic | 1 |
| C | Carbonyl | 0 |
| O | Primary alcohol | −0.5 |
| O | Secondary alcohol | −0.75 |
| O | Tertiary alcohol | −0.25 |

Calibration graphs for *n*-butane, 2-butanone and 2-pentanone based on the peak areas were recorded and used as reference components. The alkanes were determined by means of the *n*-butane calibration and oxidation products by means of the ketone calibration. Contributions of the various types of atoms to the ECN of the uncalibrated compounds used are given in Table I.

The relative mass response factors for uncalibrated compounds were calculated using the following equation:

$$f = \frac{M_{rx}\mathrm{ECN}_r}{M_{rr}\mathrm{ECN}_x}$$

where $r$ = reference compound; $x$ = uncalibrated compound and $M_r$ = molecular mass.

## RESULTS AND DISCUSSION

*Qualitative analysis*

In these investigations the oxidation of $C_1$–$C_6$ alkanes was carried out. In all instances alkyl hydroperoxides could be identified as the main reaction product by means of their mass spectra. For *tert.*-butyl hydroperoxide an authentic reference standard (80% *tert.*-butyl hydroperoxide in dibutyl peroxide; Aldrich, Steinheim, Germany) was used in addition and the identity of this compound in chromatograms could be verified by comparing the retention times and mass spectra.

TABLE II

MASS SPECTRA (RELATIVE INTENSITY, %) OF THE ALKYL HYDROPEROXIDES

h.p. = hydroperoxide; H.p. = Hydroperoxy.

| *m/z* | Compound (molecular mass) | | | | | | | | | | | | | | |
|---|---|---|---|---|---|---|---|---|---|---|---|---|---|---|---|
| | Methyl-h.p. (48) | Ethyl-h.p. (62) | 1-H.p.-propane (76) | 2-H.p.-propane (76) | 1-H.p.-2-methylpropane (90) | 2-H.p.-2-methylpropane (90) | 1-H.p.-butane (90) | 2-H.p.-butane (90) | 1-H.p.-pentane (104) | 2-H.p.-pentane (104) | 3-H.p.-pentane (104) | 1-H.p.-2-methylbutane (104) | 1-H.p.-3-methylbutane (104) | 2-H.p.-2-methylbutane (104) | 2-H.p.-3-methylbutane (104) |
| 19 | 6.0 | 3.7 | | 3.0 | | | | 3.0 | | 1.5 | | | | 0.5 | 0.8 |
| 20 | | | | | | | | | | | | | | | |
| 21 | | | | | | | | | | | | | | | |
| 22 | | | | | | | | | | | | | | | |
| 23 | | | | | | | | | | | | | | | |
| 24 | | | | | | | | | | | | | | | |
| 25 | | 1.9 | | | | | | 1.1 | | | | | | | 1.0 |
| 26 | | 8.8 | 12.4 | 4.0 | 3.0 | 4.6 | | 10.4 | 2.9 | 3.2 | 10.4 | 1.5 | | 4.0 | 4.5 |
| 27 | | 33.1 | 52.9 | 13.1 | 30.0 | 17.7 | 31.2 | 34.3 | 41.2 | 22.1 | 41.7 | 8.2 | | 14.9 | 13.4 |
| 28 | | | | | | | 1.4 | 11.2 | | 6.6 | | | | 3.7 | 7.5 |
| 29 | 100.0 | 100.0 | 60.3 | 21.2 | 32.6 | 30.2 | 47.1 | 56.0 | 63.2 | 20.9 | 65.5 | 59.4 | 31.9 | 14.9 | 26.8 |
| 30 | 20.9 | 10.6 | 10.3 | | 5.6 | | 2.5 | 3.0 | | 0.7 | 6.0 | 1.8 | | 0.5 | |
| 31 | 26.9 | 35.3 | 100.0 | 3.3 | 22.2 | 23.6 | 42.2 | 16.4 | 41.9 | 5.1 | 40.5 | 11.1 | 8.9 | 7.5 | 1.9 |
| 32 | | | | | 19.3 | | | | | 1.2 | | | | | 0.6 |
| 33 | 1.8 | | | | | | 4.4 | | | | | | | | |
| 34 | | | | | | | 1.9 | | | | | | | | |
| 35 | | | | | | | | | | | | | | | |
| 36 | | | | | | | | | | | | | | | |
| 37 | | | 1.6 | 2.9 | 1.5 | 4.1 | | 2.4 | | 1.6 | | | | | 3.3 |
| 38 | | | 5.1 | 4.4 | 7.4 | 6.8 | 3.7 | 3.0 | | 3.2 | 3.3 | 1.5 | | 2.2 | 5.2 |
| 39 | | | 17.7 | 15.7 | 39.3 | 39.2 | 25.0 | 22.4 | 40.4 | 23.5 | | 37.1 | 47.5 | 15.2 | 29.8 |
| 40 | | | 2.9 | 3.4 | 5.5 | 9.7 | 4.7 | 3.3 | 3.1 | 4.4 | | | | 2.7 | 6.7 |
| 41 | | 1.8 | 52.9 | 39.6 | 100.0 | 100.0 | 100.0 | 69.4 | 100.0 | 32.6 | 40.9 | 100.0 | 98.1 | 19.7 | 46.2 |
| 42 | | 6.2 | 28.5 | 14.2 | 36.3 | 12.8 | 26.8 | 11.2 | 89.7 | 21.3 | 14.1 | 20.0 | 55.0 | 11.9 | 21.6 |
| 43 | | 22.1 | 75.7 | 100.0 | 91.9 | 79.5 | 45.4 | 73.9 | 94.1 | 100.0 | 70.7 | 40.1 | 100.0 | 100.0 | 100.0 |
| 44 | | 11.0 | 7.4 | 9.7 | 5.6 | 4.4 | 16.2 | 19.4 | 38.2 | 16.2 | 5.2 | 5.2 | 31.2 | 3.7 | 25.3 |
| 45 | | 30.9 | 2.9 | 58.2 | 7.7 | 1.8 | 6.6 | 100.0 | 14.0 | 70.6 | 3.2 | 4.2 | 8.9 | 3.3 | 68.5 |
| 46 | | 8.1 | | 1.5 | | | | 3.1 | | 1.9 | | | | | 1.8 |
| 47 | 67.5 | 17.5 | 6.9 | | | | 4.7 | | | | | | | | |
| 48 | 77.6 | | | | | | | | | | | | | | |
| 49 | | | | | | 1.3 | | 0.8 | | | | | | | |
| 50 | | | | | | 5.0 | | 4.5 | | 1.5 | 1.2 | | | 1.5 | 1.8 |
| 51 | | | | | | 4.1 | | 3.7 | | 1.9 | 1.5 | | | 1.8 | 1.6 |
| 52 | | | | | | | | 0.8 | | 0.7 | | | | | |
| 53 | | | | | | 4.1 | | 4.2 | 5.1 | 4.1 | 4.2 | 3.2 | 1.9 | 4.5 | 3.3 |
| 54 | | | | | | | | 0.8 | | | | | | | |

| | | | | | | | | | | | | | |
|---|---|---|---|---|---|---|---|---|---|---|---|---|---|
| 55 | | | | 8.6 | 10.6 | 11.2 | 11.9 | 68.4 | 39.7 | 19.3 | 36.4 | 69.8 | 35.8 | 26.1 |
| 56 | | | | 11.9 | 19.4 | 40.5 | 19.7 | 14.7 | 2.2 | 1.5 | 43.1 | 9.6 | 1.8 | 1.6 |
| 57 | | 6.2 | | 35.3 | 73.3 | 50.1 | 43.3 | 29.4 | 2.5 | 55.0 | 66.9 | 19.3 | 4.2 | 2.2 |
| 58 | | 12.2 | 4.8 | | 22.1 | 1.5 | 4.0 | 14.7 | 2.9 | 25.3 | 11.9 | 4.5 | 13.4 | |
| 59 | | 14.4 | 1.9 | | 78.1 | 0.8 | 16.9 | | 1.7 | 100.0 | | | 23.8 | |
| 60 | | 7.4 | | | 3.1 | | 0.7 | | | 3.1 | | | 0.7 | |
| 61 | | | 4.5 | | | | 11.2 | | 5.9 | | | | | 5.9 |
| 62 | 24.3 | | | | | | | | | | | | | |
| 63 | 0.7 | | | | | | | | | | | | | |
| 64 | | | | | | | | | | | | | | |
| 65 | | | | | | | | | | | | | | |
| 66 | | | | | | | | | | | | | | |
| 67 | | | | | | | | | | | | | | |
| 68 | | | | | | | | | 0.7 | | | | | |
| 69 | | | | | | | | 13.2 | 0.7 | | | 1.5 | | 0.9 |
| 70 | | | | | | | | 30.1 | 8.8 | 6.0 | 18.6 | 23.8 | 6.3 | 5.2 |
| 71 | | | | | | 2.2 | | 17.6 | 16.9 | 23.8 | 12.6 | 11.9 | 22.4 | 19.3 |
| 72 | | | | 8.9 | | 5.6 | 6.0 | | 0.8 | 1.2 | | | 3.7 | 2.7 |
| 73 | | | | | | | 1.5 | | 4.7 | | | | 11.2 | 4.8 |
| 74 | | | | 3.7 | | | | | | | | | | |
| 75 | | | | | 6.6 | | | | | 12.6 | | | 10.4 | |
| 76 | | 4.4 | 6.7 | | | | | | | | | | | |
| 77 | | | | | | | | | | | | | | |
| 78 | | | | | | | | | | | | | | |
| 79 | | | | | | | | | | | | | | |
| 80 | | | | | | | | | | | | | | |
| 81 | | | | | | | | | | | | | | |
| 82 | | | | | | | | | | | | | | |
| 83 | | | | | | | | | | | | | | |
| 84 | | | | | | | | | | | | | | |
| 85 | | | | | | | | | | | | | | |
| 86 | | | | | | | | | 4.3 | 6.0 | | | | 3.3 |
| 87 | | | | | | | | | 0.3 | | | | | |
| 88 | | | | | | | | | | | | | | |
| 89 | | | | | | | | | | | | | 1.0 | |
| 90 | | | | | 1.5 | 1.5 | 2.3 | | | | | | | |
| 91 | | | | | | | | | | | | | | |
| 92 | | | | | | | | | | | | | | |
| 93 | | | | | | | | | | | | | | |
| 94 | | | | | | | | | | | | | | |
| 95 | | | | | | | | | | | | | | |
| 96 | | | | | | | | | | | | | | |
| 97 | | | | | | | | | | | | | | |
| 98 | | | | | | | | | | | | | | |
| 99 | | | | | | | | | | | | | | |
| 100 | | | | | | | | | | | | | | |
| 101 | | | | | | | | | | | | | | |
| 102 | | | | | | | | | | | | | | |
| 103 | | | | | | | | | | | | | | |
| 104 | | | | | | | | | 1.3 | 2.2 | | | 0.4 | |
| 105 | | | | | | | | | | | | | | |
| 106 | | | | | | | | | | | | | | |

The mass spectra obtained with the GC–MS system used here differ in relative intensities from the mass spectra in the NBS–Wiley Library and literature data [13]. Nevertheless, all characteristic fragments are present and the identity of the hydroperoxides is unambiguous.

Fig. 2 shows a chromatogram with FID for a reaction mixture of alkanes and hydrogen peroxide after a reaction time of 25 min. All possible simple hydroperoxides are present in the reaction mixture. Chromatographic separation of 1-hydroperoxy-2-methylpropane and 2-hydroperoxybutane could not be achieved under the conditions used here, but the overlap of the two peaks could be recognized by means of the MS analysis.

Fig. 3 and Table II presents the mass spectra of the hydroperoxides detected, normalized on PFTBA.

The intensity of the molecular ion peaks decreases significantly from $C_1$ to $C_6$ hydroperoxides. The relative stabilities of the molecular ions decreased in the order *sec.*-hydroperoxides ≥ *tert.*-hydroperoxides > primary hydroperoxides. For primary $C_5$ and all $C_6$ hydroperoxides molecular ions could not be detected.

The characteristic fragments resulting from elimination of $HO_2$ (M − 33) and $H_2O_2$ (M − 34) are present in the mass spectra of all alkyl peroxides with more than two carbon atoms and the M − 33 peak is more intense than the M − 34 peak. Elimination of $H_2O$ (M − 18) and OH (M − 17) is also observed in most spectra, the former peak being more intense than the latter.

Ions resulting from α-fragmentation are generally less intense but give important information on the position of the hydroperoxide group in the molecule. Alkyl hydroperoxides with the hydroperoxide group in the 2-position yield fragments at *m/z* 45 ($C_2H_5O^+$) and the hydroperoxide group in the 3-position results in fragments at *m/z* 59 ($C_3H_7O^+$).

The base peaks in most of the mass spectra of hydroperoxides are typical hydrocarbon fragments; in some instances a contribution of oxygen-containing fragments to the base peak cannot be excluded (*e.g.*, *m/z* 29 in ethyl hydroperoxide and *m/z* 43 in 2-hydroperoxypropane).

Using this system, hydroperoxides of alkyl-substituted aromatic compounds and chlorinated hydrocarbons could also be synthesized, but only in low yields. Fig. 4 shows the mass spectrum of 1,2-dichlorohydroperoxyethane as an example.

*Quantitative analysis*

In order to recognize losses of hydroperoxides during the analytical procedure and to verify the applicability of the ECN concept to alkyl hydroperoxides, reaction mixtures of single hydro-

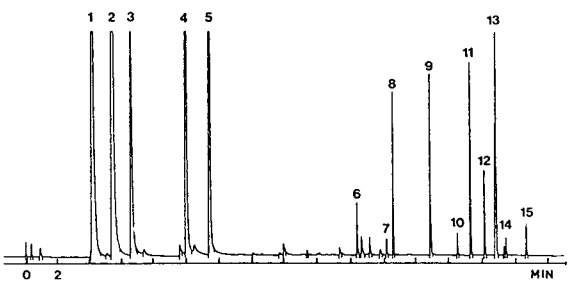


Fig. 2. Chromatogram of a reaction mixture of alkanes and hydrogen peroxide obtained using FID. 1–5 = alkanes (propane, isobutane, *n*-butane, isopentane, *n*-pentane). 6–15 = Alkyl hydroperoxides: 6 = 2-hydroperoxypropane; 7 = 1-hydroperoxypropane; 8 = 2-methyl-2-hydroperoxypropane; 9 = 2-hydroperoxybutane; 10 = 1-hydroperoxybutane; 11 = 2-methyl-2-hydroperoxybutane; 12 = 2-methyl-3-hydroperoxybutane; 13 = 2- and 2-hydroperoxypentane; 14 = 2-methyl-1-hydroperoxybutane and 3-methyl-1-hydroperoxybutane; 15 = 1-hydroperoxypentane. Peaks not marked = other oxidation products (mostly ketones).

TABLE III

DETECTION LIMITS (3σ) FOR ALKYL HYDROPEROXIDES

| Compound | Detection limit | |
|---|---|---|
| | pg[a] | ppb (v/v)[b] |
| 2-Hydroperoxypropane | 127 | 27 |
| Primary $C_4$ hydroperoxides | 103 | 18 |
| 2-Hydroperoxybutane | 108 | 19 |
| *tert.*-Butylhydroperoxide | 98 | 17 |
| Primary $C_5$ hydroperoxides | 94 | 14 |
| Secondary $C_5$ hydroperoxides | 98 | 15 |
| Secondary $C_6$ hydroperoxides | 91 | 12 |

[a] Absolute detection limits.

[b] Resulting detection limits for the vapour-phase concentration in the reaction vessel.

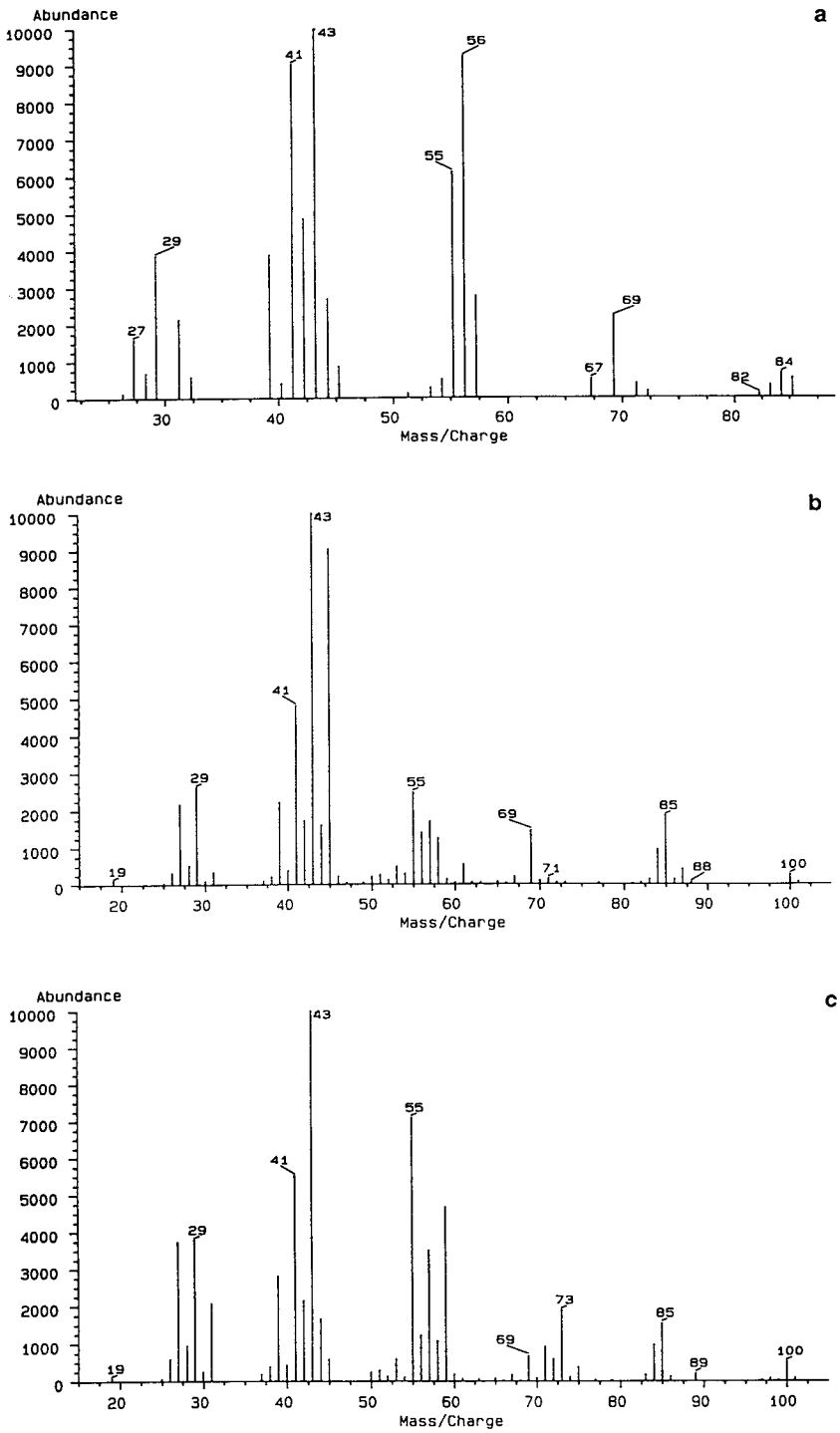


Fig. 3. Mass spectra of the hydroperoxides derived from the oxidation of *n*-hexane. (a) 1-Hydroperoxyhexane, $CH_3(CH_2)_5OOH$ ($M_r$ 118); (b) 2-hydroperoxyhexane, $CH_3CH(OOH)(CH_2)_3CH_3$ ($M_r$ 118); (c) 3-hydroperoxyhexane, $CH_3CH_2CH(OOH)(CH_2)_2CH_3$ ($M_r$ 118).

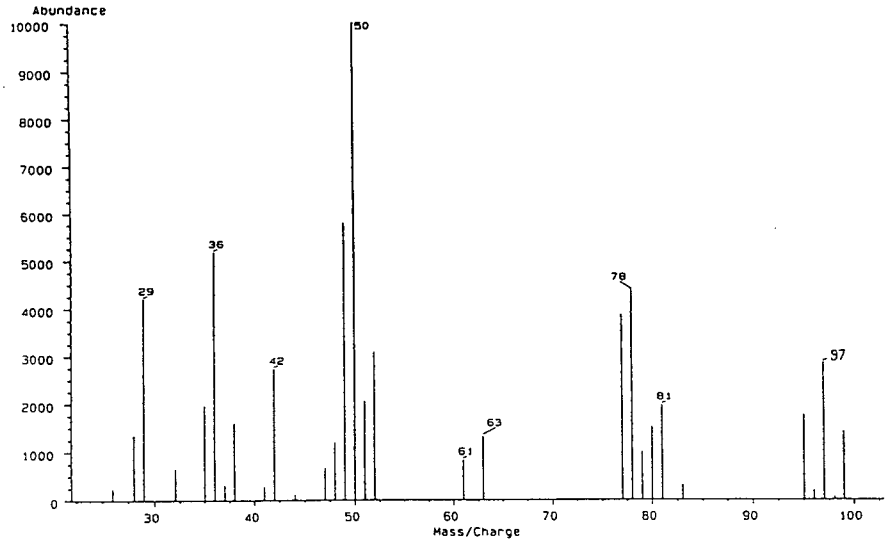


Fig. 4. Mass spectra of 1,2-dichloroethyl hydroperoxide and characteristic fragments (a molecular peak could not be detected).

| Elimination of | Molecular mass for the 3 possible chlorine compositions and their relative intensities in parentheses | | |
|---|---|---|---|
| | 130 (10:) | 132 (6,5:) | 134 (1) |
| $O_2H$ (M − 33) | 97 | 99 | 101 |
| $H_2O_2$ (M − 34) | 96 | 98 | 100 |
| $^{35}Cl$ | 95 | 97 | – |
| $^{37}Cl$ | – | 95 | 97 |
| OH and $^{35}Cl$ | 78 | 80 | – |
| $H_2O$ and $^{35}Cl$ | 77 | 79 | – |
| OH and $^{37}Cl$ | – | 78 | 80 |
| $H_2O$ and $^{37}Cl$ | | 79 | 81 |

carbons were investigated. Reaction mixtures of propane, isobutane, *n*-butane, isopentane, *n*-pentane and *n*-hexane were analysed before starting the reaction and after a reaction time of 25 min. Using the amount of degradation of the educt and the amount of products, mass balances for carbon were established. Recoveries of 94–102% were determined for these alkanes. Therefore, the ECN concept was applicable to the determination of hydroperoxides.

For methane and ethane no carbon balances could be established because cold trapping and the column capacity for these very volatile compounds were insufficient. Peak splitting and peak broadening occurred and quantitative analysis was impossible.

In Table III the detection limits of the hydroperoxides are listed. Detection limits ($3\sigma$) were derived using the ECN concept. The detection limits of this system might be improved if sample loops of larger volumes are applied.

## CONCLUSION

A sensitive GC method for the identification and determination of alkyl hydroperoxides has been developed. Mass spectra of $C_1$–$C_6$ hydroperoxides have been recorded. Detection limits of the hydroperoxides ranged between 91 and 127 pg absolute. With this system, very unstable hydroperoxides such as chlorinated hydroperoxides could also be synthesized and determined.

ACKNOWLEDGEMENT

We are grateful to the Eurotrac subproject Lactoz for financial support.

REFERENCES

1 C.N. Hewitt and G.L. Kok, *J. Atmos. Chem.*, 12 (1991) 181.
2 R.S. Deelder, M.G.F. Kroll and J.A.M. van den Berg, *J. Chromatogr.*, 125 (1976) 307.
3 G.L. Kok, K. Thompson, A.L. Lazarus and S.E. McLaren, *Anal. Chem.*, 58 (1986) 1192.
4 W. Czerwinsky and E. Kurek, *J. Chromatogr.*, 286 (1984) 275.
5 L. Cerveny, A. Marhoul and V. Ruzicka, *J. Chromatogr.*, 74 (1972) 118.
6 G.T. Cairns, R. Ruiz Diaz, K. Selby and D.J. Waddington, *J. Chromatogr.*, 103 (1975) 381.
7 U. Stanescu, A. Farcas and V. Petruta, *Chromatographia*, 15 (1982) 183.
8 P. Warneck and K. Bächmann, in R.A. Cox (Coordinator), *Eurotrac Annual Report, Part 8, Lactoz*, International Scientific Secretariat, Garmisch-Partenkirchen, 1988, p. 106.
9 P.D. Lightfoot, R.A. Cox, J.N. Crowley, M. Destriau, G.D. Hayman, M.E. Jenkin, G.K. Moortgat and F. Zabel, *Atmos. Environ.*, 26A, No. 10, (1992).
10 J.C. Sternberg, W.S. Gallaway and D.T.L. Jones, in N. Brenner, J.E. Callen and M.D. Weiss (Editors), *Gas Chromatography*, Academic Press, New York, 1962, pp. 231–267.
11 J.T. Scanlon and D.E. Willis, *J. Chromatogr. Sci.*, 23 (1985) 333.
12 A.D. Jorgenson, K.C. Picel and V.C. Stamoudis, *Anal. Chem.*, 62 (1990) 683.
13 A.R. Burgess, R.D.G. Lane and D.K. Sen Sharma, *J. Chem. Soc.*, (1969) 341.

*Journal of Chromatography A*, 653 (1993) 293–302
Elsevier Science Publishers B.V., Amsterdam

CHROM. 25 452

# Reversed-phase thin-layer chromatographic separations of enantiomers of dansyl-amino acids using β-cyclodextrin as a mobile phase additive[☆]

Joseph W. LeFevre[☆☆]

*Chemistry Department, Virginia Polytechnic Institute and State University, Blacksburg, VA 24061 (USA)*

(First received June 8th, 1993; revised manuscript received July 25th, 1993)

ABSTRACT

The DL-racemates of nine proteinogenic amino acids were resolved by reversed-phase thin-layer chromatography after conversion to their 5-dimethylamino-1-naphthalene sulfonyl (dansyl) derivatives. The chiral selector β-cyclodextrin was used in the mobile phase along with either aqueous acetonitrile or aqueous methanol as an organic modifier. DL-Histidine was separated as both its mono- and didansyl derivatives. It was determined that it was the cyclic nature of two imino acids DL-proline and DL-pipecolic acid that prevented their enantiomeric separations under the conditions employed. The DL-racemates of four non-proteinogenic amino acids, two of which are involved in the urea cycle, were also separated.

## INTRODUCTION

The resolution of racemates using optically active cyclodextrins (CDs) as chiral selectors continues to be a topic of much interest. The cyclodextrins, which are designated α, β or γ, are cyclic molecules consisting of either six, seven or eight α-D-glucose units, respectively, bonded through 1,4-linkages. These molecules have been used to separate a wide variety of racemates by high-performance liquid chromatography (HPLC) [1], gas chromatography (GC) [2], high-performance capillary electrophoresis (HPCE) [3], and thin-layer chromatography (TLC) [4]. The cyclodextrins form diastereomeric inclusion complexes which allow hydrogen bonding interactions to occur with the unidirectional 2- and 3-hydroxyl groups located at the mouth of the cyclodextrin cavity [5].

The separation of 5-dimethylamino-1-naphthalene sulfonyl (dansyl, Dns)-DL-racemates of several amino acids by reversed-phase TLC using β-cyclodextrin (β-CD) in the mobile phase was first reported by Armstrong *et al.* [4]. This work was extended by Lepri *et al.* [6] who compared two different types of reversed-phase TLC. Both groups were successful in resolving DL-racemates of the same eight proteinogenic and the same three non-proteinogenic amino acids. Armstrong achieved only partial resolution of Dns-DL-tryptophan and Lepri failed to resolve it at all. This constitutes the first report on the application of this methodology to the resolution of the DL-racemates of the remaining ten common amino acids.

Complete resolution of nine of the remaining ten proteinogenic amino acid DL-racemates is reported in this paper. DL-Proline was only

☆ In memory of my father, the late David A. LeFevre, and his contributions to electrochemistry.

☆☆ Permanent address: Chemistry Department, State University of New York at Oswego, Oswego, NY 13126, USA.

0021-9673/93/$06.00 

TABLE I

REVERSED-PHASE TLC DATA FOR THE SEPARATION OF Dns-AMINO ACIDS

Solvents: A = MeOH–0.20 *M* β-CD (35:65, v/v); B = $CH_3CN$–0.20 *M* β-CD (32:68, v/v); C = $CH_3CN$–0.2 *M* β-CD (20:80, v/v); D = MeOH–0.2 *M* β-CD (55:45, v/v); E = MeOH–saturated β-CD (60:40, v/v); F = MeOH–0.2 *M* β-CD (50:50, v/v).

| Dns-Amino acid | Abbreviation | $R_{F(D)}$ | $R_{F(L)}$ | $\alpha$ [a] | $R_s$ [b] | Solvent [c] |
|---|---|---|---|---|---|---|
| DL-Alanine | Dns-DL-Ala | 0.47 | 0.40 | 1.43 | 1.64 | A |
| DL-*allo*-Isoleucine | Dns-DL-*allo*-Ile | 0.38 | 0.30 | 1.43 | 3.25 | B |
| DL-Asparagine | Dns-DL-Asn [d] | 0.69 | 0.60 | 1.39 | 1.53 | C |
| DL-Arginine | Dns-DL-Arg | 0.65 | 0.55 | 1.52 | 1.69 | C |
| DL-Citrulline | Dns-DL-Cit | 0.63 | 0.54 | 1.45 | 1.52 | C |
| DL-Cystine | N,N′-Di-Dns-DL-Cys-Cys | 0.42 | 0.37 | 1.23 | 1.52 | D |
| DL-Glutamine | Dns-DL-Gln | 0.66 | 0.57 | 1.46 | 1.86 | C |
| DL-Histidine | N-(α)-Mono-Dns-DL-His | 0.64 | 0.58 | 1.28 | 1.13 | C |
| | N-(α),N-(im)-Di-Dns-DL-His [e] | 0.22 | 0.19 | 1.20 | 0.94 | E |
| DL-Isoleucine | Dns-DL-Ile | 0.40 | 0.33 | 1.35 | 1.71 | B |
| DL-Lysine | N,N′-Di-Dns-DL-Lys | 0.39 | 0.35 | 1.19 | 1.02 | E |
| N-Methyl-DL-valine | Dns-DL-N-Me-Val [e] | 0.28 | 0.24 | 1.18 | 0.94 | F |
| DL-Ornithine | N,N′-Di-Dns-DL-Orn | 0.40 | 0.35 | 1.24 | 1.20 | E |
| DL-Pipecolic acid | Dns-DL-Pip | 0.25 | 0.25 | 1.00 | 0 | F |
| DL-Proline | Dns-DL-Pro | 0.41 [f] | 0.39 [f] | 1.10 [f] | 0.63 [f] | F |
| DL-Tyrosine | N,O-Di-Dns-DL-Tyr | 0.26 | 0.23 | 1.15 | 0.94 | E |

[a] $\alpha = [(1 - R_{F(L)})/R_{F(L)}]/[(1 - R_{F(D)})/R_{F(D)}]$.
[b] $R_s = 2$ (distance between the two spots)/(sum of the widths of the two spots).
[c] Solutions contained urea and sodium chloride (see Experimental section).
[d] Part of the D-spot began to elute near the solvent front. The main body of this spot was used for these calculations.
[e] The identity of the D- *vs.* L-spot was not confirmed for this derivative.
[f] These are only approximate values because of overlap of the spots.

partially resolved by this technique. In addition, four non-proteinogenic amino acid DL-racemates were resolved. Two of these, DL-citrulline and DL-ornithine, are important compounds in the urea cycle. Table I lists the Dns-amino acids along with their abbreviations and separation data.

## EXPERIMENTAL

### *Materials*

The reversed-phase TLC was performed with glass-backed, chemically bonded octadecylsilane ($C_{18}$) plates. Whatman $LKC_{18}F$ plates (200 μm thickness, 20 × 5 cm) were used to separate the dansylated DL-pairs and to purify N-(α),N-imidazole (im)-Di-Dns-DL-His. A Whatman $PLKC_{18}F$ plate (1000 μm thickness, 20 × 20 cm) was used to purify N-(α)-mono-Dns-DL-His for proton nuclear magnetic resonance ($^1H$ NMR) spectroscopy. Both types of plates contained a preabsorbent layer. Whatman $MKC_{18}F$ plates (200 μm thickness, 1 × 3 in.; 1 in. = 2.54 cm) were used to analyze the mono-and di-Dns-His samples subjected to acid hydrolysis and/or UV light. All three types of reversed-phase plates were obtained from Whatman (Clifton, NJ, USA). The normal-phase TLC plates consisted of aluminum-backed Merck Kieselgel 60 $F_{254}$ (0.2 mm thickness, 20 × 20 cm) and glass-backed Merck Kieselgel 60 $F_{254}$ (0.25 mm thickness, 20 × 5 cm), both available from EM Science (Gibbstown, NJ, USA). β-cyclodextrin hydrate, sodium chloride, urea and dansyl chloride (Dns-Cl), were obtained from Aldrich (Milwaukee, WI, USA). Methanol (MeOH) and acetone (both HPLC grade), and sodium hydrogencarbonate ($NaHCO_3$) were obtained from Fisher Scientific (Fair Lawn, NJ, USA). Acetonitrile ($CH_3CN$, Nanograde) was purchased from Mal-

linckrodt (Paris, KY, USA). All amino acids were purchased from Sigma (St. Louis, MO, USA) as were the following standard Dns-amino acids: Dns-L-Ala, Dns-L-Asn, Dns-L-Arg, Dns-L-Cit, N,N′-Di-Dns-L-Cys-Cys, Dns-L-Gln, N,N′-di-Dns-L-Lys, Dns-L-Pro and N,O-di-Dns-L-Tyr. A Mineralight lamp (Model UVGL-25; UVB, Inc., San Gabriel, CA, USA) was used to visualize the TLC plates at 366 nm.

*Synthesis of Dns-DL-racemates*

A modified version of the procedures reported by Gray [7] and Chimiak and Polonski [8] was used to prepare the following Dns derivatives: DL-Ala, D-*allo*-Ile, DL-Asn, DL-, D- and L-Ile, DL-Lys, N-Me-DL-Val, DL- and L-Orn, DL- and L-Pip and DL-Pro. To 1000 $\mu$l of a 1 m*M* solution of the amino acid in 0.1 *M* $NaHCO_3$ were added 1000 $\mu$l of 15 m*M* Dns-Cl in acetone in a 5-ml conical vial. The vial was covered and the homogeneous yellow solution was stirred for 2 h at room temperature. The excess Dns-Cl was removed by extracting one or two times with diethyl ether. The pH of the aqueous layer was adjusted to 4 using 0.2 *M* hydrochloric acid and the neutralized Dns-derivative was extracted one or two times with ethyl acetate (EtOAc). The combined EtOAc extracts were dried with anhydrous magnesium sulfate. After evaporation to dryness the crude products were dissolved in EtOAc–MeOH (95:5; 200–600 $\mu$l, depending upon the yield) for reversed-phase TLC. The same procedure was used to prepare N,O-di-Dns-DL-Tyr with the following exception. Since DL-Tyr is not soluble in 0.1 *M* $NaHCO_3$, 0.2 *M* sodium hydroxide was added dropwise to dissolve the DL-Tyr, and the pH was adjusted to 10.

A slightly different work-up procedure was used to prepare the mono-Dns derivatives of the basic amino acids DL-Arg and DL-Cit, and the N-($\alpha$)-mono-Dns derivative of DL- and L-His. After removal of the excess Dns-Cl and acidifying to pH 1, excess $CH_3CN$ was added to the aqueous solution to form a lower-boiling azeotrope. The solution was evaporated to dryness on a rotary evaporator. The crude samples were purified (along with Dns-DL-Asn and Dns-DL-Gln) by normal-phase TLC prior to analysis by reversed-phase TLC.

Another modified work-up procedure was used to prepare N-($\alpha$),N-(im)-di-Dns-DL-His. Since the imidazole dansyl group is sensitive to acid [7], the crude reaction mixture was not acidified. Instead, after removal of excess Dns-Cl by extraction with EtOAc, the solution was simply evaporated to dryness with excess $CH_3CN$. The crude sample was dissolved in MeOH and purified in the dark by reversed-phase TLC (see *Reversed-phase TLC methods*).

*Normal-phase TLC methods*

The following five mono-Dns-amino acids were purified by normal-phase TLC: DL-Asn, DL-Arg, DL-Cit, DL-Gln and DL- and L-His. Each was dissolved in approximately 500 $\mu$l of MeOH and was streaked on a glass-backed, normal-phase TLC plate. The plates were developed in a solvent system composed of either EtOAc–$CHCl_3$–MeOH–acetic acid (AcOH) 50:30:20:1, v/v) [9] for Dns-DL-Asn ($R_F = 0.10$), Dns-DL-Cit ($R_F = 0.10$) and Dns-DL-Gln ($R_F = 0.13$) or EtOAc–$CHCl_3$–MeOH–AcOH (40:30:50:2, v/v) for Dns-DL-Arg ($R_F = 0.17$) and N-($\alpha$)-mono-Dns-DL- and L-His ($R_F = 0.14$). The appropriate band was visualized using long-wavelength UV light, scraped off the plate, and each derivative was eluted with 1–2 ml of MeOH. The purified samples were evaporated to dryness and redissolved in MeOH (Dns-DL-Cit and N-($\alpha$)-mono-Dns-DL- and L-His 100 $\mu$l each, Dns-DL-Gln 200 $\mu$l, and Dns-DL-Asn and Dns-DL-Arg 300 $\mu$l each) in preparation for reversed-phase TLC analysis.

*Reversed-phase TLC methods*

In order to increase the solubility of $\beta$-CD in water, a saturated solution of urea in water was prepared first [4]. This solution was then made 0.6 *M* in NaCl. The appropriate amount of $\beta$-CD was then added. Less than 1 $\mu$l of each solution of Dns-amino acid was spotted on a $20 \times 5$ cm TLC plate and developed from 3 to 6 h at room temperature in a $225 \times 54$ mm I.D. chamber.

Purification of N-($\alpha$)-mono-Dns-DL-His for $^1H$ NMR spectroscopy was accomplished by preparative reversed-phase chromatography using MeOH–2% aqueous AcOH (65:35, v/v) as the solvent [10]. A pure sample of N-($\alpha$),N-(im)-di-

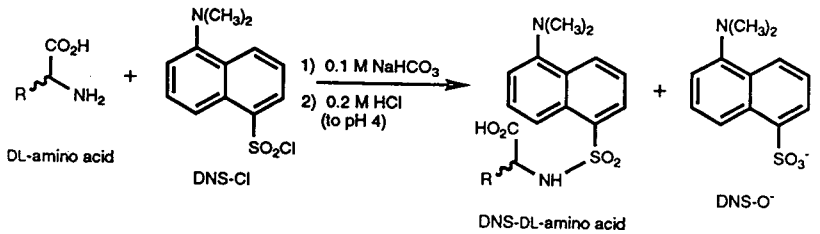


Fig. 1. General reaction for the formation of mono-Dns-DL-amino acids.

Dns-DL-His was obtained by reversed-phase chromatography in the dark using MeOH–0.01 *M* $Na_2HPO_4$ (75:25, v/v) [10] as the solvent. The pure samples were eluted from the silica gel with MeOH. The di-Dns derivative of DL-His was eluted in the dark. The $^1H$ NMR spectra were run in $C^2H_3O^2H$ using residual $C^2H_3OH$ as an internal standard ($\delta$4.78). A Bruker WP-270 NMR spectrometer was used to record the spectra.

## RESULTS AND DISCUSSION

The preparation of the Dns-DL-racemates was straightforward (see Experimental section for details). The general reaction for the preparation of the mono-Dns derivatives appears in Fig. 1. In the cases where the side chain contained a sulfhydryl group (Cys), a phenolic hydroxyl group (Tyr), an amino group (Lys and Orn), or an imidazole group (His), a di-Dns derivative was formed (Fig. 2). Under the reaction conditions employed the guanidinium group of Arg, and the amide group in Asn, Cit and Gln showed no reactivity [7].

The separation data ($R_F$, $\alpha$, $R_s$) for 15 Dns-amino acid DL-racemates appear in Table I. In each case where separation occurred, the D-isomer eluted ahead of the L-isomer (Fig. 3). This is consistent with earlier observations made on

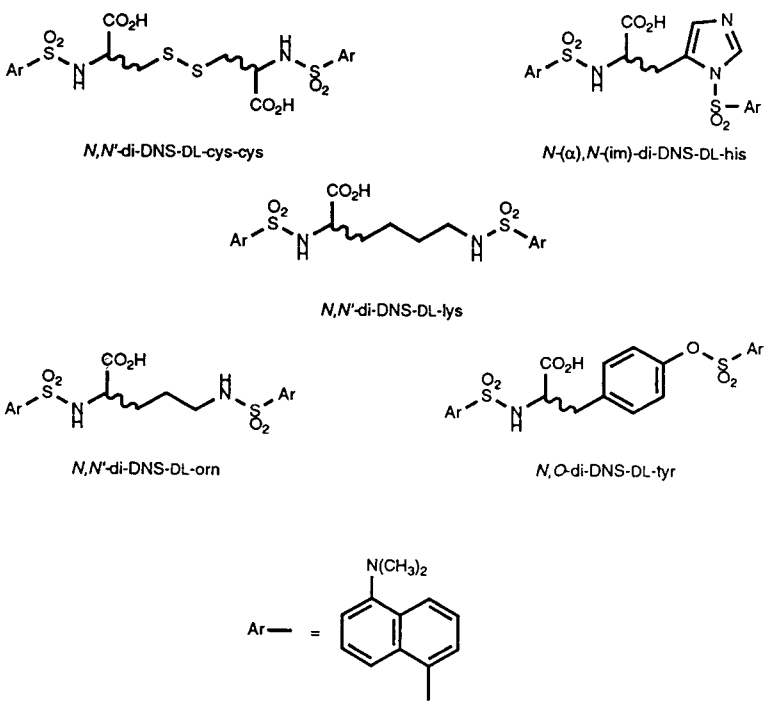


Fig. 2. Structures of the di-Dns-amino acids.

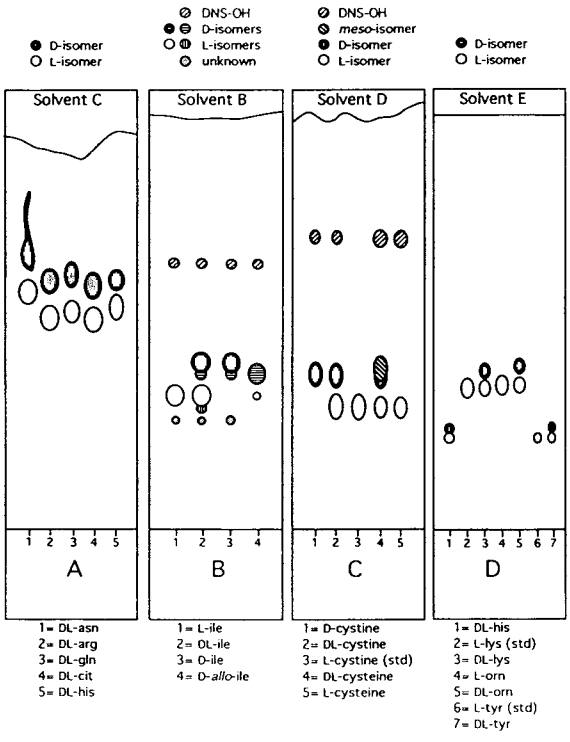


Fig. 3. Reversed-phase TLC diagrams of Dns-DL-amino acid separations. For solvents, see Table I. Plates A and B represent mono-Dns derivatives, plates C and D di-Dns derivatives.

different Dns-amino acid DL-racemates [4]. Since the separation method is believed to be based upon the preferential "fit" of one optical isomer over another into the $\beta$-CD cavity, it is obvious that the D-isomers are more tightly complexed with the $\beta$-CD in the mobile phase (higher $R_F$ values) than the corresponding L-isomers (lower $R_F$ values). In reversed-phase HPLC using a bonded $\beta$-CD as the stationary phase, the L-isomers elute prior to the corresponding D-isomers, again reflecting the stronger complexation of the D-isomers with the $\beta$-CD [11]. The exact mechanism of separation in either process (TLC or HPLC) is unknown. Presumably, the carboxyl group and/or the NH group of the primary sulfonamide of the D-isomer is/are capable of hydrogen bonding with the 2- or 3-hydroxyls near the mouth of the $\beta$-CD cavity to a greater extent than the L-isomer, thereby contributing to the enantioselectivity. In addition, with $\beta$-CD in the mobile phase, multiple complexation to more than one $\beta$-CD molecule is possible [12].

It was found during work-up that adjusting the pH of the crude, aqueous solution to 4 and extracting with EtOAc avoided large amounts of the fluorescent blue by-product dansyl sulfonic acid (Dns-OH) formed from the hydrolysis of Dns-Cl. This was necessary to avoid streaking upon development of the reversed-phase plates. At pH 4 the Dns-OH is essentially deprotonated (Fig. 1) and the majority remains in the aqueous layer. This extraction procedure could not be used for the mono-Dns derivatives of the basic amino acids Arg, Cit and His which were not soluble in EtOAc at pH 7 or less.

The solvent of choice for resolving the mono-Dns derivatives of DL-Asn, Arg, Cit, Gln and His was $CH_3CN$–0.2 $M$ $\beta$-CD (20:80, v/v) (Fig. 3A). All of these compounds had similar $R_F$ values (between 0.54 for Dns-L-Cit and 0.69 for Dns-D-Asn). The Dns-OH had an $R_F$ value of 0.59 in this solvent system, and effectively prevented the clear measurement of $\alpha$ and $R_s$ values for each of these enantiomeric pairs. It was easily removed by normal-phase TLC (see Experimental section) prior to reversed-phase TLC. It was not necessary to purify the Dns derivatives of the remaining amino acids since the Dns-OH had a much higher $R_F$ value than the compounds of interest.

There was some question as to whether N-($\alpha$)-mono-Dns-DL-His or N-($\alpha$),N-(im)-di-Dns-DL-His was initially isolated and separated (Fig. 3A). Some earlier reports using similar reaction conditions indicated that the di-Dns derivative was formed [13–15], but in one study the mass spectrum showed no parent ion at molecular mass 621 [14]. Other researchers [10,16] simply stated that Dns-His was formed without indicating whether it was the mono- or di-Dns derivative. Furthermore, the reversed-phase TLC conditions used in this work for separating D- and L-Dns-His (Table I, solvent C) were very different from the conditions used to separate the D- and L-isomers of the di-Dns derivatives of Lys, Orn and Tyr (Table I, solvent E). The Dns-His sample was much more polar than these three di-Dns derivatives, showing similar polarity to the mono-Dns derivatives of the amino acids Asn, Arg, Cit and Gln.

Since no standard samples of either mono- or di-Dns-His were readily available, the identity of

the initial Dns-DL-His sample (Fig. 3A) was confirmed as N-(α)-mono-Dns-DL-His by TLC, specific chemical reactions, and $^1$H NMR spectroscopy as described below.

First, it is known that the dansyl group on the α-nitrogen atom of both mono- and di-Dns-His is stable to acid hydrolysis, but the one on the imidazole nitrogen atom of di-Dns-His is not [7]. Therefore, hydrolysis of di-Dns-His produces N-(α)-mono-Dns-His and Dns-OH. A sample of Dns-DL-His was subjected to hydrolysis with 6 *M* HCl at 110°C for 12 h. Normal-phase TLC of the starting material using 1-butanol saturated with 0.2 *M* NaOH [17] showed a single, green fluorescent spot at $R_F = 0.15$. If di-Dns-His was present, acid hydrolysis would have resulted in the disappearance of this spot and the appearance of two new spots, one at a lower $R_F$ value [17] (corresponding to the more polar compound N-(α)-mono-Dns-DL-His) and a second new spot at $R_F = 0.56$ (corresponding to Dns-OH). In the event, acid hydrolysis resulted in a TLC that was essentially unchanged from that of the starting material. When a sample of di-Dns-DL-His, which was prepared later, was subjected to the same acid hydrolysis conditions, the starting material at $R_F = 0.36$ (same solvent system) had disappeared after 30 min and two major spots were produced, corresponding to N-(α)-mono-Dns-DL-His at $R_F = 0.15$ and Dns-OH at $R_F = 0.56$.

The second piece of evidence for N-(α)-mono-Dns-His came from a specific, colorimetric reaction. The Pauly reaction [18] utilizes diazotized sulfanilic acid and produces a yellow to red color with compounds containing an imidazole ring whose nitrogen atom at the 1 position is not derivatized. Only N-(α)-mono-Dns-His, therefore, would be expected to react. When a sample of pure Dns-DL-His was spotted on silica gel and sprayed with the Pauly reagent [19,20], a red spot corresponding to the azo dye of N-(α)-mono-DNS-His resulted. A negative result was seen for N-(α),N-(im)-di-Dns-DL-His. These reactions are summarized in Fig. 4.

The third line of support for the mono-Dns derivative was provided by $^1$H NMR spectroscopy. After purification of a crude sample of N-(α)-mono-Dns-DL-His by preparative reversed-phase TLC (see Experimental section), $^1$H NMR analysis showed a six-proton singlet at δ2.86 corresponding to the N,N-dimethyl group of the disubstituted naphthalene ring, and a relatively simple aromatic region (δ7.0–8.5). A sample of di-Dns-His would be expected to show two six-proton singlets in the δ2.7–2.9 region corresponding to two sets of N,N-dimethyl groups. In fact, this was found to be the case. A pure sample of N-(α),N-(im)-di-Dns-DL-His showed two singlets at δ2.77 and 2.79 and a much more complicated aromatic region due to the presence of two disubstituted naphthalene rings rather than one. Therefore, the TLC data, the hydrolysis and Pauly reactions, and $^1$H NMR spectroscopy clearly indicated that the Dns-His samples originally prepared and separated in this paper corresponded to N-(α)-mono-Dns-His and not the di-Dns derivative.

The N-(α),N-(im)-di-Dns-His sample is quite sensitive to UV light. Initial attempts to purify this compound by both normal- and reversed-phase TLC were unsuccessful. During development, the plates were monitored by long-wavelength UV light, which caused partial destruction of the compound. When the purification was carried out in the dark on reversed-phase TLC, a pure sample resulted. Exposure of a portion of this sample dissolved in MeOH to long-wavelength UV light for 30 min resulted in complete destruction of the starting material [$R_F = 0.49$; solvent MeOH–0.01 *M* $Na_2HPO_4$ (75:25, v/v), reversed-phase TLC] and the appearance of eight new spots, two of which could be identified as N-(α)-mono-Dns-DL-His ($R_F = 0.79$) and Dns-OH ($R_F = 0.89$). The behavior of the di-Dns-His on reversed-phase TLC relative to other Dns-amino acids clearly indicated that the Dns-His sample separated by Macek *et al.* [10] was di-Dns-His and not the mono-Dns derivative.

A portion of the N-(α),N-(im)-di-Dns-DL-His sample sample was subjected to reversed-phase TLC using β-CD in the mobile phase (Fig. 3D). Although resolution of the D- and L-isomers did occur ($\alpha = 1.20$, $R_s = 0.94$), the separation was not as efficient as the one for N-(α)-mono-Dns-DL-His ($\alpha = 1.28$, $R_s = 1.13$). Therefore, the NH group at the 1 position of the free imidazole ring of the mono-Dns derivative contributes signifi-

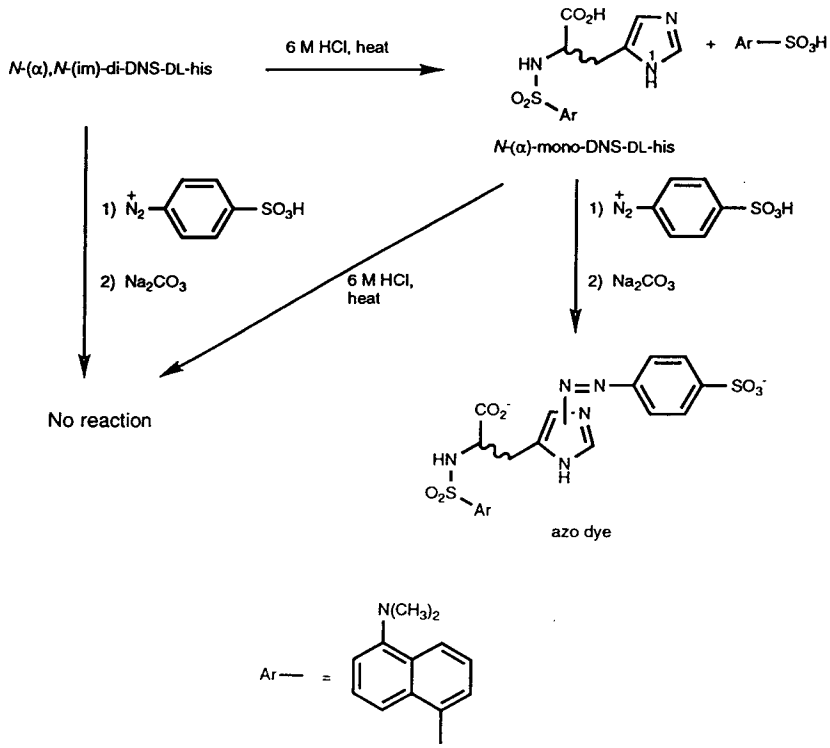


Fig. 4. Reactions of the mono- and di-Dns derivatives of DL-histidine.

cantly to the enantioselection, presumably by hydrogen bonding to the β-CD.

Because of the presence of two chiral centers Dns-Ile exists in four stereoisomeric forms (Fig. 5). All four stereoisomers were separated by this technique (Fig. 3B). The sample of DL-Ile from Sigma used in the preparation of the derivatives was labeled as containing all four stereoisomers. Reversed-phase TLC analysis showed two major spots and three minor spots, plus Dns-OH. The two major spots corresponded as expected to Dns-D- and L-Ile. The first major spot ($R_F$ = 0.33) was identified as Dns-L-Ile by comparison with a sample synthesized from L-Ile. The second major spot ($R_F$ = 0.40) was identified as Dns-D-Ile by comparison with a sample synthesized from the corresponding D-amino acid (which also contained traces of its diastereomer the non-proteinogenic amino acid D-*allo*-Ile). The first minor spot ($R_F$ = 0.38), corresponding to Dns-D-*allo*-Ile, was identified by comparison with a sample synthesized from D-*allo*-Ile (which also contained traces of the diastereomer L-Ile). The

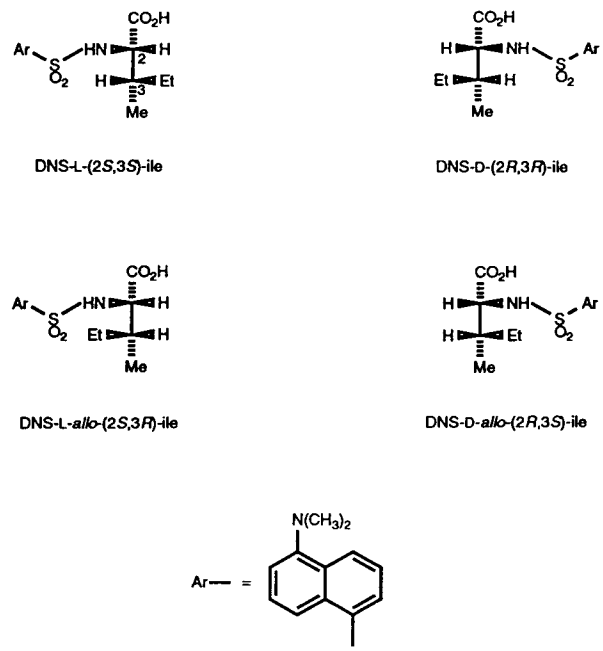


Fig. 5. Structures of the Dns-DL-isoleucines.

second minor spot at $R_F = 0.30$ corresponded to the remaining isomer L-*allo*-Ile. The third minor spot was not identified.

DL-Cysteine (Cys) was separated as the N,N′-di-Dns dimer of DL-cystine (Cys-Cys). Under the conditions employed in the dansylation reaction the –SH (thiol) group of Cys is oxidized to the corresponding –S–S– (disulfide) dimer, Cys-Cys, which subsequently is didansylated, once on each nitrogen atom [21]. Thus, dansylation of L-Cys yields N,N′-di-Dns-L-Cys-Cys and D-Cys yields N,N′-di-Dns-D-Cys-Cys. Dansylation of DL-Cys yields not only the di-Dns-L-(25%) and D-(25%) isomers of Cys-Cys, but also the *meso* compound di-Dns-D-Cys-L-Cys (50%). Therefore, reversed-phase TLC gave spots with identical $R_F$ values for the di-Dns derivatives of both D-Cys-Cys and D-Cys (0.38) and for both L-Cys-Cys and L-Cys (0.31). When a DL-mixture of Cys was dansylated, a third major spot was visible ($R_F$ = 0.39) corresponding to the *meso* compound (Fig. 3C).

As is evident from Table I, excellent $\alpha$ and $R_s$ values were obtained for all mono-Dns-amino acids (except proline and pipecolic acid). The di-Dns-derivatives of His, Lys, Orn and Tyr did not separate as well as the others (Fig. 3D). Because of the less polar nature of these derivatives, it was necessary to use more organic modifier (MeOH) relative to aqueous $\beta$-CD to get the compounds to move up the reversed-phase plate than in the case of the mono-Dns derivatives. The lower $R_s$ values were presumably due to the fact that derivatization of the side chain resulted in reduced hydrogen bonding potential. The Dns-OH by-product produced in the syntheses of these di-Dns derivatives eluted near the solvent front and no attempts were made to draw these complex, elongated patterns in Fig. 3D.

It was not possible to completely separate Dns-DL-Pro using this methodology. Proline is a cyclic imino acid rather than an amino acid, and thus forms a secondary sulfonamide upon dansylation rather than a primary sulfonamide. Dns-DL-Pipecolic acid (Pip), the six-membered ring analogue of proline (Fig. 6) could not be separated at all. Lam and Karmen [22] experienced similar difficulty with these two imino

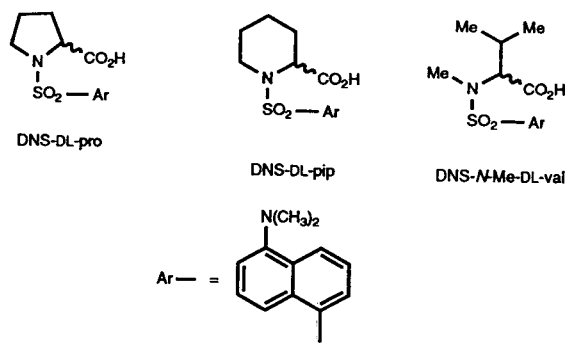


Fig. 6. Structures of the secondary sulfonamide Dns-DL-amino acids.

acids. They used a copper(II)-L-proline chiral mobile phase additive in order to form diastereomeric copper(II) complexes with enantiomeric Dns-amino acid derivatives using reversed-phase HPLC. Although the mechanism of separation using Cu(II) complexes is obviously different than with $\beta$-CD, it is interesting to note that the presence of a secondary sulfonamide was mentioned as a possible reason for the lack of formation of the proper diastereomeric copper(II) complexes, and hence, lack of separation. The Dns-D- and L-isomers of Pro and Pip were eventually separated by Lam and Karmen [22] by forming complexes with copper(II)-L-aspartame.

In order to determine whether it was the cyclic nature of these imino acids or the presence of the secondary sulfonamide that was responsible for the lack of separation, a sample of Dns-N-methyl-DL-valine (Fig. 6) was synthesized from the corresponding non-proteinogenic amino acid. This derivative is of comparable molecular mass and polarity to Dns-DL-Pro and Dns-DL-Pip and is a secondary sulfonamide, but is not cyclic. Reversed-phase TLC analysis showed nearly complete resolution of this DL-pair ($R_s = 0.94$). Presumably then, it is the cyclic nature of these imino acids that prevents enantioselection by $\beta$-CD rather than the fact that they are secondary sulfonamides. Reversed-phase TLC separation of Dns-DL-valine using the same solvent system as Dns-N-Me-DL-Val (Table I, solvent F) resulted in a much improved separation ($R_s$ = 2.07). Dns-DL-Val is a primary sulfonamide and,

therefore, an NH group is available for hydrogen bonding to one of the 2- or 3-hydroxyl groups of β-CD thus improving the enantioselectivity. Dns-N-Me-DL-Val, being a secondary sulfonamide, lacks this NH group. The fact that this DL-pair can be resolved indicates that a primary sulfonamide group is not a necessary condition for enantioselection by β-CD.

Zukowski *et al.* [23] recently reported the enantiomeric separations of DL-Pro, DL-Pip and other imino acids as their 9-fluorenylmethyl chloroformate (FMOC) derivatives using an (*R*)-(−)-1-(1-naphthyl)ethyl carbamoylated-β-CD column and HPLC. Baseline separations were obtained using non-aqueous polar mobile phases containing triethylamine, AcOH and $CH_3CN$. The chiral recognition mechanism under non-aqueous conditions is still not clear, but it has been hypothesized that rather than inclusion complex formation, external adsorption at the mouth of the cyclodextrin cavity may be occurring [24].

An enantioseparation of DL-Pro has also been performed by LeFevre [25], who made diastereomeric Mosher amides of the methyl esters of DL-Pro. A normal-phase HPLC column was used for the baseline separation using *n*-heptane and diethyl ether in the mobile phase.

Finally, it was of interest to separate the DL-enantiomers of the non-proteinogenic amino acids DL-citrulline and DL-ornithine since these are important compounds in the urea cycle. Dns-DL-Cit ($R_s = 1.52$, Fig. 3A) and di-Dns-DL-Orn ($R_s = 1.20$, Fig. 3D) were both completely resolved by this technique as was Dns-DL-Arg ($R_s = 1.69$, Fig. 3A).

## CONCLUSIONS

The reversed-phase TLC method described above, which uses β-cyclodextrin as a chiral selector, provides a simple, sensitive technique for separating enantiomers of dansyl amino acids. The system is capable of separating both mono- and di-dansyl derivatives with the former showing better $R_s$ values. This work, in conjunction with that of Armstrong *et al.* [4], makes possible the resolution of all but two (proline and tryptophan) of the nineteen common, optically active amino acids found in proteins by reversed-phase TLC. Other applications of this method are currently being investigated.

## ACKNOWLEDGEMENT

Financial support from the Chemistry Department at the State University of New York at Oswego is gratefully acknowledged as is Dr. David G.I. Kingston of Virginia Polytechnic Institute and State University for supplying laboratory space and selected chemicals during my sabbatical leave.

## REFERENCES

1 W.L. Hinze, T.E. Riehl, D.W. Armstrong, A. Alak and T.J. Ward, *Anal. Chem.*, 57 (1985) 237.
2 T. Koscielski, D. Sybilska and J. Jurczak, *J. Chromatogr.*, 280 (1983) 131.
3 A. Guttman, A. Paulus, A.S. Cohen, N. Grinberg and B.L. Karger, *J. Chromatogr.*, 448 (1988) 41.
4 D.W. Armstrong, F.-Y. He and S.M. Han, *J. Chromatogr.*, 448 (1988) 345.
5 D.W. Armstrong, T.J. Ward, R.D. Armstrong and T.E. Beesley, *Science*, 232 (1986) 1132.
6 L. Lepri, V. Coas, P.G. Desideri and L. Checchini, *J. Planar Chromatogr.*, 3 (1990) 311.
7 W.R. Gray, *Methods Enzymol.*, 25B (1972) 121.
8 A. Chimiak and T. Polonski, *Org. Prep. Proceed. Int.*, 5 (1973) 117.
9 N. Seiler and J. Wiechmann, *Experientia*, 20 (1964) 559.
10 K. Macek, Z. Deyl and M. Smrž, *J. Chromatogr.*, 193 (1980) 421.
11 D.W. Armstrong and W. DeMond, *J. Chromatogr. Sci.*, 22 (1984) 411.
12 D.W. Armstrong, F. Nome, L.A. Spino and T. Golden, *J. Am. Chem. Soc.*, 108 (1986) 1418.
13 Y. Tapuhi, D.E. Schmidt, W. Lindner and B.L. Karger, *Anal. Biochem.*, 115 (1981) 123.
14 N. Seiler, H.H. Schneider and K.D. Sonnenberg, *Anal. Biochem.*, 44 (1971) 451.
15 W. Lindner, J.N. LePage, G. Davies, D.E. Seitz and B.L. Karger, *J. Chromatogr.*, 185 (1979) 323.
16 D. Morse and B.L. Horecker, *Anal. Biochem.*, 14 (1966) 429.
17 M. Cole, J.C. Fletcher and A. Robson, *J. Chromatogr.*, 20 (1965) 616.
18 H. Pauly, *Z. Physiol. Chem.*, 42 (1904) 508.
19 B.N. Ames and H.K. Mitchell, *J. Am. Chem. Soc.*, 74 (1952) 252.
20 R.W. Cowgill, *Anal. Chem.*, 27 (1955) 1519.

21 E. Schulze and V. Neuhoff, *Hoppe-Seyler's Z. Physiol. Chem.*, 357 (1976) 225.
22 S. Lam and A. Karmen, *J. Liq. Chromatogr.*, 9 (1986) 291.
23 J. Zukowski, M. Pawloska and D.W. Armstrong, *J. Chromatogr.*, 623 (1992) 33.
24 D.W. Armstrong, S. Chen, C. Chang and S. Chang, *J. Liq. Chromatogr.*, 15 (1992) 545.
25 J.W. LeFevre, *Ph.D. Dissertation*, Virginia Polytechnic Institute and State University, Blacksburg, VA, 1984, pp. 47–51.

*Journal of Chromatography A*, 653 (1993) 303–312
Elsevier Science Publishers B.V., Amsterdam

CHROM. 25 413

# Strategy for setting up single-capillary isotachophoresis–zone electrophoresis

N.J. Reinhoud, U.R. Tjaden* and J. van der Greef

*Division of Analytical Chemistry, Leiden/Amsterdam Center for Drug Research, Leiden University, P.O. Box 9502, 2300 RA Leiden (Netherlands)*

(First received March 29th, 1993; revised manuscript received July 6th, 1993)

ABSTRACT

A strategy is described for the optimization of capillary zone electrophoresis (CZE) with isotachophoretic (ITP) preconcentration in a single-capillary set-up. CZE with indirect UV absorbance detection is used as a tool in setting up ITP–CZE. The electropherograms obtained with indirect detection give an immediate insight into the migration order of possible leading and terminating ions and of the analyte ions. Furthermore, information is obtained on the ionic composition of the sample matrix. The separation window in the ITP step can be chosen in such a way that a sample clean-up is achieved before zone electrophoresis is started. The described approach is applicable for setting up an ITP–CZE analysis in both the cationic and anionic modes. The usefulness of the strategy is illustrated by setting up the ITP–CZE of three cationic antimuscarinic drugs. Applying the developed strategy, combined with liquid–liquid extraction, concentrations of homatropine and scopolamine down to 100 ng/ml could easily be determined.

## INTRODUCTION

One of the challenges in the application of capillary zone electrophoretic (CZE) separations in the analysis of biological samples is to achieve relevant determination limits. For a number of drugs this means that concentrations in the nanomolar range or lower have to be measured. To take full advantage of the separation power of CZE for trace analysis of biological samples, two approaches are considered to improve the determination limits. One is to increase the detection sensitivity. Several highly sensitive detection systems such as laser-induced fluorescence detection and electrochemical detection have been described [1–3]. However, these detection systems are only applicable to those analytes which show appropriate detection characteristics or can only be applied after a derivatization procedure. Especially for analyte concentrations at or below the nanomolar level, derivatization procedures are liable to involve artefact formation [4].

Another approach for improving the determination limits in CZE is to increase the sample loadability of the system. For reasons of separation efficiency, injection volumes in CZE are usually not higher than 1% of the total volume of the separation system. This means that the injection volumes are in the range 0.1–70 nl. Although absolute detection limits of femtomoles seem very impressive, the corresponding sample concentration detection limits are in the micromolar range, which is at least a factor 1000 away from trace analysis. One way to increase the loadability of the CZE system is to apply off-line concentrating sample pretreatment methods such as the use of extraction procedures in combination with an evaporation step. In these

* Corresponding author.

0021-9673/93/$06.00 

procedures millilitres of sample can be pretreated, concentrated and analysed.

Electrophoretic analyte focusing techniques provide an elegant way to increase the loadability in CZE. These focusing techniques, such as the coupling of isotachophoresis (ITP) with CZE and field amplified injection procedures, are based on the application of local differences in electrical field strength during the injection or the focusing step to permit stacking of the analyte ions [5–14]. The coupling of ITP with CZE has been described by several workers [5–10]. Improvements in determination limits by up to a factor of 1000 have been reported. In a recent paper we described the possibility of automated ITP–CZE for anionic separations in a single capillary using backpressure programming [15]. Sample volumes up to 55% of the total capillary volume were focused isotachophoretically and analysed in the CZE step. A hydrodynamic pressure was used for removal of the terminator buffer before the CZE was started. The ITP conditions prevented excessive zone broadening. The procedure was reproducible, quantitative and automated.

In this paper, a strategy is described for anionic and cationic separations using ITP–CZE in a single capillary. Four focusing procedures are described, two for each ionic mode. In both ionic modes the CZE run can take place in either the leading or the terminating buffer, depending on the configuration used. The choice of the leading and terminating buffer ions, which defines the actual separation window, is made after analyte and matrix analysis by CZE using indirect detection. Three antimuscarinic (atropinic) drugs, neostigmine, homatropine and scopolamine [16], were used as test compounds.

## EXPERIMENTAL

### *Apparatus*

An untreated fused silica capillary (100 $\mu$m I.D.) (SGE, Ringwood, Victoria, Australia) was used. A programmable injection system for capillary electrophoresis (PRINCE, Lauerlabs, Emmen, Netherlands) equipped with a reversible polarity power supply and possibility for pressurized and electrokinetic injection was used for the analyte focusing process.

On-capillary UV absorbance detection took place using a Spectra 100 UV–Vis detector (Spectra-Physics, Mountain View, CA, USA). The signal was registered on a BD 40 chart recorder (Kipp & Zn, Delft, Netherlands).

### *Chemicals*

Scopolamine hydrobromide, homatropine hydrobromide and neostigmine bromide were obtained from Sigma (St. Louis, MO, USA), crystal violet, triethylamine (TEA) (99%), diethanolamine (DEtOHA) (99%), triethanolamine (TEtOHA) (97%), 2,4,6-collidine (2,4,6-trimethylpyridine) (99%) and pyridine (99%) from Janssen Chimica (Beerse, Belgium), phosphoric acid, tris(hydroxymethyl)aminomethane (Tris), lithium hydroxide, sodium hydroxide, potassium hydroxide and ammonium acetate from Merck (Darmstadt, Germany) and dichloromethane (99%) from J.T. Baker (Deventer, Netherlands). In all experiments deionized water obtained with a Milli-Q system (Millipore, Bedford, MA, USA) was used.

### *Extraction of spiked plasma and urine samples*

The extraction procedure used is similar to that described for atropine [17]. Stock solutions of 1 mg/ml scopolamine hydrobromide, homatropine hydrobromide and neostigmine bromide were prepared in water and kept frozen (253 K) until used. Dilutions of the drugs were added to 225 $\mu$l of untreated blank plasma and urine from healthy volunteers until a final volume of 250 $\mu$l. The pH was increased by adding 50 $\mu$l of 1 mol/l lithium hydroxide solution. The samples were extracted by adding 600 $\mu$l of dichloromethane followed by vortex mixing for 1 min. The samples were centrifuged for 5 min at 1000 $g$. The upper layer was discarded and 500 $\mu$l of the lower layer were transferred into another vial and evaporated to dryness under reduced pressure using a Speedvac SVC 100H evaporation centrifuge (Savant Instruments, Farmingdale, NY, USA). After evaporation to dryness, the residues were dissolved in 500 $\mu$l of terminating buffer for ITP–CZE or CZE buffer for CZE analysis.

*Analyte focusing*

The analyte focusing procedure for the three antimuscarinic drugs consisted of five steps (Fig. 1A).

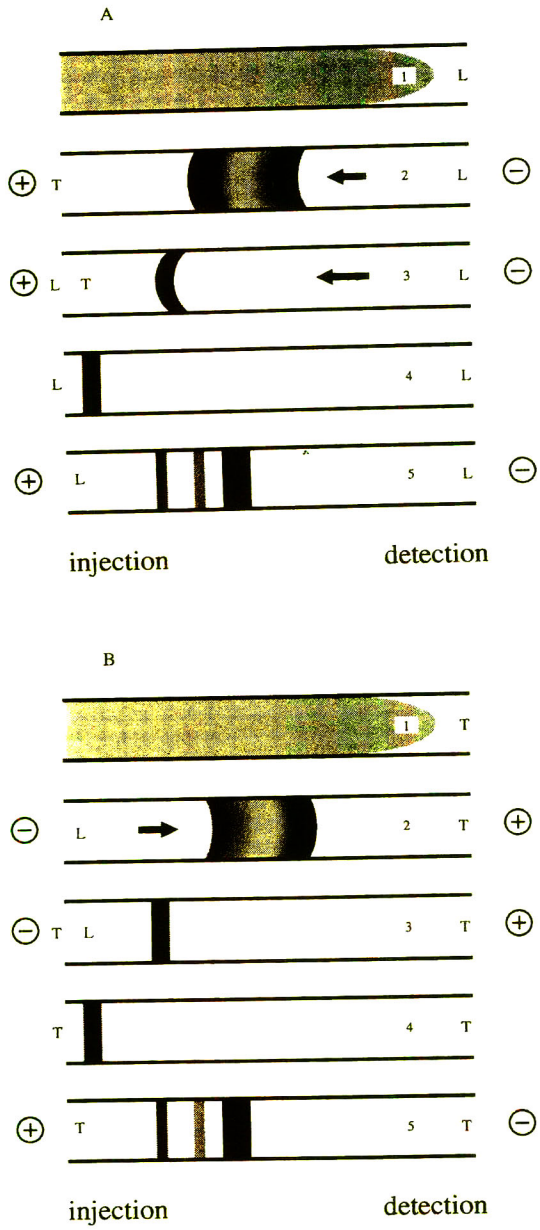


Fig. 1. Schematic representation of the ITP–CZE procedure for cations, (A) using the leading buffer (L) as CZE background electrolyte in combination with a negative backpressure (arrows) and (B) using the terminating buffer (T) as CZE background electrolyte and a positive backpressure. A reversal of the voltage is necessary in procedure B.

*Step 1.* After filling the capillary and the ITP cathode vial with leading buffer, the capillary is loaded with sample.

*Step 2.* The sample vial is replaced by the anode vial containing terminating buffer. A hydrodynamic backpressure is applied to counter balance the migration velocity of the analyte ions.

*Step 3.* When the focusing process is completed, the voltage is switched off and the vial containing terminating buffer is replaced with a vial containing CZE buffer which is the same as the leading buffer. The voltage is turned on with a similar hydrodynamic backpressure but with a lower voltage than used in step 2. As a result, the highly concentrated plug of analyte cations moves into the direction of the capillary inlet.

*Step 4.* When the concentrated analyte ions approach the capillary inlet the hydrodynamic backpressure is switched off and the CZE (step 5) is started.

## RESULTS AND DISCUSSION

In each ionic mode of ITP–CZE the CZE step can take place in either the leading or the terminating buffer, resulting in four analyte focusing procedures (Figs. 1 and 2). The ITP–CZE procedure which will be applied for the cationic test compounds as given in Fig. 1A will now be discussed. The differences from the other three procedures will be indicated rather than discussing all procedures in detail. The procedure for ITP–CZE of anions as given in Fig. 2B has been described in detail elsewhere [15].

*Analyte focusing*

When during the focusing step (step 2) a positive voltage is applied at the capillary inlet, the analyte cations will migrate in the direction of the cathode because of the electrophoretic and electroosmotic mobility. A hydrodynamic pressure is applied to counterbalance the migration velocity of the analyte ions. In contrast to conventional ITP, the analyte ions do not move into the capillary during the focusing step but are concentrated and fixed at a position in the capillary by the hydrodynamic backpressure. The terms positive and negative backpressure are

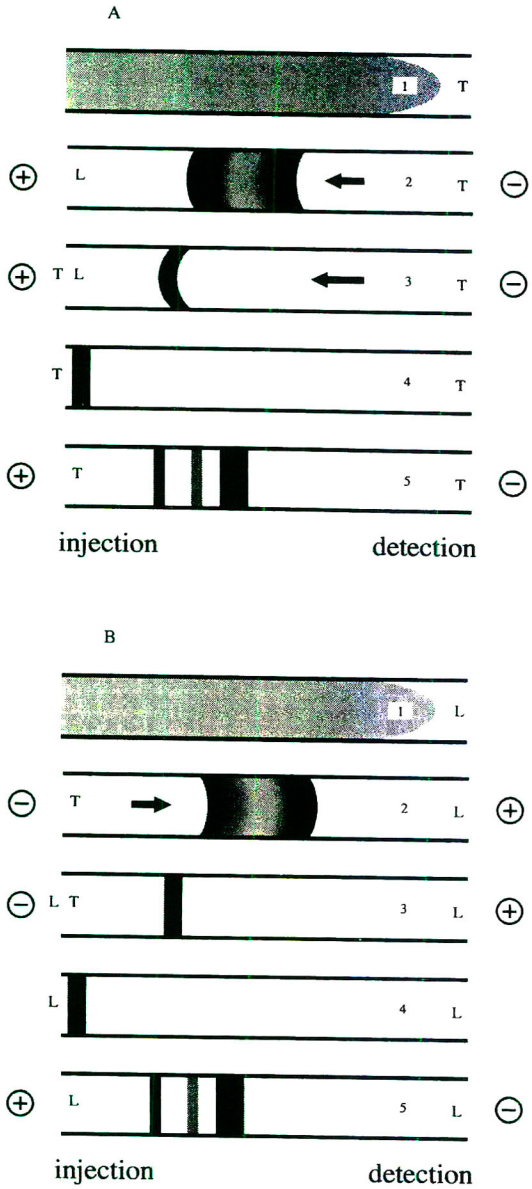


Fig. 2. Schematic representation of the ITP–CZE procedure for anions (A) using the terminating buffer (T) as CZE background electrolyte in combination with a negative backpressure (arrows), and (B) using the leading buffer (L) as CZE background electrolyte and a positive backpressure. A reversal of the voltage is necessary in procedure B.

used to describe the direction in which the hydrodynamic backpressure is applied: a positive backpressure induces a flow in the direction of the capillary outlet and a negative backpressure results in a flow in the opposite direction.

In step 3, the highly concentrated plug of analyte cations is moving hydrodynamically in the direction of the capillary inlet. Zone broadening is counteracted by the isotachophoretic conditions that still exist. The plug of terminating buffer that is still in the capillary is removed at the capillary inlet.

The most critical point in the procedure is the timing of the moment to switch off the hydrodynamic backpressure (step 4) and to start the CZE (step 5). This is done at the moment the analytes are about to leave the capillary. When the CZE step is started too early, the remaining plug of terminating ions causes an inhomogeneous electric field and influences the efficiency and migration times in the CZE step. When the CZE step is started too late the analyte ions have left the capillary. In the first few runs a visible dye is used for precise timing of the moment that the sample ions are near the capillary inlet. When reproducible migration times in the focusing step are obtained, the procedure can be automated and the dye is no longer needed. Timing is also possible by monitoring the increase in current during step 3. The plug of terminating buffer raises the total resistance of the capillary, which means that at constant voltage the current increases until the terminating buffer has left the capillary.

The procedures for ITP–CZE using negative backpressure (Figs. 1A and 2A) differ from those using positive backpressure (Figs. 1B and 2B) in that in step 3 the backpressure is increased to mobilize the focused sample zone in the direction of the capillary inlet. In step 4 the backpressure is reduced to zero and the CZE run is started without reversal of the voltage. This means that the migration order of ions is the same in the ITP and CZE steps. In the procedures with reversal of the voltage, a reversal of the migration order of the analyte ions also takes place when switching from ITP to CZE. This phenomenon did not affect the efficiency or resolution in ITP–CZE with respect to CZE separations of relatively clean samples [15].

*ITP as sample clean-up for CZE*

The choice of the buffer system determines the extent to which the ITP focusing step can be used in sample clean-up for the CZE analysis. In

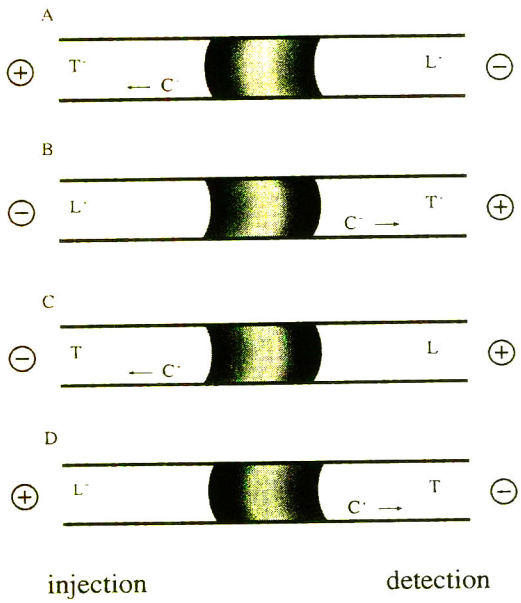


Fig. 3. The migration direction of the neutral species and counter ions ($C^+$, $C^-$) in the focusing step (Figs. 1 and 2, step 2) of the ITP–CZE procedure. Situations A and C are favourable with respect to sample clean-up.

Fig. 3 a summary is given of the different focusing steps in ITP–CZE. The migration direction of the ions with a lower mobility than the terminating ions is either in the direction of the capillary inlet or in the direction of the detector. Obviously, with respect to sample clean-up, the cationic mode with negative backpressure (Figs. 1A and 3A) and the anionic mode with positive backpressure (Figs. 2B and 3C) are favourable. In both instances the ions with a lower mobility than the terminating ions, including the neutral species and the counter ions, are removed and diluted in the inlet vial during the focusing step.

The focusing step is completed when all ions move isotachophoretically under steady-state conditions [18]. The more complex a sample is with respect to ion composition and ionic strength, the more time it takes to reach a true isotachophoretic state. Therefore, a sample pretreatment before the ITP–CZE step that results in a decrease in ionic strength of the sample matrix will reduce the focusing time in ITP–CZE. In the case of large variations in the composition of the sample matrix (*e.g.*, urine), a pretreatment step is likely to improve both the reproducibility and the efficiency in ITP–CZE. These aspects will be demonstrated below, where a strategy is given and discussed for setting up an ITP–CZE system for the three cationic test compounds.

*Choice of CZE buffer*

The first step in the optimization procedure for ITP–CZE will always be the optimization of the CZE step. Several papers are available describing CZE separations and methods for optimization [1–3]. However, in ITP–CZE the CZE buffer will also be a leading (or terminating) buffer. This will influence the choice of the background electrolyte for CZE.

With respect to sample clean-up it is favourable to use the leading buffer as the background electrolyte in CZE. Another aspect in favour of using the leading buffer concerns the band broadening caused by conductivity differences between the sample zones and the background electrolyte [19]. When a highly concentrated sample zone after the focusing step is switched to zone electrophoresis, band broadening takes place because of differences in conductivity of the sample zone and the background electrolyte [15]. The sample zone itself disturbs the homogeneity of the electric field in the electrophoresis tube. Zone broadening because of differences in conductivity is described by the equation

$$dz = \frac{L}{\kappa} \cdot d\kappa \qquad (1)$$

where $d\kappa$ is the conductivity difference between the sample zone and the background electrolyte, $\kappa$ is the conductivity of the background electrolyte, $L$ is the electrophoretic migration distance and $dz$ is the zone broadening due to the conductivity difference [19]. Because the conductivity of the leading buffer is always higher than that of the analyte ions, the band broadening will be less when the leading buffer is used as the background electrolyte than when the terminating buffer is used as the background electrolyte in the CZE step, for similar values of $d\kappa$.

Finally, using a leading buffer as background electrolyte for CZE is convenient with respect to current monitoring for the precise timing of the moment to switch from ITP to CZE (Figs. 1 and 2, step 4). Because at the time of switching the capillary is filled with the background electrolyte

for CZE the current will be high (typically in the microampere range) when using a leading buffer as the background electrolyte for CZE. When a terminating buffer is used as the background electrolyte for CZE the current will be considerably lower at the time of switching (typically in the high nanoampere range). Fluctuations in the current caused by ripples in the power supply make precise timing difficult, especially in the latter instance.

Addition of selectivity-enhancing compounds to the background electrolyte is allowed as long as those additives are non-ionic (*i.e.*, non-ionic detergents, non-ionic complex-forming agents, organic modifiers). With ionic additives care must be taken that they do not disturb the ITP conditions.

The ionic strength of the CZE buffer should be chosen so that the concentrating properties in the ITP step are high, but not so high that the analyte precipitates (*e.g.*, 5–100 mmol/l). The pH of the CZE buffer affects the electroosmotic flow-rate, which influences the efficiency of the ITP step. A high electroosmotic flow-rate will result in a mixing of zones in ITP. Therefore, at high pH additives are used that reduce the electroosmotic flow-rate, *e.g.*, hydroxypropylmethylcellulose (HPMC).

In conventional CZE the background electrolyte should have a buffering capacity to maintain a constant pH during separation. In ITP and ITP–CZE the counter ion should have this buffering capacity. Under steady-state conditions in ITP the analyte ions are focused between the leading and terminating ions. The counter ions are present throughout the separation tube. This means that the best way to buffer the system is by means of the counter ions.

The most important parameters in the initial conditions of the CZE background electrolyte will be the choice of pH, the buffering counter ions and the additives used. The choice of the leading and terminating ions can be made after studying the ITP separation window. In the ITP–CZE analysis of the cationic test compounds the migration order of the analyte, leading and terminating ions was not changed on switching from triethylamine to sodium as leading ion. However, changing the pH, the percentage of organic modifier or buffering counter ion might affect the migration order.

*ITP separation window*

One of the advantages in ITP–CZE is that most of the matrix constituents can be removed in the focusing step. The choice of the leading and terminating ions determines the focusing window. All compounds outside the separation window in the ITP step migrate under zone electrophoretic conditions. When maximum sample clean-up is desired a system is chosen where the CZE step takes place in the leading buffer. Complete removal of all counter ions and neutral species from the capillary is then expected (Figs. 1A, 2B, 3A and 3C).

However, matrix ions with a higher mobility than that of the leading ions in this instance migrate into the separation capillary even during the focusing step. When such ions are present in the matrix at a high concentration then it is advisable to trap them within the ITP window or to use these ions as leading ions. Otherwise, these ions may cause an inhomogeneity in the electrical field during the CZE run. For the optimization of ITP–CZE it is therefore necessary to have information on the ionic composition of the sample matrix. A conventional CZE system with indirect UV absorbance detection [20] is particularly suitable as a screening method for the main matrix components (Fig. 4).

Ions with a higher mobility than the leading ions giving a strong signal in the detection system may cause a drift in the baseline. These ions should also be trapped within the ITP separation window. Because of their detection properties these ions cannot be used as leading ions in a conventional detection system. In that particular event a leading ion with a higher mobility should be used.

With respect to sample clean-up the terminating ion should be chosen so that the mobility is just below that of the analyte ion with the lowest mobility.

*Choice of the leading and terminating buffer*

Several reviews on ITP are available that detail buffer systems and ionic mobilities of

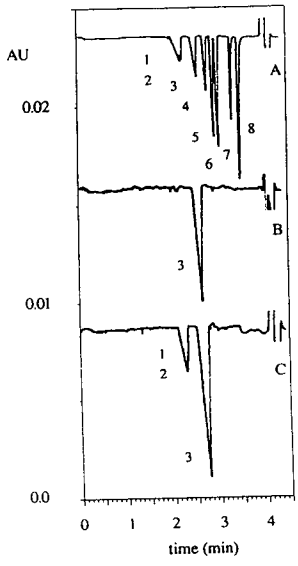


Fig. 4. Electropherograms of (A) a mixture of cations (2.5 mmol/l in background electrolyte), (B) human plasma (diluted 1:19 in background electrolyte) and (C) human urine (diluted 1:19 in background electrolyte). A voltage of 25 kV (4.7 $\mu$A) was applied over the 900 × 0.1 mm I.D. separation capillary. Indirect UV absorbance detection took place at 550 mm from the injection end at 200 nm using a 10 mmol/l collidine buffer adjusted to pH 8.0 with phosphoric acid. Injection was performed (A) hydrodynamically using 10 mbar for 6 s or (B, C) electrokinetically at 6 kV for 6 s. The cationic mixture consisted of ammonium (1), potassium (2), sodium (3), lithium (4), TEA (5), DEtOHA (6), Tris (7) and TEtOHA (8). At 4 min a system peak appeared together with the electroosmotic flow marker (acetonitrile).

compounds which are most helpful in setting up an ITP–CZE separation [18,21]. The ionic mobility of a compound is defined as the electrophoretic mobility of the compound when it is fully ionized. For ions such as sodium and chloride tabulated values can be used without correction for pH. For weak acids and bases the effective electrophoretic mobility can be calculated using the relationship between the p$K_a$, pH and ionic mobility [21]. This relationship is given by the equation

$$\mu_{HA} = \mu_{A^-} \cdot \frac{1}{1 + \frac{[H^+]}{K_a}} \quad (2a)$$

for compounds with one p$K_a$, where $\mu_{A^-}$ is the ionic mobility and $K_a$ the protolysis constant. For dibasic acids this equation becomes

$$\mu_{H_2A} = \frac{\mu_{HA^-} + \mu_{A^{2-}} \cdot \frac{K_{a_2}}{[H^+]}}{\frac{[H^+]}{K_{a_1}} + 1 + \frac{K_{a_2}}{[H^+]}} \quad (2b)$$

where $K_{a_1}$ and $K_{a_2}$ are the dissocation constants for a dihydric acid and the ionic mobilities are given by $\mu_{A^{2-}}$ and $\mu_{HA^-}$.

Eqns. 2a and 2b correct for the fraction of the compound that is not in the ionic form. Only the ionized fraction contributes to the electrophoretic mobility of an ion. Using the conditions in Fig. 4A for Tris the effective mobility is calculated to be $1.55 \cdot 10^{-8}$ m$^2$ V$^{-1}$ s$^{-1}$ (migration time 3.40 min, electroosmotic flow marker 4.05 min, electrical field strength 25 kV per 90 cm, at pH 8.0). According to eqn. 2a, effective mobility of $1.48 \cdot 10^{-8}$ m$^2$ V$^{-1}$ s$^{-1}$ is expected, which is close to the measured effective electrophoretic mobility (the tabulated value for the ionic mobility of Tris is $2.95 \cdot 10^{-8}$ m$^2$ V$^{-1}$ s$^{-1}$ [21] and the p$K_a$ of Tris is 8.0). In the same system sodium, which is always fully ionized, has an effective electrophoretic mobility of $5.05 \cdot 10^{-8}$ m$^2$ V$^{-1}$ s$^{-1}$, which is approximately the same as the ionic mobility [18], as expected.

As shown in Fig. 6, a CZE system applying indirect detection can be used for selecting suitable leading and terminating ions in ITP–CZE. Especially in those instances where additives to the buffer are used, tabulated values are not always available. The electropherogram gives a good insight into the migration order of the leading, terminating and sample ions. To make a good comparison possible it is necessary that the indirect detection system is similar to the chosen CZE buffer in the ITP–CZE analysis with respect to additives, counter ion and pH.

Based on data obtained by the indirect detection system, the final choice of leading and terminating ions can be made. For plasma and urine samples sodium is most likely the main cationic compound, which is confirmed by the electropherograms in Fig. 4. Therefore, when the mobility of the analyte ions is lower, sodium can be used as the leading ion.

*Application of ITP–CZE to spiked plasma and urine samples*

The first step in the ITP–CZE analysis of the three antimuscarinic test compounds in spiked plasma and urine was the optimization of the CZE system. At pH 5.0 the compounds were baseline separated (Fig. 5). Therefore, an acetate buffer adjusted to pH 5.0 was chosen as the background electrolyte for CZE. To permit a high loadability of the system, a separation capillary of 900 × 0.1 mm I.D. was used. The current at 25 kV was reduced by adding 50% methanol to the buffer. To reduce the CZE run times the detector was placed at 550 mm from the capillary inlet. This offered the additional advantage of allowing the application of a negative hydrostatic backpressure by raising the electrode vial at the capillary outlet.

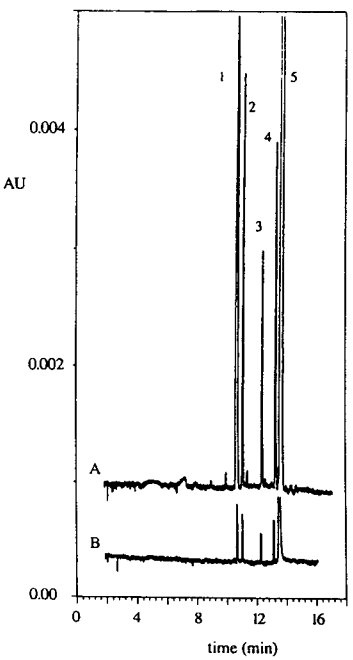


Fig. 5. (A) ITP–CZE of 280 nl and (B) CZE of 28 nl of the three test compounds neostigmine (2), homatropine (3), scopolamine (4) and of the dye crystal violet (5). Peak 1 is an unidentified system peak. In both instances a concentration of a 1 μg/ml of the test compounds and 10 μg/ml for the dye was injected. The leading buffer was 10 mmol/l TEA in 50% methanol adjusted to pH 5.0 with acetic acid. The terminating buffer consisted of 10 mmol/l β-alanine in 50% methanol adjusted to pH 5.0 with acetic acid. UV absorbance detection took place at 550 mm from the injection end at 200 nm. The detector settings were the same for both electropherograms. ITP–CZE was performed as described in Fig. 1A.

The second step was the selection of the ITP separation window. Depending on the separation window set by the leading and terminating ions, ITP can be used for sample clean-up for CZE. Therefore, an indirect detection system was used to study the main matrix components in urine and plasma (Fig. 4). Conditions for the indirect detection of urine and plasma were chosen so that semi-quantitative information was obtained rapidly. The electropherograms of urine and plasma were compared with an electropherogram of a mixture of cations. The main cationic component in urine and plasma was sodium, as expected. Therefore, sodium was chosen as a leading ion in the ITP–CZE method. Especially urine contains a considerable concentration of cations with higher mobility such as potassium and ammonium ions (Fig. 4C). These ions did not disturb the final ITP–CZE analysis, otherwise one of these ions could be chosen as the leading ion.

The choice of β-alanine as terminating ion was made in a similar way using indirect detection. However, to make a good comparison with the migration order in ITP–CZE possible, the conditions of the indirect system were carefully chosen. The buffer consisted of acetate at pH 5.0 in 50% methanol. The only difference to the conditions of the CZE background electrolyte in the final ITP–CZE system was the use of pyridine as UV-absorbing co-ion instead of sodium. Fig. 6 clearly demonstrates the separation window between the leading and terminating ions.

Depending on the separation window, the complexity of the matrix and the analyte concentration, ITP [22–24] and ITP–CZE can be used for the analysis of plasma and urine samples without any or with minor pretreatment (*e.g.*, filtration). In Fig. 7 the electropherograms obtained after ITP–CZE of 10 μg/ml antimuscarinic drugs in urine with the without pretreatment are shown. For trace analysis it is unlikely that the selectivity in ITP–CZE without an additional pretreatment will be sufficient. Interferences in the CZE analysis will by definition

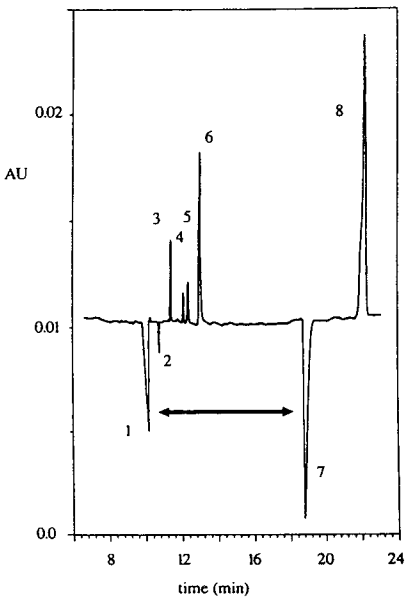


Fig. 6. Representation of the ITP separation window (arrow) using CZE with an indirect detection system. The background electrolyte consisted of 10 mmol/l pyridine in 50% methanol adjusted to pH 5.0 with acetic acid. The migration order of neostigmine (3), homatropine (4), scopolamine (5) and crystal violet (6) can be easily determined with respect to possible leading (1, TEA) and terminating (7, β-alanine) ions. Peak 2 is an unidentified system peak and peak 8 is pyridine. For electrophoretic conditions, see Fig. 4.

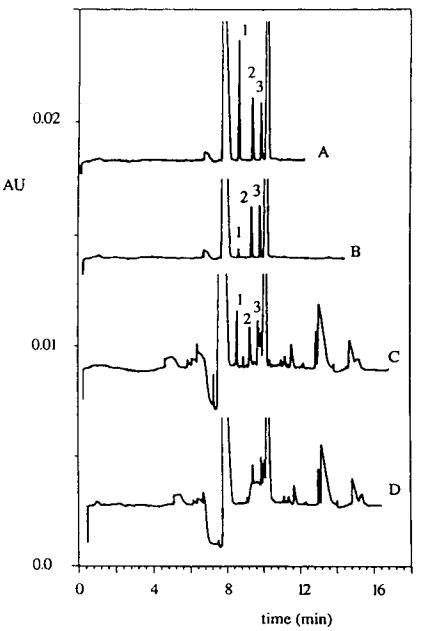


Fig. 7. ITP–CZE of 92 nl (10 μg/ml) of neostigmine (1), homatropine (2) and scopolamine (3), (A) in buffer, (B) in urine after dichloromethane extraction and (C) in urine without any pretreatment, in comparison with (D) blank urine. ITP–CZE was performed as described in Fig. 1A. Sodium acetate (10 mmol/l) at pH 5.0 in 50% methanol was used as the leading buffer and as the CZE background electrolyte. The termination ion was β-alanine. During the focusing step (Fig. 1A, step 2) a voltage of 10 kV and a backpressure of 22 mbar were applied. For the hydrodynamic mobilization of the sample zones (Fig. 1A, step 3) the backpressure was increased to 30 mbar at the same voltage. The focusing step took 5.5 min for runs A and B and 15 min for C and D.

migrate within the separation window in the ITP step because the separation principle in both electrophoretic modes is the same. The use of spacer ions in the ITP step may enhance the selectivity of the final analysis, but in the case of comigrating zones in CZE the ITP step will not give additional selectivity.

The selectivity is considerably enhanced by applying a liquid–liquid extraction with dichloromethane prior to the ITP–CZE step (Figs. 7–9). As can be seen in Fig. 7B, the extraction recovery for neostigmine is low. Scopolamine and homatropine can be measured at a concentration level of 100 ng/ml in plasma (Fig. 9) and urine (Fig. 8) after extraction. Although it is likely that the determination limits can be lowered using a concentration step by dissolving the evaporated extract in a smaller volume, no attempts were made to optimize the method.

## CONCLUSIONS

Two ITP–CZE procedures for cationic and two ITP–CZE procedures for anionic separations are given. A strategy is described for setting up an ITP–CZE analysis. Information on the migration order of leading ions, terminating ions and analyte ions can be obtained using CZE with indirect UV absorbance detection. Furthermore, information on the ionic composition of the matrix can be obtained. Indirect detection permits tuning of the ITP separation window when ITP is used for sample clean-up for CZE.

The applicability of the described strategy is

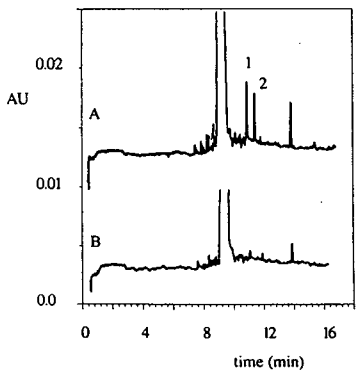


Fig. 8. ITP–CZE of 1.8 μl of (A) 100 ng/ml homatropine (1) and scopolamine (2) in urine and (B) blank urine after dichloromethane extraction. ITP–CZE conditions as in Fig. 7 except for the backpressure in the focusing step (Fig. 1A, step 2), which was 30 mbar at a voltage of 15 kV. The voltage was decreased to 10 kV at a constant backpressure to mobilize the focused analyte zones (Fig. 1A, step 3) towards the capillary inlet. The focusing step took 25 min before the CZE step was started at 25 kV. Crystal violet was no longer used as a dye. The current in step 3 increased from 0.1 to 3.1 μA.

demonstrated for the optimization of ITP–CZE of homatropine, scopolamine and neostigmine in spiked urine and plasma samples. Depending on the analyte concentrations plasma and urine samples can be analysed without pretreatment. However, because the separation mechanisms in both ITP and CZE are based on the same principle, an additional sample pretreatment will be needed in the case of comigrating matrix interferences. The coupling of a sample pretreatment based on separation mechanism other than

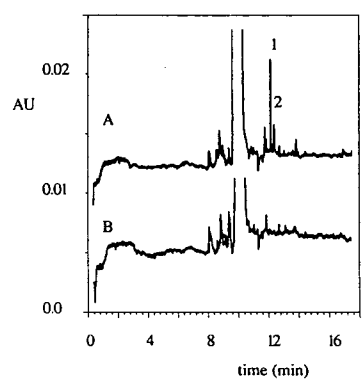


Fig. 9. ITP–CZE of 1.8 μl of (A) 100 ng/ml homatropine (1) and scopolamine (2) in plasma and (B) blank plasma after dichloromethane extraction. ITP–CZE conditions as in Fig. 8.

electrophoresis in combination with the tremendous concentrating properties of ITP makes the highly efficient separation power of CZE applicable for trace analysis.

## REFERENCES

1 R.A. Wallingford and A.G. Ewing, *Adv. Chromatogr.*, 29 (1989) 1.
2 W.G. Kuhr, *Anal. Chem.*, 62 (1990) 403R.
3 W.G. Kuhr and C.A. Monnig, *Anal. Chem.*, 64 (1992) 389R.
4 C.M.B. van den Beld, U.R. Tjaden, N.J. Reinhoud, D.S. Stegehuis and J. van der Greef, *J. Controlled Release*, 13 (1990) 129.
5 F. Foret, V. Sustacek and P. Bocek, *J. Microcol. Sep.*, 2 (1990) 229.
6 D.S. Stegehuis, H. Irth, U.R. Tjaden and J. van der Greef, *J. Chromatogr.*, 538 (1991) 393.
7 D. Kaniansky and J. Marak, *J. Chromatogr.*, 498 (1990) 191.
8 V. Dolnik, K.A. Cobb and M. Novotny, *J. Microcol. Sep.*, 2 (1990) 127.
9 R.L. Chien and D.S. Burgi, *Anal. Chem.*, 64 (1992) 489A.
10 F. Foret, E. Szoko and B.L. Karger, *J. Chromatogr.*, 608 (1992) 3.
11 R.L. Chien and D.S. Burgi, *Anal. Chem.*, 64 (1992) 1046.
12 D.S. Burgi and R.L. Chien, *Anal. Chem.*, 63 (1991) 2042.
13 C. Schwer and F. Lottspeich, *J. Chromatogr.*, 623 (1992) 345.
14 F.E.P. Mikkers, F.M. Everaerts and T.P.E.M. Verheggen, *J. Chromatogr.*, 169 (1979) 11.
15 N.J. Reinhoud, U.R. Tjaden and J. van der Greef, *J. Chromatogr.*, 641 (1993) 155.
16 I.R. Innes and M. Nickerson, in L.S. Goodman and A. Gilman (Editors), *The Pharmaceutical Basis of Therapeutics*, Collier–MacMillan, London, 4th ed., 1970, Ch. 25.
17 T. Okuda, M. Nishida, I. Sameshima, K. Kyoyama, K. Hiramatsu, Y. Takehara, K. Kohriyama, *J. Chromatogr.*, 567 (1991) 141.
18 F.M. Everaerts, J.L. Beckers and T.P.E.M. Verheggen, *Isotachophoresis: Theory, Instrumentation and Practice*, Elsevier, Amsterdam, 1976.
19 S. Hjertén, *Electrophoresis*, 11 (1990) 665.
20 E.S. Yeung and W.G. Kuhr, *Anal. Chem.*, 63 (1991) 275A.
21 J. Pospichal, P. Gebauer and P. Bocek, *Chem. Rev.*, 89 (1989) 419.
22 P. Oefner, R. Häfele, G. Bartsch and G. Bonn, *J. Chromatogr.*, 516 (1990) 251.
23 T. Hirokawa, H. Takemina, Y. Kiso, R. Takiyama, M. Morio, K. Fujii and H. Kikuchi, *J. Chromatogr.*, 305 (1984) 429.
24 V. Dolnik and P. Boček, *J. Chromatogr.*, 225 (1981) 455.

*Journal of Chromatography A*, 653 (1993) 313–319
Elsevier Science Publishers B.V., Amsterdam

CHROM. 25 443

# Effect of cetyltrimethylammonium chloride on electroosmotic and electrophoretic mobilities in capillary zone electrophoresis

Takashi Kaneta*, Shunitz Tanaka and Mitsuhiko Taga

*Department of Chemistry, Faculty of Science, Hokkaido University, Kita-ku, Sapporo 060 (Japan)*

(First received March 30th, 1993; revised manuscript received July 21st, 1993)

ABSTRACT

The effect of a cationic surfactant, cetyltrimethylammonium chloride (CTAC), on the electroosmotic mobility and the electrophoretic mobility of organic anions in capillary zone electrophoresis was investigated. The electroosmotic mobility showed four stepwise changes, including a reversal, with increasing CTAC concentration. The behaviour, especially the reversal of the electroosmotic mobility, was explained by assuming the formation of hemimicelles on the capillary wall. That is, CTAC first adsorbs individually by electrostatic interactions and then begins to associate into hemimicelles by Van der Waals attraction. The formation of hemimicelles changes the surface charge of the capillary wall from negative to positive and causes the reversal of the electroosmotic mobility. The effective electrophoretic mobilities of organic anions such as benzoic acid analogues were also influenced by the CTAC concentration. It was concluded that the behaviour was due to the interaction with hemimicelles on the capillary wall and also ion association with the monomer of CTAC and the interaction of micelles in bulk solution.

## INTRODUCTION

Capillary zone electrophoresis (CZE) is one of the most powerful separation techniques and many excellent separations by CZE have been reported in the last decade [1–4]. The separation in CZE is performed in a narrow fused-silica capillary tube filled with an electrolyte solution. On applying a high electric field to both ends of the capillary, an electroosmotic flow from the anode to cathode is generated that carries sample solutes to a detector. The apparent electrophoretic mobilities of cationic species increase because the electroosmotic mobility is added to the electrophoretic mobility. In contrast, those of anionic species decrease because these species migrate electrophoretically in the opposite direction to the electroosmotic flow. If the electrophoretic mobilities of the anionic species are close to or larger than the electroosmotic mobility, it takes a long time to detect them or sometimes it is difficult to detect them under ordinary CZE conditions. The control of the electroosmotic mobility is very important for improving the separation and shortening the analysis time in CZE. The electroosmotic mobility can be varied by altering the composition of the background electrolyte. Especially cationic surfactants have a large effect on electroosmotic mobility [5,6]. On increasing the concentration of a cationic surfactant, the electroosmotic mobility decreases and then the direction of the flow is reversed. This reversed electroosmotic flow is advantageous in the separation of anions [7,8].

On the other hand, it is essential for optimization of the separation selectivity in micellar

* Corresponding author. Present address: Department of Science and Technology, Faculty of Engineering, Kyushu University, Hakozaki, Higashi-ku, Fukuoka 812, Japan.

0021-9673/93/$06.00 

electrokinetic capillary chromatography (MECC) to investigate the ability of various kinds of surfactants, because a selectivity different from that in MECC using sodium dodecyl sulphate, which is the most popular surfactant in MECC, is to be expected when using cationic surfactants. However, there are few reports on the utility of cationic surfactants in MECC [9,10]. The effect of cationic surfactants on electroosmotic and electrophoretic mobilities has been hardly studied in detail.

We have previously reported the migration behaviour of inorganic anions in MECC using cetyltrimethylammonium chloride (CTAC) as a cationic surfactant [11]. The separation selectivity for these inorganic anions could be controlled by adding CTAC to the migrating electrolyte solution. We have also evaluated the interaction between inorganic anions and CTAC by using the effective electrophoretic mobility. In this work, the dependence of the electroosmotic mobility on the concentration of CTAC was investigated in detail. With increasing CTAC concentration, the electroosmotic mobility showed four stepwise changes including a reversal. These stepwise changes and the reversal cannot be explained only the electrostatic interaction between CTAC and the capillary wall. The formation of hemimicelles has been discussed by Emmer *et al.* [12], but they did not show experimental evidence for hemimicelle formation [12]. The hemimicelle theory proposed by Fuerstenau and co-workers [13,14] was introduced to explain the behaviour of the electroosmotic mobility. The effective electrophoretic mobilities of some organic anions as test solutes were also investigated in the presence of CTAC. It was demonstrated that the electrophoretic mobilities of these anions were controlled by the interaction with (1) the monomer of CTAC based on ion-pairing equilibria, (2) the hemimicelles formed on the capillary wall and (3) the micelles in the bulk solution.

## EXPERIMENTAL

### *Apparatus*

Fused-silica capillary tubes (500 mm × 50 μm I.D.) were obtained from GL Sciences (Tokyo, Japan). An HCZE-30PN0.25 high-voltage power supply (Matsusada Precision Devices, Shiga, Japan) was used. A Model $CV^4$ variable-wavelength absorbance detector (ISCO, Lincoln, NE, USA) was used to measure the absorbance at 210 nm. Detection was carried out by measuring the absorbance on the column at a position 20 cm from the positive or negative end of the capillary tube. The signal was recorded with an FBR-251A strip-chart recorder (Toa Electronic). The pretreatment of the capillary and the method of sample injection were described in a previous paper [11]. The electroosmotic mobility of the bulk solution was evaluated from the methanol peak. The signs of the electroosmotic and electrophoretic mobilities were defined such that the direction of migration from the cathode to the anode was positive. The migration voltage was kept constant at 15 kV and the current was varied from 8 to 14 μA with increasing surfactant concentration. All experiments were performed at room temperature (*ca.* 22°C).

### *Materials*

All reagents were of analytical-reagent grade and were used without further purification. Cetyltrimethylammonium chloride (CTAC), benzoic acid and tropic acid were obtained from Wako (Osaka, Japan) and cinnamic acid, hydrocinnamic acid and 2-phenylpropanoic acid from Tokyo Kasei Kogyo (Tokyo, Japan). All organic acids were dissolved in methanol and the concentrations of the standard solutions were 10 m*M*. Sample solutions were prepared by diluting each standard solution to 0.5 m*M* with methanol. The background electrolyte solution was prepared as follows: the required amounts of CTAC were dissolved with water and then 0.5 ml of 1 *M* potassium dihydrogenphosphate and 1.0 ml of 1 *M* tris(hydroxymethyl)aminomethane (Tris) were added to the solution. After the pH of the solution had been adjusted by adding 1 *M* citric acid, the solution was diluted to 50 ml. The final concentrations of phosphate and Tris were 10 and 20 m*M*, respectively. For an experiment under acidic conditions, 4 m*M* phosphoric acid solution (pH 2.7) was used as the electrolyte solution and the solution had the same conductivity as the other buffer solutions.

## RESULTS AND DISCUSSION

We first studied the dependence of the electroosmotic mobility on CTAC concentration. The relationship between CTAC concentration and electroosmotic mobility is shown in Fig. 1. These curves can be divided into the four sections, where the electroosmotic mobility decreases gently (I), changes considerably and turns in the opposite direction (II), hardly changes at concentrations from $1 \cdot 10^{-4}$ to $5 \cdot 10^{-3}$ *M* (III) and then changes considerably again (IV). The electroosmotic mobility depends on the pH of the background electrolyte until the CTAC concentration is $1 \cdot 10^{-4}$ *M* (sections I and II), but not above that concentration (sections III and IV).

This behaviour of the electroosmotic mobility is similar to the dependence of the zeta potential of quartz on the concentration of primary alkylammonium acetates as reported by Fuerstenau [13]. According to his explanation, the surfactants adsorb as individual ions in section I. In section II, the surfactant ions in the Stern layer next to the surface increase and once these ions are close enough together Van der Waals attraction acts between their hydrocarbon chains to associate into hemimicelles. Section III appears to be the onset of multi-layer adsorption. However, as the second layer would not be held strongly on the capillary wall by coulombic force and these ions in the second layer are stripped off by the streaming liquid, the zeta potential does not change much in this section. Although Fuerstenau did not find section IV, we can interpret it as follows. The surfactant ions in the second layer would not be stripped off in section IV because the interaction between CTAC should be stronger beyond the critical micellar concentration (cmc) in the bulk solution, which is about 1 m*M* [15].

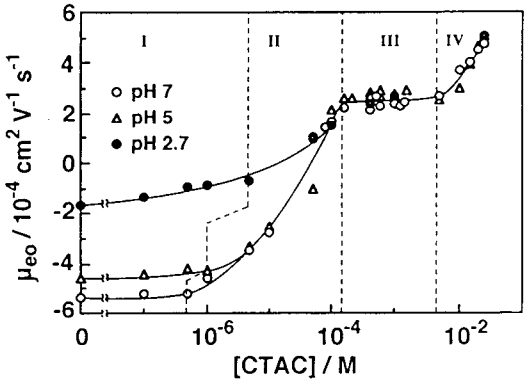


Fig. 1. Effect of CTAC concentration on electroosmotic mobility. Buffers: 10 m*M* phosphoric acid–20 m*M* Tris–citric acid (pH 7.0 and 5.0) and 4 m*M* phosphoric acid (pH 2.7). Migration voltage: 15 kV (9–14 $\mu$A). Room temperature (22°C). ○ = pH 7; △ = pH 5; ● = pH 2.7.

In the range of lower CTAC concentrations (section I), the electroosmotic mobility depends on the pH of the background electrolyte solution because the electroosmotic mobility is mainly governed by the degree of ionization of the silanol groups on the capillary wall. As the dissociation constant of the silanol groups is about $10^{-5.3}$ in an aqueous solution [16], the degree of dissociation of the silanol groups should vary widely in the pH range 3–7. It is considered that the adsorption of the surfactants on the capillary wall can be attributed to the electrostatic interaction between $CTA^+$ and the dissociated silanol groups at lower CTAC concentrations [17].

In section II, the electroosmotic mobility changes considerably and reversed electroosmotic flow is observed. The electroosmotic mobility in this region still shows a dependence on pH. This region corresponds to the portion of hemimicelle formation reported by Fuerstenau and both the electrostatic interaction and Van der Waals attraction contribute to the adsorption of CTAC. The excess positive charges of the adsorbing CTAC with the formation of hemimicelles causes the reversal of the electroosmotic flow. On the other hand, the reversed electroosmotic mobility in sections III and IV is no longer affected by pH. This suggests that the adsorption of the surfactant ions in this region should result from Van der Waals attraction rather than coulombic force.

Fuerstenau and co-workers [14] calculated the Van der Waals energy per methylene group between adjacent chains of adsorbed surfactant, $\phi$, from the measurement of the zeta potential of quartz. This value is in agreement with the values for the formation of the micelle in a bulk solution. The evidence is substantially in favour of the hemimicelle theory. We have previously

reported the effect of cationic surfactants having different alkyl chain lengths ($n = 10$, 12, 14) on the electroosmotic mobility [18]. The value of $\phi$ obtained from our results [from the slope of the plot of carbon number of the alkyl chain *versus* the logarithm of the concentration of the surfactants at zero electroosmotic mobility ($C_0$)] is $1.05kT$, and this value is in excellent agreement with Fuerstenau's results. This provides proof of the formation of hemimicelles on the capillary wall, although the conditions in the previous work were different from those in this study. A schematic illustration of hemimicelle formation on the capillary wall is shown in Fig. 2. Initially, cationic surfactant ions adsorb on the capillary wall as individual ions and neutralize the charge of the capillary wall. Then the adsorbing cationic surfactants begin to associate into two-dimensional patches of ions and form hemimicelles. Accompanied by the hemimicelle formation, the electroosmotic mobility changes considerably. When the net charge on the capillary wall changes from negative to positive owing to the adsorption of excess cationic surfactants due to the formation of hemimicelles, reversal of the electroosmotic flow occurs.

The effect of the cationic surfactant on the electrophoretic mobility of solutes was investigated. We first studied the migration behaviour of some organic acids as test solutes. The effective electrophoretic mobilities of the acidic solutes depend on the pH of the background electrolyte based on the acid dissociation equilibria. The effective electrophoretic mobility was obtained by subtracting the electroosmotic mobility from the observed electrophoretic mobility. The acid dissociation constants of these organic acids were evaluated according to the linear model of Khaledi *et al.* [19] as shown in Table I. These values are near 4.5 and some values agree with the literature values [20]. The order of the migration velocity at pH 4.6 (hydrocinnamic acid > 2-propanoic acid = cinnamic acid > tropic acid > benzoic acid) was the same as that of the dissociation constants. At pH 7.0, where all solutes should exist in the dissociated form, the order of the migration velocity was tropic acid > 2-propanoic acid = hydrocinnamic acid > cinnamic acid > benzoic acid, which is in agreement with the order of their molecular masses. We considered that these organic acids were appropriate model solutes to study the interaction with CTAC.

Fig. 3 shows the dependence of the effective electrophoretic mobility of benzoic acid on CTAC concentration. The pH of 7.0 of the background electrolyte guarantees that benzoic acid is in the dissociated form. An interesting behaviour was observed in the range of CTAC concentrations from 0 to 25 m*M*. The curve showing the relationship between CTAC concentration and the effective electrophoretic mobility of benzoic acid also possesses four distinct sec-

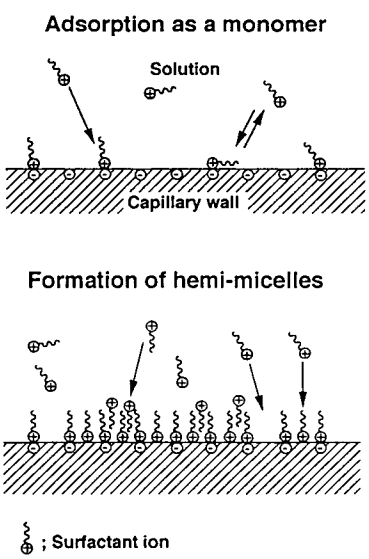


Fig. 2. Schematic illustration of hemimicelle formation on the capillary wall.

TABLE I

ACID DISSOCIATION CONSTANTS ($pK_a$) OF ORGANIC ACIDS

| Compound | $pK_a$ | Lit. [19] |
|---|---|---|
| Tropic acid | 4.2 | 4.12 |
| Benzoic acid | 4.2 | 4.204 |
| 2-Phenylpropanoic acid | 4.5 | 4.38 |
| Hydrocinnamic acid | 4.7 | 4.664 (35°C)[a] |
| Cinnamic acid | 4.5 | 4.438 |

[a] Temperature specified for one value only.

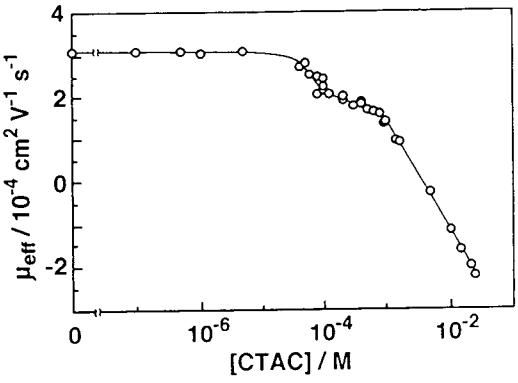


Fig. 3. Effect of CTAC concentrations on the electrophoretic mobility of benzoate ion. Buffer: 10 m*M* phosphoric acid–20 m*M* Tris–citric acid (pH 7.0). Other conditions as in Fig. 1.

tions: (I) a portion section where there is no change in the effective electrophoretic mobility, (II) a section where the electrophoretic mobility decreases considerably, (III) a section where the slope is gentle and (IV) a section where the effective electrophoretic mobility decreases rapidly again. We can relate this behaviour to the dependence of the electroosmotic mobility on CTAC concentration. In section I, CTAC behaves as a monomer individually at the surface of the capillary wall and in the bulk solution. There is only the ion association equilibria between the solutes and the cationic surfactants in this section. The interaction is not so strong that the change in the electrophoretic mobility of benzoic acid is very small in this section. In section II, where the surfactants form hemimicelles on the capillary wall, benzoate ions interact strongly with the hemimicelles and the electrophoretic mobility decreases considerably. As the second layer does not form in section III as mentioned above, the interaction with hemimicelles is held constant in this portion. However, the effective electrophoretic mobility of benzoate ion decreases slightly owing to the ion association equilibria between benzoate ions and surfactant monomers in the bulk solution. In section IV, the effective electrophoretic mobility decreases considerably again because benzoate ions begin to interact with the micelles in the bulk solution.

The migration behaviour of anions under ion association equilibrium below the cmc could be presented by the following equation [11]:

$$\frac{1}{\mu_{eff}} = \frac{K_{IA}}{\mu_{ep}} \cdot C_{sf} + \frac{1}{\mu_{ep}} \quad (1)$$

where $\mu_{eff}$ is the effective electrophoretic mobility, $K_{IA}$ is the ion association constant between the anion and CTAC and $C_{sf}$ is the CTAC concentration. The curves of $C_{sf}$ *vs.* $\mu_{eff}^{-1}$ for benzoic acid and tropic acid are shown in Fig. 4. Two clear inflection points can be seen. In the solution without CTAC, the electrophoretic mobility of benzoate ion is larger than that of tropate ion because the molecular mass of benzoic acid is smaller than that of tropic acid. At CTAC concentrations, >0.1 m*M* (the first inflection point), the effective electrophoretic mobility of benzoate ion becomes smaller than that of tropate ion because benzoate ion interacts more strongly than tropate ion with hemimicelles of CTAC. $\mu_{eff}^{-1}$ increases linearly on the basis of the ion association equilibria until the CTAC concentration reaches the cmc in the bulk solution. The second inflection point indicates the cmc of CTAC in the bulk solution under this experimental conditions. Beyond this point, $\mu_{eff}^{-1}$ increases considerably owing to the interaction with the micelles formed in the bulk solution. The slope of the $\mu_{eff}^{-1}$ *vs.* $C_{sf}$ line provides the ion association constant between organic anions and CTAC on the basis of eqn. 1. Fortunately, there is little change in the electroosmotic mobility

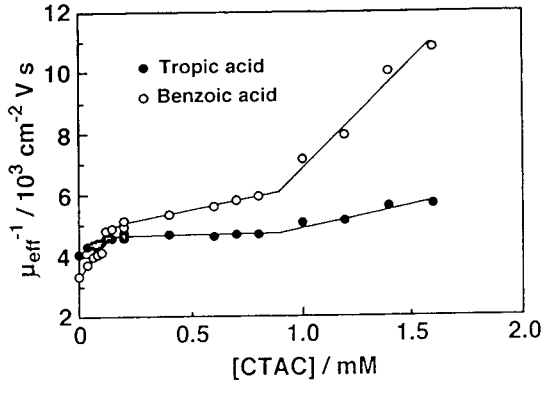


Fig. 4. $C_{sf}$ *vs.* $\mu_{eff}^{-1}$ plots for (○) benzoate and (●) tropate ions. Conditions as in Fig. 3.

within the range of concentrations 0.2–1.0 m*M* (section III in Fig. 1). Hence we can determine the conditional ion association constants directly from the slope of the line plotted within this limited concentration range. The values obtained were 280 l $mol^{-1}$ for benzoate ion, 280 l $mol^{-1}$ for 2-phenylpropanoate ion and 350 l $mol^{-1}$ for hydrocinnamate ion. The slope for tropate ion was so small that we could not estimate it. The intercept of the $C_{sf}$ *vs.* $\mu_{eff^{-1}}$ line gives the effective electrophoretic mobility of the anion interacting with hemimicelles.

The effective electrophoretic mobility of the anion changes notably even at very low concentrations. The change in the electrophoretic mobility of benzoic acid and tropic acid resulting from the interaction with the hemimicelles (below the first inflection point in Fig. 4) has the almost same slope as that with the micelles in the bulk solution (beyond the second inflection point in Fig. 4). It is speculated that the interaction with the hemimicelles will be similar to that with the micelles in the bulk solutions and the interaction may consist of both hydrophobic interaction and electrostatic interaction.

Chromatograms of organic anions (A) without and (B) with 0.08 m*M* CTAC are shown in Fig. 5. The analyte ions migrate to the cathode in Fig. 5A, whereas they migrate to the anode in Fig. 5B. It is notable that in spite of the much lower concentration of CTAC than the cmc, the migration order in Fig. 5B is different from that in Fig. 5A. As cinnamic acid has the strongest interaction with hemimicelles, the peak shows serious tailing.

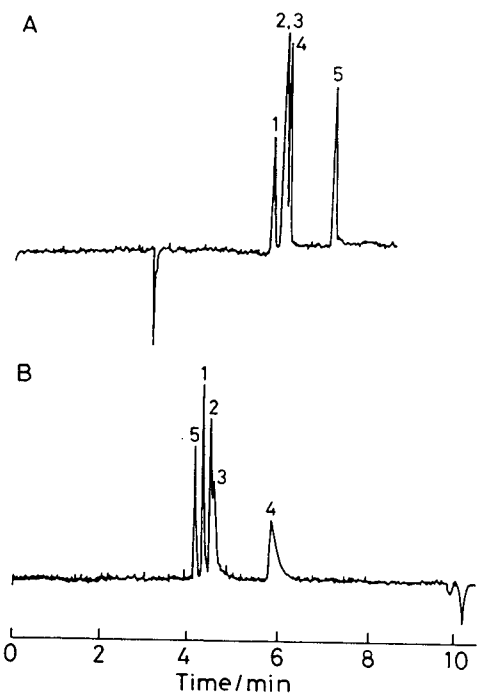


Fig. 5. Chromatograms of organic anions (A) without CTAC and (B) with 0.08 m*M* CTAC. Peaks: 1 = tropic acid; 2 = 2-phenylpropanoic acid; 3 = hydrocinnamic acid; 4 = cinnamic acid; 5 = benzoic acid. Buffer: 10 m*M* phosphoric acid–20 m*M* Tris–citric acid (pH 7.0). Migration voltage: 15 kV (9 μA). Other conditions as in Fig. 1.

## CONCLUSIONS

The electroosmotic mobility was greatly influenced by a cationic surfactant and showed four stepwise changes, including reversal, with increasing CTAC concentration. The alternation of the electroosmotic mobility can be interpreted by the adsorption of CTAC on the capillary wall due to both the electrostatic interaction and Van der Waals attraction. At very low concentrations, CTAC adsorbed as individual ions by the electrostatic interaction between CTAC and silanol groups on the capillary wall, then it began to associate into hemimicelles by Van der Waals attraction between the hydrophobic carbon chains of CTAC. The reversed electroosmotic mobility can be explained by the excess positive charges of adsorbing CTAC on the capillary wall. The formation of hemimicelles facilitates the adsorption of CTAC beyond the amount required to neutralize negative charges of silanol on the capillary wall. The electrophoretic mobilities of organic anions also showed a similar behaviour to that of the electroosmotic mobility, reflecting the state of the capillary wall. On increasing the CTAC concentration, the electrophoretic mobilities of organic anions decrease as a result of the interaction of ion association with CTAC monomers, the interaction with hemimicelles and the interaction with the micelles in the bulk solution. The interaction with monomer and hemimicelles of a cationic surfac-

tant such as CTAC could provide a unique separation selectivity in the CZE and MECC separation of anions and also the interaction with the micelles in a bulk solution.

## REFERENCES


1 J.W. Jorgenson and K.D. Lukacs, *Anal. Chem.*, 53 (1981) 1298.
2 M.J. Gordon, X. Haung, S.L. Pentoney, Jr. and R.N. Zare, *Science*, 242 (1988) 224.
3 W.G. Kuhr, *Anal. Chem.*, 62 (1990) 403R.
4 H.H. Lauer and J.B. Ooms, *Anal. Chim. Acta*, 250 (1991) 45.
5 J.C. Reijenga, G.V.A. Aben, Th.P.E.M. Verheggen and F.M. Everaerts, *J. Chromatogr.*, 260 (1983) 241.
6 T. Tsuda, *J. High Resolut. Chromatogr. Chromatogr. Commun.*, 10 (1987) 622.
7 X. Huang, J.A. Luckey, M.J. Gordon and R.N. Zare, *Anal. Chem.*, 61 (1989) 766.
8 W.R. Jones and P. Jandik, *J. Chromatogr.*, 546 (1991) 411.
9 K. Otsuka, S. Terabe and T. Ando, *J. Chromatogr.*, 332 (1985) 219.
10 D.E. Burton, M.J. Sepaniak and M.P. Maskarinec, *J. Chromatogr. Sci.*, 25 (1987) 514.
11 T. Kaneta, S. Tanaka, M. Taga and H. Yoshida, *Anal. Chem.*, 64 (1992) 798.
12 A. Emmer, M. Jansson and J. Roeraade, *J. Chromatogr.*, 547 (1991) 544.
13 D.W. Fuerstenau, *J. Phys. Chem.*, 60 (1956) 981.
14 P. Somasundaran, T.W. Healy and D.W. Fuerstenau, *J. Phys. Chem.*, 68 (1964) 3562.
15 M.J. Rosen, *Surfactants and Interfacial Phenomena*, Wiley, New York, 1978.
16 C. Schwer and E. Kenndler, *Anal. Chem.*, 63 (1991) 1801.
17 W.J. Lambert and D.L. Middleton, *Anal. Chem.*, 62 (1990) 1585.
18 T. Kaneta, S. Tanaka and H. Yoshida, *J. Chromatogr.*, 538 (1991) 385.
19 M.G. Khaledi, S.C. Smith and J.K. Strasters, *Anal. Chem.*, 63 (1991) 1820.
20 J.A. Dean (Editor), *Lange's Handbook of Chemistry*, McGraw-Hill, New York, 13th ed., 1973.

*Journal of Chromatography A*, 653 (1993) 321–327
Elsevier Science Publishers B.V., Amsterdam

CHROM. 25 415

# Separation of pyridinecarboxylic acid isomers and related compounds by capillary zone electrophoresis

# Effect of cetyltrimethylammonium bromide on electroosmotic flow and resolution

George M. Janini*, King C. Chan, Jeffrey A. Barnes, Gary M. Muschik and Haleem J. Issaq

*Program Resources, Inc./DynCorp, NCI-Frederick Cancer Research and Development Center, P.O. Box B, Frederick, MD 21702 (USA)*

(First received May 24th, 1993; revised manuscript received July 6th, 1993)

ABSTRACT

The effect of the addition of cetyltrimethylammonium bromide (CTAB) to the buffer system in capillary electrophoresis on electroosmotic flow (EOF) is examined. At a CTAB concentration of $2.5 \cdot 10^{-4}$ *M*, EOF is anodal (flow towards the positive detector column end). With bare silica columns, anodal EOF first increases with increasing pH, up to a maximum in the pH range 4–6 depending on CTAB concentration, then decreases as pH is further increased. Optimum resolution of pyridinecarboxylic acid isomers is obtained at pH 2.7 with a 10 m*M* phosphate buffer and 30 m*M* CTAB. Using the same buffer system, optimum resolution for hydroxy-substituted pyridinecarboxylic acid isomers is obtained at pH 7.5. The use of CTAB results in a dramatic improvement in peak shape. Preliminary results, using an excimer laser operated at 248 nm, show that the fluorescence intensity of isonicotinic acid is substantially enhanced with the addition of 0.3% hydrogen peroxide to the phosphate buffer system.

## INTRODUCTION

Nicotinic (*m*-pyridinecarboxylic) acid and nicotinamide are water-soluble vitamins that have many important biological functions [1–3], and isonicotinic (*p*-pyridinecarboxylic) acid is a metabolite of isoniazid, which is an anti-tuberculosis drug [4]. Several methods have already been described for the separation and analysis of pyridinecarboxylic (PC) acid derivatives [1–15]. These include colorimetric [5,6], fluorimetric [7,8], gas chromatographic–mass spectrometric [9] and ion-exchange [10] methods and HPLC with various types of detectors [1,3,4,11–15]. The colorimetric and fluorimetric methods have been criticized for excessive analysis time and lack of sensitivity [1], and several of the HPLC methods have been faulted for complicated sample pre-treatment procedures [1,3]. Roberts *et al.* [15] encountered severe problems due to poor peak shapes when analyzing *o*-pyridinecarboxylic (picolinic) acid and related compounds by reversed-phase HPLC, that could only be corrected by addition of the analytes to the mobile phase. Mawatari *et al.* [1,4] reported the fluorimetric determination of 3- and 4-substituted pyridines by HPLC with postcolumn UV irradiation and subsequent fluorescence detection. This interesting approach resulted in signifi-

* Corresponding author.

cant enhancement of sensitivity; however, post-column sample treatment may result in extra peak broadening and, more importantly, the use of organic solvents in the mobile phase results in decreased fluorescence intensity.

The recent development of capillary zone electrophoresis (CZE) has provided the potential for achieving rapid high-resolution separations of macromolecules as well as small ionic and ionizable compounds [16,17]. Furthermore, the introduction of micellar electrokinetic capillary chromatography (MECC) has allowed the extension of CZE methods for the separation of neutral compounds [18,19]. Because of its strong separation power and its compatibility with aqueous solutions, CZE is particularly suited for the separation of PC acids and related compounds and their analysis in biological fluids. Only three reports on the use of capillary electrophoresis for the analysis of these compounds have been reported; Fujiwara *et al.* [20] and Nishi *et al.* [21] reported the use of MECC for the analysis of water-soluble vitamins including nicotinic acid and Tanaka *et al.* [2] used a tube isotachophoretic method for the separation of nicotinic acid derivatives.

In this study we report the use of capillary electrophoresis with and without micellar additives for the separation of PC acid isomers and related compounds. A number of strategies have been investigated including pH optimization, column coating and control of electroosmosis with the use of cetyltrimethylammonium bromide (CTAB). Preliminary results on the use of an excimer laser at 248 nm for the simultaneous photochemical activation and on-column laser-induced fluorescence (LIF) detection of these compounds will also be presented.

## EXPERIMENTAL

A Beckman CZE System 2000 (Model P/ACE) equipped with a UV detector, an autosampler, a liquid-cooled column cartridge and a System Gold software package was used in this study. All experiments were conducted at 25°C. Injections were made using the pressure mode for 2–5 s. The buffers were prepared by dissolving the appropriate amount of reagent in distilled and deionized water and were degassed and filtered through 0.2-$\mu$m nylon 66 filters. A Fisher Accumet pH meter 25 (Fisher Scientific, Fair Lawn, NJ, USA) was used to measure pH levels. Fused-silica capillaries (Polymicro Technologies, Phoenix, AZ, USA) were prepared for use by conditioning with NaOH, water and the appropriate buffer. All columns were 57 cm (50 cm, injector–detector) $\times$ 75 $\mu$m I.D., unless otherwise specified. Mesityl oxide was used as a neutral marker to monitor the electroosmotic flow. The LIF system was laboratory built as has been described previously [22]. Excitation was provided by a KrF pulsed excimer laser operating at 248 nm (Model GX-500), (Potomac Photonics, Lanham, MD, USA). All chemicals were obtained from Aldrich (Milwaukee, WI, USA).

## RESULTS AND DISCUSSION

### *Effect of CTAB on electroosmotic flow*

Cationic surfactants such as CTAB adsorb on the capillary wall surface by dynamic electrostatic interactions between the positively charged tertiary ammonium ion and the negatively charged Si–$O^-$ group [23–25]. A bilayer of CTAB molecules is formed at the capillary wall with a positive charge directed towards the center of the capillary. At a given applied field strength and buffer system, the magnitude and direction of electroosmotic flow (EOF) is controlled solely by the capillary wall surface charge density [26]. The amount of negative charge density on fused-silica surfaces is determined by the degree of ionization of Si–OH groups present on the surface. The ionization constant of the Si–OH group on fused-silica surfaces is not precisely determined, but it is estimated to be about $1 \cdot 10^{-3}$ [26]. As negative charge is built up at the surface with increasing pH, electroosmotic flow increases. This is clearly illustrated in Fig. 1 (curve □), which shows the effect of pH on EOF with a bare fused-silica capillary in the pH range 3–8. The addition of CTAB to the buffer system, which dynamically adsorbs to the surface, initially slows down the EOF and eventually reverses its direction [23–25,27–29]. The magnitude of change in EOF and the point at which it changes

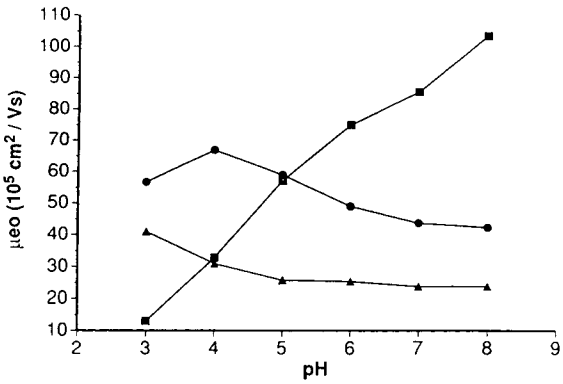


Fig. 1. Electroosmotic mobility ($\mu_{eo}$) *versus* pH. Buffer: 15 m*M* phosphate; neutral marker: mesityl oxide. (□) Column: 50 cm × 75 μm I.D. untreated fused silica; applied voltage: + 25 kV; $\mu_{eo}$: positive; (○) Column as for □; buffer additive $2.5 \cdot 10^{-4}$ *M* CTAB; applied voltage: − 25 kV; $\mu_{eo}$: negative; (▲) Column: 50 cm × 50 μm I.D., $C_8$; buffer additive: $2.5 \cdot 10^{-4}$ *M* CTAB; applied voltage: − 25 kV; $\mu_{eo}$: negative.

direction depends on the nature of the capillary surface, pH and the concentration of CTAB in the buffer system [28]. Tsuda [25] and Huang *et al.* [27] both reported reversal of EOF at a surfactant concentration of approximately $3.5 \cdot 10^{-4}$ *M* with bare capillaries, and Pfeffer and Yeung [28] reported a much lower surfactant concentration (*ca.* 1 μ*M* CTAB) for the reversal of flow with a fused-silica column coated with hydrophobic cross-linked polymer PS-264.

In this work we measured the EOF with bare and $C_8$-coated fused-silica capillaries as a function of pH using buffers modified with CTAB. Fig. 1 (curve ○) shows the dependence of EOF on pH with a bare fused-silica column at a CTAB concentration of $2.5 \cdot 10^{-4}$ *M* and Fig. 1 (curve ▲) shows a corresponding plot with a $C_8$-coated column. In both situations the direction of EOF is reversed towards the positive electrode. At any given CTAB concentration, EOF with the bare silica column increases as the pH is increased from pH 3, plateaus then decrease with further increase in pH. The pH at which EOF is maximum varies slightly depending on the concentration of CTAB. Assuming that EOF is directly proportional to surface charge density, it could only be concluded that $Si–O^-$ is a more favorable CTAB adsorption site compared to Si–OH. As pH is increased from 3 to 4, the underlying silica surface turns more negative with increased ionization of Si–OH groups and more CTAB is bound to the surface, resulting in higher net positive charge density. As pH is further increased, more Si–OH groups are ionized with no concomitant increase in CTAB binding because of surface saturation. As a result, the net surface charge density turns more and more negative and EOF decreases with increasing pH. The results of the EOF *vs.* pH experiment with the $C_8$ column (Fig. 1, curve ▲) show that EOF is slower at any given pH compared to the bare silica column. This is presumably because the hydrophobic, $C_8$-coated surface does not bind the tertiary ammonium ion as strongly as does the negatively charged silica surface. However, even the lowest concentration of CTAB (1 μ*M*) [28] is sufficient for flow reversal because with $C_8$ bonding most of the surface hydroxy groups are effectively eliminated, especially at low pH, and any slight CTAB binding will develop a positive surface charge density.

*Strategies for separating pyridinecarboxylic acid isomers*

A number of capillary electrophoresis modes of operation (normal polarity or cathodal, reversed polarity or anodal and MECC) were investigated to arrive at the optimum conditions for the resolution of PC acid isomers. First the normal polarity (cathodal) mode, where the injector end is positive and the EOF is towards the negative electrode, was explored. Fig. 2 shows the effect of pH on the migration relative to mesityl oxide (MO) of *o*-PC (picolinic) acid, *m*-PC (nicotinic) acid and *p*-PC (isonicotinic) acid. The p*K* values of these compounds at 25°C are as follows [30]: picolinic acid, $pK_1 = 1.06$ and $pK_2 = 5.37$; nicotinic acid, $pK_1 = 2.07$ and $pK_2 = 4.73$ and isonicotinic acid, $pK_1 = 1.70$ and $pK_2 = 4.89$. Strictly speaking, these compounds are not zwitterionic even though they possess a positive charge on the pyridine nitrogen at pH < 3, and turn negative at pH > 3 due to the ionization of the carboxylic acid. This dependence of charge on pH is reflected in the trend shown in Fig. 2. The acids migrate faster than MO at pH < 3; the slowest migrating acid being picolinic acid, the

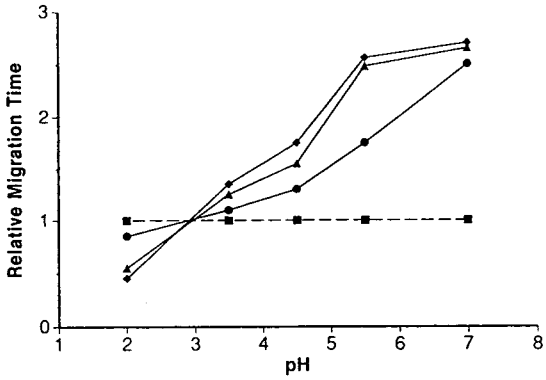


Fig. 2. The effect of pH on the migration order and separation of PC acid isomers. Column: 50 cm × 75 μm I.D. fused silica. Applied voltage: 25 kV; buffer: 25 m*M* phosphate at pH 2.0–4 and pH 5.5–7; 50 m*M* acetate at pH 4.5. □ = MO; ○ = *o*-PC (picolinic) acid; ◆ = *m*-PC (nicotinic) acid; ▲ = *p*-PC (isonicotinic) acid.

isomer that carries the smallest positive charge, at any given pH in this range of pH. As the pH is increased above pH 3 the order of elution is reversed and picolinic acid now carries the smallest negative charge in the pH range and is eluted first. The isomers are best separated at pH ≈ 4.5; however, the peaks exhibit excessive peak asymmetry, the severity of which depends on the pH. Similar problems of poor peak shape that were attributed to a property of the compounds rather than instrumental deficiencies were encountered by Roberts *et al.* [15] during the development of HPLC methods in the analysis of similar compounds.

Fig. 3 is an electropherogram of the PC isomers and nicotinamide under optimum conditions with respect to separation and peak shape. Fig. 4 shows the separation of hydroxy-substituted PC acids, namely, 3-hydroxypicolinic acid (3HPA), 2-hydroxynicotinic acid (2HNA) and 6-hydroxynicotinic acid (6HNA), under two sets of experimental conditions. Although the three isomers could be separated as shown at pH 5.5, peak shape problems are severe and highly dependent on pH. Peak shapes obtained with new columns are reasonable (Figs. 3 and 4); however, peak shape quickly deteriorates with repeated injections. Column reconditioning with NaOH and water did not seem to restore the original conditions. The addition of organic

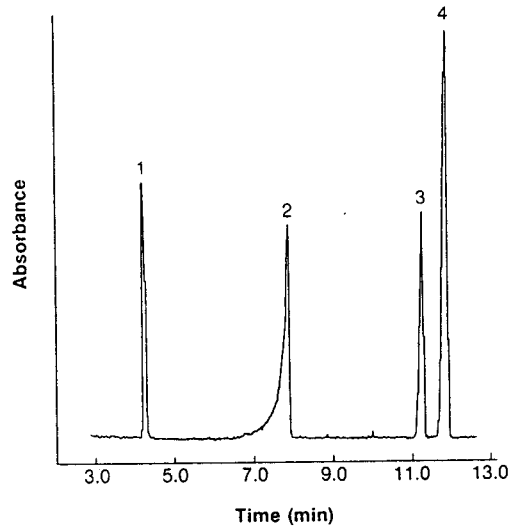


Fig. 3. Separation of PC acid derivatives. Buffer: 50 m*M* acetate, pH 5.5; applied voltage: 25 kV; detection: UV 254 nm; instrument: Beckman Model P/ACE System 2000. Column 50 cm × 75 μm I.D. fused silica. Peaks: 1 = nicotinamide; 2 = picolinic acid; 3 = isonicotinic acid; 4 = nicotinic acid.

solvents, salts and urea to the buffer system was attempted (unpublished results) but did not result in any improvement in peak shape, especially for the most troublesome solutes, namely picolinic acid (Fig. 3) and 3-hydroxypicolinic acid (Fig. 4).

A dramatic improvement in peak shape was obtained by the addition of CTAB to the run-

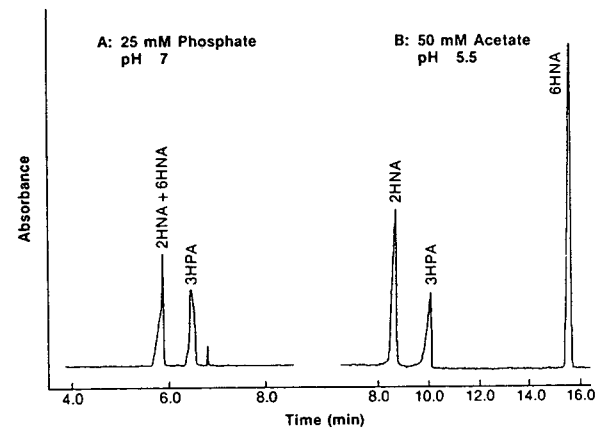


Fig. 4. Separation of hydroxypyridinecarboxylic acid isomers. Applied voltage: 25 kV; detection: UV 280 nm. Other conditions as in Fig. 3.

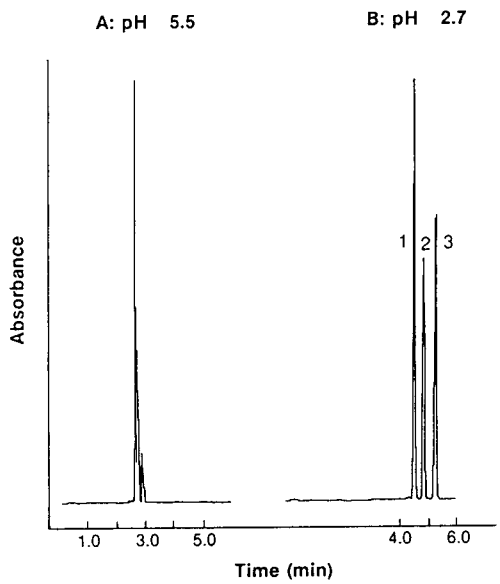


Fig. 5. Separation of PC acid isomers using a CTAB-modified buffer. Buffer: 10 m*M* phosphate + 30 m*M* CTAB; applied voltage: 20 kV. Other conditions as in Fig. 3. Peaks: 1 = picolinic acid; 2 = isonicotinic acid; 3 = nicotinic acid.

ning buffer as shown in Figs. 5 and 6. A range of pH and CTAB concentrations was tested to arrive at the best conditions for the separation of these compounds. It was determined that CTAB

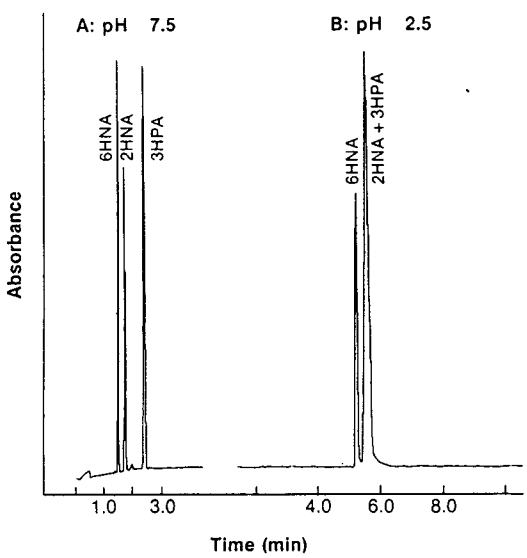


Fig. 6. Separation of hydroxypyridinecarboxylic acid isomers using a CTAB-modified buffer. Experimental conditions as in Fig. 5.

concentrations up to the critical micelle concentration (CMC) of about $1 \cdot 10^{-3}$ *M* [28] result in shorter analysis time but only slight improvement in peak shape. Even though the use of high CTAB concentrations (up to 30 m*M*) resulted in high current values (*ca.* 100 $\mu$A with 10 m*M* phosphate buffer, 50 cm × 75 $\mu$m I.D. column at 20 kV), it was necessary as it resulted in dramatically improved peak shape at all pH values. MECC is best suited for the separation of neutral compounds, but it has also been shown to improve the separation of some ionic compounds [19]. Analytes of opposite charge to the micelles interact rather strongly with the micelles through ionic forces, while analytes of similar charge interact weakly due to electrostatic repulsion. The separation of PC isomers at pH 2.7 (Fig. 5B), where both the analytes and micelles are positively charged, might be slightly affected by interactions with the micelles, but the order of migration is largely dependent on analyte $pK_1$ values. On the other hand, comparison of Fig. 4A to Fig. 6A shows that the separation of hydroxypyridinecarboxylic acid isomers in neutral and basic media where the analytes are negatively charged, is greatly influenced by interaction with the micelles. The MECC separation of PC acid isomers also depends on the buffer pH. Fig. 5 shows that complete resolution of the three isomers is obtained at pH 2.7, while higher-pH buffers will result in overlapping peaks. In contrast, Fig. 6 shows that the hydroxy-substituted isomers are better resolved at slightly basic pH values.

The concentration of the individual components of the standard mixtures used to generate Figs. 5 and 6 was about 1–10 $\mu$g/ml. The limit of detection obtained under the conditions specified in the Experimental section and figure captions without any attempt at sample stacking was in the range of $1 \cdot 10^{-5}$ to $1 \cdot 10^{-6}$ *M*. In an attempt to improve the limit of detection, the use of LIF was also investigated. PC acids absorb UV light but their native fluorescence is not particularly strong. Mawatari *et al.* [1,4] previously reported the detection of isonicotinic acid using HPLC coupled with postcolumn photochemical reaction and fluorescence detection. In their study, hydrogen peroxide present in the mobile phase

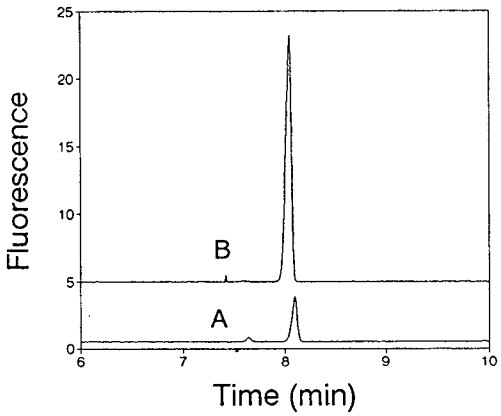


Fig. 7. Effect of $H_2O_2$ on the fluorescence signal of isonicotinic acid. (A) Buffer: 12 m*M* phosphate, pH 7.7; (B) buffer: 12 m*M* phosphate with 0.3% $H_2O_2$, pH 7.7; applied voltage: 15 kV; injection: gravity, 10 cm for 15–20 s; isonicotinic acid concentration: 1 $\mu$g/ml.

reacted with the analyte to give maximum fluorescence upon irradiation with UV light for about 2.5 min. It was felt that the application of this procedure to capillary electrophoresis, using a UV laser, may have distinct advantages such as the elimination of the postcolumn reactor, instantaneous photochemical reaction, and simultaneous on-column LIF detection. Preliminary results are shown in Fig. 7 which indicates a substantial enhancement in fluorescence signal. The results are encouraging and the subject will be further explored in future communications from this laboratory.

## CONCLUSIONS

The CZE separation of pyridinecarboxylic acid isomers presented a challenge because of peak shape problems that seem to be a property of the compounds rather than instrumental deficiencies. The separation and peak shape of these compounds is highly dependent on pH. The addition of CTAB to the buffer provided several advantages including: (1) highly improved peak shape; (2) faster analysis time; (3) better control of EOF and better reproducibility of migration times.

## ACKNOWLEDGEMENTS

The content of this publication does not necessarily reflect the views or policies of the Department of Health and Human Services, nor does mention of trade names, commercial products, or organizations imply endorsement by the US Government.

## REFERENCES

1 K. Mawatari, F. Iinuma and M. Watanabe, *Anal. Sci.*, 7 (1991) 733.
2 S. Tanaka, T. Kaneta, H. Yoshida and H. Ohtaka, *J. Chromatogr.*, 521 (1990) 158.
3 A. Durrer, B. Walther, A. Racciatti and B. Testa, *J. Chromatogr.*, 495 (1989) 256.
4 K. Mawatari, F. Iinuma and M. Watanabe, *Anal. Sci.*, 6 (1990) 515.
5 D.K. Chaudhuri, *Ind. J. Med. Res.*, 39 (1951) 491.
6 W.T. Robinson, L. Cosyns and M. Kraml, *Clin. Biochem.*, 11 (1978) 46.
7 B.R. Clark, R.M. Halpern and R.A. Smith, *Anal. Biochem.*, 68 (1975) 54.
8 P.C. Ioannou, *Talanta*, 34 (1987) 857.
9 G. Karlaganis, E. Peretti and B.H. Lauterburg, *J. Chromatogr.*, 420 (1987) 171.
10 G.M. McCreanor and D.A. Bender, *Br. J. Nutr.*, 56 (1986) 577.
11 N. Hengen, V. Seiberth and M. Hengen, *Clin. Chem.*, 24 (1978) 1740.
12 J.X. de Vries, W. Gunthert and R. Ding, *J. Chromatogr.*, 221 (1980) 161.
13 J.B. Tarr, *Biochem. Med.*, 26 (1981) 330.
14 R.W. McKee, Y.A. Kang-Lee, M. Panaqua and M.E. Swendseid, *J. Chromatogr.*, 230 (1982) 309.
15 D.W. Roberts, R.J. Ruane and I.D. Wilson, *J. Chromatogr.*, 471 (1989) 437.
16 J.W. Jorgenson and K.D. Lukacs, *Anal. Chem.*, 53 (1981) 1298.
17 R.A. Wallingford and A.G. Ewing, *Adv. Chromatogr.*, 29 (1990) 1.
18 S. Terabe, K. Otsuka, K. Ichikawa, A. Tsuchiya and T. Ando, *Anal. Chem.*, 56 (1984) 111.
19 G.M. Janini and H.J. Issaq, *J. Liq. Chromatogr.*, 15 (1992) 927.
20 S. Fujiwara, S. Iwase and S. Honda, *J. Chromatogr.*, 447 (1988) 133.
21 H. Nishi, N. Tsumagari, T. Kakimotu and S. Terabe, *J. Chromatogr.*, 465 (1989) 331.
22 K.C. Chan, G.M. Janini, G.M. Muschik and H.J. Issaq, *J. Liq. Chromatogr.*, 16 (1993) 1877.
23 S. Terabe, K. Ishikawa, K. Utsuka, A. Tsuchiya and T. Ando, presented at the *26th International Liquid Chromatography Symposium, Kyoto, January 25–26, 1983.*

24 J.C. Reijenga, G.V.A. Aben, Th.P.E.M. Verheggen and F.M. Everaerts, *J. Chromatogr.*, 260 (1983) 241.
25 T. Tsuda, *J. High. Resolut. Chromatogr. Chromatogr. Commun.*, 10 (1987) 622.
26 M.A. Hayes and A.G. Ewing, *Anal. Chem.*, 64 (1992) 512.
27 X. Huang, J.A. Luckey, M.J. Gordon and R.N. Zare, *Anal. Chem.*, 61 (1989) 766.
28 W.D. Pfeffer and E.S. Yeung, *Anal. Chem.*, 62 (1990) 2178.
29 H.-T. Chang and E.S. Yeung, *Anal. Chem.*, 65 (1993) 650.
30 A. Albert and E.P. Serjeant, *Ionization Constants of Acids and Bases*, Wiley, New York, 1962.

*Journal of Chromatography A*, 653 (1993) 329–335
Elsevier Science Publishers B.V., Amsterdam

CHROM. 25 404

# High-resolution separation of DNA restriction fragments by capillary electrophoresis in cellulose derivative solutions

Yoshinobu Baba*, Naomi Ishimaru, Kazuko Samata and Mitsutomo Tsuhako

*Kobe Women's College of Pharmacy, Kitamachi, Motoyama, Higashinada-ku, Kobe 658 (Japan)*

(First received March 16th, 1993; revised manuscript received June 17th, 1993)

ABSTRACT

The performance and the efficiency of several cellulose derivatives as a molecular sieving agent for the capillary electrophoretic separation of DNA restriction fragments were investigated. All fragments up to 12 000 base pairs (bp) in the 1-kbp DNA ladder were resolved using linear polyacrylamide-coated capillaries filled with a buffer solution containing 0.5% cellulose derivative and the separation was completed within 17 min. High-concentration (0.7%) cellulose derivative solutions are effective for the complete separation of small fragments (50–1000 bp) of a *Hin*cII and a *Hae*III digest of $\Phi$X174 DNA. A plate number of $0.5–1 \cdot 10^6$ plates per metre was achieved. The migration time and the resolution of DNA fragments were manipulated by varying several parameters, such as the size (viscosity) and the concentration of cellulose derivatives and the applied field strength. Some guidelines are presented for choosing these parameters, depending on the size of the DNA fragments being separated.

## INTRODUCTION

Slab gel electrophoresis is the standard method used to separate, identify and purify DNA fragments and is successfully applied to the mapping of double-stranded DNA restriction fragments, polymerase chain reaction (PCR) analysis, restriction fragment length polymorphism (RFLP) analysis and Southern blotting [1,2]. Although slab gel electrophoresis is simple and capable of resolving a broader molecular weight range of DNA fragments, the technique is time-consuming, labour-intensive and non-quantitative.

Capillary electrophoresis (CE) is an automated technique offering the benefits of rapid separation and high resolution of DNA restriction fragments [3,4]. DNA restriction fragments of 100–120 000 base pairs (bp) are separated within 20 min by capillary gel electrophoresis (CGE) using capillaries filled with cross-linked polyacrylamide gel [5–7] and linear polyacrylamide [5]. High-speed and high-resolution separation of DNA restriction fragments can be performed by using CE in entangled polymer solutions [6–16]. The performance of a few hydrophilic polymers has been tested in the separation of DNA fragments [6–16]. Very little, however, is known about the effect of changes in the structure and physical properties of the hydrophilic polymers on the electrophoretic behaviour of DNA fragments in the capillary.

In this paper, we investigate the use of several types of cellulose derivatives, whose basic structure is shown in Fig. 1 and features are listed in Table I, as entangled polymers for the CE separation of double-stranded DNA restriction fragments in the size range 100–12 000 bp. We examined the effect of the structure and the physical properties of cellulose derivatives on the resolving power of CE in cellulose derivative

* Corresponding author.

0021-9673/93/$06.00 

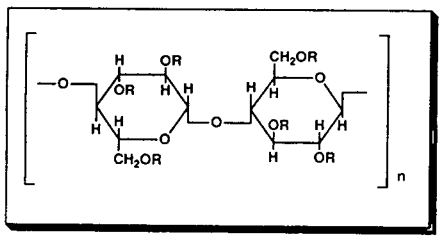

**Cellulose Derivative**

| | | | |
|---|---|---|---|
| Methyl Cellulose | –H | $-CH_3$ | |
| Hydroxypropyl Methyl Cellulose | –H | $-CH_3$ | $-CH_2CH(OH)CH_3$ |
| Hydroxypropyl Cellulose | –H | $-CH_2CH(OH)CH_3$ | |

Fig. 1. Structure of cellulose derivatives.

solutions, *i.e.*, how wide a range of molecular mass of DNA fragments can be separated with high resolution. For this purpose, we prepared and used capillaries in which linear polyacrylamide was chemically bound to the capillary inner surface by using a bifunctional reagent such as 3-methacryloxypropyltrimethoxysilane [17]. The reduction in the electroosmotic flow by capillary wall deactivation was effective for high-performance separation of a complex mixture of DNA fragments due to improved resolution and reproducibility [8,10,11,15].

## EXPERIMENTAL

### *Chemicals*

The DNA restriction fragments of a ΦX174 DNA/*Hae*III digest (0.24 μg/μl) and a ΦX174 DNA/*Hin*cII (0.29 μg/μl) digest were purchased from Toyobo (Osaka, Japan). A 1-kilo base pair (kbp) DNA ladder (1.0 μg/μl) was obtained from Gibco BRL (Tokyo, Japan). The ΦX174 DNA/*Hae*III digest contained eleven fragments of 72, 118, 194, 234, 271, 281, 310, 603, 872, 1078 and 1357 bp. The ΦX174 DNA/*Hin*cII digest contained thirteen fragments of 79, 162, 210, 291, 297, 335, 341, 345, 392, 495, 612, 770 and 1057 bp. The 1-kbp DNA ladder contained 23 fragments of 75, 134, 154, 201, 220, 298, 344, 396, 506, 517, 1018, 1636, 2036, 3054, 4072, 5090, 6108, 7126, 8144, 9162, 10180, 11198 and 12216 bp. The DNA samples were diluted ten-fold with Milli-Q water and stored at −18°C until use. Cellulose derivatives (Fig. 1) listed in Table I were a gift from ShinEtsu Chemicals (Tokyo, Japan). 3-Methacryloxypropyltrimethoxysilane was purchased from ShinEtsu Chemicals. All other chemicals were of analytical-reagent or electrophoretic grade from Wako (Osaka, Japan).

### *Preparation of linear polyacrylamide-coated capillary and running buffer*

Polyimide-coated fused-silica capillaries (375 μm O.D., 100 μm I.D., Polymicro Technologies, Phoenix, AZ, USA) of 42.5 cm effective length and 50 cm total length were used. Linear polyacrylamide-coated capillaries were prepared as previously described [17] with slight modification. The capillary was leached by passing 1 *M* NaOH solution for 15 min by using a vacuum injection system [18], and subsequently rinsed with Milli-Q water for 15 min and acetonitrile for 15 min. A solution of 0.4% 3-methacryloxypropyltrimethoxysilane and 0.4% acetic

TABLE I

CELLULOSE DERIVATIVES USED FOR THE ENTANGLED POLYMER IN CAPILLARY ELECTROPHORESIS

| Cellulose | Abbreviation | Viscosity[a] (cP) | Methyl group (%) | Hydroxypropyl group (%) |
|---|---|---|---|---|
| Methyl cellulose | MC-4000 | 4290 | 30.0 | 0 |
| | MC-8000 | 7980 | 29.8 | 0 |
| Hydroxypropyl cellulose | HPC-11000 | 11000 | 0 | 63.3 |
| Hydroxypropyl methyl cellulose | HPMC-4000a | 4550 | 27.8 | 5.6 |
| | HPMC-4000b | 4390 | 29.0 | 9.3 |
| | HPMC-15000 | 15900 | 28.7 | 5.8 |

[a] Viscosity of a 2% cellulose aqueous solution measured at 20°C.

acid in acetonitrile was continuously passed through the capillary for 1 h. The capillary was then rinsed with acetonitrile for 15 min and Milli-Q water for 15 min. The acrylamide solution (3% T and 0% C[a]) was prepared in a buffer solution [50 m*M* tris(hydroxymethyl)-aminomethane (Tris), 50 m*M* boric acid and 2.5 m*M* EDTA] and carefully degassed in an ultrasonic bath for 10 min. Solutions of 10% (v/v) N,N,N′,N′-tetramethylethylenediamine (TEMED) and 10% (w/v) ammonium peroxydisulphate were prepared freshly. Polymerization was initiated by the addition of 20 μl of ammonium peroxydisulphate solution and 80 μl of TEMED solution into 5 ml of acrylamide solution. The polymerizing solution was quickly passed through the capillary for 10 min and left to polymerize for 30 min. The capillary was then rinsed with Milli-Q water for 15 min to remove polyacrylamide that had not reacted with the silanol group on the capillary inner surface.

Running buffer used in this study was 50 m*M* Tris–borate, 2.5 m*M* EDTA and an appropriate amount of cellulose derivative (pH 8.3) and prepared as follows (because it took a very long time to dissolve the cellulose derivative when it was added to water directly). Cellulose derivative (0.5 g) was added to *ca.* 40 ml of hot Milli-Q water (>70°C) with stirring. After the mixed solution became a hot aqueous slurry, 20 ml of a buffer solution (250 m*M* tris–borate and 12.5 m*M* EDTA) were added to the hot aqueous slurry. The aqueous slurry was cooled to below 20°C, which resulted in an aqueous solution. The resultant solution was diluted to 100 ml with Milli-Q water.

*Apparatus*

CE separations in cellulose derivative solutions were carried out by using a Waters Quanta 4000 capillary electrophoresis system. The DNA fragment mixture was introduced electrophoretically at negative polarity of 10 kV for 10 s into the capillary and separated by a linear polyacrylamide-coated capillary filled with running buffer at negative polarity of 10–20 kV (200–400 V/cm, 18–22 μA) at room temperature (24–27°C). Electrokinetic injection was used for the separation because this technique yielded a more efficient separation than pressure injection [11]. DNA fragments were detected at 254 nm.

[a] C = g N,N′-methylenebisacrylamide (Bis)/% T; T = (g acrylamide + g Bis)/100 ml solution.

## RESULTS AND DISCUSSION

Fig. 2 shows examples of the separations of the 1-kbp DNA ladder using the linear polyacrylamide-coated capillary filled with buffer solution including 0.5% cellulose derivatives (MC-4000, HPMC-4000a and HPMC-4000b) which have similar viscosity but are different in the structure and composition of the alkyl

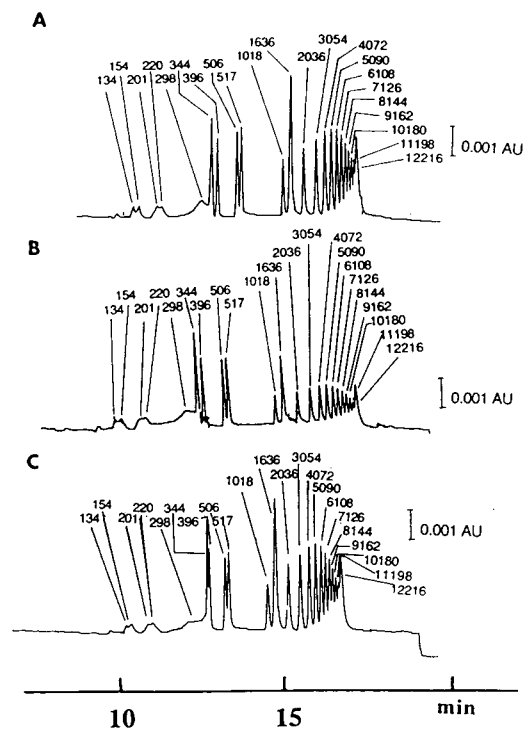


Fig. 2. CE separation of the 1-kbp DNA ladder. Linear polyacrylamide-coated capillary: 100 μm I.D., 375 μm O.D., total length 50 cm; effective length 42.5 cm. Running buffer: 50 m*M* Tris–borate, 2.5 m*M* EDTA and 0.5% cellulose derivative (pH 8.3). Cellulose derivative: (A) MC-4000, (B) HPMC-4000a and (C) HPMC-4000b. Field: 200 V/cm. Current: 18 μA. Injection: 10 kV for 10 s. Temperature: room temperature. Detection: 254 nm. Resolved fragments are labelled by their size in base pairs.

groups, as listed in Table I. The 1-kbp DNA ladder provides a good reference for the examination of the resolving power of the polymer solutions because it covers a broader molecular weight range of DNA fragments. The fragments were identified by their sizes in base pairs, the assignments agreeing with the reported separation of the 1-kbp DNA ladder obtained in a polyacrylamide gel-filled capillary, where peaks were assigned by spiking with slab gel isolated fragments [5]. The peak for DNA of 75 bp could not be assigned owing to very low detectability.

It can be seen in Fig. 2 that all separations of individual ladder fragments, obtained at 200 V/cm, are excellent and provide results very similar to those previously reported using cross-linked gel-filled capillaries [5–7], capillaries filled with a methylcellulose solution [6,7,10,15] and capillaries filled with an agarose solution [14]. The mixture of DNA fragments ranging from 134 to 8144 bp is baseline resolved; larger fragments ranging from 9162 to 12 216 bp are almost completely resolved, and yet the separation was completed within only 17 min. Additionally, the 506- and 517-bp pair, differing by only 11 bp, which are usually not separated on the slab gel electrophoresis [5,10], was completely resolved. The plate number of each peak in each separation was estimated to be in the range $0.5–1 \cdot 10^6$ plates per metre. The results in Fig. 2 illustrate that a change in the structure and the composition of alkyl groups on cellulose derivatives does not affect the performance and the efficiency of the separation of DNA fragments.

Fig. 3 illustrates the separations of the 1-kbp DNA ladder fragments using cellulose derivatives (MC-8000, HPC-11000 and HPMC-15000) with different viscosities. The efficiency of DNA separations under the conditions used can be compared with that in other media, as shown in Fig. 2. The representative cases of Fig. 3A and B show that the separation is equivalent to that obtained using cellulose derivatives of relatively low viscosity. However, poor resolution of DNA fragments was obtained using HPMC-15000, as shown in Fig. 3C. We tried to improve the resolution of DNA fragments by changing the concentration of HPMC-15000, but did not achieve a better resolution. In addition, HPMC-

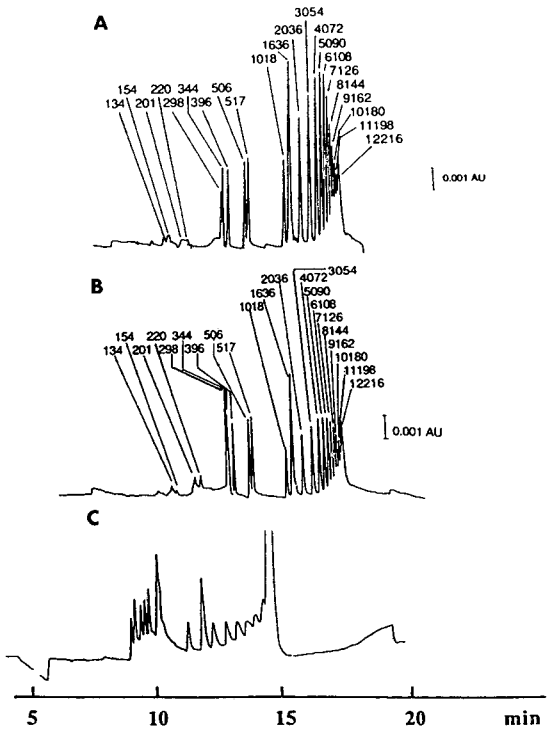


Fig. 3. Effect of the viscosity of cellulose derivative on the CE separation of the 1-kbp DNA ladder. Cellulose derivative: (A) MC-8000, (B) HPC-11000 and (C) HPMC-15000. Other conditions as in Fig. 2.

15000 buffer is inadequate for the entangled polymer solution, because it is too viscous to be easily loaded into the capillary.

The influences of the concentration of cellulose derivatives on the separation of the 1-kbp DNA ladder fragments are shown in Figs. 4 (HPMC-4000b) and 5 (HPC-11000). CE in 0.1% HPMC-4000b cellulose solution failed to resolve each fragment of the 1-kbp DNA ladder (Fig. 4A), but some peaks of DNA fragments were separated using 0.3% HPMC-4000b, as shown in Fig. 4B. The 0.7% HPMC-4000b cellulose solution (Fig. 4C) gave a better resolution of small fragments up to 517 bp than the 0.5% solution (Fig., 2C), but fragments larger than 6108 bp were not separated using the 0.7% solution. The separation time (24 min) of Fig. 4C is longer than that (17 min) of Fig. 2C. In the CE separation using 0.7% HPC-11000 (Fig. 5C) as well as 0.7% HPMC-4000b (Fig. 4C) cellulose solution, small DNA fragments up to 517 bp

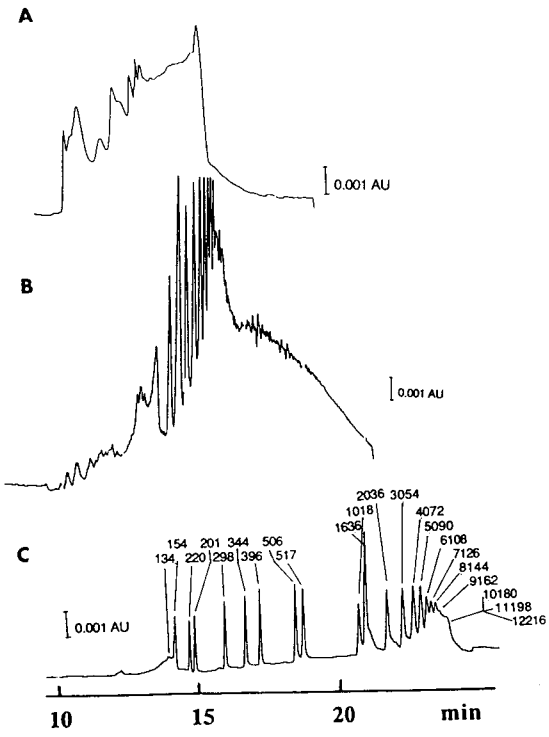


Fig. 4. Effect of the concentration of HPMC-4000b on the CE separation of the 1-kbp DNA ladder. Concentration of HPMC-4000b: (A) 0.1%, (B) 0.3% and (C) 0.7%. Other conditions as in Fig. 2.

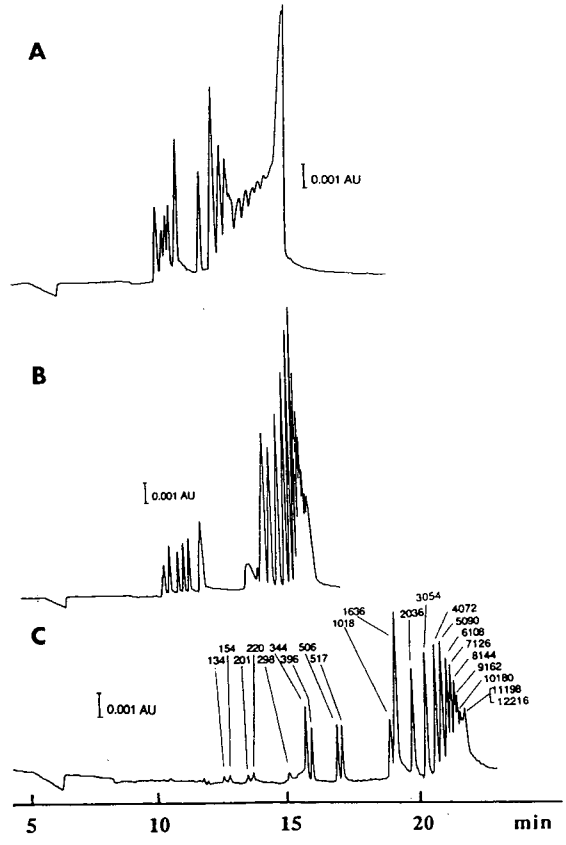


Fig. 5. Effect of the concentration of HPC-11000 on the CE separation of the 1-kbp DNA ladder. Concentration of HPC-11000: (A) 0.1%, (B) 0.3% and (C) 0.7%. Other conditions as in Fig. 2.

were baseline resolved, but the resolution of fragments larger than 8144 bp was poor. In addition, a longer separation time was required. The resolving power of HPC-11000 at lower concentration (Fig. 5A and B) seems to be higher than that of HPMC-4000b (Fig. 4A and B). These results show that an individual cellulose derivative solution has a characteristic limiting polymer concentration to exhibit the molecular sieving effect, and that a high-viscous cellulose derivative, which has longer chain length of polymer, can be an effective sieving agent even at a lower concentration, as will be discussed below.

The separation mechanism for DNA fragments using hydrophilic polymer solutions in CE has been investigated by Grossman and Soane [12,13]. The transient pores are formed by the entanglement of the polymer chains when the polymer volume fraction, $\Phi$, is higher than the polymer volume fraction at which the polymer chains begin to interact with one another. Such a polymer volume fraction, $\Phi^*$, is called the overlap threshold and expressed as:

$$\Phi^* = N^{-0.8} \quad (1)$$

where $N$ is the number of segments in the cellulose polymer chain. Eqn. 1 predicts that the overlap threshold will decrease with an increase in the chain length of the cellulose derivative, and this can be proved by the results, as shown in the comparison of HPC-11000 (Fig. 5) with HPMC-4000b (Fig. 4). The overlap threshold of hydroxyethyl cellulose, whose molecular mass is 191 800 and $N$ value is 1026, is calculated to be 0.39% [12,13]. The overlap thresholds of HPMC-4000b and HPC-11000 are estimated to

be 0.6 and 0.3%, respectively, because, according to the manufacturer, HPMC-4000b and HPC-11000 have average molecular masses of 90 000 and 250 000, respectively. These values agree roughly with the experimental values of 0.5% for HPMC-4000b and 0.3% for HPC-11000.

Transient pores with a broader distribution of size than the permanent pores in the gels must be present in the polymer network. The entangled polymer solution is therefore characterized by an average pore size, $\xi(\Phi)$, which is expressed as follows [12,13]:

$$\xi(\Phi) = a\Phi^{-0.75} \quad (2)$$

where $\Phi$ is the polymer volume fraction and $a$ is the length of a polymer segment. As expected from eqn. 2, the effective pore diameters should decrease with increasing concentration of cellulose derivative, providing improved separation of small fragments. The small DNA fragments in the 1-kbp ladder exhibit significant improvement in resolution when the concentration of cellulose derivative is increased from 0.1 to 0.7%, as shown in Figs. 4 and 5.

Fig. 6 illustrates the effect of the applied field on the separation of the 1-kbp DNA ladder using 0.5% HPMC-4000b. The migration time of each fragment decreases with an increase in the applied field. The efficiency of this separation increases, as expected, with fields up to about 300 V/cm. However, at a field of 400 V/cm, the resolving power of cellulose derivative solution decreases, because band broadening results from the stretching of DNA.

Fig. 7 demonstrates the use of 0.7% MC-4000 polymer solution for the separation of small DNA fragments in the range 72–1353 bp. This range of the *Hin*cII and *Hae*III restriction fragments of $\Phi$X174 DNA is crucial to DNA fragment typing using the PCR technique. Resolution is excellent and efficiency exceeded $1 \cdot 10^6$ plates/m. It can be seen from Fig. 7 that, in spite of the high resolution, no separation between the 335-, 341- and 345-bp fragments (Fig. 7a), or between the 271- and 281-bp fragments (Fig. 7b), was obtained. The same situation was also reported by other research groups [11]. However, these unseparated pairs can be completely baseline resolved by adding ethidium bromide to the buffer solution [11,16].

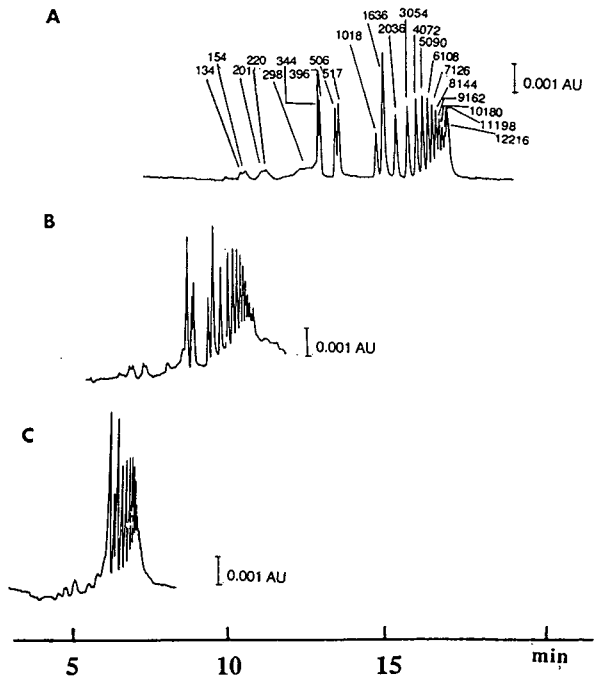


Fig. 6. Effect of the applied field on the CE separation of the 1-kbp DNA ladder. Cellulose derivative: 0.5% HPMC-4000b. Field: (A) 200 V/cm, (B) 300 V/cm and (C) 400 V/cm. Other conditions as in Fig. 2.

All cellulose derivatives tested here, except for HPMC-15000, can be used in the separation of double-stranded DNA restriction fragments. The size (viscosity) and the concentration of cellulose derivative are the most important parameters to manipulate the migration time and resolution. The choices within these parameters depend primarily on the size of the DNA fragments being separated. High-concentration (0.7–0.9%) cellulose derivative solutions are most effective for separating small fragments of DNA (50–100 bp). Their resolving power is extremely high, and fragments of DNA that differ in size by as little as 5–10 bp can be separated from one another. Although they can be run with high resolution, high-concentration polymer solutions have the disadvantage of being more difficult to load into the capillary than low-concentration polymer solutions owing to very high viscosity.

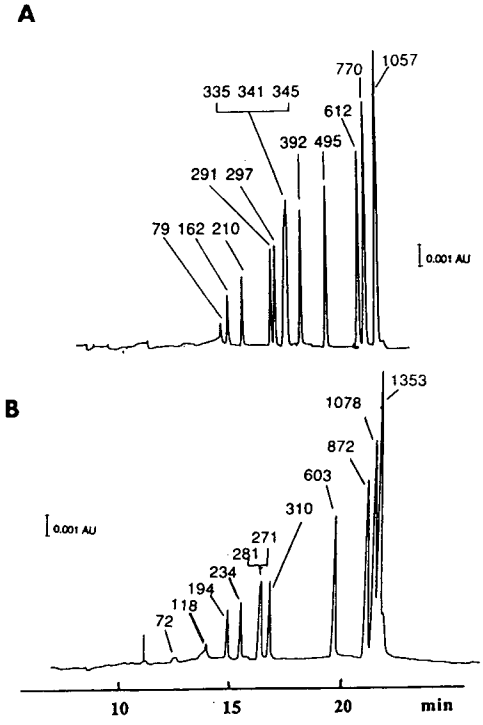


Fig. 7. CE separation of the DNA restriction fragment mixtures of (A) a *Hin*cII restriction digest of ΦX174 DNA and (B) the *Hae*III restriction digest of ΦX174 DNA. Running buffer: 50 m*M* Tris–borate, 2.5 m*M* EDTA and 0.7% MC-4000 (pH 8.3). Other conditions as in Fig. 2. Resolved fragments are labelled by their size in base pairs.

Low-concentration polymer solutions have a slightly lower resolving power than high-concentration polymer solutions but have a wider range of separation. DNAs from 100 bp to approximately 10 kbp in length can be separated with high resolution using 0.4–0.5% cellulose derivative solutions.

In this study, we demonstrate that the use of several cellulose derivatives as molecular sieving agents for CE represents an excellent approach for high-resolution separation of a broader molecular weight range of DNA restriction fragments. CE with cellulose derivative solutions has real potential as a powerful tool for gene diagnosis, such as RFLP analysis and single-strand conformation polymorphism (SSCP) analysis.

ACKNOWLEDGEMENTS

We acknowledge Associate Professor Makoto Otsuka at Kobe Women's College of Pharmacy for his helpful discussions on the nature of cellulose derivatives. We are indebted to Mr. Fumio Kobayashi at ShinEtsu Chemicals for his gift of cellulose derivatives. This work was partially supported by a Grant-in-Aid for Creative Basic Research (Human Genome Program), a Grant-in-Aid for Cancer Research and a Grant-in-Aid for Scientific Research from the Japan Ministry of Education, Science, and Culture.

REFERENCES

1 J. Sambrook, E.F. Fritsch and T. Maniatis, *Molecular Cloning: A Laboratory Manual*, Cold Spring Harbor Laboratory Press, New York, 2nd ed., 1987.
2 D. Rickwood and B.D. Hames (Editors), *Gel Electrophoresis of Nucleic Acids—A Practical Approach*, IRL Press, Oxford, 2nd ed., 1990.
3 Y. Baba and M. Tsuhako, *Trends Anal. Chem.*, 11 (1992) 280.
4 Y. Baba and M. Tsuhako, *BioIndustry*, 10 (1993) 299.
5 D.N. Heiger, A.S. Cohen and B.L. Karger, *J. Chromatogr.*, 516 (1990) 33.
6 Y. Baba, C. Sumita, K. Hide, N. Ishimaru, K. Samata, A. Tanaka and M. Tsuhako, *J. Liq. Chromatogr.*, 16 (1993) 955.
7 C. Sumita, Y. Baba, K. Hide, N. Ishimaru, K. Samata, A. Tanaka and M. Tsuhako, *J. Chromatogr.*, submitted for publication.
8 M. Zhu, D.L. Hanse, S. Burd and F. Gannon, *J. Chromatogr.*, 480 (1989) 311.
9 A.M. Chin and J.C. Colburn, *Am. Biotechnol. Lab.*, 7 (10A) (1989) 16.
10 M. Strege and A. Lagu, *Anal. Chem.*, 63 (1991) 1233.
11 H.E. Schwartz, K. Ulfelder, F.J. Sunzeri, M.P. Busch and R.G. Brownlee, *J. Chromatogr.*, 559 (1991) 267.
12 P.D. Grossman and D.S. Soane, *Biopolymers*, 31 (1991) 1221.
13 P.D. Grossman, in P.D. Grossman and J.C. Colburn (Editors), *Capillary Electrophoresis Theory and Practice*, Academic Press, San Diego, 1992, Ch. 8.
14 P. Bocek and A. Chrambach, *Electrophoresis*, 13 (1992) 31.
15 W.A. Mac Crehan, H.T. Rasmussen and D.M. Northrop, *J. Liq. Chromatogr.*, 15 (1992) 1063.
16 K. Ulfelder, H.E. Schwartz, J.H. Hall and F.J. Sunzeri, *Anal. Biochem.*, 200 (1992) 260.
17 S. Hjertén, *J. Chromatogr.*, 347 (1985) 191.
18 Y. Baba, T. Matsuura, K. Wakamoto, Y. Morita, Y. Nishitsu and M. Tsuhako, *Anal. Chem.*, 64 (1992) 1221.

*Journal of Chromatography A*, 653 (1993) 336–340
Elsevier Science Publishers B.V., Amsterdam

CHROM. 25 509

# Short Communication

# Chiral high-performance liquid chromatographic separation of the three stereoisomers of 2,6-diaminopimelic acid without derivatisation

Takashi Nagasawa

*Department of Bioscience and Technology, Iwate University, Morioka, Iwate 020 (Japan)*

John R. Ling*

*Department of Biochemistry, School of Life Sciences, The University of Wales, Aberystwyth SY23 3DD, Wales (UK)*

Ryoji Onodera

*Laboratory of Animal Nutrition and Biochemistry, Miyazaki University, Miyazaki 889-21 (Japan)*

(First received June 15th, 1993; revised manuscript received August 16th, 1993)

ABSTRACT

The peptidoglycan component of most bacterial cell walls contains the amino acid, 2,6-diaminopimelic acid (DAP), which can exist in three stereoisomeric forms. A chiral ligand-exchange HPLC method is described that is capable of separating mixtures of these isomers without derivatisation so that they may be used as substrates in subsequent biological experiments. The conditions for separation were optimised so that DAP was eluted from the chiral column, MCI gel CRS10w, with a mobile phase of 2 m*M* $CuSO_4$–methanol (98:2, v/v) at 40°C. The elution times for the DD-, *meso*- and LL-isomers were 10.5, 14.6 and 34.7 min, respectively, as confirmed by circular dichroism.

## INTRODUCTION

Bacterial cell walls are structurally diverse, yet most Gram-positive and Gram-negative bacteria contain peptidoglycans in which the amino acid, 2,6-diaminopimelic acid (DAP), is a common component [1]. Because of its apparent uniqueness to bacteria, DAP has been extensively used to study bacterial cell wall biosynthesis [2] and degradation [3], to classify bacteria taxonomically [4] and as a marker to estimate bacterial biomass. This latter function has been exploited in widely different ecosystems, such as porcine digesta [5] and leaf litter [6], but most frequently its use has been within the digestive tracts of ruminant animals [1]. However, questions about the accuracy of DAP as a marker have been raised as a result of investigations into its metab-

* Corresponding author.

0021-9673/93/$06.00 

olism by rumen microorganisms. It has been shown that DAP can be metabolised in both its free [7] and bacterially bound [8] forms, by both rumen bacteria [9] and protozoa [10], both *in vitro* [7–10] and *in vivo* [11]. The fact that DAP can exist in three stereoisomeric forms namely, DD-, *meso*- and LL-DAP, undoubtedly affects its metabolism by rumen microorganisms. Yet nothing is known about these aspects of DAP metabolism, primarily because no simple, rapid method exists for the production of free DAP isomers, that is, without derivatisation.

To advance our studies of DAP metabolism within the rumen microbial ecosystem, we required a method for the rapid separation of underivatised DAP stereoisomers, including those contained in commercially available [$^3$H]DAP, so that substrates suitable for subsequent microbial incubations and enzymic studies could be produced. A Cu-based ligand-exchange HPLC method, developed from the pioneering work of Davankov *et al.* [12], that is capable of such chiral separations is reported here.

## EXPERIMENTAL

### *Sources of DAP*

Samples of DAP, supplied as mixtures of the DD-, *meso*- and LL-isomers, were obtained from Sigma (St. Louis, MO, USA). A sample of authentic LL-DAP was kindly given by Dr P.J. White, Department of Microbiology, The University of Sheffield, UK.

### *Paper chromatography*

Descending chromatography was performed on paper (Whatman No. 1) with a solvent composed of methanol–water–10 *M* HCl–pyridine, (32:7:1:4, v/v), as described by Rhuland *et al.* [13]. The isomers were detected by spraying with ninhydrin (0.2% w/v in acetone) and heating them at 95°C for 5 min.

### *HPLC equipment*

The chiral HPLC column (MCI gel CRS10w, 100 mm × 4.0 mm I.D.) was purchased from Mitsubishi Kasei (Tokyo, Japan). The HPLC equipment (Shimadzu, Kyoto, Japan) consisted of a LC-6A pump unit (elution flow-rate, 1.0 ml/min), a SPD-6AV UV–Vis detector (set at 254 nm) and a Chromatopac CR-6A data processor. The column temperature was maintained by a circulating water bath. Samples containing DAP were dissolved in distilled water. The mobile phase was composed of an aqueous solution of $CuSO_4$, usually with the addition of methanol.

### *Circular dichroism (CD) analysis*

Before eluates from the chiral HPLC column were subjected to CD analysis, copper ions were removed from these fractions by a column (40 mm × 8 mm I.D.) of Chelex 100 resin (50–100 mesh, sodium form; Bio-Rad, Tokyo, Japan), according to the method of Armstead and Ling [14]. CD spectra were obtained by the use of a J-20 automatic recording spectropolarimeter (Japan Spectroscopic, Tokyo, Japan).

## RESULTS AND DISCUSSION

DAP possesses two chiral carbons and, because of the particular configuration of the substituent groups around these, it can exist in four possible forms, namely as the (*R*,*R*)-, (*S*,*S*), (*R*,*S*)- and (*S*,*R*)-isomers. However, since the latter two forms are indistinguishable, they are usually referred to as the *meso*-isomer, and the three resulting stereoisomeric forms are commonly known as DD-, LL- and *meso*-DAP.

The chromatographic resolution of these three stereoisomers is a technically difficult problem. Several methods for separating DAP have been reported. The most frequently used are ion-exchange column chromatography [15], thin-layer chromatography [15] and gas–liquid chromatography [16,17], but none of these methods is capable of resolving any of the DAP isomers.

By contrast, paper chromatography has been successfully used to separate the isomers of DAP [13,18]. In the present study, using the method of Rhuland *et al.* [13], the LL-isomer was separated after development of the chromatogram for 7 h, though at that time the DD- and *meso*-isomers were still unresolved. Only after 23 h development were all three isomers completely separated with mobilities, relative to LL-DAP, of

0.77 and 0.85 for the DD- and *meso*-isomers, respectively. Therefore, although paper chromatography allows satisfactory separation of the DAP isomers, it is a time-consuming and tedious method, with at best, only semi-quantitative recovery of the required isomers.

Several approaches based on HPLC procedures have been applied to the problem of separating these DAP isomers. Wiseman and Nichols [19] prepared a chiral mobile phase, containing N,N-di-*n*-propyl-L-alanine, which resolved all three isomers, but, of course, the DAP isomers were contaminated with the eluent containing the chiral compound. An alternative approach is to derivatise the DAP prior to HPLC separation; Zanol and Gastaldo [20] derivatised DAP with the chiral reagent, Nα-(2,4-dinitro-5-fluorophenyl)-L-alaninamide (Marfey's reagent), which allowed them to separate the three isomers. Precolumn derivatisation of DAP with *o*-phthaldialdehyde is another approach, but this appears to be less successful, since it resulted in only partial resolution of the stereoisomers [21,22]. Nevertheless, because derivatisation of the DAP is a prerequisite for all of these HPLC methods, none is suitable for the production of DAP stereoisomeric substrates which can be used for subsequent biological experimentation. The only remaining approach is to use HPLC that relies upon a chiral column, rather than a chiral mobile phase or derivatisation method. The MCI gel CRS10w column, used in the present study, was composed of a silica stationary phase coated with the chiral N,N-dioctyl-L-alanine.

The effects of varying the major chromatographic conditions of this chiral ligand-exchange HPLC system upon the retention times of the three stereoisomers of DAP were investigated; Fig. 1 shows the results. Increasing the molarity of the $CuSO_4$ in the mobile phase decreased retention times, but had little effect upon the separation of the DD- and *meso*-isomers (Fig. 1A). Subsequent elutions were all performed with 2 m*M* $CuSO_4$. The addition of methanol to the mobile phase significantly reduced the back-pressure in the system. It also caused a more rapid elution of all stereoisomers, but increasing its concentration to 5% (v/v) or more caused the DD- and *meso*-isomers to be incompletely re-

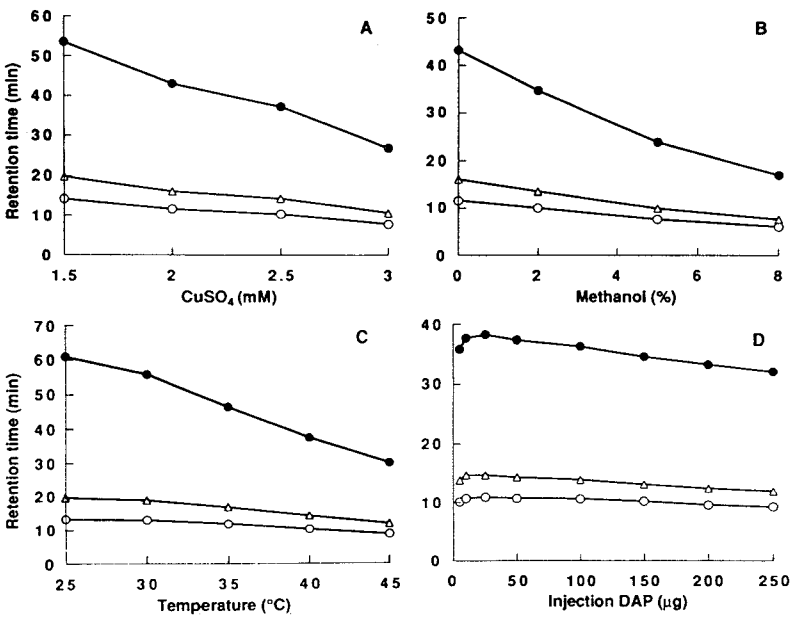


Fig. 1. Effects of (A) $CuSO_4$, and (B) methanol concentrations in the mobile phase, (C) column temperature, and (D) amount of sample on the retention times of a mixture of (○) DD-, (△) *meso*- and (●) LL-isomers of DAP eluted from a column of MCI gel CRS10w. The mobile phase in B was 2 m*M* $CuSO_4$, and in C and D it was 2 m*M* $CuSO_4$–methanol (98:2, v/v). The column temperature in A, B and D was 40°C, and the sample size in A, B and C was 10 μg DAP.

solved (Fig. 1B). The effect of column temperature is shown in Fig. 1C; retention times were inversely related to this parameter. The effect of the amount of DAP mixture loaded on to the column was investigated; samples up to approximately 150 μg had negligible influence upon either the degree of resolution, or the retention times of the three stereoisomers (Fig. 1D).

The operating conditions chosen for any chromatographic system are always a compromise of its component parameters. To ensure that the LL-isomer was eluted within a reasonably short time, yet with the DD- and *meso*-isomers still completely resolved, the following conditions were chosen as optimal; a mobile phase consisting of 2 m*M* $CuSO_4$–methanol (98:2, v/v), with the column operating at 40°C and with a sample size of less than 150 μg DAP. Using these parameters, the results of a typical chromatogram demonstrating the separation of the three peaks of a standard stereoisomeric mixture of DAP is shown in Fig. 2. The proportions of the peak areas, when a sample of 10 μg DAP was eluted, were 25, 50 and 25% for peaks 1, 2 and 3, respectively.

CD analysis was used to confirm the identity of the three peaks of Fig. 2. At 210 nm the differential absorption values of the eluates derived from peaks 1, 2 and 3 were −0.60, −0.17 and +0.43, respectively, with a value of −0.18 for water. This information, together with the observation that the authentic LL-DAP co-eluted with peak 3 (34.7 min), and the fact that the standard DAP is known to contain the DD-, *meso*- and LL-isomers in the ratio 1:2:1, allowed the correct identification of each stereoisomer. The three peaks and their retention times were recorded as DD- (10.5 min), *meso*- (14.6 min) and LL-DAP (34.7 min).

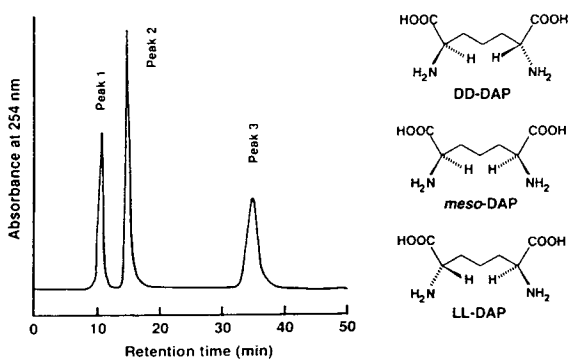


Fig. 2. Elution profile of a mixture of the three stereoisomers of DAP eluted from a column of MCI gel CRS10w with a mobile phase of 2 m*M* $CuSO_4$–methanol (98:2, v/v). The column temperature was 40°C, and the sample size was 10 μg DAP. Peaks 1, 2 and 3 were identified as DD-, *meso*- and LL-DAP, respectively, each with the structure as shown.

When DAP stereoisomers, especially in radiolabelled form, are being prepared as substrates for biological experimentation, such as microbial metabolic studies [9,11], an initial ion-exchange purification step should be included, as recommended by Masson and Ling [8]; they reported that in commercially available [$^3$H]DAP as much as 20% of the radiolabel was present in compounds other than DAP. This step, followed by separation of the DAP by the chiral HPLC method as described above, and with the subsequent removal of the copper ions [14] and methanol (by a stream of nitrogen gas, or by freeze-drying) from the mobile phase, will allow the production of pure DAP isomers.

The method developed in this present study, based on a chiral ligand-exchange HPLC procedure, is the first to report the rapid separation, collection and identification of the three stereoisomers of DAP in their underivatised forms. Studies to resolve the metabolism of these stereospecific compounds by rumen microorganisms are currently underway.

## ACKNOWLEDGEMENT

The authors wish to acknowledge the financial support from the Japanese Ministry of Education, Science and Culture, under its International Scientific Research Program: Joint Research scheme.

## REFERENCES

1 J.R. Ling, in S. Hoshino, R. Onodera, H. Minato and H. Itabashi (Editors), *The Rumen Ecosystem —The Microbial Metabolism and its Regulation*, Japan Scientific Societies Press, Tokyo, 1990, p. 83.
2 N. Nanninga, F.B. Wientjes, E. Mulder and C.L. Woldringh, in S. Mohan, C. Dow and J.A. Cole (Editors), *Prokaryotic Structure and Function: A New Perspective*, Cambridge University Press, Cambridge, 1992, p. 185.

3 J.-V. Höltje and E.I. Tuomanen, *J. Gen. Microbiol.*, 137 (1991) 441.
4 K.H. Schleifer and P.H. Seidl, in M. Goodfellow and D. Minnikin (Editors), *Chemical Methods in Bacterial Systematics*, Vol. 20, Academic Press, New York, 1985, p. 201.
5 A.M. Rowan, P.J. Moughan and M.N. Wilson, *Anim. Feed Sci. Technol.*, 36 (1992) 129.
6 M.O. Gessner, M.A. Bauchrowitz and M. Escautier, *Microbial Ecol.*, 22 (1991) 285.
7 R. Onodera and M. Kandatsu, *Nature (London) New Biol.*, 244 (1973) 31.
8 H.A. Masson and J.R. Ling, *J. Appl. Bacteriol.*, 60 (1986) 341.
9 A.M. Denholm and J.R. Ling, *Appl. Environ. Microbiol.*, 55 (1989) 212.
10 R. Onodera, H. Takashima and J.R. Ling, *J. Protozool.*, 38 (1991) 421.
11 H.A. Masson, A.M. Denholm and J.R. Ling, *Appl. Environ. Microbiol.*, 57 (1991) 1714.
12 V.A. Davankov and A.V. Semechkin, *J. Chromatogr.*, 141 (1977) 313.
13 L.E. Rhuland, E. Work, R.F. Denman and D.S. Hoare, *J. Am. Chem. Soc.*, 77 (1955) 4844.
14 I.P. Armstead and J.R. Ling, *J. Chromatogr.*, 586 (1991) 259.
15 J.R. Ling and P.J. Buttery, *Brit. J. Nutr.*, 39 (1978) 165.
16 N.P. Sen, E. Somers and R.C. O'Brien, *Anal. Biochem.*, 28 (1969) 345.
17 C.W. Moss, F.J. Diaz and M.A. Lambert, *Anal. Biochem.*, 44 (1971) 458.
18 H.R. Perkins, *Nature*, 208 (1965) 872.
19 J.S. Wiseman and J.S. Nichols, *J. Biol. Chem.*, 259 (1984) 8907.
20 M. Zanol and L. Gastaldo, *J. Chromatogr.*, 536 (1991) 211.
21 M.E.R. Dugan, W.C. Sauer, K.A. Lien and T.W. Fenton, *J. Chromatogr.*, 582 (1992) 242.
22 R. Puchala, H. Piór, G.W. Kulasek and J.A. Shelford, *J. Chromatogr.*, 623 (1992) 63.

*Journal of Chromatography A*, 653 (1993) 341–347
Elsevier Science Publishers B.V., Amsterdam

CHROM. 25 480

# Short Communication

# Development of a method for simultaneous determinations of nitrogen oxides, aldehydes and ketones in air samples

Andreas H.J. Grömping, Uwe Karst and Karl Cammann*

*Lehrstuhl für Analytische Chemie, Anorganisch-Chemisches Institut, Westfälische-Wilhelms-Universität Münster, W-4400 Münster (Germany)*

(First received April 27th, 1993; revised manuscript received July 12th, 1993)

ABSTRACT

Nitrogen oxides, aldehydes and ketones are important environmental toxins which frequently occur together (*e.g.* in automobile exhaust and in tobacco smoke). In this paper a convenient method for a simultaneous analysis of nitrogen oxides, aldehydes and ketones in air is presented for the first time. This method is based on the well-established and practical 2,4-dinitrophenylhydrazine method for the determination of aldehydes and ketones. Detection limits for the determination of nitrogen oxides were 10 ppb (v/v) using solid sorbents, 50 ppb (v/v) using impingers (sampling at 0.8 l/min for 15 min), and 150 ppb (v/v) using passive sampling devices (sampling for 4 h).

## INTRODUCTION

Nitrogen dioxide as well as aldehydes and ketones often occur together in gaseous samples, *e.g.* automobile exhaust [1,2], gas-stove exhaust [3], and tobacco smoke [2,4]. Both are formed as combustion byproducts underlining the necessity of a method for their simultaneous determination. Recognition of their toxicity has stimulated a rapid development of new analytical techniques for these compounds.

The classical methods for the analysis of formaldehyde, such as the pararosaniline (PRA) method [5], the chromotropic acid (CTA) method [6] and the 3-methyl-2-benzthiazolonhydrazine (MBTH) method [7], are based on colorimetric techniques. Since some of the methods suffer from interferences, different methods using chromatographic separations have been proposed [8–10]. In recent years the 2,4-dinitrophenylhydrazine (DNPH) method has become the most important method for the analysis of aldehydes and ketones [11–17], since a large number of these compounds can be determined simultaneously.

Nitrogen oxides are determined with the Saltzman technique (see ref. 18) or the triethanolamine method [19], both of which are based on colorimetric techniques. As the simultaneous determination of nitrogen oxides, aldehydes and ketones is very important, Kaul-

* Corresponding author.

0021-9673/93/$06.00 

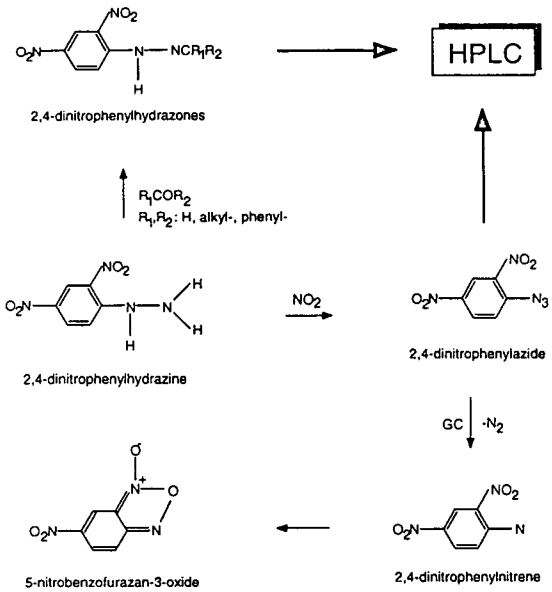


Fig. 1. Basic reactions mentioned in this paper.

bach [20] proposed a simultaneous determination of these compounds using two different colorimetric methods, the Saltzman method for the detection of nitrogen dioxide and the PRA method for the determination of formaldehyde. Unfortunately, two analytical procedures have to be performed to determine only formaldehyde and nitrogen dioxide which makes this method very time consuming.

The interferences of nitrogen dioxide with the determination of aldehydes and ketones using the DNPH method have been described recently [13]. In this paper the development of the first fast and convenient method for the simultaneous determination of aldehydes, ketones, and nitrogen oxides in gaseous samples using only one reagent [21] based on their reactions with DNPH (see Fig. 1) is described.

## EXPERIMENTAL

### *Reagents*

Formaldehyde (37%, w/v), methanol, hydrochloric acid and sulphuric acid were Merck analytical grade. Deionized, twice distilled water and methanol purified by distillation over a 1-m column filled with Raschig rings were used as eluents for HPLC. Acetonitrile (liquid chromatography grade) was purchased from Merck. Nitrogen monoxide (99.8% pure) and nitrogen dioxide (98% pure) were purchased from Messer-Griesheim.

### *Apparatus*

Portable air sampling pumps, Models S 2500 and Alpha 1 from DuPont were used. The HPLC system used consisted of an Alltech Model 100 A pump or a Knauer HPLC pump and a Rheodyne Model 7125 injection valve or a Rheodyne Model 7126 pneumatic injection valve, both with 20-$\mu$l sample loops. Detectors used were a Zeiss Model PMQ 3 UV–visible absorbance detector with a Uvicon 6-$\mu$l cell or a Knauer UV–visible absorbance detector. As detection wavelength either 300 nm (absorbance maximum of dinitrophenylazide) or 345 nm (absorbance maximum of dinitrophenylhydrazones) was chosen. A Machery–Nagel Poligosil $C_{18}$ (5 $\mu$m, 20 × 4 mm) guard column and a Machery–Nagel Poligosil $C_{18}$ (5 $\mu$m, 250 × 4 mm) analytical column were used. Injections were done via a Knauer injection loop of 20 $\mu$l volume.

For the identification of the different formaldehyde derivatives a GC–MS system was used, which consisted of a Hewlett-Packard Model 5890 series II gas chromatograph, a Hewlett-Packard Ultra 2 column (50 m × 0.32 mm), and a Hewlett-Packard Model 5970 mass-selective detector.

### *Chromatographic separation*

Karst *et al.* [13] solved the problem of the separation of dinitrophenylazide and formaldehyde–dinitrophenylhydrazone which have a similar chromatographic behavior using a complex gradient for baseline separation. We used an isocratic solvent system to separate the two compounds. Typically, the chromatographic separation was carried out at a flow-rate of 1.0 ml/min, with acetonitrile–water (60:40) as eluent.

### *Formaldehyde standard solution*

The formaldehyde standard solution was prepared by diluting 1 ml of commercial formaldehyde solution (37%, w/v) to 100 ml with purified water. A final concentration of 0.124

mol/l was determined according to the method used by Harris [22].

*Air sampling*

Impingers were filled with solutions of DNPH in organic solvents. Using a personal sampling pump, an air stream of 0.8 l/min was drawn through the impinger. A trap filled with methanol–dry ice prevented the solvents from vaporizing into the pump. Sampling of candle smoke was carried out as described in a previous paper [23].

Sampling with solid sorbents coated with DNPH was investigated as well. Coating of Chromosorb P with DNPH, preparation of the sampling tubes, and desorption utilized the procedure of Binding *et al.* [24] with the modifications described below. This technique was applied to the sampling of nitrogen oxides as well as aldehydes and ketones. In order to reduce the blank, the DNPH was recrystallized twice from 6 *M* hydrochloric acid and then twice from acetonitrile. Next, 5 g DNPH were suspended in 20 ml acetonitrile (instead of dissolving in dimethylformamide [24]) and 6 g Chromosorb P added. The suspension was treated for 5 min in an ultrasonic bath. The next modification of the procedure of Binding *et al.* [24] was to remove all acetonitrile with a rotavapor without any remaining solvent. This solid sorbent was used to prepare sampling tubes as described below.

Finally, the possibilities of diffusive sampling were studied. For this purpose diffusive samplers as described by Levin *et al.* [25] were used. Elution was done by shaking the filter for a few minutes with 5 ml acetonitrile in a 10-ml glass vial. In each case, 20 $\mu$l of the absorbing or desorbing solution were analyzed after sampling by means of HPLC.

*Synthesis of the hydrazone standards*

A solution of 5 m*M* 2,4-dinitrophenylhydrazine in 15 ml of 40% (w/v) sulphuric acid was diluted with 25 ml ethanol. To this solution 5 m*M* of the carbonyl compound were added as 10% (w/v) solution. The precipitate was washed with water and recrystallized from ethanol. Characterization of the hydrazones was performed using spectroscopic methods and mass spectrometry.

*Synthesis of the azide standard*

Gaseous nitrogen dioxide was passed into an acidified (0.1 ml of concentrated hydrochloric acid) solution of DNPH in 60 ml acetonitrile. The color of the solution changed from orange to yellow. The progress of the reaction was monitored by HPLC. The solvent was removed in vacuo, and the residue was dried and characterized using spectroscopic methods and MS [13].

## RESULTS AND DISCUSSION

*Identification of the reaction product between nitrogen oxides and DNPH*

The identification of the reaction products of nitrogen oxides and DNPH has been described in a previous paper [13]. The main reaction product could be identified as 2,4-dinitrophenylazide (see Fig. 1); an important by-product is 2,4-dinitrochlorobenzene. Spectroscopic data of the 24,-dinitrophenylazide: IR (KBr): 3050 (s, C–H), 2100 (s, C–N), 1600 9s), 1500, (s), 1320 (s), 1270 (s), 905 (m), 825 (m). MS (GC) (see bottom of Fig. 1) 181 (100%) [$M^+$], 165 (12%) [M − O], 105 (9%), 104 (10%), 77 (27%), 75 (47%), 74 (37%). UV (methanol): maximum at 300 nm. $^1$H NMR ($C^2HCl_3$): 8.82 (s, 1H), 8.47 (d, 1H), 7.49 (d, 1H).

*Air sampling with impingers*

Nitrogen dioxide was diluted in a gas-tight flask (volume 1 l). This was connected to two impingers in series with a personal air sampling pump. The impingers were filled with a solution of 1.5 mg DNPH in 2.5 ml acetonitrile. Because of the hydrophilicity of $NO_2$, for a better solubility the solution was diluted with 1 ml water and acidified with 0.1 ml 1 *M* HCl to allow an efficient sampling of nitrogen dioxide. Finally, an air stream of 0.5 l/min was drawn through the gas-tight flask and the impingers for 15 min.

To study the reproducibility, ten 8-l samples (each corresponding to 0.5 ml pure $NO_2$) were taken. The data have a standard deviation of 6%. This corresponds to a deviation of 14% at

the 95% confidence level. The correlation between the peak height of dinitrophenylazide and the quantity of $NO_2$ added was studied injecting eight different amounts of $NO_2$ (0–1.0 ml) into the gas-tight apparatus. The linear regression has a correlation coefficient of 0.998.

Air sampling of aldehydes and ketones is usually done without addition of water to the absorbing solution. To work under the same conditions for nitrogen dioxide measurements, a solution of 1.5 mg DNPH in 2.5 ml acetonitrile and 0.1 ml HCl was used without addition of water. Again a linear correlation was observed with the same correlation coefficient. In blank measurements no dinitrophenylazide could be detected. Therefore, the limit of detection (LOD) for $NO_2$ was determined corresponding to a signal-to-noise ratio of 3:1 to be 50 ppb (v/v) for a 7.5-l sample.

Nitric oxide was detected by oxidation to nitrogen dioxide using potassium dichromate. A tube (100 × 4 mm) was filled with 200 mg potassium dichromate and acidified with 2–3 drops of concentrated phosphoric acid (see Fig. 2). This tube was inserted in line before the impingers. Different quantities of nitric oxide were then drawn through this oxidation layer and the impinger as was done for the nitrogen dioxide. A linear correlation between peak height of dinitrophenylazide and addition of nitric oxide was observed, injecting seven different volumes of NO (0–0.7 ml) into the apparatus. A correlation coefficient of 0.996 was obtained for the linear diagram of signal *vs.* volume. Thus, it is possible to determine the sum of nitric oxide and nitrogen dioxide ($NO_x$) by connecting the impinger to a tube containing an oxidation layer of acidified $K_2Cr_2O_7$. For the determination of nitric oxide, the difference of a measurement with an oxidation layer and without an oxidation layer can be determined. Because potassium dichromate oxidizes alcohols to aldehydes and ketones [26], formaldehyde and higher homologues cannot be analyzed with this method.

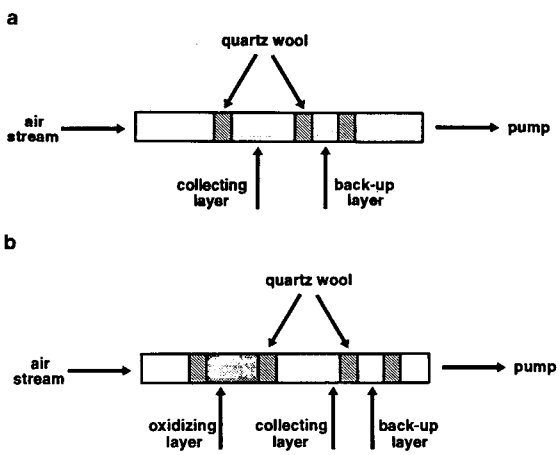


Fig. 2. Sampling with solid sorbents. (a) Determination of nitrogen oxide, aldehydes and ketones; (b) determination of the sum of nitrogen dioxide and nitric oxide ($NO_x$).

*Air sampling with solid sorbents*

Using solid sorbent tubes, prepared according to Binding *et al.* [24], nitrogen dioxide could not be detected. The reproducibility was very poor and linear calibration curves could not be obtained. In order to allow an efficient sampling of the hydrophilic nitrogen dioxide, 0.5 ml demineralized water were added to 2.5 g of the dry solid sorbent. Once again, different quantities of nitrogen dioxide were drawn through tubes filled with this solid sorbent. A linear calibration curve was obtained with a correlation coefficient of 0.997 for more than three orders of magnitude (see Fig. 3a). Addition of 0.2 $\mu$l pure $NO_2$ (diluted with nitrogen to 8 l) corresponds to an LOD of 10 ppb (v/v) $NO_2$.

For sampling of aldehydes and ketones these sampling phases are used without addition of water. To study the possibilities for the determination of $NO_2$ of this dry sampling phase another calibration curve was taken (see Fig. 3b). In the lower concentration range its linearity is better than that of the wet sampling phase ($r > 0.999$). But its capacity is restricted so that sampling above a concentration of 10 ppm (v/v) is not recommended.

Using the procedure described above, the sampling of NO with solid sorbents was tested as well. For this purpose the tubes were filled with an oxidation layer of 200 mg potassium dichromate acidified with 2–3 drops of concentrated phosphoric acid in front of the sampling layer. The calibration curve is linear with a correlation coefficient of 0.994. Fig. 4 shows the difference

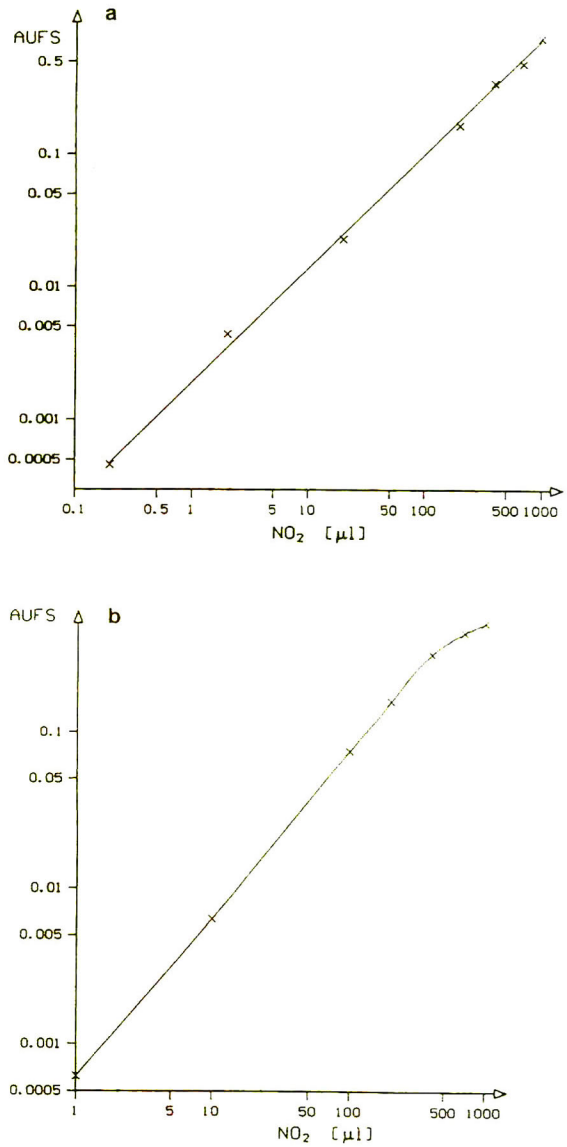


Fig. 3. Correlation between peak height of dinitrophenylazide and addition of $NO_2$: sampling with solid sorbents. (a) Wet sampling phase, (b) dry sampling phase. Column: Polygosil $C_{18}$ (5 $\mu$m, 250 × 4 mm); flow-rate: 1.0 ml/min; eluent: acetonitrile–water (60:40); detection wavelength: 300 nm; injection volume: 20 $\mu$l.

between sampling with and without an oxidation layer. Because of different alcohols which had been oxidized (see Fig. 4b) to aldehydes/ketones, several peaks besides the dinitrophenylazide peak emerged.

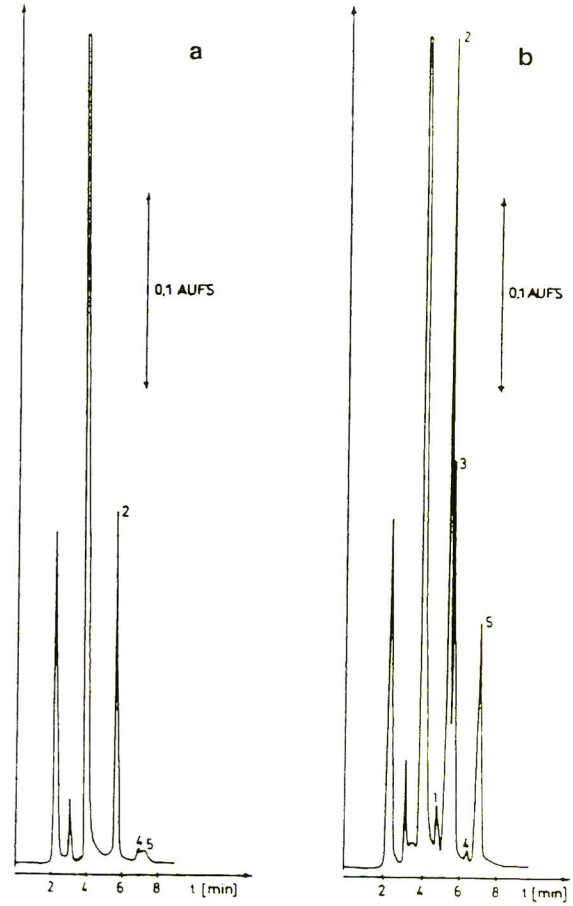


Fig. 4. Chromatogram of automobile exhaust (a) without and (b) with oxidation layer. Column: Polygosil $C_{18}$ (5 $\mu$m, 250 × 4 mm); flow-rate: 1.0 ml/min; eluent: acetonitrile–water (60:40); detection wavelength: 345 nm; injection volume: 20 $\mu$l. Peaks: 1 = dinitrophenylazide; 2 = formaldehyde–dinitrophenylhydrazone; 3 = unknown; 4 = acetaldehyde–dinitrophenylhydrazone; 5 = acrolein–dinitrophenylhydrazone.

*Air sampling with passive samplers*

For measurements in working areas, passive samplers are often used. Therefore, the suitability of passive samplers based on the reaction with DNPH was studied for the determination of nitrogen dioxide. A passive sampler was placed in the middle of a 144-l plexiglas box. Five different volumes of nitrogen dioxide (0–1.0 ml) were injected through a septum. A linear calibration curve with a correlation coefficient of 0.999 was obtained. The LOD corresponds to

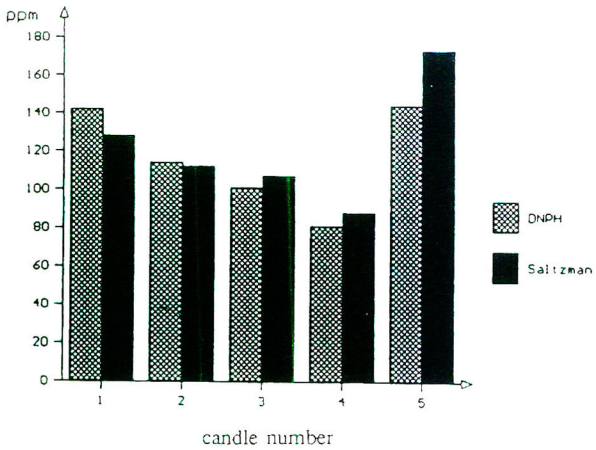


Fig. 5. Comparison of DNPH and Saltzman methods by analyzing smoke of different candles. Sampling with impingers; DNPH method: column: Polygosil $C_{18}$ (5 $\mu$m, 250 × 4 mm); flow-rate: 1.0 ml/min; eluent: acetonitrile–water (60:40); detection wavelength: 300 nm; injection volume: 20 $\mu$l.

150 ppb (v/v) $NO_2$ for a signal-to-noise ratio of 3:1.

*Comparison to the Saltzman method*

A widely used procedure for the determination of nitrogen oxides in air is the collection of a sample in an impinger filled with water followed by spectrophotometric determination using the Saltzman method [27,28]. In order to compare the methods, the DNPH impinger techniques and the Saltzman method were applied to the analysis of candle smoke. Similar values were obtained with both methods (see Fig. 5). The observed deviations were not greater than those observed with one single method during several repetitive measurements. According to Wiederholt *et al.* [28] the LOD for the Saltzman method is 200 ppb (v/v). Since an LOD of 50 ppb (v/v) for the impinger techniques and an LOD of 10 ppb (v/v) with solid sorbents was obtained in this study the detection of nitrogen oxides was improved by at least a factor of 4.

## ACKNOWLEDGEMENTS

Financial support of the Bundesministerium für Forschung und Technologie (AZ.:325-4007-07INR223) and the Institut für Chemo- und Biosensorik is gratefully acknowledged.

## REFERENCES

1 W. Forth, D. Henschler and W. Rummel, *Allgemeine und Spezielle Pharmakologie und Toxikologie*, Wissenschaftsverlag Zürich, Zurich, 5th ed., 1987.
2 G. Creech, R.T. Johnsson and J.O. Stoffer, *J. Chromatogr. Sci.*, 20 (1983) 67–72.
3 T.G. Matthews and T.C. Howell, presented at the *3rd Int. Conf. on Indoor Quality and Climate, Stockholm, 1984.*
4 C. Jermini, A. Weber and E. Grandjean, *Int. Arch. Occup. Environ. Health*, 36 (1977) 169.
5 R.R. Miksch, D.W. Anthon, L.Z. Fanning, L.D. Hollowell, K. Revzan and J. Glanville, *Anal. Chem.*, 53 (1981) 2118–2123.
6 American Public Health Association Intersociety Committee; M. Katz (Editor), *Methods of Sampling and Analysis*, American Public Health Association, Washington, DC, 2nd ed., 1977, pp. 300–307.
7 E. Sawicki, T.R. Hauser, T.W. Stanley and W. Elbert, *Anal. Chem.*, 33 (1961) 93–96.
8 S.J. Swarin and F. Lipari, *J. Liq. Chromatogr.*, 6 (1983) 425–444.
9 G.R. Möhlmann, *Appl. Spectr.*, 39 (1985) 98–101.
10 P. Bisgaard, L. Molhave, B. Rietz and P. Wilhardt, *Am. Ind. Hyg. Assoc. J.*, 45 (1984) 425–429.
11 A. Grömping and K. Cammann, *Fresenius' Z. Anal. Chem.*, 335 (1989) 796–801.
12 K. Cammann, M. Faust, A. Grömping, U. Meyer and B. Winter, *VDI-Berichte*, No. 838 (1990) 91–100.
13 U. Karst, N. Binding, K. Cammann and U. Witting, *Fresenius' J. Anal. Chem.*, 345 (1993) 48–52.
14 A. Grömping, *Diploma Thesis*, Westfälische-Wilhelms-Universität Münster, Münster, 1989.
15 A. Grömping, *Ph.D. Thesis*, Westfälische-Wilhelms-Universität Münster, Münster, 1991.
16 R.H. Beasley, C.E. Hoffmann, M.L. Rueppel and J.W. Worley, *Anal. Chem.*, 52 (1980) 1110–1114.
17 J.-O. Levin, K. Andersson, R. Lindahl and C.-A. Nilsson, *Anal. Chem.*, 57 (1985) 1032–1035.
18 J.E. Sickles, P.M. Grohse, L.L. Hodson, C.A. Salmons, K.W. Cox, A.R. Turner and E.D. Estes, *Anal. Chem.*, 62 (1990) 338–346.
19 R.S. Braman, M.A. de la Cantera and Q.X. Han, *Anal. Chem.*, 58 (1986) 1537–1541.
20 S. Kaulbach, *Z. Ges. Hygiene*, 35 (1989) 55–57.
21 K. Cammann, A. Grömping and U. Karst, *Deutschland Pat. DPA*, 41 06 875 (1991).
22 D.C. Harris, *Quantitative Chemical Analysis*, Wiley, New York, 1984.
23 A.H.J. Grömping and K. Cammann, *Chromatographia*, 35 (3/4) (1993) 142–148.
24 N. Binding, S. Thiewens and U. Witting, *Staub-Reinhalt. Luft*, 46 (1986) 444–446.

25 J.-O. Levin, R. Lindahl and K. Andersson, *Environ. Tech. Lett.*, 9 (1988) 1423–1430.
26 A. Streitwieser, Jr. and C.H. Heathcock, *Organische Chemie*, Verlag Chemie, Weinheim, 1980.
27 B.E. Saltzman, *Anal. Chem.*, 26 (1954) 1949–1954.
28 E. Wiederholt, H. Hartkamp and K. Gutsche, *CLB, Chem. Labor Betr.*, 36 (1985) 338–342.

*Journal of Chromatography A*, 653 (1993) 348–353
Elsevier Science Publishers B.V., Amsterdam

CHROM. 25 407

# Short Communication

# High-performance liquid chromatographic determination of thiocyanate anion by derivatization with pentafluorobenzyl bromide

Xiaoyu Liu and Zihou Yun*

*Department of Chemistry, Beijing Normal University, 100875 Beijing (China)*

(First received April 15th, 1993; revised manuscript received June 24th, 1993)

ABSTRACT

This paper describes, for the first time, a high-performance liquid chromatographic method for the determination of thiocyanate anion as its pentafluorobenzyl derivative. The method is based on pre-column derivatization of thiocyanate anion with α-bromo-2,3,4,5,6-pentafluorobenzyl (PFB · Br). The derivative and chromatographic conditions were investigated. It is found that of different derivative solvents, such as acetone, acetonitrile and dichloromethane, acetone is the best. The chromatographic conditions were optimized by using a Zorbax ODS column and methanol–water (80:20, v/v) as mobile phase at a flow-rate of 1.0 ml/min and the eluent was monitored by a UV detector operating at 254 nm. The detection limit is 2.7 ng, and the method is both sensitive and selective. It has been successfully applied to the analysis of waste water of an electroplate and the saliva of regular smokers. Recoveries thus obtained were 93.7–102% and 92.1–101%, respectively.

## INTRODUCTION

Thiocyanate has been extensively used for various purposes, such as dyeing, medicine, photography, catalysis, prevention of erosion, etc. [1]. Several authors have demonstrated *in vivo* conversion of thiocyanate to cyanide by an erythrocytic enzyme, and suggested the physiological effects of its conversion [2]. In addition, since thiocyanate has a long plasma half-life, its concentration is a good index of long-term exposure to cigarette smoke [3]. Finally, the thyreostatic effect of the thiocyanate anion, produced by inhibiting iodine transport in the thyroid, is well known [4].

A number of publications have been devoted to the determination of thiocyanate by chromatographic methods, such as derivative gas chromatography, ion chromatography and ion-exchange chromatography [5]. In derivative gas chromatography, α-bromo-2,3,4,5,6-pentafluorobenzyl (PFB · Br), which is highly sensitive to electron-capture detection (ECD), is widely employed as the derivative reagent with which thiocyanate reacts to give a high yield and stable product, which is then quantitatively analysed by GC [5]. This method has high sensitivity and selectivity, and thus is of recent interest. However, its disadvantages are obvious: (1) in pre-column derivatization the thiocyanate anion

* Corresponding author.

0021-9673/93/$06.00 

reacts with PFB · Br in dichloromethane, which is an unsuitable solvent for ECD because of the existence of the halide element and (2) because derivatization occurs in $CH_2Cl_2$ solvent, phase-transfer catalysts (PTCs) are required to transfer the thiocyanate anion from the aqueous solution to the organic phase, thus making the procedure both complicated and time-consuming.

In this report, we first present a novel procedure for derivative determination of thiocyanate by HPLC. Thiocyanate reacts with PFB · Br and acetone used as the solvent. After derivatization, the product in high yield and with high stability is applied to HPLC, and detected by UV detection. The principal advantage of the approach lies in the fact that the derivative reaction takes place in a homogeneous phase, therefore no PTC is required. In addition, the selectivity of the procedure is better than that of previous methods. The method is comparatively easy to operate and suitable for microanalysis. At the end of this paper, the present method is utilized to analyse the waste water of an electroplate and saliva samples from regular smokers.

## EXPERIMENTAL

### *Reagents*

Methanol, dichloromethane, acetone, acetonitrile and potassium thiocyanate were obtained from the Chemical Reagent Company of Beijing, α-bromo-2,3,4,5,6-pentafluorobenzyl was purchased from Aldrich. All reagents used were analytical grade. Distilled and deionized water was used in the preparation of all solutions.

### *Apparatus*

A Varian 5060 liquid chromatograph equipped with a UV-100 detector, a 3090A integrator, a Zorbax ODS analytical column (5 μm, 250 mm × 4.6 mm) and a Spectra-Focus fast-scanning UV detector was used.

### *Standard solution*

A solution of PFB · Br in dichloromethane (4 μl/ml) and a solution of PFB · Br in acetone (7 μl/ml) were stored in a refrigerator. Potassium thiocyanate standard solutions (0.1 mol/l) and hexadecyl trimethyl ammonium bromide (HDTMAB) solution (0.1 mol/l) were prepared by dissolving solid potassium thiocyanate and HDTMAB in water.

### *$CH_2Cl_2$ as derivative solvent*

A 0.1-ml aliquot of 0.001 mol/l aqueous potassium hydroxide solution, 0.1 ml of standard solution of thiocyanate anion, 0.1 ml of HDTMAB solution and 0.5 ml of a solution of PFB · Br in dichloromethane were added in succession to a 5-ml glass-stoppered test tube. The reaction mixture was shaken mechanically at 30°C for 20 min. After reaction, 3 ml of water were added. The mixture was stirred, and then centrifuged at 3500 rpm for 10 min.

### *Acetone as derivative solvent*

A 0.1-ml aliquot of 0.001 mol/l aqueous potassium hydroxide solution, 0.1 ml of standard solution of thiocyanate anion and 0.5 ml of a solution of PFB · Br in acetone were added in succession to a 5-ml glass-stoppered test tube. The reaction mixture was shaken mechanically at 30°C for 20 min.

### *Chromatographic conditions*

Chromatographic separation was carried out on an ODS column at 30°C. The mobile phase was MeOH–water (80:20), the flow-rate was 1.0 ml/min, and the UV detector was set at 254 nm (see Fig. 1A).

### *Sample analysis*

A 0.1-ml volume of waste water of an electroplate from Beijing Electroplate Plant and 0.1 ml of saliva from a smoker who had been smoking for 20 years were derivatized and determined according to the method for standard solution (see Fig. 1B and C); acetone was used as derivative solvent.

### *Recoveries*

Recoveries were determined by analysis of samples spiked with 290, 407 or 581 ng of potassium thiocyanate.

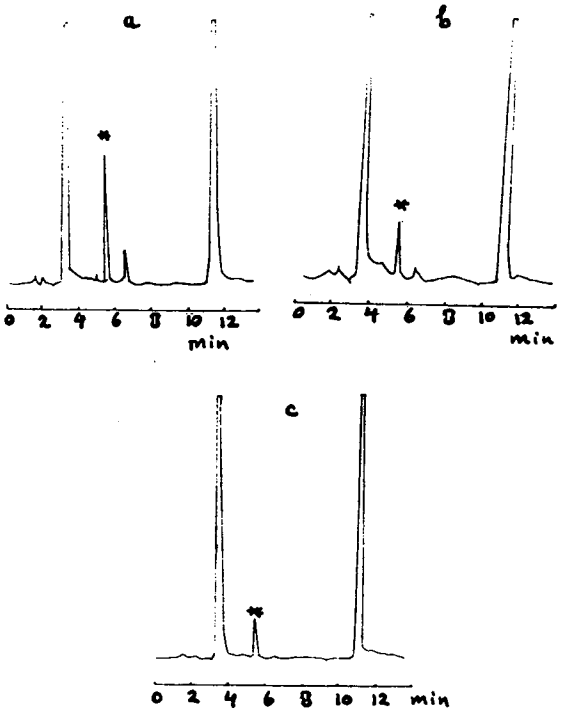


Fig. 1. Chromatogram of the standard solution and the samples. (a) Standard solution, (b) waste water of an electroplate, (c) saliva from a regular smoker. * = Derivative product.

## RESULTS AND DISCUSSION

### *Optimization of derivative conditions*

When the concentration of thiocyanate anion was about $1.0 \cdot 10^{-2}$ to $1.0 \cdot 10^{-2}$ mol/l, the volume of neat PFB · Br required to ensure a constant formation of thiocyanate derivative was 2 $\mu$l (see Fig. 2).

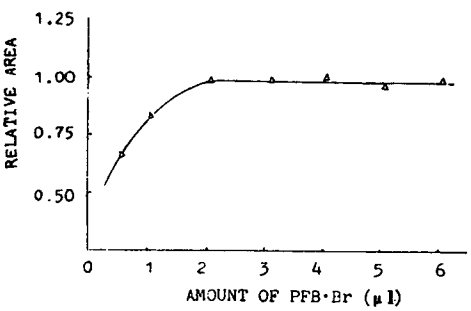


Fig. 2. Optimization of the amount of PFB · Br used in the derivatization.

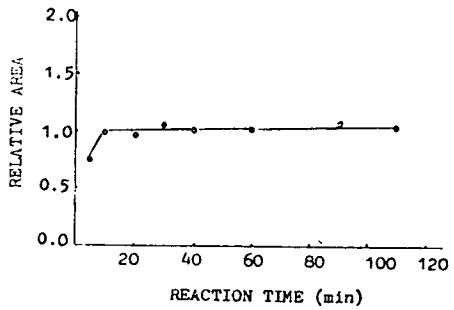


Fig. 3. Optimization of the reaction time of the derivatization.

Thiocyanate reacts rapidly with PFB · Br, requiring only 15 min to reach constant yield (see Fig. 3). A reaction time of 20 min was enough for practical use. The derivative product, which was stored at room temperature for a day or in a refrigerator for a week, was still stable (see Fig. 4).

When the temperature of the derivative reaction was set at 20°C, 30°C or 40°C, the derivative yields were almost unchanged. Thus 30°C was selected as the reaction temperature.

When the concentration of potassium hydroxide was $1.0 \cdot 10^{-5}$ to 1.0 mol/l and the concentration of sulphuric acid $0.5 \cdot 10^{-5}$ to 0.5 mol/l, the derivative yield of the reaction system studied was almost invariable (see Fig. 5). In our study 0.1 ml of $1.0 \cdot 10^{-3}$ mol/l potassium hydroxide was added to the system. The pH value is 8.3.

When $CH_2Cl_2$ is used as the derivative solvent, PTCs, such as HDTMAB, etc., are required to transfer thiocyanate anion from water to the organic phase. This leads to a complicated

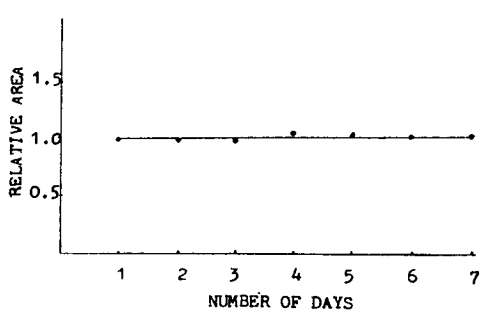


Fig. 4. Test of the stability of the derivative product stored in a refrigerator for a week.

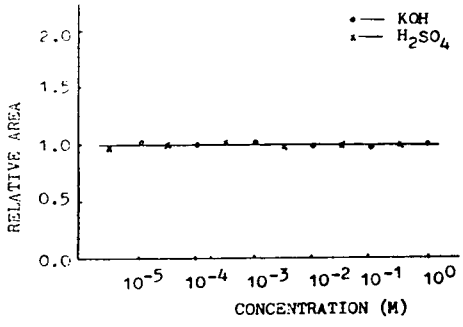


Fig. 5. Influence of the basicity and acidity on the derivative reaction.

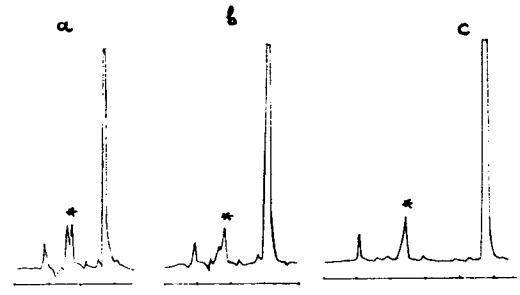


Fig. 6. Chromatogram of standard solution with different ratios of mobile phase (methanol–water) and dichloromethane as derivative solvent: (a) 87:13, (b) 85:15, (c) 80:20. * = Derivative product.

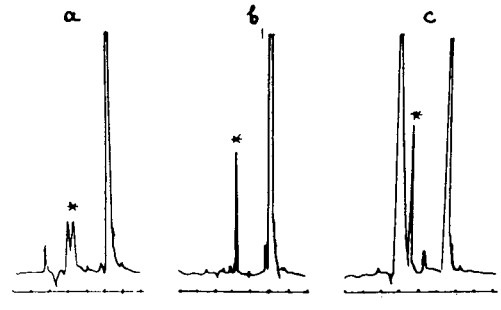


Fig. 7. Chromatogram of standard solution with different derivative solvents. (a) Dichloromethane, (b) acetonitrile, (c) acetone. * = Derivative product.

and time-consuming operation. In order to avoid using PTCs, we adopted two other solvents, *i.e.* acetone and acetonitrile, both of which are soluble in water. The different derivative yields of the reaction in the above three solvents are listed in Table I. it is seen from the table that the derivative yield in acetone is almost the same as in dichloromethane. This is why we selected acetone as the reaction solvent.

The other reason why we chose acetone lies in its selectivity. As is well known, thiocyanate anion is a dual nucleophilic reagent. When it reacts with PFB · Br, two products, namely PFB · SCN and PFB · NCS, are possible (see Fig. 6). However, it is found that the ratio of the two compounds in the derivative reaction varies as the solvent changes (see Fig. 7). Table II illustrates the results of this phenomenon. It shows that when acetone is employed only one chromatographic peak emerges, while in dichloromethane and acetonitrile solutions two chromatographic peaks are formed with different yield ratios of the two possible products. The reaction selectivity thus increases in the order: $CH_2Cl_2 > CH_3CN > CH_3COCH_2$. This interesting phenomenon relates to the organic solvent effect, and can be accounted for in terms of the well-established hard and soft acid and base (HSAB) theory [6].

TABLE I

COMPARISON OF THE DERIVATIVE YIELD IN THREE DIFFERENT SOLVENTS

| Solvent | Reaction temperature (°C) | Relative yield[a] |
|---|---|---|
| $CH_3COCH_3$ | 30 | 101.0% |
| $CH_3CN$ | 30 | 90.3% |
| $CH_3CN$ | 70 | 97.3% |
| $CH_2Cl_2$ | 30 | 100.0% |

[a] For the convenience of comparison, we suppose the yield of the derivatization in $CH_2Cl_2$ to be 100%.

TABLE II

SELECTIVITY OF THE PRODUCT IN DIFFERENT SOLVENTS

| Solvent | Number of peaks | Product ratio[a] |
|---|---|---|
| $CH_3COCH_3$ | 1 | 0 |
| $CH_3CN$ | 2 | 0.04 |
| $CH_2Cl_2$ | 2 | 0.60 |

[a] The product ratio is defined as the ratio of the areas of the two peaks. The mobile phase is MeOH–water (87:13).

*Chromatographic conditions*

The maximum absorption wavelength of the derivative product was determined at 210 nm by the Spectra-Focus fast-scanning UV detector. Because there are interference peaks near this point, the detector wavelength chosen was 254 nm.

Because iodide, nitrite, sulphide and cyanide can react with PFB · Br, and acetone has a peak when detected at 254 nm, the optimal ratio of MeOH–$H_2O$ is 80:20 (v/v) to avoid interference. When these anions do not coexist with thiocyanate, a ratio of MeOH–$H_2O$ of 87:13 (v/v) can be chosen and the rate of analysis is quicker.

*Interference*

In our experiments, it is demonstrated that chloride, fluoride, sulphate, sulphite, thiosulphate, phosphate, acetate, carbonate, nitrate, chromate and oxalate anions do not react with PFB · Br. Thus, these anions do not interfere in the determination of thiocyanate. Iodide, nitrite, cyanide and sulphide anions do react with PFB · Br. However, their products can be separated by using a different mobile phase composition to avoid interference.

*Linearity and detection limit*

A linear relationship between the peak area and the amount of the thiocyanate anion was obtained for potassium thiocyanate standard solution concentrations of $1.0 \cdot 10^{-3}$, $5.0 \cdot 10^{-3}$, $7.0 \cdot 10^{-3}$, $1.0 \cdot 10^{-2}$, $1.5 \cdot 10^{-2}$ and $2.0 \cdot 10^{-2}$ mol/l. The regression equation is:

$$y = -0.01938 + 0.4868x$$

The correlation coefficient is 0.9962.

When the signal-to-noise ratio is 2.0 and acetone is used as solvent, the detection limit is 2.7 ng.

*Precision and accuracy*

To assess the accuracy and precision of the method, the intra-day ($n = 10$) and inter-day ($n = 5$) reproducibility of the assay were determined at a concentration of $1.0 \cdot 10^{-2}$ mol/l potassium thiocyanate. The results are reported in Table III.

Repeatability of injection of the same system ($n = 10$) was acceptable. The relative standard deviation (R.S.D.) was 3.83%.

TABLE III

ACCURACY AND PRECISION OF THE METHOD

| | Intra-day ($n = 10$) | Inter-day ($n = 5$) |
|---|---|---|
| Mean peak area | 27 609 | 27 965 |
| S.D. | 800.4 | 878.0 |
| R.S.D. | 2.90% | 3.14% |

*Samples analysis*

Waste water of an electroplate and saliva from a smoker who had been smoking for 20 years were analysed by the method presented above. The concentration of thiocyanate was $1.402 \cdot 10^{-4}$ g/ml and $1.014 \cdot 10^{-4}$ g/ml, respectively.

Analytical recoveries were determined for the samples of waste water of an electroplate and of the saliva by spiking with standards of potassium thiocyanate at concentrations ranging from $5.0 \cdot 10^{-3}$ to $1.0 \cdot 10^{-2}$ mol/l. The recoveries of the added potassium thiocyanate are shown in Table IV.

## CONCLUSIONS

Determination of thiocyanate anion at trace concentrations by derivatization HPLC using acetone as derivative solvent has been studied in this paper. It is found that, compared with

TABLE IV

RECOVERY OF SAMPLES

| Sample | Labelled amount (ng) | $n$ | Recovery | | |
|---|---|---|---|---|---|
| | | | Mean | S.D. | R.S.D. |
| Waste water | | | | | |
| | 290 | 4 | 96.3 | 2.42 | 2.51 |
| | 407 | 4 | 97.7 | 1.07 | 1.09 |
| | 581 | 4 | 99.2 | 2.14 | 2.16 |
| Saliva | | | | | |
| | 290 | 4 | 94.5 | 1.72 | 1.80 |
| | 407 | 4 | 98.6 | 2.34 | 2.37 |
| | 581 | 4 | 97.3 | 1.96 | 2.01 |

dichloromethane using acetone as derivative solvent, the method is simpler and more selective. From the results mentioned above, the present method is applicable to the determination of thiocyanate in real samples. It may be useful for the determination of thiocyanate anion in biological and environmental specimens.

REFERENCES

1 Y.G. Hou, S.C. Lin and X.Z. Chi, *J. Beijing Normal Univ. (Natur)*, 24 (1988) 51.
2 T. Toida, T. Togawa, S. Tanabe and T. Imanari, *J. Chromatogr.*, 308 (1984) 133.
3 Z.H. Yao, X.M. Xu, Z.S. Wu, M. Zhang, Z. Wang, X.G. Hong and S.E. Yu, *Zhonghua Yixue Zazhi*, 67 (1987) 190.
4 S.-H. Chen, H.-L. Wu, M. Tanaka, T. Shono and K. Funazo, *J. Chromatogr.*, 504 (1990) 257.
5 S.-H. Chen, H.-L. Wu, M. Tanaka, T. Shono and K. Tunazo, *J. Chromatogr.*, 396 (1987) 129.
6 B.F. Tang, Z. Xie and Z.J. Chen, *Solvent Effects in Organic Chemistry*, Chemical Engineering, Beijing, 1987, p. 204.

*Journal of Chromatography A*, 653 (1993) 354–358
Elsevier Science Publishers B.V., Amsterdam

CHROM. 25 417

# Short Communication

# Studies on the retention and thermodynamic properties of aromatic compounds on two types of crown ether polysiloxane stationary phase

Li Li[☆], Cai-Ying Wu*, Ling-Shouang Cai and Zhao-Rui Zeng

*Department of Chemistry, Wuhan University, Wuhan 430072, Hubei Province (China)*

(First received March 29th, 1993; revised manuscript received July 5th, 1993)

ABSTRACT

We separated 37 aromatic compounds, including twelve groups of positional isomers, on two new types of crown ether polysiloxane, di(*tert.*-butylbenzo)-propyl-15-crown-5 polysiloxane (PSO-DTB-3-15C5) and dibenzopropyl-15-crown-5 polysiloxane (PSO-DB-3-15C5). It is shown that when these new crown ethers polysiloxanes are used as stationary phases in capillary column gas chromatography they possess excellent chromatographic properties and are unique in the separation of some polar aromatic positional isomers, especially phenols and nitro compounds. The mechanism and retention are discussed by measuring various thermodynamic parameters: the enthalpy of solution, $\Delta H$, the entropy of solution, $\Delta S$, the free energy of solution, $\Delta G$, and differences in $\Delta H$ [$\Delta(\Delta H)$] and $\Delta S$ [$\Delta(\Delta S)$]. The results were compared with those obtained on OV-1701 and PEG 20M GC columns.

## INTRODUCTION

It is well known that crown ethers are useful chromatographic stationary phases because of their high chemical stability and good selectivity [1–4] resulting from the cavity structure and the strong electronegative effect of heteroatoms on the crown ether ring. The polymeric crown ether stationary phases (PCSPs) are superior to small molecule crown ethers, because the latter have poor thermal stability and are associated with poor column efficiency, coating difficulty and column bleeding at high temperature, while the former may alleviate some of these problems. In recent years, many polymeric crown ethers have been used in GC, and their chromatographic properties have been studied [5–10].

We coated fused-silica capillaries with two new types of crown ether and demonstrated excellent chromatographic properties, such as a wide range of operating temperature, high column efficiency, good thermal stability and unique selectivity in the separation of some polar aromatic positional isomers, especially phenols and nitro compounds. In order to study the retention and separation mechanism of these PCSPs, thermodynamic parameters of solution, the enthalpy of solution ($\Delta H$), the entropy of solution ($\Delta S$), the free energy of solution ($\Delta G$) and the differences in $\Delta H$ [$\Delta(\Delta H)$] and $\Delta S$ [$\Delta(\Delta S)$] were

* Corresponding author.
☆ Present address: Hengyang Medical College, Hengyang 421001, Hunan Province, China.

0021-9673/93/$06.00 

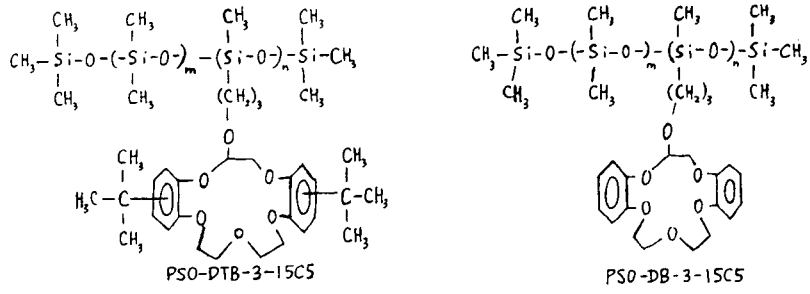


Fig. 1. Structures of the crown ether polysiloxanes used in this study.

measured. The last two parameters are independent of column temperature: $\Delta(\Delta H)$ and $\Delta(\Delta S)$ reflect the forces of interaction and the goodness of fit of solute molecules within the cavity of the crown ether. Thirty-seven aromatic compounds can be separated on these two new PCSPs between 90 and 240°C.

*Theoretical*

Two well-known equations can be applied. First:

$$\ln k' = \frac{-\Delta H}{R} \cdot \frac{1}{T} + \frac{\Delta S}{R} - \ln \beta \quad (1)$$

The slope $\Delta H/R$ and the intercept $(\Delta S/R - \ln \beta)$ of the graph of $\ln k'$ against $1/T$ were calculated by the least-squares method from at least five measurements within the temperature range 90–240°C. Solution enthalpy, $\Delta H$, is the measure of the forces of interaction between solute molecules and stationary phase; solution entropy, $\Delta S$, reveals the degree of mixing of the solute molecules and stationary phase. Second:

$$\ln \alpha = \frac{-(\Delta H_1 - \Delta H_2)}{RT} + \frac{\Delta S_1 - \Delta S_2}{R} = \frac{-\Delta(\Delta H)}{RT} + \frac{\Delta(\Delta S)}{R} \quad (2)$$

Here the difference in the enthalpy of solution, $\Delta(\Delta H)$, and the difference in the entropy of solution, $\Delta(\Delta S)$, were calculated by the least-squares method, as in eqn. 1.

## EXPERIMENTAL

*Instrumentation*

An SC-7 gas chromatograph (Sichuan Analytical Apparatus Plants, Sichuan, China) equipped with a capillary split injection system and a flame ionization detector was used.

*Gas chromatographic procedure*

PSO-DTB-3-15C5 and PSO-DB-3-15C5 were prepared by hydrosilylation as previously described [2]. Their structures are shown in Fig. 1 and their chromatographic properties are listed in Table I.

The carrier gas was nitrogen at a linear velocity of 12–15 cm/s. The injector temperature was maintained at 250–280°C and the detector temperature was held at 280°C. A split ratio of 100:1 was used throughout. The retention time ($t_R$) of all aromatic compounds and the separation factor ($\alpha$) of all isomeric pairs were measured at 10°C intervals in the temperature range

TABLE I

CHROMATOGRAPHIC PROPERTIES OF THE CROWN ETHER POLYSILOXANES USED IN THIS STUDY

| Stationary phase | Column No. | Column dimensions: length (m) × I.D. (mm) | Column efficiency (plates/m) | Capacity factor ($k'$) | Peak asymmetry |
|---|---|---|---|---|---|
| PSO-DTB-3-15C5 | 1 | 9 × 0.25 | 4500 | 3.63 | 1.05 |
| | 2 | 14.5 × 0.25 | 4590 | 5.01 | 1.03 |
| PSO-DB-3-15C5 | 1 | 14 × 0.25 | 4443 | 3.8 | 1.05 |
| | 2 | 14.5 × 0.25 | 5206 | 4.98 | 1.01 |

TABLE II

THE VALUES OF $\Delta H$, $\Delta S$ AND $\Delta G$ ON PCSPs, OV-1701 AND PEG 20M

Units: $\Delta H$ = kJ/mol; $\Delta S$ = J/mol/K; $\Delta G$ = kJ/mol.

| | Elution order | PSO-DTB-3-15C5 | | | PSO-DB-3-15C5 | | | OV-1701 | | | PEG-20M | | |
|---|---|---|---|---|---|---|---|---|---|---|---|---|---|
| | | $-\Delta H$ | $-\Delta S$ | $-\Delta G$ | $-\Delta H$ | $-\Delta S$ | $-\Delta G$ | $-\Delta H$ | $-\Delta S$ | $-\Delta G$ | $-\Delta H$ | $-\Delta S$ | $-\Delta G$ |
| Dichlorobenzene | *p* | 42.15 | 103.76 | 3.448 | 39.69 (*m*) | 100.58 (*m*) | 2.174 (*m*) | 36.71 (*m*) | 49.53 (*m*) | 18.24 (*m*) | 41.33 (*m*) | 57.31 (*m*) | 19.96 (*m*) |
| | *o* | 41.92 | 102.68 | 3.620 | 41.00 (*p*) | 103.17 (*p*) | 2.518 (*p*) | 37.54 (*p*) | 51.18 (*p*) | 18.45 (*p*) | 42.17 (*p*) | 58.00 (*p*) | 20.46 (*p*) |
| | *m* | 43.12 | 103.93 | 3.354 | 41.86 (*o*) | 103.24 (*o*) | 3.351 (*o*) | 38.25 (*o*) | 51.40 (*o*) | 19.08 (*o*) | 42.64 (*o*) | 57.62 (*o*) | 21.15 (*o*) |
| Cresol | *o* | 55.26 | 128.12 | 7.471 | 53.71 | 123.21 | 7.753 | | | | 57.35 (*m*) | 75.58 (*m*) | 29.16 (*m*) |
| | *m* | 57.59 | 131.69 | 8.470 | 55.49 (*p*) | 125.18 (*p*) | 8.798 (*p*) | 45.70 | 64.91 | 21.49 | 59.29 (*p*) | 77.49 (*p*) | 30.39 (*p*) |
| | *p* | 57.91 | 132.11 | 8.633 | 55.37 (*m*) | 124.51 (*m*) | 8.928 (*m*) | 47.26 | 67.08 | 22.24 | 59.17 (*o*) | 76.91 (*o*) | 30.48 (*o*) |
| Nitrochlorobenzene | *m* | 51.41 | 112.49 | 9.451 | 47.50 | 102.51 | 9.264 | 45.87 | 59.48 | 23.68 | 50.71 | 62.86 | 27.26 |
| | *p* | 51.62 | 112.07 | 9.818 | 48.23 | 103.18 | 9.744 | 45.94 | 59.15 | 23.88 | 51.63 | 63.77 | 27.84 |
| | *o* | 52.24 | 112.90 | 10.13 | 49.35 | 104.59 | 10.34 | 46.97 | 60.37 | 24.45 | 53.22 | 65.40 | 23.79 |
| Dinitrobenzene | *o* | 59.12 | 116.89 | 15.52 | 66.19 | 130.20 | 17.63 | 53.49 | 66.27 | 28.77 | 52.43 | 52.80 | 32.74 |
| | *m* | 60.92 | 120.14 | 16.11 | 67.53 | 132.36 | 18.16 | 54.31 | 67.04 | 29.30 | 52.94 | 53.45 | 33.00 |
| | *p* | 59.63 | 116.06 | 16.34 | 68.51 | 132.53 | 19.08 | 55.82 | 68.16 | 30.39 | 57.58 | 59.20 | 35.50 |
| Methylnaphthalene | $\beta$ | 50.12 | 109.25 | 9.370 | 48.03 | 104.67 | 8.988 | 45.99 | 59.04 | 23.97 | 48.05 | 58.24 | 26.32 |
| | $\alpha$ | 51.44 | 111.16 | 9.977 | 48.58 | 104.59 | 9.568 | 46.47 | 59.43 | 24.30 | 49.63 | 58.50 | 26.81 |
| Quindine | *n* | 49.16 | 107.00 | 9.249 | 49.08 | 105.92 | 9.572 | 45.24 | 58.10 | 23.57 | 48.90 | 57.82 | 27.33 |
| | Iso | 49.13 | 105.59 | 9.745 | 50.38 | 107.75 | 10.19 | 45.92 | 58.53 | 24.09 | 49.84 | 58.87 | 27.88 |
| Anthracene | an- | 62.50 | 116.15 | 19.18 | 67.79 (ph) | 126.71 (ph) | 20.53 (ph) | 55.71 (ph) | 63.07 (ph) | 32.19 (ph) | | | |
| phenanthrene | ph- | 62.89 | 116.56 | 19.41 | 67.96 | 126.79 | 20.67 | 56.13 | 63.69 | 32.37 | | | |
| Nitrotoluene | *m* | 50.38 | 109.58 | 9.507 | 50.49 | 109.83 | 9.523 | 38.38 (*o*) | 45.62 (*o*) | 21.36 (*o*) | 45.90 (*o*) | 55.79 (*o*) | 25.09 (*o*) |
| | *p* | 50.65 | 109.41 | 9.840 | 50.96 | 109.83 | 9.993 | 39.79 (*m*) | 47.06 (*m*) | 22.24 (*m*) | 45.53 (*m*) | 53.34 (*m*) | 25.64 (*m*) |
| | *o* | 51.39 | 110.49 | 10.18 | 52.37 | 111.99 | 10.60 | 41.28 (*p*) | 49.45 (*p*) | 22.83 (*p*) | 46.71 (*p*) | 54.86 (*p*) | 26.25 (*p*) |
| Dinitrotoluene | 3,4- | 43.50 | 97.77 | 7.032 | 41.52 | 94.03 | 6.447 | 53.22 (2, 6) | 65.42 (2, 6) | 28.82 (2, 6) | | | |
| | 2,3- | 46.11 | 100.93 | 8.463 | 45.80 | 100.52 | 8.306 | 54.13 (2, 5) | 65.85 (2, 5) | 29.56 (2, 5) | | | |
| | 2,6- | 58.37 | 116.31 | 14.99 | 58.76 | 116.35 | 15.36 | 55.18 (2, 4) | 66.42 (2, 4) | 30.40 (2, 4) | | | |
| | 2,5- | 61.31 | 120.55 | 16.34 | 61.83 | 120.54 | 16.87 | 56.44 (3, 5) | 68.36 (3, 5) | 30.94 (3, 5) | | | |
| | 2,4- | 61.38 | 118.47 | 17.19 | 62.59 | 119.97 | 17.84 | 57.98 (3, 4) | 68.88 (3, 4) | 32.29 (3, 4) | | | |
| | 3,5- | 62.44 | 120.30 | 17.57 | 63.12 | 120.54 | 18.16 | | | | | | |
| Phenyl dihydroxide | *o* | 61.27 | 126.87 | 13.95 | 59.98 | 123.13 | 14.05 | | | | | | |
| | *p* | 65.93 | 133.77 | 16.03 | 67.53 | 133.27 | 17.82 | | | | | | |
| | *m* | 69.03 | 139.01 | 17.18 | 69.30 | 135.85 | 18.63 | | | | | | |
| Tetrahydronaphthalene | | 46.77 | 109.08 | 6.083 | 42.55 | 101.16 | 4.817 | | | | | | |
| Indene | | 40.33 | 97.94 | 3.798 | 40.62 | 99.73 | 3.421 | | | | | | |
| Triphenylisomer | *o* | 57.09 | 105.75 | 17.65 | 74.66 | 143.17 | 21.26 | | | | | | |
| | *m* | 64.67 | 111.99 | 22.90 | 77.04 | 137.01 | 25.94 | | | | | | |
| | *p* | 64.13 | 109.25 | 23.38 | 77.79 | 136.68 | 26.81 | | | | | | |
| Decahydronaphthalene | *trans* | 40.69 | 102.26 | 2.547 | 36.47 | 97.77 | −0.0018 | | | | | | |
| | *cis* | 41.97 | 103.09 | 3.517 | 36.79 | 95.94 | 1.004 | | | | | | |

90–240°C and at least five data points were obtained for each compound. Correlation coefficients of ln $k'$ *versus* $1/T$ plots were higher than 0.99. Solution free energy ($\Delta G$) values at 373K were calculated.

## RESULTS AND DISCUSSION

Table II shows that the size of the $\Delta G$ values agrees with the retention order of isomers. Aromatic compounds are well separated on the two new PCSP columns, while their $\Delta G$ values are smaller than those on OV-1701 and polyethylene glycol (PEG) 20M; hence, the two new PCSP columns produce smaller retention times for the same compounds than PEG-20M. The range of $\Delta G$ values on PSO-DB-3-15C5 is larger than on PSO-DTB-3-15C5, resulting in better separation of the isomers on PSO-DB-3-15C5.

Table II also shows that 3,4-DNT and 2,3-DNP are well separated on the two new PCSP columns, but they cannot be separated on OV-

TABLE III

THE VALUES OF $\Delta(\Delta H)$ AND $\Delta(\Delta S)$ ON PCSPs, OV-1701 AND PEG-20M

Units: $\Delta(\Delta H)$ = kJ/mol; $\Delta(\Delta S)$ = J/mol/K.

| | | PSO-DTB-3-15C5 | | PSO-DB-3-15C5 | | OV-1701 | | PEG-20M | |
|---|---|---|---|---|---|---|---|---|---|
| | | $\Delta(\Delta H)$ | $\Delta(\Delta S)$ | $\Delta(\Delta H)$ | $\Delta(\Delta S)$ | $\Delta(\Delta H)$ | $\Delta(\Delta S)$ | $\Delta(\Delta H)$ | $\Delta(\Delta S)$ |
| Dichlorobenzene | *o/p* | 0.2314[a] | 1.116[a] | −1.309 (*p/m*) | −2.572 (*p/m*) | | | | |
| | *m/p* | −0.9727 | −0.167 | −2.158 (*o/m*) | −2.634 (*o/m*) | | | | |
| Cresol | *m/o* | −2.327 | −3.552 | −1.784 (*p/o*) | −1.985 (*p/o*) | −1.561 | 2.1656 | −1.819 | 1.330 |
| | *p/o* | 2.641 | −3.961 | −1.664 (*m/o*) | −1.299 (*m/o*) | | | 0.120 | −0.576 |
| Nitrochloro-benzene | *p/m* | −0.2148[a] | 0.4110[a] | −0.7481 | −0.6963 | 0.071 | 0.339 | 0.920 | −0.915 |
| | *o/m* | −0.8267 | −0.3654 | −1.845 | −2.074 | 1.100 | −0.887 | 2.513 | 2.629 |
| Dinitrobenzene | *m/o* | −1.778 | −3.168 | −1.346 | −2.192 | 0.820 | −0.770 | 0.509 | −0.651 |
| | *p/o* | −0.5057[a] | 0.8572[a] | −2.323 | −2.295 | 2.327 | −1.887 | 5.144 | −6.398 |
| Methyl-naphthalene | *α/β* | −1.625 | −2.635 | −0.5729[a] | 0.09677[a] | 0.481 | −0.39 | 0.584 | −0.259 |
| Quindine | iso/*n* | 0.1784[a] | 1.299[a] | −1.260 | −1.680 | 0.682 | −0.436 | 0.944 | −1.047 |
| Anthacene phenanthrene | ph/an | −0.3649 | −0.4322 | −0.2142 (an/ph) | −0.193 (an/ph) | | | | |
| Nitrotoluene | *p/m* | −0.3524[a] | 0.1379[a] | −0.8089 | −0.8230 | | | | |
| | *o/m* | −1.093 | −0.9212 | −1.971[a] | −2.591[a] | | | | |
| Dinitrotoluene | 2,3/3,4 | −2.614[a] | −3.203[a] | −4.294 | −6.537 | | | | |
| | 2,6/3,4 | −16.69 | −22.65 | −17.27 | −22.41 | | | | |
| | 2,5/3,4 | −19.63 | −26.93 | −19.52 | −24.87 | | | | |
| | 2,4/3,4 | −19.68 | −24.80 | −21.08 | −26.01 | | | | |
| | 3,5/3,4 | −20.74 | −26.60 | −21.55 | −26.43 | | | | |
| Phenyl dihydroxide | *p/o* | −5.160 | −6.934 | −7.597 | −10.29 | | | | |
| | *m/o* | −8.251 | −12.10 | −9.262 | −12.61 | | | | |
| Decahydro-naphthalene | *cis* | −1.304 | −0.8846 | −0.3097 | 1.904 | | | | |
| | *trans* | | | | | | | | |
| Diphenylbenzene | *m/o* | −7.560 | −6.242 | −0.471[a] | 11.04[a] | | | | |
| | *p/o* | −7.119 | −3.732 | −0.8229[a] | 11.33[a] | | | | |

[a] The correlation coefficient is less than 0.6.

1701 and PEG 20M. *o*-Cresol and *p*-cresol cannot be separated on OV-1701 but are separated on PEG 20M. They can be even better resolved on the two new PCSPs.

The retention of solute on the PCSPs depends mainly on hydrogen bonds formed by the high electron cloud density on the crown ether ring, the fit of the solute molecules within the crown ether cavity and dipole–dipole interaction between isomeric analytes and PCSPs. Both $\Delta H$ and $\Delta S$ contribute to the retention order of positional isomers. The $\Delta S$ values on the two new PCSPs show small differences, and all are larger, more than 40–80 J/mol · K larger, than on OV-1701 and PEG 20M columns and 20–40 J/mol · K larger than on PSOB-3-18C6 [11]. This shows that the steric hindrance due to the crown ether moiety is greater. From Table II we known that the $\Delta H$ values of positional isomers, which do not form hydrogen bonds, are similar, while the $\Delta H$ values of cresol isomers, which can form hydrogen bonds with PCSPs and PEG-20M, give values which are about 10 kJ/mol higher than on OV-1701.

From Table III, the $\Delta(\Delta H)$ values of all isomers are larger than on the OV-1701 column, hence the PCSPs are more effective for the separation of isomers. Most $\Delta(\Delta H)$ values on PSO-DB-3-15C5 are higher than for the same compounds on PSO-DTB-3-15C5.

For fifteen pairs of isomers the correlation coefficients of ln $\alpha$ *versus* $1/T$ plots are higher than 0.9 on the PSO-DTB-3-15C5 column. The same is true of the PSO-DB-3-15C5 column. For six pairs of isomers on the PSO-DTB-3-15C5 column and four pairs of isomers on the PSO-DB-3-15C5 column, the correlation coefficients of ln $\alpha$ *versus* $1/T$ plots are smaller than 0.6. The results show that the plots of ln $\alpha$ *versus* $1/T$ of these compounds are non-linear and that the influence of temperature on these isomers is not the same. These isomers are *o*/*p*-dichlorobenzene, *p*/*m*-nitrochlorobenzene, *p*/*o*-dinitrobenzene, *n*/iso-quindine, *p*/*o*-nitrotoluene and 2,3/3,4-dinitrotoluene on PSO-DTB-3-15C5 and $\alpha$/$\beta$-methylnaphthalene, *o*/*m*-nitrotoluene, *m*/*o*-diphenylbenzene and *p*/*o*-diphenylbenzene on PSO-DB-3-15C5.

The graphs of ln $k'$ against $1/T$ on the PCSPs clearly show that the separation efficiency of aromatic compounds on PSO-DB-3-15C5 is better than on PSO-DTB-15C5. The optimum temperature range is 200–210°C, at which temperatures seventeen aromatic compounds can be separated. If two compounds have a point of intersection, this indicates that these two compounds cannot be separated at this temperature. There are many points of intersection in the temperature range 130–170°C.

## CONCLUSIONS

Two new PCSPs exhibit good chromatographic properties and high selectivity for aromatic compounds. Solution thermodynamic parameters show that hydrogen bonding forces and dipole forces caused by the high electron density of the crown ether ring are the main cause of the separation. Both $\Delta H$ and $\Delta S$ contribute to the retention order of positional isomers.

## REFERENCES

1 Y. Jin, R. Fu and Z. Huang, *J. Chromatogr.*, 469 (1989) 153.
2 R. Fu, A. Zhang *et al.*, *Sepu*, 4 (1992) 199.
3 I.M. Kolthoff, *Anal. Chem.*, 51 (1979) IR.
4 E.V. Zagorevskaya and N.Y. Kovaleva, *J. Chromatogr.*, 365 (1986) 7.
5 C.-Y. Wu, X.-C. Zhou, Z.-R. Zeng, X.-R. Lu and L.-F. Zhang, *Anal. Chem.*, 63 (1991) 1874.
6 C.-Y. Wu, J.-S. Cheng, W.-H. Gao, Z.-Y. Zeng, X.-R. Lu and S.-L. Gong, *J. Chromatogr.*, 594 (1992) 243.
7 D.D. Fine, H.L. Gearhart, II and H.A. Mottola, *Talanta*, 32 (1985) 751.
8 C.A. Rouse, A.C. Finlinson, B.J. Tarbet, J.C. Pixton, N.M. Djordjevic, K.E. Markides and M.L. Lee, *Anal. Chem.*, 60 (1988) 901.
9 C.-Y. Wu, H.-Y. Li, Y.-Y. Chen and X.-R. Lu, *J. Chromatogr.*, 504 (1990) 279.
10 J.S. Bradshaw, M.M. Schirmer, Zoltan Juvance, K.E. Markides and M.L. Lee, *J. Chromatogr.*, 540 (1991) 279.
11 C.-Y. Wu, J.-S. Cheng and Z.-R. Zeng, *Chromatographia*, 35 (1993) 33.

*Journal of Chromatography A*, 653 (1993) 359–362
Elsevier Science Publishers B.V., Amsterdam

CHROM. 25 440

# Short Communication

# Comparison of mass spectrometric techniques for the analysis of trace amounts of 1-methylaminoanthraquinone, used as smoke dye in exploding money suitcases

Anthonie M.A. Verweij* and Peter J.L. Lipman

*Department of General Chemistry, Forensic Science Laboratory of the Ministry of Justice, Volmerlaan 17, 2288 GD Rijswijk (Netherlands)*

(First received May 19th, 1993; revised manuscript received July 9th, 1993)

ABSTRACT

Results are presented for different chromatographic and mass spectrometric methods of analysis of the smoke dye MAAQ. When applying gas chromatography various mass spectrometric (ionization) methods can be employed to reach the low picogram range, but for difficult samples full of other dirt preference has to be given to an MS–MS method in the daughter (negative) ion mode. The results of LC–thermospray-MS and LC–thermospray-MS–MS are somewhat less sensitive.

## INTRODUCTION

The dye 1-methylaminoanthraquinone (MAAQ), C.I. 60505, is used as a smoke dye in explosive devices installed in suitcases used to transport banknotes. During a robbery, activation of the explosive device causes a cloud of dye particles to be deposited on clothes, banknotes and other objects. Laboratory tests can determine the presence of the dye on articles such as banknotes and clothes and thus can link a suspect to the robbery.

For the analysis of MAAQ gas chromatography–mass spectrometry is the method of choice [1]. Electron impact (EI) and positive- or negative-ion chemical ionization (CI) are used as ionization methods. In this paper attention is given to the use of tandem mass spectrometric methods using gas chromatography with the common ionization methods and thermospray (TSP) liquid chromatography, thus giving excellent selectivity and/or good sensitivity compared with the more conventional GC–MS methods for the analysis of small amounts of the smoke dye.

## EXPERIMENTAL

### *Materials/extraction*

Pellets containing 1-methylaminoanthraquinone together with potassium chlorate and cane sugar were a gift from ICI. MAAQ was obtained in pure state by a dichloromethane extraction of the crushed pellets. All other reagents used were of analytical grade.

* Corresponding author.

0021-9673/93/$06.00 

Solutions of MAAQ in methanol (100 ng/μl) were spotted five times in 10-μl quantities at several points on the banknote. After drying the spots, the banknote was extracted three times with methanol. The methanol was evaporated by a gentle stream of nitrogen and the residue dissolved in 100 μl of methanol. Recovery of MAAQ appeared to be of the order of 25%.

*Apparatus*

*GC.* A Varian 3400 gas chromatograph was used, with a J&W DB-5 fused-silica column (30 m × 0.25 mm I.D., film thickness 0.25 μm). The oven was programmed from 100°C to 250°C at 10°C/min. The carrier gas was helium. The flow-rate was *ca.* 1 ml/min and the split ratio was *ca.* 10:1.

*HPLC.* A Waters 600-MS programmable pump equipped with a U6K injector was used to pump 0.4 ml/min (methanol–50 m*M* ammonium acetate in water of pH 4.0; 85:15) through a Waters 4-μm Nova-Pack $C_{18}$ 150 mm × 3.9 mm HPLC cartridge column. Post column, an extra 0.8 ml/min ammonium acetate in water was

TABLE I

RESULTS (STANDARD SOLUTIONS) FOR THE VARIOUS CHROMATOGRAPHIC/MASS SPECTROMETRIC METHODS IN THE ANALYSIS OF MAAQ

Abbreviations: EI = Electron impact ionization; CI = Chemical ionization; MID = Multiple ion detection; SIM = Single-ion monitoring; SRM = Selected reaction monitoring; TSP = Thermospray interface.

| Chromatography | Ionization technique | Scan type | Detection limit (pg) ($S/N \approx 3$) |
|---|---|---|---|
| 1 Gas | EI | Full scan | 100 |
| 2 Gas | CI, positive ion[a] | Full scan | 50 |
| 3 Gas | CI, negative ion[a] | Full scan | 5 |
| 4 Gas | EI | MID 237, 220 | 20 |
| 5 Gas | CI, positive ion[a] | SIM 238 | 10 |
| 6 Gas | CI, negative ion[a] | SIM 237 | 2 |
| 7 Gas | EI<br>MS–MS daughter ion[b] | SRM 237 > 164 | 100 |
| 8 Gas | CI, positive ion[a]<br>MS–MS Daughter ion[c] | SRM 238 > 165 | 10 |
| 9 Gas | CI, negative ion[a]<br>MS–MS daughter ion[d] | SRM 237 > 195 | 10 |
| 10 Liquid | TSP (positive)[e] | Full scan | 100 |
| 11 Liquid | TSP (positive)[e] | SIM 238 | 10 |
| 12 Liquid | TSP (positive)[e]<br>MS–MS daughter ion[f] | SRM 238 > 139 | 100 |

[a] Reaction gas, isobutane; pressure, 8150 mT.

MS–MS parameters:

| | Collision offset voltage | MSMSC | Argon pressure (mT) |
|---|---|---|---|
| [b] | −27.5 | 0 | 3.5 mT |
| [c] | −30.0 | 10 | 3.5 mT |
| [d] | +35.0 | 0 | 3.5 mT |
| [f] | −30.0 | 10 | 3.0 mT |

[e] TSP–MS parameters: vaporizer temperature, 145°C; source temperature, 200°C; repeller, 30 V; multiplier voltage, 1500 V; dynode power, 15 kV; scan time, 1.20 s. GC–MS parameters: Source temperature, 150°C; scan time 0.5 s; multiplier voltage, 1500 V; dynode power 15 kV.

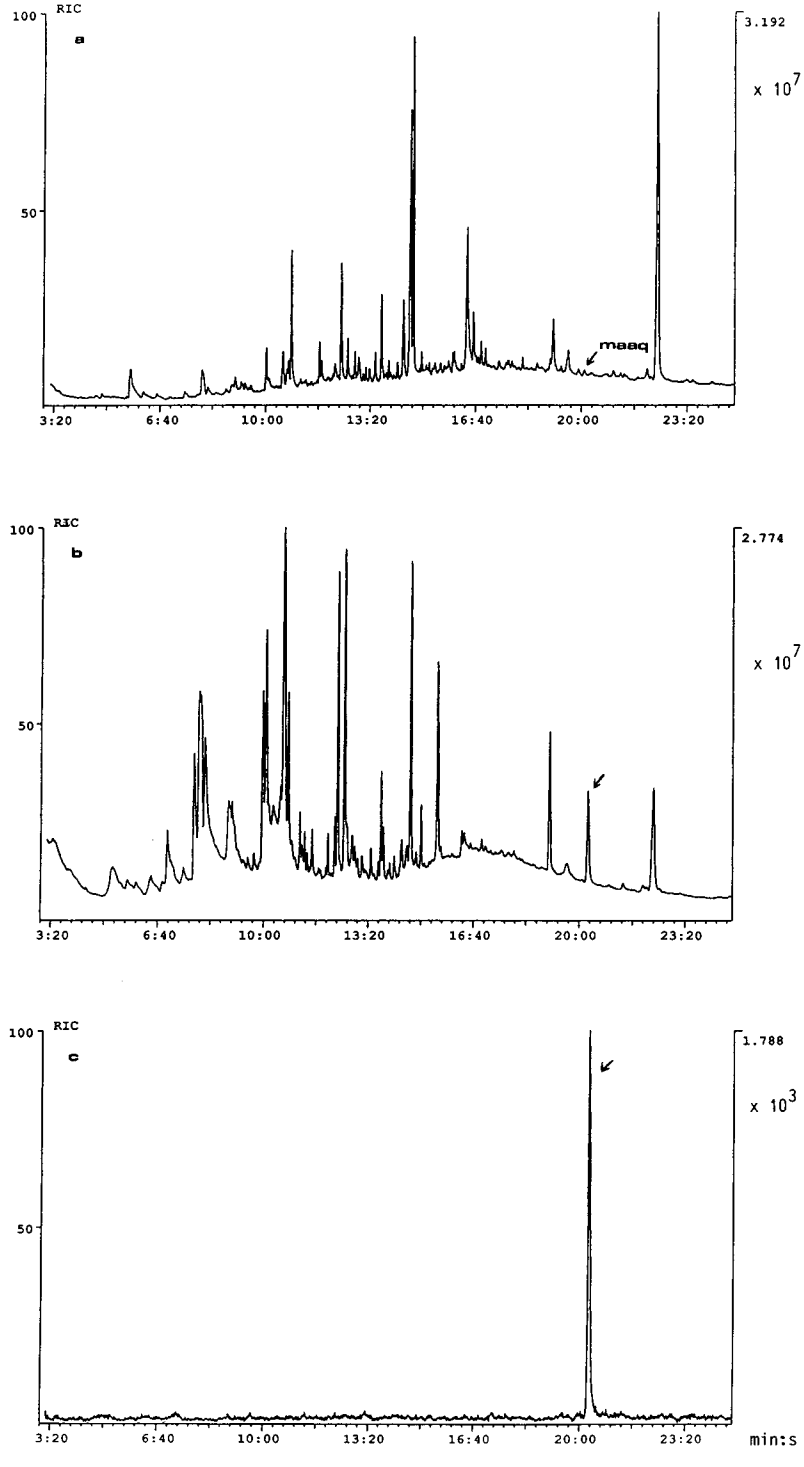


Fig. 1. RIC traces of an extracted banknote supplied with MAAQ. (a) EI full scan, (b) negative-ion CI full scan, (c) MS–MS negative-ion CI (237 > 195).

added by a Waters 590-MS isocratic pump for ionizing enhancement in thermospray applications.

*MS.* A Finnigan MAT TSQ 700 tandem quadrupole mass spectrometer coupled to a DECstation 2100 was used. In gas chromatography the column was directly coupled to the mass spectrometer, while the liquid chromatograph was connected to the mass spectrometer by the Finnigan MAT TSP-2 interface. The operating conditions of the TSP interface, such as the repeller voltage, vaporizer temperature, source temperature and ionic strength of the eluent, were all optimized. These parameters are given in the footnotes to Table I.

*MS–MS* experiments in the daughter-ion mode [2–4] were done using argon (99.999%) as collision gas for the $M^-$ ion generated by negative-ion isobutane CI (in gas chromatography) and the $[M + H]^+$ ions generated by the thermospray interface (in liquid chromatography). In order to obtain optimum selectivity not the full scan but selected reaction monitoring (SRM) technique [2,3] was applied. Collision offset voltage, argon pressure and MSMSC factor (a correction factor for increasing the transmission of ions in the MS–MS mode) were optimized for several ions in the MS–MS spectrum and the most intense ion in the MS–MS spectrum was chosen for MS–MS experiments. For these parameters see the footnotes to Table I.

## RESULTS AND DISCUSSION

In Table I the results of the various chromatographic and mass spectrometric methods that can be used in the analysis of MAAQ are tabulated. Some attention was paid to the LC–TSP method, which gave no results with negative ions. With the TSP interface only $[M + H]^+$ ions of MAAQ were created, even when the pH of the eluent was varied between 3.5 and 10.0. In LC–TSP the detection limits for the full scan and MS–MS daughter methods were in the high picogram range, whereas the SIM method had a detection limit in the low picogram range. In GC sensitivities in the low picogram range can be found for negative-ion CI in full scan mode, both negative- and positive-ion CI in SIM mode and both negative- and positive-ion CI in MS–MS in the daughter-ion mode.

However, the best method of analysing trace amounts of MAAQ in embarrassing samples full of all kind of dirt is without doubt the GC–CI-MS–MS method in the daughter negative-ion mode for reasons of both selectivity and sensitivity.

In the MS–MS method in the daughter-ion mode the chemical noise (caused by all kind of compounds in the extract) is efficiently suppressed and the selectivity for MAAQ raised, by choosing to pass the molecular ion of MAAQ (237) through the first quadrupole, an ion that dissociates by collision with argon in the second quadrupole to the ion 195, the ion which is chosen only to pass the third quadrupole. (This is also called selected reaction monitoring.) See Table I for the appropriate parameters.

Furthermore, negative-ion CI is better suited to compounds with electronegative group(s), thus giving better selectivity.

It can be seen from Fig. 1, in which an MS–MS reconstructed ion chromatogram (RIC) is compared with the RICs for EI and negative-ion CI for an extract of an MAAQ-spiked banknote, that the chemical noise level in the EI and CI chromatograms is quite high compared with the MS–MS chromatogram.

## REFERENCES

1 R.M. Martz, D.J. Reuter and L.D. Lasswell III, *J. Forensic Sci.*, 28 (1983) 200–207.
2 J. Yinon, in A. Meahly and R.L. Williams (Editors), *Forensic Science Progress*, Vol. 5, Springer, Berlin, 1991, pp. 1–29.
3 W.A.M. Niessen and J. van der Greef, *Liquid Chromatography–Mass Spectrometry*, Marcel Dekker, New York, 1992, pp. 51–55.
4 A.M.A. Verweij, P.J.L. Lipman and P.G.M. Zweipfenning, *J. Forensic Sci. Int.*, 54 (1992) 67–74.

*Journal of Chromatography A*, 653 (1993) 363–368
Elsevier Science Publishers B.V., Amsterdam

CHROM. 25 465

# Short Communication

# Determination of polycyclic aromatic hydrocarbons from bitumen concrete roads in drainage water by microextraction, large-volume sampling and gas chromatography–mass spectrometry with selected ion monitoring

R. Kubinec, P. Kuráň, I. Ostrovský and L. Soják*

*Chemical Institute, Faculty of Natural Sciences, Comenius University, Mlynská dolina CH-2, 84215 Bratislava (Slovak Republic)*

(First received April 14th, 1993; revised manuscript received July 27th, 1993)

ABSTRACT

A method for the determination of ppt levels of polycyclic aromatic hydrocarbons in drinking and drainage water based on microextraction, large-volume injection of a toluene extract into a split–splitless injector and gas chromatography–mass spectrometry with selected ion monitoring is described. The elimination of solvent from the target analytes by controlling the temperature of the injector equipped with a liner packed with Chromosorb W coated with OV-1 was achieved.

## INTRODUCTION

A possible contamination threat to ground water appeared when bitumen concrete was used as a road construction material. By mass, this type of concrete contains 1.5–2.0% of road tars; the basic compounds present in these tars, such as polycyclic aromatic hydrocarbons (PAHs) are partially soluble in water [1]. Therefore, all "eluates" from this material such as rain water and drainage water could be contaminated and could threaten ground water. Many PAHs are serious environmental contaminants because of their carcinogenicity, mutagenicity and toxicity. The US EPA lists sixteen PAHs as "priority pollutants" of the environment. Under the standards adopted by the European Community (Netherlands), the reference concentration of PAHs (the *A* limit) in ground water for the most dangerous PAH, benzo[*a*]pyrene, is 10 ng $l^{-1}$, for fluoranthene and pyrene 20 ng $l^{-1}$ and for phenantrene and anthracene 100 ng $l^{-1}$[2].

For the analysis of such very dilute samples, preconcentration and selective preseparation are required in order to achieve the required sensitivity. For preconcentration and clean-up of environmental samples, microextration has been widely utilized. The enrichment factors obtained, *i.e.*, $10^2$–$10^3$, can be increased to $10^5$ by further

* Corresponding author.

0021-9673/93/$06.00 

preconcentration of the extracts with the aid of large-volume sampling. The introduction of large-volume sampling in capillary gas chromatography (GC) is becoming increasingly important in various application areas [3], especially in the analysis of very dilute environmental samples [4].

The analysis of such extracts is greatly facilitated by using GC–mass spectrometry with selected ion monitoring (MS-SIM) owing to the reduced matrix interference for components of interest. Selective detection by MS-SIM results in improved detection limits and leads to more reliable analytical results.

The aim of this work was to study the applicability of the off-line coupling of microextraction of PAHs from water with large-volume sampling of extracts using a split–splitless injector for GC–MS-SIM analysis of ppt and sub-ppt concentrations of PAHs in drainage water from bitumen concrete roads and in drinking water respectively.

## EXPERIMENTAL

### *Materials*

The test blocks were made of either bitumen concrete or bitumen-free concrete. They were 138 mm high and 20 mm wide. The test blocks were extracted with 1500 ml of drinking water (the water to block surface area ratio was 10 ml of water to 1 $cm^2$ of surface area) during a 7-day period at $20 \pm 2°C$. A 1000-ml volume of each extract was used for PAH determination.

All solvents used were of analytical-reagent grade or of higher purity (Merck, Darmstadt, Germany). All individual PAHs used were of 99% minimum purity.

### *Instrumentation*

An HP 5890 Series II gas chromatograph was equipped with a split–splitless capillary inlet injector. Helium was used as the carrier gas. An HP 5971A mass-selective detector was used for detection with an ionization energy of 70 eV. Selected ion monitoring was used for the detection of selected PAH ions ($m/z$ 154, 178, 202, 228, 252, 276, 300 and 302) [1]. The measured values and resulting characteristics were processed by the computer which is part of the GC–MS system.

### *GC analysis*

A glass capillary column (20 m × 320 μm I.D.), coated with OV-1 and immobilized by γ-irradiation as the stationary phase with a film thickness of 0.4 μm, was used for the separation of PAHs. The separation was temperature programmed with an isothermal period at 80°C for 16 min, then increased at 15°C $min^{-1}$ to 300°C and an isothermal period at 300°C for 6 min.

### *Microextraction of PAHs*

A volume of 800 ml of water was extracted with 2 ml of toluene for 1 min with intensive shaking, followed by ultrasonic extraction for 10 min at ambient temperature (Tesla UG 160/320 TA). For the determination of PAHs in drinking water, 1 ml of the toluene extract layer [5] was then transferred into a glass separator and preconcentrated to 250 μl. For the analysis of the drainage water, the large extract volumes were introduced into the injector linear without any preconcentration. A model sample of PAHs in water was prepared from drinking water and 80 μl of PAH solution in methanol.

### *Large-volume sampling*

All injections were made with a 100-μl injection syringe (Hamilton). The injection port was rearranged with a splitless insert of 4 mm I.D. (Hewlett-Packard). The insert was packed like a short packed column with silanized Chromosorb W (60–80 mesh) coated with 4% (w/w) of OV-1 stationary phase immobilized by dicumyl peroxide. The length of the packing material was 5 cm. After the flash injection of 70 μl of sample (100 μl $s^{-1}$), the solvent was purged out using a split with a purge flow of 60 ml $min^{-1}$ helium 80°C (*i.e.*, 30°C below the boiling point of toluene used as the solvent) for 2.8 min. After this split period, the system was turned to the splitless mode and the injection port was heated ballisticaly to 300°C for 5 min for thermal desorption of the analyte compounds. Because the head of the analytical capillary column was still at 80°C, thermally desorbed compounds condensed in it. After 16 min this preconcentration

period was stopped, the split was opened, the injection port was cooled to 80°C and the analysis was continued with the temperature programme of the capillary column.

*Quantification*

Quantitative data were obtained on the basis of external calibration.

## RESULTS AND DISCUSSION

The reproducibilities of peak areas from seven replicate measurements for large-volume injection of 70 $\mu$l of a standard PAH sample with corresponding concentrations of 1 and 10 ng $l^{-1}$ in water are given in Tables I and II. The average precision of peak-area measurement of PAHs for a 1 ng $l^{-1}$ concentration is 21.4% and for 10 ng $l^{-1}$ it is 11.6%; hence, according to expectation, the precision of peak-area measurements increases with increasing concentration of PAHs. The detection limits that were calculated on the basis of the average peak areas of PAHs for a concentration of 1 ng $l^{-1}$ and their standard deviations for the 99% confidence level are also given in Table I. It is clear from Table I that the detection limits of PAHs for large-volume injection are in the range 0.2–1 ng $l^{-1}$.

TABLE II

REPRODUCIBILITY OF PEAK AREAS OF PAH STANDARDS FOR A CONCENTRATION OF 10 ng $l^{-1}$ (ppt) PER COMPOUND

Abbreviations as in Table I.

| PAH | *X* | SD | R.S.D. (%) |
|---|---|---|---|
| Phenanthrene | 141 149 | 13 979 | 9.9 |
| Anthracene | 145 145 | 17 925 | 11.7 |
| Fluoranthene | 166 390 | 19 933 | 12.0 |
| Pyrene | 153 717 | 15 495 | 10.1 |
| Benz[*a*]anthracene | 81 840 | 7739 | 9.5 |
| Chryzene | 119 259 | 11 013 | 9.2 |
| Benzo[*b*]fluoranthene | 99 852 | 9707 | 9.7 |
| Benzo[*k*]fluoranthene | 126 642 | 15 608 | 12.3 |
| Benzo[*e*]pyrene | 114 262 | 11 627 | 10.2 |
| Benzo[*a*]pyrene | 63 955 | 7924 | 12.3 |
| Perylen | 131 853 | 5961 | 19.7 |
| Indeno[1,2,3-*cd*]pyrene | 97 284 | 11 972 | 12.3 |

The average PAH recoveries by liquid–liquid microextraction from water and large-volume sampling for three concentration levels, obtained from three measurements, are given in Table III. The recoveries of the compounds were calculated from the normalized peak areas for spiked samples of water and reference solutions using large-volume sampling (70 $\mu$l). The results show

TABLE I

REPRODUCIBILITY OF PEAK AREAS OF PAH STANDARDS AT A CONCENTRATION OF 1ng $l^{-1}$ (ppt) PER COMPOUND

*X* = average peak area measured from seven trials; S.D. = standard deviation; R.S.D. = relative standard deviation; MDL = method detection limit.

| PAH | *X* | S.D. | R.S.D. (%) | MDL (ppt) |
|---|---|---|---|---|
| Phenanthrene | 36 426 | 6798 | 18.7 | 0.7 |
| Anthracene | 38 615 | 10 250 | 26.5 | 0.9 |
| Fluoranthene | 40 043 | 8751 | 21.8 | 0.8 |
| Pyrene | 37 768 | 5812 | 15.3 | 0.6 |
| Benz[*a*]anthracene | 22 315 | 6127 | 27.3 | 1.0 |
| Chryzene | 31 951 | 9385 | 29.4 | 1.1 |
| Benzo[*b*]fluoranthene | 28 380 | 6254 | 22.0 | 0.8 |
| Benzo[*k*]fluoranthene | 35 365 | 2287 | 6.5 | 0.2 |
| Benzo[*e*]pyrene | 35 851 | 8432 | 25.0 | 0.9 |
| Benzo[*a*]pyrene | 19 933 | 4527 | 22.7 | 0.8 |
| Perylene | 46 493 | 9815 | 21.1 | 0.8 |
| Indeno[1,2,3-*cd*]pyrene | 25 720 | 5062 | 20.0 | 0.7 |

TABLE III

PAH RECOVERY BY LIQUID–LIQUID MICROEXTRACTION FROM WATER AND LARGE-VOLUME SAMPLING AT VARIOUS PAH CONCENTRATIONS

Average results for three measurements.

| PAH | Concentration (ng $l^{-1}$) | | | | | |
|---|---|---|---|---|---|---|
| | 10 | | 50 | | 100 | |
| | Recovery (%) | R.S.D. (%) | Recovery (%) | R.S.D. (%) | Recovery (%) | R.S.D. (%) |
| Phenanthrene | 186 | 136 | 97.8 | 2.7 | 94.1 | 3.4 |
| Anthracene | 170 | 66 | 77.8 | 3.2 | 77.8 | 9.6 |
| Fluoranthene | 137 | 21 | 84.6 | 3.4 | 97.9 | 2.1 |
| Pyrene | 130 | 25 | 83.9 | 3.4 | 97.1 | 0.9 |
| Chrysene | 130 | 19 | 83.9 | 7.6 | 71.8 | 2.1 |
| Benzo[*a*]pyrene | 106 | 37 | 48.1 | 6.2 | 44.6 | 4.2 |
| Perylene | 93 | 16 | 53.1 | 2.9 | 43.0 | 2.8 |

that relatively high recoveries and good reproducibilities for concentrations of 50 and 100 ng $l^{-1}$ of individual PAHs were achieved. The higher recoveries and higher R.S.D. values for lower concentrations (10 ng $l^{-1}$) of PAHs (in comparison with those in Table II) may be caused by the presence of interfering compounds in the water analysed in the former instance and because the whole analytical procedure is included in the latter. The interference may influence the quantitative results of the GC–MS-SIM determination of PAHs at lower concentration levels.

The method was applied to the ultra-trace determination of PAHs in drinking water and in water extracts of bitumen concretes and bitumen-free concretes. The chromatogram of PAHs from a tar used for bitumen concrete test blocks is shown in Fig. 1, that of PAHs from drinking water used for leaching the concrete

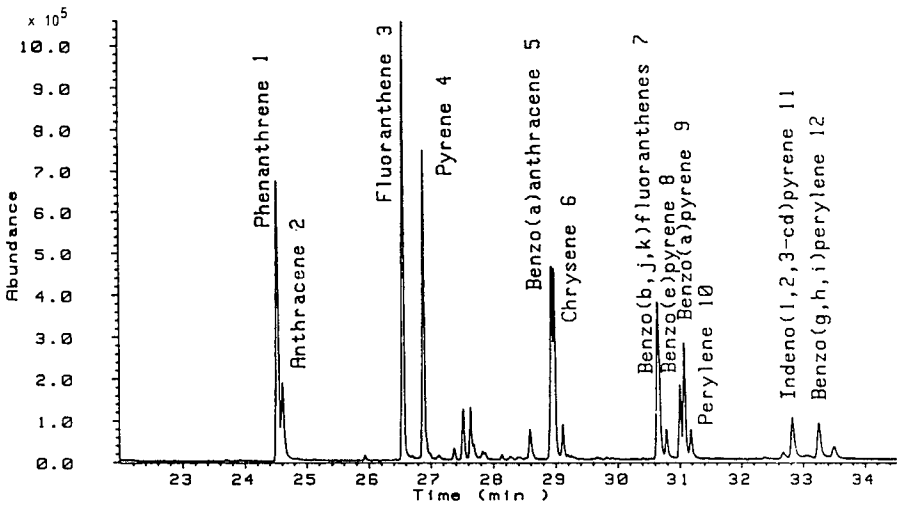


Fig. 1. Chromatogram of PAHs from tar obtained by GC–MS-SIM.

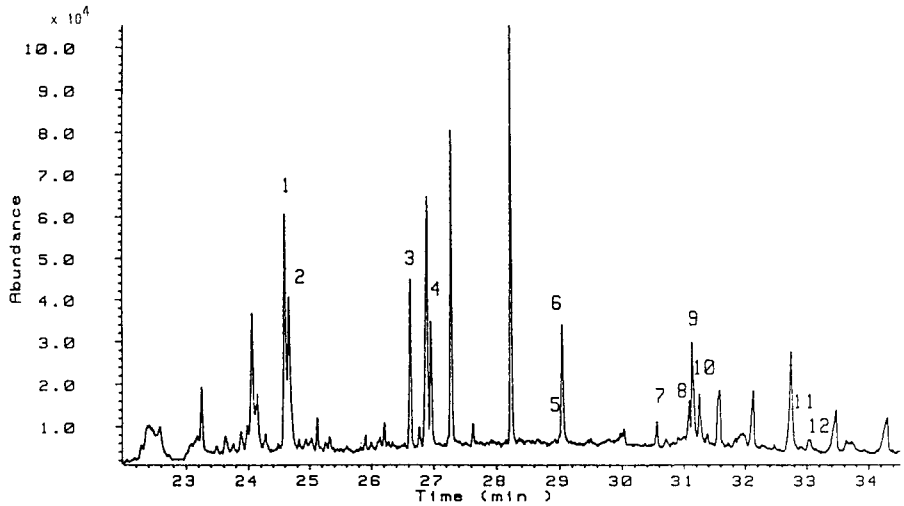


Fig. 2. Chromatogram of PAHs from drinking water obtained by GC–MS-SIM. Peak identifications as in Fig. 1.

test blocks in Fig. 2 and that of PAHs from the drainage water of bitumen concrete test blocks in Fig. 3. The results for the determination of PAHs in these samples by using the external standard method are given in Table IV. The concentration of PAHs in the drinking water sample are in the range 0.7–3.5 ng $l^{-1}$ (ppt) (and lower than these values in the case of co-elution PAHs with impurities) and in the drainage water in the range 4–15 000 ng $l^{-1}$. The latter results can be correlated with the characteristics of the water solubility of PAHs [1], which decreases with increasing number of condensed rings in the PAH molecule. Nevertheless, the PAH isomers with a linear structure, *e.g.*, anthracene, are less soluble than those of an angular structure (phenanthrene). However, micelle formation by detergents and other soluble organic compounds can increase the solubility of PAHs [1]. The relatively high concentrations of PAHs determined in bitumen-free concrete probably resulted from contamination of the cement during the burning period in its manufacture (*e.g.*, burning of used tyres).

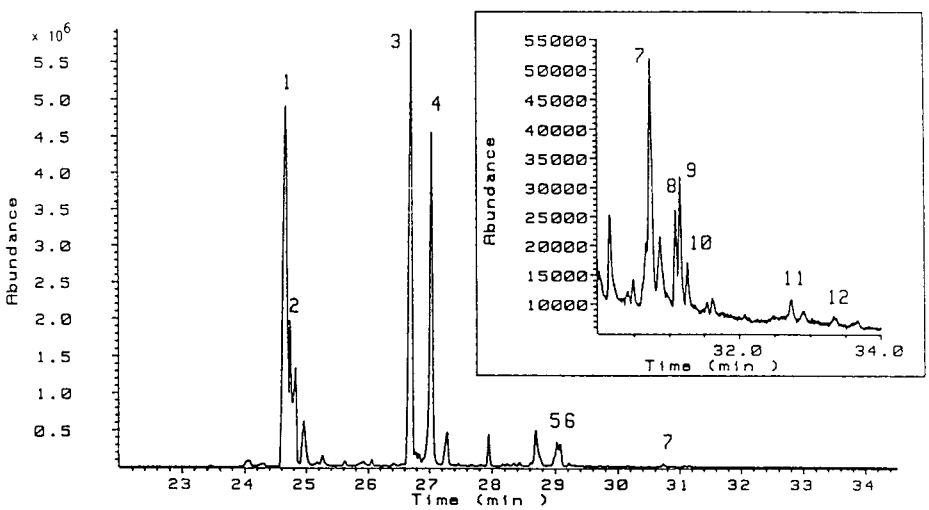


Fig. 3. Chromatogram of PAHs from drainage water obtained by GC–MS-SIM. Peak identifications as in Fig. 1.

TABLE IV

PAH CONCENTRATIONS IN WATER SAMPLES AND THEIR SOLUBILITY IN WATER AT 25°C

| PAH | Concentration (ng $l^{-1}$) | | | Solubility in water (ng $l^{-1}$) |
|---|---|---|---|---|
| | Drinking water | Bitumen-free concrete eluate | Bitumen concrete eluate | |
| Phenanthrene | 2.6 | 26.0 | 13 600 | 1 290 000 |
| Anthracene | 1.8 | 9.0 | 4700 | 73 000 |
| Fluoranthene | 3.5 | 326.0 | 15 000 | 260 000 |
| Pyrene | 2.5 | 888.0 | 11 500 | 135 000 |
| Benz[*a*]anthracene | ND[a] | 68.0 | 920 | 14 000 |
| Chryzene | 3.0 | 64.0 | 600 | 2000 |
| Benzo[*b*,*jk*]fluoranthene | 0.7 | 25.0 | 150 | – |
| Benzo[*e*]pyrene | 1.5 | 10.0 | 40 | 3800 |
| Benzo[*a*]pyrene | 3.2 | 16.0 | 60 | 400 |
| Perylene | 2.8 | 5.0 | 17 | 400 |
| Indeno[1,2,3-*cd*]pyrene | ND | 2.0 | 5 | – |
| Benzo[*ghi*]perylene | ND | 1.5 | 4 | 300 |

[a] ND = not determined.

The results obtained indicate that owing to the extremely high enrichment factors connected with the use of microextraction and large-volume sampling, and application of MS-SIM detection, the proposed method allows the determination of PAHs at ppt concentrations in drinking and contaminated waters.

REFERENCES

1 M.L. Lee, M.V. Novotny and K.D. Bartle, *Analytical Chemistry of Polycyclic Aromatic Compounds*, Academic Press, New York, 1981, p. 10.
2 J.E.T. Moen, J.P. Cornet and C.W.A. Evers, in J.W. Assink and W.J. van den Brink (Editors), *Contaminated Soil*, Martinus Nijhoff, Dordrecht, 1986, p. 441.
3 P. Sandra, in K.J. Hyver (Editor), *High Resolution Gas Chromatography*, Hewlett-Packard, Avondale, PA, 1989, Ch. 3.
4 J. Staniewski, H.G. Janssen, C.A. Cramers and J.A. Rijks, *J. Microcol. Sep.*, 4 (1992) 331.
5 J. Hrivňák, *Anal. Chem.*, 57 (1985) 2159.

*Journal of Chromatography A*, 653 (1993) 369–373
Elsevier Science Publishers B.V., Amsterdam

CHROM. 25 433

# Short Communication

# Sampling method of organotin compounds in air using a quartz-fibre filter and an activated carbon-fibre filter for gas chromatographic determination

Kuniaki Kawata*, Megumi Minagawa and Yoshimaru Fujieda

*Niigata Prefectural Research Laboratory for Health and Environment, 314-1 Sowa, Niigata 950-21 (Japan)*

Akio Yasuhara

*The National Institute for Environmental Studies, 16-2 Onogawa, Tsukuba, Ibaraki 305 (Japan)*

(First received May 25th, 1993; revised manuscript received July 13th, 1993)

ABSTRACT

A sampling method using quartz-fibre filters and an activated carbon-fibre filter was developed for gas chromatographic determination of organotin compounds in air. The organotin compounds investigated were dibutyltin chloride (DBTC), tributyltin chloride (TBTC), diphenyltin chloride (DPTC) and triphenyltin chloride (TPTC). The chlorides collected on filters were extracted ultrasonically with benzene and converted into propyl derivatives using propylmagnesium bromide. The derivatives were analysed by capillary gas chromatography (GC) equipped with a flame photometric detector adjusted for tin detection. The collection efficiencies and recoveries of the organotin compounds were quantitative. The minimum detectable concentrations were 0.2 ng/m$^3$ for DBTC and TBTC, 0.3 ng/m$^3$ for DPTC and 0.4 ng/m$^3$ for TPTC. This method was successfully applied to the determination of organotin compounds in indoor air.

## INTRODUCTION

Tributyltin and triphenyltin compounds have been used as antifouling agents for painting ship bottoms and fishing nets, and as wood preservatives; dibutyltin and diphenyltin compounds have been used as stabilizers for halogen-containing polymers. They are toxic to fish species and other aquatic animals, and exist as contaminants in water [1], sediment [2] and biota [3]. They are not thought to exist in air because of their very low volatilities [4]. Therefore, there have been few investigations on their existence in the environmental air.

A few reports have described attempts to collect some organotin compounds from the working atmosphere for gas chromatographic determinations: chromosorb 102 resin collection for butyltin compounds [5] and glass-fibre filter collection for dialkyltin compounds [6]. However, these methods cannot be applied to the determination of organotin compounds in the environmental air because the detection limits of these methods are much higher than the mini-

* Corresponding author.

0021-9673/93/$06.00 

mum allowable environmental concentration levels.

We used a quartz-fibre filter and an activated carbon-fibre filter, which are effective in the collection of airborne pesticides [7–10], for the collection of organotin compounds in air, *i.e.* dibutyltin dichloride (DBTC), tributyltin chloride (TBTC), diphenyltin dichloride (DPTC) and triphenyltin chloride (TPTC). Some reports have shown that organotin compounds in water and biota can be analysed after propylation by gas chromatography (GC) coupled with flame photometric detection (FPD) with a tin filter [11,12]; this method is selective and sensitive. This report presents the results of organotin compound collection using quartz-fibre filter and activated carbon-fibre filter for GC–FPD determination after propylation.

## MATERIALS AND METHODS

### *Apparatus and materials*

An automated sequential air sampler, GS-10D (Tokyo Dylec, Tokyo, Japan), was used for sample collection. An ultrasonic apparatus, EN-20S-1A (Shimada, Tokyo, Japan), and a centrifugal apparatus, KN70 (Kubota, Tokyo, Japan), were used for the extraction procedure. The gas chromatograph used was a GC-7AG (Shimadzu) equipped with an FPD. A fused-silica HP-1 column (10 m × 0.53 mm I.D., coated with methylsilicone in 2.65 $\mu$m thickness) was purchased from Hewlett-Packard.

TPTC and 2 *M* propylmagnesium bromide (tetrahydrofuran solution) were purchased from Tokyo Kasei Kogyo (Tokyo, Japan). DPTC was obtained from Aldrich (Milwaukee, WI, USA). Other reagents were obtained from Wako (Osaka, Japan).

Quartz-fibre filters (Toyo Pallflex 2500 Qatup) and activated carbon-fibre filters (Toyobo KF Paper P-175) were shaped into circles of 47 mm diameter for sample collection.

### *Sample collection and determination*

Air was sampled through two quartz-fibre collection filters at the front and through an activated carbon-fibre collection filter at the rear at 5 l/min for 24 h using the automated sequential air sampler. Each sampled filter was extracted ultrasonically with 10 ml of 1 *M* HCl–methanol for 10 min followed by centrifugation at 1700 *g* for 10 min, and the supernatant was decanted. The extraction was repeated with 10 ml of 1 *M* HCl in methanol and then twice with 2.5 ml of benzene. The extracts were combined, washed with 15 ml of 10% NaCl, dried over $Na_2SO_4$ and concentrated to 1 ml by blowing with nitrogen gas. A 1-ml volume of 2 *M* propylmagnesium bromide was added to the sample, shaken and allowed to stand for 30 min in a water bath at 40°C. A 10-ml volume of 0.5 *M* $H_2SO_4$ was added to decompose excess propylmagnesium bromide, then 10 ml of methanol were added. The resulting solution was extracted twice with 2.5 ml of *n*-hexane. The combined organic phases were concentrated to 0.5 ml by blowing with nitrogen gas. The solution was analysed by GC. GC conditions were as follows: column temperature, 110°C (held for 2 min) to 250°C (held for 2 min) increasing at 8°C/min; injector and detector temperature, 280°C; injection mode, direct injection; carrier gas flow-rate, 10 ml/min; detector, FPD with tin filter ($\lambda = 611.1$ nm).

## RESULTS AND DISCUSSION

### *Extraction solvent*

Extraction efficiencies for the organotin compounds from the quartz-fibre collection filter and the activated carbon-fibre collection filter were determined by adding known amounts of organotin compounds (25 $\mu$g of DBTC and TBTC and 75 $\mu$g of DPTC and TPTC) to each filter as an ethanolic solution. The filter was allowed to stand for 20 min in order to evaporate the ethanol, then the organotin compounds were extracted from the filter as described above by using ten different solvents. All organotin compounds were extracted quantitatively from the quartz-fibre collection filter by each extraction solvent; for example, 96 ± 5.9% DBTC, 92 ± 4.2% TBTC, 99 ± 3.6% DPTC and 95 ± 4.9% TPTC ($n = 4$) were extracted with benzene. On the other hand, it was hard to extract quantitatively the organotin compounds from the activated carbon-fibre collection filter. As shown in

TABLE I

EXTRACTION EFFICIENCIES FOR ORGANOTIN COMPOUNDS FROM ACTIVATED CARBON-FIBRE COLLECTION FILTER

| Solvent | Extraction efficiency (%) | | | |
|---|---|---|---|---|
| | TBTC | TPTC | DBTC | DPTC |
| *n*-Hexane | 34 | 11 | 19 | 0.6 |
| *n*-Hexane–ethanol (4:1, v/v) | 49 | 14 | 30 | 0.6 |
| Dichloromethane | 46 | 60 | 73 | 1.8 |
| Dichloromethane–ethanol (4:1, v/v) | 49 | 63 | 96 | 3.6 |
| Benzene–ethanol (4:1, v/v) | 50 | 84 | 78 | 11 |
| Toluene | 55 | 86 | 53 | 6.0 |
| Toluene–ethanol (4:1, v/v) | 45 | 95 | 81 | 14 |
| Xylene | 45 | 73 | 32 | 2.4 |
| Xylene–ethanol (4:1, v/v) | 39 | 84 | 83 | 20 |
| Benzene | 99 ± 38[a] | 93 ± 1.7[a] | 68 ± 5.1[a] | 26 ± 3.8[a] |
| Benzene[b] | 92 ± 12[a] | 91 ± 4.2[a] | 66 ± 3.3[a] | 21 ± 0.9[a] |

[a] Mean ± standard deviation ($n = 4$).
[b] Added: 1 μg of DBTC, 1 μg of TBTC, 3 μg of DPTC and 3 μg of TPTC.

Table I, TBTC and TPTC were extracted quantitatively from the filter by benzene, and DBTC by dichloromethane–ethanol (4:1, v/v), but DPTC could not be extracted by any solvent investigated. However we need not consider the low extraction efficiencies of DBTC and DPTC by benzene from the activated carbon-fibre collection filter, because both compounds can be collected by the quartz-fibre collection filters, as described later. The extraction efficiencies for 1–3 μg of the organotin compounds were almost equal to those for 25–75 μg of the compounds, as shown in Table I. Therefore, benzene was chosen as the best solvent.

*Retention efficiencies*

It is difficult to determine the collection efficiencies of filters for organotin compounds, because it is impossible to prepare air samples containing known amounts of organotin compounds [6]. Hence, we estimated the collection efficiency from the retention efficiency [13,14].

Retention efficiencies for organotin compounds of quartz-fibre collection filters were determined by adding known amounts of the organotin compounds (125 μg of DBTC and TBTC and 175 μg of DPTC and TPTC) to a quartz-fibre collection filter as an ethanolic solution. Air was passed at 5 l/min for 24 h through the filter ($F_1$) with back-up from another two quartz-fibre collection filters ($F_2$ and $F_3$) at room temperature. The retention efficiencies of DBTC, DPTC and TPTC were quantitative, but TBTC evaporated from the quartz-fibre collection filters by passing air, suggesting the need for another back-up filter ($F_3$). Some experiments were carried out by adding the activated carbon-fibre collection filter as a back-up filter ($F_3$). The results are shown in Table II. Retention efficiencies of the organotin compounds were quantitative.

TABLE II

RETENTION EFFICIENCIES OF ORGANOTIN COMPOUNDS

| Collection filter[a] | Retention efficiency[b] (%) | | | |
|---|---|---|---|---|
| | DBTC | TBTC | DPTC | TPTC |
| $F_1$ | 86 ± 2.2 | 18 ± 5.7 | 93 ± 8.5 | 94 ± 4.5 |
| $F_1 + F_2$ | 95 ± 3.4 | 67 ± 4.4 | 96 ± 8.4 | 98 ± 4.4 |
| $F_1 + F_2 + F_3$ | 96 ± 3.3 | 91 ± 5.7 | 96 ± 8.4 | 98 ± 4.4 |

[a] $F_1$ and $F_2$ = quartz-fibre collection filters; $F_3$ = activated carbon-fibre collection filter.
[b] Mean ± standard deviation ($n = 4$).

The minimum detectable concentrations with signal-to-noise ratio of 3 based on peak height were 0.2 ng/m$^3$ for DBTC and TBTC, 0.3 ng/m$^3$ for DPTC and 0.4 ng/m$^3$ for TPTC. These values were about 100–2000 times lower than those achieved with previous methods.

*Stabilities of organotin compounds on the collection filters*

The storage stabilities of the organotin compounds on the collection filters were investigated. The collection filters with 50 $\mu$g of DBTC and TBTC and 150 $\mu$g of DPTC and TPTC added were stored for a known period. The results are shown in Table III. The organotin compounds were more stable on the collection filters at −20°C than at 15°C. DBTC, DPTC and TPTC remained almost unchanged in quantity for at least 7 days on the collection filters during storage at −20°C; under the same conditions, TBTC was stable for at least 7 days on the quartz-fibre filter, and for at least 4 days on the activated carbon-fibre collection filter. Therefore, the collection filters should be stored at −20°C and be analysed within 4 days after sampling.

*Application to environmental samples*

This sampling and analytical method was applied to organotin compounds in air in houses. TPTC was detected in some samples in concentrations ranging from 0.4 to 0.6 ng/m$^3$. No

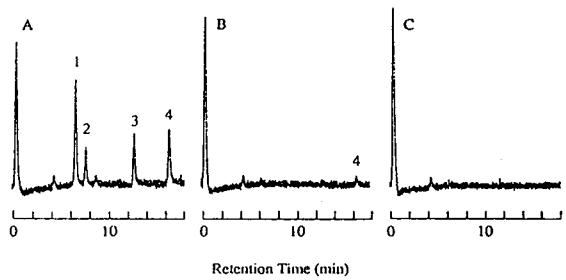


Fig. 1. GC–FPD chromatograms of organotin compounds. (A) Standard. (B) Sample. (C) Procedural blank. 1 = Dibutyldipropyltin; 2 = tributylpropyltin; 3 = diphenyldipropyltin; 4 = triphenylpropyltin.

TPTC was detected from the second quartz-fibre filter ($F_2$) or the activated carbon-fibre filter ($F_3$). Hence, TPTC in air was collected quantitatively by the first quartz-fibre filter ($F_1$). The detected TPTC came from wood preservatives applied to timber used in building the houses. Typical gas chromatograms of standards, a sample and a procedural blank are shown in Fig. 1. The organotin compounds could be analysed without interferences.

REFERENCES

1 R.J. Maguire, Y.K. Chau, G.A. Bengert and E.J. Hale, *Environ. Sci. Technol.*, 37 (1982) 698.
2 N.S. Makkar, A.T. Kronick and J.J. Cooney, *Chemosphere*, 18 (1989) 2043.
3 J.W. Short and J.L. Sharp, *Environ. Sci. Technol.*, 23 (1989) 740.

TABLE III

STABILITIES OF ORGANOTIN COMPOUNDS ON COLLECTION FILTERS

| Collection filter | Storage temperature (°C) | Storage time (days) | Recovery[a] (%) | | | |
|---|---|---|---|---|---|---|
| | | | TBTC | TPTC | DBTC | DPTC |
| Quartz fibre | 15 | 4 | 88 | 91 | 86 | 90 |
| | | 7 | 85 | 90 | 76 | 87 |
| | −20 | 4 | 99 | 96 | 90 | 92 |
| | | 7 | 92 | 98 | 88 | 93 |
| Activated carbon fibre | 15 | 4 | 49 | 33 | 87 | 85 |
| | | 7 | 41 | 30 | 63 | 76 |
| | −20 | 4 | 92 | 92 | 98 | 94 |
| | | 7 | 73 | 80 | 94 | 92 |

[a] Mean ($n$ = 2).

4 R.J. Maguire, J.H. Carey and E.J. Hale, *Agric. Food Chem.*, 31 (1983) 1061.
5 B. Zimmerli and H. Zimmermann, *Z. Anal. Chem.*, 304 (1980) 23.
6 S. Vainiotalo and L. Häyri, *J. Chromatogr.*, 523 (1990) 273.
7 N. Moriyama, H. Murayama, E. Kitajima, Y. Urushiyama and K. Kawata, *Eisei Kagaku*, 36 (1990) 290.
8 K. Kawata, N. Moriyama, M. Kasahara and Y. Urushiyama, *Bunseki Kagaku*, 39 (1990) 423.
9 K. Kawata, N. Moriyama and Y. Urushiyama, *Bunseki Kagaku*, 39 (1990) 601.
10 K. Kawata, *J. Environ. Chem.*, 2 (1992) 181.
11 K. Takami, T. Okumura, H. Yamasaki and M. Nakamoto, *Bunseki Kagaku*, 37 (1988) 117.
12 H. Kurosaki, H. Yokoyama and K. Ozaki, *Bunseki Kagaku*, 40 (1991) T65.
13 E.M. Roper and C.G. Wright, *Bull. Environ. Contam. Toxicol.*, 33 (1984) 476.
14 V.B. Stein, T.A. Amin and R.S. Narang, *J. Assoc. Off. Anal. Chem.*, 70 (1987) 721.

*Journal of Chromatography A*, 653 (1993) 374–379
Elsevier Science Publishers B.V., Amsterdam

CHROM. 25 476

# Short Communication

# Analysis of *Fusarium* mycotoxins by supercritical fluid chromatography with ultraviolet or mass spectrometric detection

J. Christopher Young*

*Plant Research Centre, Agriculture Canada, Ottawa K1A 0C6 (Canada)*

David E. Games

*Mass Spectrometry Research Unit, Department of Chemistry, University College of Swansea, Singleton Park, Swansea SA2 8PP, Wales (UK)*

(Received July 7th, 1993)

ABSTRACT

Supercritical fluid chromatography (SFC) on packed high-performance liquid chromatographic columns combined with ultraviolet and moving belt (MB)-mass spectrometry (MS) was applied to the separation and identification of some *Fusarium* mycotoxins in *F. roseum* liquid culture extracts. Mycotoxins observed included the trichothecenes 4-deoxynivalenol (DON), isoDON, 3-acetylDON, 3,15-diacetylDON, calonectrin, 15-deacetylcalonectrin, and 7-hydroxyisotrichodermol, as well as culmorin, culmorone and sambucoin. SFC separations were rapid; retention times were typically less than about 6 min. Detection limits for a variety of mycotoxin standards analyzed by SFC–MB-MS ranged from 10 to 250 mg.

## INTRODUCTION

The utility of supercritical fluid chromatography (SFC) on capillary and packed columns with flame ionization and single wavelength ultraviolet (UV) detection for the separation of a variety of *Fusarium* mycotoxins was demonstrated recently [1]. These detectors provide only partial information on the nature of a particular mycotoxin by virtue of congruence of retention times with those of standards. Further characterization of individual mycotoxin constituents requires additional information. The SFC–MS analysis of only a few trichothecene mycotoxins (standards only) on capillary columns has been reported [2–4]. This study was initiated to determine the efficacy of coupling packed column SFC with a full scan UV detector or, via moving belt (MB) interface, with a mass spectrometer (MS) for the characterization of natural mixtures of mycotoxins (see Fig. 1 for

* Corresponding author.

0021-9673/93/$06.00 

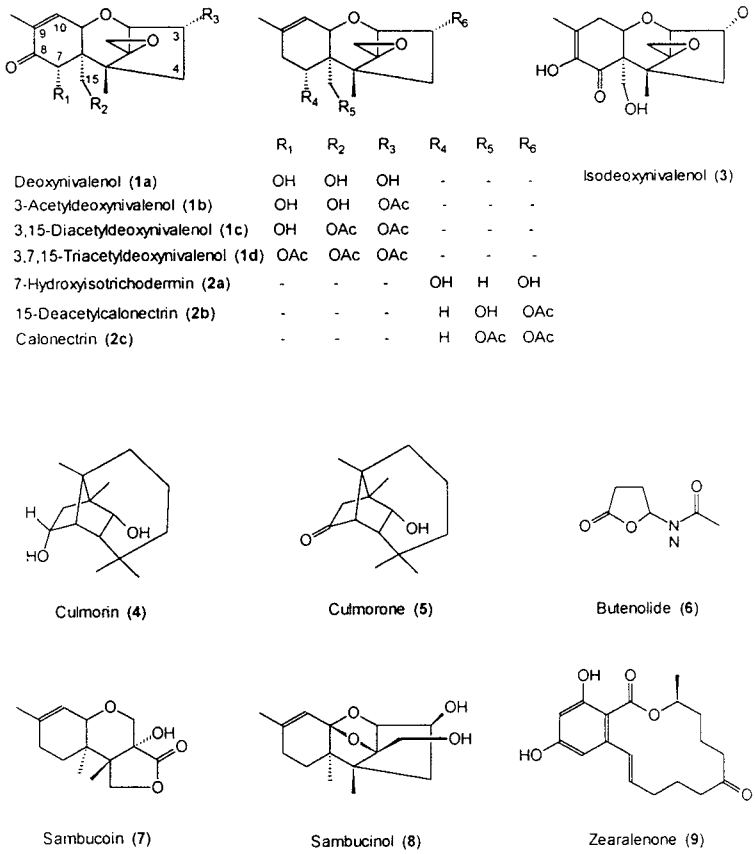


Fig. 1. Structures of some *Fusarium* mycotoxins.

structures of typical *Fusarium* mycotoxins) isolated from several *Fusarium roseum* liquid culture extracts.

## MATERIALS AND METHODS

### *Mycotoxins and reagents*

Mycotoxin standards were obtained from liquid cultures of various *Fusarium* spp. (prepared in the Plant Research Centre laboratories, Ottawa, Canada). Natural mixtures of mycotoxins were obtained from liquid culture extracts of *F. roseum*. All reagents and solvents were of analytical-reagent grade. Instrument-grade carbon dioxide supplied in cylinders with a dip tube (BOC, London, UK) and glass-distilled methanol were used as eluents.

### *Supercritical fluid chromatography*

SFC analyses were conducted with supercritical carbon dioxide containing 10% methanol on a Hewlett-Packard 1084B liquid chromatograph (LC) (Hewlett-Packard, Avondale, PA, USA) modified for SFC [5] at (1) 60°C and pressure 250 bar at a flow-rate of 2 ml/min on a 250 × 2 mm I.D. stainless-steel column of 3-$\mu$m Hypersil connected to a Spectra-Physics scanning ultraviolet detector or (2) at 50°C and pressure 315 bar at a flow-rate of 4 ml/min on a 250 × 4.6 mm I.D. stainless-steel column of Spherisorb Amino 3 $\mu$m connected via a LC–MS moving belt (MB) interface (VG Analytical, Wythenshawe, UK) to a VG-7070E (VG Analytical, Manchester, UK) mass spectrometer operating in the electron ionization (EI) mode at 70 eV or in the chemical ionization (Cl) mode with ammonia or methane.

The liquid carbon dioxide and pump heads were cooled to −25°C using a Neslab RTE-4Z refrigerated bath (Neslab Instruments, Newington, NH, USA).

## RESULTS AND DISCUSSION

### *Supercritical fluid chromatography–ultraviolet detection of Fusarium mycotoxins*

Fig. 2 shows the three dimensional SFC chromatogram for UV detection, from 200–325 nm, of extract I from a *Fusarium roseum* liquid culture. This chromatogram implies the presence of at least two major compounds with UV spectra beyond end absorption. Full spectrum scans of the two major peaks, at 4.93 and 5.13 min, were congruent with those for iso-4-deoxynivalenol (IDON) (**3**) and 4-deoxynivalenol (DON) (**1a**), respectively, and occurred at the same retention times as standards. Confirmation of structure assignment was assured by examination of their respective mass spectra (see below). Fig. 2 also reveals that there are no other major UV absorbing components.

Depending upon the UV absorption cut off of the solvent system used for traditional high-performance liquid chromatography (HPLC), detection at low wavelengths (at or below 200 nm) may not be possible and components with only low wavelength absorption would be missed.

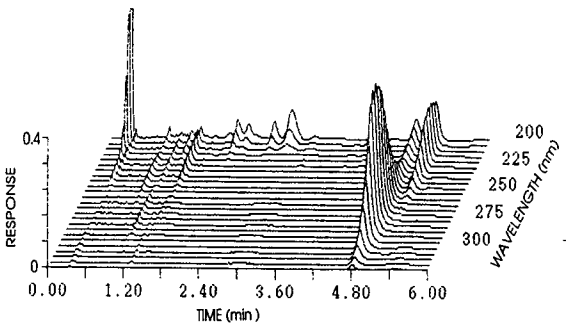


Fig. 2. Three-dimensional chromatogram of *Fusarium roseum* liquid culture extract I. Separation by SFC with eluent supercritical $CO_2$ containing 10% methanol at 60°C and pressure 250 bar at a flow-rate of 2 ml/min on 250 × 2 mm I.D. 3-$\mu$m Hypersil column. Detection by UV spectrometry from 200 to 325 nm.

SFC with $CO_2$ and methanol modifier is only limited by the range of the detector. The chromatogram at 200 nm (Fig. 2) clearly indicates the presence of other components with low wavelength absorption. However, end absorption spectra are of little diagnostic value. Since *Fusarium* mycotoxins without UV spectra are known, other methods of detection are required in order to discover the presence of such components.

### *Supercritical fluid chromatography–mass spectrometric detection of Fusarium mycotoxins*

The SFC effluent was linked, via a moving-belt interface, to a mass spectrometer operated under EI conditions. The retention times and detection limits of a variety of *Fusarium* mycotoxin standards were determined. The results summarized in Table I show that SFC–MB-MS detection limits were in the range of 10–250 ng. These are higher than those observed under GC-MS conditions [6].

### *SFC–MS analysis of Fusarium roseum culture extracts*

Reanalysis of extract I by SFC–MS under EI

TABLE I

DETECTION LIMITS OF SELECTED *FUSARIUM* MYCOTOXINS ANALYZED BY SUPERCRITICAL FLUID CHROMATOGRAPHY–MOVING BELT INTERFACE-MASS SPECTROMETRY

SFC with eluent supercritical $CO_2$ containing 10% methanol at 50°C and a pressure of 316 bar at a flow-rate of 4 ml/min on 250 × 4.6 mm I.D. stainless-steel column of Spherisorb Amino 3 $\mu$m. Detection on a magnetic sector VG 7070E mass spectrometer operating in the electron ionization mode.

| Compound | Detection limit (ng) |
|---|---|
| 3-Acetyldeoxynivalenol (**1b**) | 100 |
| Butenolide (**6**) | 20 |
| Culmorin (**4**) | 50 |
| 4-Deoxynivalenol (**1a**) | 150 |
| Sambucinol (**7**) | 30 |
| Triacetyldeoxynivalenol (**1c**) | 10 |
| Zearalenone (**9**) | 250 |

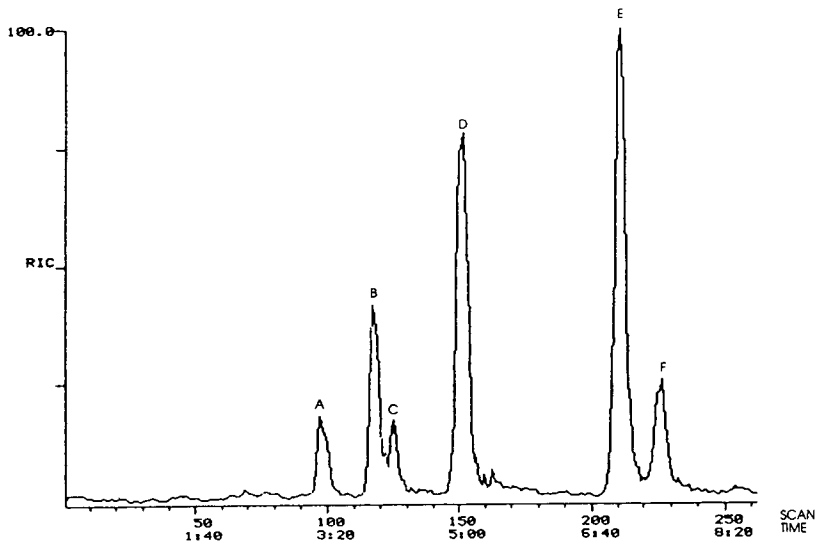


Fig. 3. Total ion mass spectrometric chromatogram of *Fusarium roseum* liquid culture extract I. Separation by SFC with eluent supercritical $CO_2$ containing 10% methanol at 50°C and pressure 315 bar at a flow-rate of 4 ml/min on 250 × 4.6 mm I.D. 3-$\mu$m Spherisorb Amino column. Moving belt interface with MS detection in EI mode. A = culmorin (**4**); B = unknown of molecular mass 342; C = 7-hydroxyisotrichodermol (**2a**); D = unknown of molecular mass 266; E = iso-4-deoxynivalenol (**3**); F = 4-deoxynivalenol (**1a**). Time in min.

conditions (chromatogram illustrated in Fig. 3) revealed the presence of at least six components. Examination of the MS of each component and comparison with those of standards led to the following peak assignments; A = culmorin (**4**), C = 7-hydroxyisotrichodermin (**2a**), E = IDON (**3**) and F = DON (**1a**). Since the MS of the remaining unknown components did not give a clear indication of molecular mass, the analysis was repeated under chemical ionization (CI) conditions by using methane and ammonia. Minor components B and D were shown, by these analyses, to have molecular masses of 342 and 266, respectively. The methane CI chromatogram (not shown) revealed that culmorin (**4**) (peak A) gave a significantly greater relative response under these conditions.

Two additional *F. roseum* extracts were analyzed by SFC–MS under EI and methane and ammonia CI conditions. Fig. 4 shows the SFC–CI-MS (ammonia) chromatogram for extract II; EI MS revealed components G and H to be culmorone (**5**) and sambucoin (**8**), respectively.

The SFC–EI-MS chromatogram for extract III, depicted in Fig. 5, suggested the presence of three major components. However detailed MS deconvolution analysis showed the first peak (I, J) to be a partially resolved mixture of calonectrin (**2c**) and 3,15-diacetyl-4-deoxynivalenol (**1c**). The remaining major components were identified as K = 15-deacetyl-calonectrin (**2b**) and L = 3-acetyl-4-deoxynivalenol (**1b**).

Although the sensitivity of SFC–MB-MS is less than that for GC–MS, there are several advantages. One is the ability to chromatograph thermally unstable or non-volatile substances without the need for derivatization prior to detection. Another is the speed of analysis. For example, the components of extracts II and III were completely eluted in less than 3 min (Figs. 4 and 5) whereas the analysis of the same extracts by GC–MS required about 12 min [6]. Although the peak widths are slightly broader than those observed by capillary GC, they are much narrower than those obtained from conventional HPLC [1].

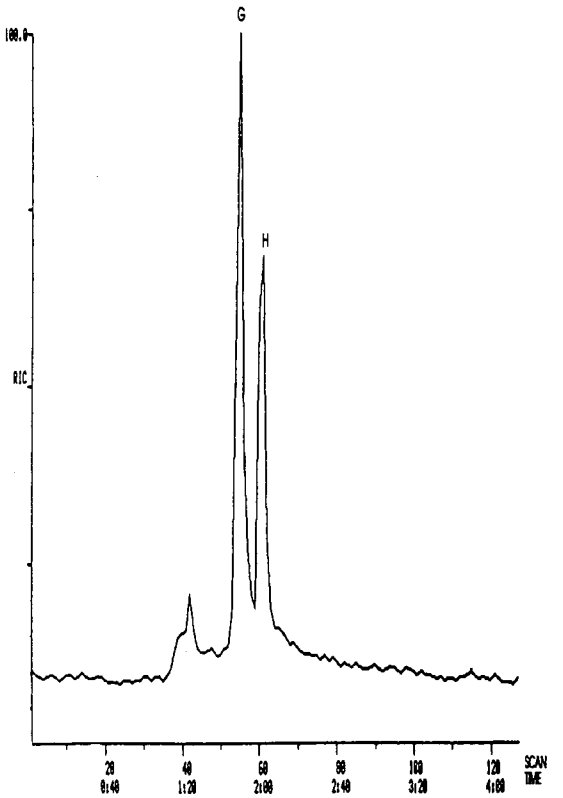


Fig. 4. Total ion mass spectrometric chromatogram of *Fusarium roseum* liquid culture extract II. Separation by SFC with eluent supercritical $CO_2$ containing 10% methanol at 50°C and pressure 315 bar at a flow-rate of 4 ml/min on 250 × 4.6 mm I.D. 3-$\mu$m Spherisorb Amino column. Moving belt interface with MS detection in Cl-$NH_3$ mode. G = culmorone (**5**); H = sambucoin (**8**). Time in min.

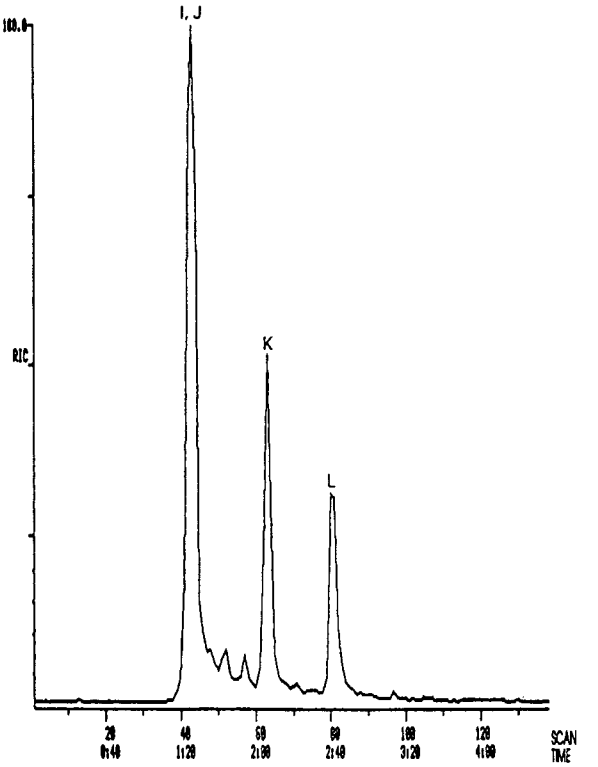


Fig. 5. Total ion mass spectrometric chromatogram of *Fusarium roseum* liquid culture extract III. Separation by SFC with eluent supercritical $CO_2$ containing 10% methanol at 50°C and pressure 315 bar at a flow-rate of 4 ml/min on 250 × 4.6 mm I.D. 3-$\mu$m Spherisorb Amino column. Moving belt interface with MS detection in EI mode. I = calonectrin (**2c**); J = 3,15-diacetyl-4-deoxynivalenol (**1c**); K = 15-deacetylcalonectrin (**2b**); L = 3-acetyl-4-deoxynivalenol (**1b**). Time in min.

## CONCLUSIONS

The full scanning UV detector can be used in conjunction with SFC for the characterization of *Fusarium* mycotoxins that have distinctive UV absorption patterns. For these and non-UV absorbing substances, the coupling of SFC with MS via the moving belt interface can provide unequivocal identification. Compared with conventional HPLC and GC, packed column SFC also offers faster analysis times.

## ACKNOWLEDGEMENTS

J.C.Y. wishes to thank D.E.G. for the opportunity to take a sabbatical study leave in the latter's laboratory. The authors thank Dr. J.D. Miller and Mr. W. Adams of the Plant Research Centre (PRC) of Agriculture Canada for providing *Fusarium roseum* culture extract material and Mr. P. Lafontaine of PRC for some GC–MS analyses. The authors are grateful to SERC for funding for mass spectrometry equipment.

This paper is PRC Contribution No. 1481.

REFERENCES

1 J.C. Young and D.E. Games, *J. Chromatogr.*, 627 (1992) 247.
2 R.D. Smith, H.R. Udseth and B.W. Wright, *J. Chromatogr. Sci.*, 23 (1985) 192.
3 H.T. Kalinowski, H.R. Udseth, B.W. Wright and R.D. Smith, *Anal. Chem.*, 58 (1986) 2421.
4 J.A. Roach, J.A. Sphon, J.A. Easterling and E.M. Calvey, *Biomed. Environ. Mass Spectrom.*, 18 (1989) 64.
5 D.R. Gere, R.D. Board and D. McManigill, *Anal. Chem.*, 54 (1982) 736.
6 J.C. Young, (1993) unpublished results.

*Journal of Chromatography A*, 653 (1993) 380–384
Elsevier Science Publishers B.V., Amsterdam

CHROM. 25 283

# Short Communication

# Rapid determination of solanum glycoalkaloids by thin-layer chromatographic scanning

F. Ferreira and P. Moyna*

*Catedra de Farmacognosia y Productos Naturales, Facultad de Química, Avenida General Flores 2124, CC 1157, Montevideo (Uruguay)*

S. Soule

*Departamento de Química Orgánica, Facultad de Ciencias, Avenida General Flores 2124, CC 1157, Montevideo (Uruguay)*

A. Vázquez

*Catedra de Farmacognosia y Productos Naturales, Facultad de Química, Avenida General Flores 2124, CC 1157, Montevideo (Uruguay)*

(First received May 27th, 1992; revised manuscript received May 7th, 1993)

ABSTRACT

A rapid quantitative TLC method for the determination of glycoalkaloids in potato leaves and tubers is described. The method includes a microscale extraction, a simple clean-up step and quantification by TLC scanning. The method is valuable for the determination of glycoalkaloids when many samples have to be evaluated as in potato breeding programmes.

## INTRODUCTION

The main potato glycoalkaloids (GAs), solanine and chaconine, are trisaccharide glycosides with a common tertiary amine aglycone, solanidine [1]. They represent 95% of the total GAs in cultivated potato varieties and play an important role in the natural defence mechanism against some economically important pests such as fungi, insects and viruses. They are toxic to humans, generally promoting gastrointestinal and neurological disorders [2].

The commercial potato cultivars contain small amounts of GAs in leaves, sprouts and tubers. Concentrations higher than 185 ppm can present risks to human consumers. Concentrations below this limit must be confirmed before delivering new varieties to the market. Wild *Solanum* species, increasingly used in breeding programmes, contain higher GA concentrations, and also GAs not present in the cultivated potato varieties. This determines the need for monitoring the GA content in the breeding processes to avoid hybrids with good resistance

* Corresponding author.

0021-9673/93/$06.00 

properties, but unsuitable for human consumption [3]. The determination of GAs in plants, potato tubers and potato products presents considerable difficulties. Almost all the common analytical methods have been tested: spectrophotometric and titrimetric determinations [4,5], quantitative TLC [6,7], GC [8,9] and HPLC [10].

The most satisfactory, from a quantitative point of view, were GC and HPLC. GC requires a hydrolytic step, which implies that only the aglycones can be detected. This represents a loss of information on the individual GAs originally present. The HPLC methods developed require the use of lengthy sample purification procedures and the use of amino columns [10]. The GAs do not have strong chromophores, so the sensitivity with UV detectors is low, and it is necessary to work with short wavelengths, losing selectivity.

In this work, a simple and economic microscale method for the TLC determination of potato GAs, with a purification step using Sep-Pak $C_{18}$ cartridges, was set up.

## EXPERIMENTAL

### *Chemicals and reagents*

A glycoalkaloid stock standard solution (1 mg/ml) was prepared by dissolving 10 mg of $\alpha$-solanine or $\alpha$-chaconine (Sigma, St. Louis, MO, USA) in 10 ml of methanol–acetic acid (99:1) and working standard solutions (0.1 mg/ml) were prepared by dilution of 1 ml of stock standard solution to 10 ml with the same solvent. Both the stock and working standard solutions were kept at −4°C and were stable for 2 months.

Sep-Pak $C_{18}$ cartridges (Millipore, Milford, MA, USA) were used for the pre-purification step. They were preconditioned by elution with methanol (3 × 3 ml) and water (3 × 3 ml).

Pre-coated silica gel TLC plates (5 × 8 cm, nylon supported, Machery–Nagel, Düren, Germany and 10 × 20 cm, glass supported, Merck, Darmstadt, Germany) were used. Both supports gave similar $R_F$ values. Reversed-phase TLC plates were RP-18 W (Macherey–Nagel). Solvents were of analytical-reagent grade.

### *Instrumental*

TLC scanning determinations were performed on a Shimadzu (Tokyo, Japan) Model 9300 TLC scanner at 560 nm for Carr–Price reagent [11] or 505 nm for Dragendorff reagent [11], using the reflection system in the zig-zag mode with an 8-mm swing width.

### *Sample preparation*

Samples of leaves or tubers (1 g) were minced with 5 ml of 1% acetic acid using a glass rod. The rod was rinsed with 1 ml of the extraction solution and the tube was capped and sonicated for 5 min. The tube was centrifuged (5000 *g*, 5 min), the solution was removed with a Pasteur pipette and the residue was re-extracted as before with 5 ml of 1% acetic acid. The combined extracts were applied to a preconditioned Sep-Pak $C_{18}$ cartridge. The cartridge was washed with 40% aqueous methanol (10 ml) and the glycoalkaloids were eluted with methanol (10 ml). The solvent was evaporated under an air current. The residue was dissolved in 500 $\mu$l of methanol and this solution was used for the quantification step.

### *TLC and quantification procedures*

Aliquots (5 $\mu$l) of the solutions were applied with an HPLC syringe in duplicate on the TLC plate together with increasing volumes (2, 4, 6 and 8 $\mu$l) of the working standard solution (in duplicate). The plate was developed to 10 cm in a 17.5 × 11.0 × 6.2 cm chamber (saturation time 30 min), using chloroform–methanol–2% aqueous ammonia (70:30:5) as the mobile phase, air dried, sprayed with Carr–Price reagent and heated for 2 min at 110°C. The spots were measured within 30 min and GAs concentrations in the samples were calculated using the calibration graph thus constructed. When the plates were developed with Dragendorff reagent, the plate was air dried, sprayed with the reagent, air-dried and measured as before in the same instrument.

## RESULTS AND DISCUSSION

### *Chromatographic system*

Both reversed- and normal-phase TLC were tested. In accordance with the results reported

for HPLC [10], the reversed-phase system is unable to give a useful separation of solanine from chaconine. The best results obtained are reported in Table I.

Many solvent systems have been reported [12] for the normal-phase TLC separation of potato GAs. Among the several we tested, the best results were obtained with two mixtures, one containing acetic acid and the other aqueous ammonia. The $R_F$ values are given in Table I.

It was not possible to reproduce the $R_F$ values reported in the literature, and the system was found to be strongly dependent on the saturation of the chamber and the progressive evaporation of the mobile phase, especially with the acetic acid mixture. It is advisable for each laboratory to standardize the system carefully before routine use.

*Detection reagents*

Several detection reagents have been used with GAs, including Dragendorff, Carr–Price and optical brightener reagents. In early attempts a clinical densitometer and Carr–Price reagent were used, but the detection conditions could not be optimized owing to instrumental limitations [6]. We compared Dragendorff and Carr–Price reagents with respect to their sensitivity and selectivity. The relative response between α-solanine and α-chaconine was similar, 0.97 for Dragendorff and 1.1 for Carr–Price reagent, making correction unnecessary for routine use. Table II summarizes the results obtained.

TABLE II

COMPARISON OF DRAGENDORFF AND CARR–PRICE REAGENTS

Stationary phase, silica gel 60; solvent, chloroform–methanol–2% aqueous ammonia (70:30:5).

| Reagent | Detection limit (μg) | Range (μg) | Correlation coefficient |
|---|---|---|---|
| Dragendorff | 0.8–1.0 | 0.8–8.0 | 0.9991 |
| Carr–Price | 0.2–0.3 | 0.2–2.0 | 0.9996 |

Typical solanine, chaconine and extract chromatograms are shown in Figs. 1 and 2. Fig. 1 shows the higher sensitivity obtained with the

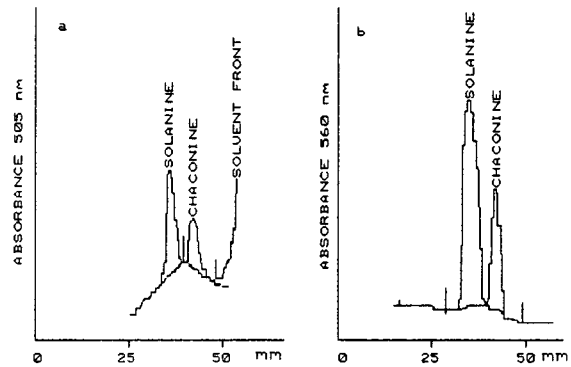


Fig. 1. Comparison of Dragendorff and Carr–Price reagents for standard solutions of α-solanine and α-chaconine. Dragendorff reagent, 5 μg of each; (b) Carr–Price reagent, 0.5 μg. Stationary phase, silica gel 60; solvent system, chloroform–methanol–2% aqueous ammonia (70:30:5).

TABLE I

SOLVENT SYSTEMS FOR THE TLC OF GLYCOALKALOIDS

$hR_F = 100\ R_F$; RP = reversed-phase $C_{18}$; NP = normal phase. All TLC was carried out on precoated plates.

| Stationary phase | Solvent | $hR_F$ | |
|---|---|---|---|
| | | Solanine | Chaconine |
| RP | MeOH–0.2% $NH_3$ (80:20) | 14 | 17 |
| | MeOH–0.2% $NH_3$ (75:25) | 14 | 20 |
| NP | $CHCl_3$–MeOH–1% $NH_3$ (50:50:1) | 88 | 92 |
| | $CHCl_3$–MeOH–1% $NH_3$ (80:20:1) | 22 | 31 |
| | $CHCl_3$–MeOH–2% $NH_3$ (70:30:5) | 35 | 45 |
| | $CHCl_3$–MeOH–AcOH (50:45:5) | 62 | 93 |

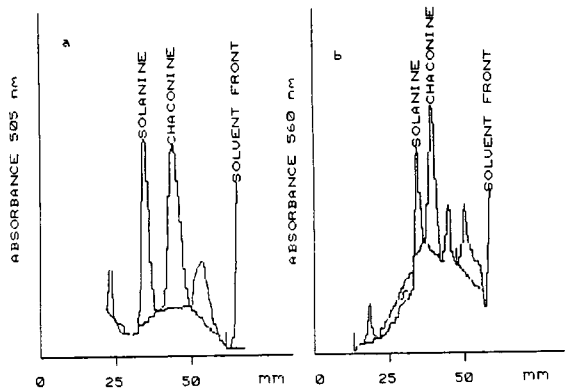


Fig. 2. Comparison of Dragendorff and Carr–Price reagents for extracts of potato leaves. Conditions as in Fig. 1.

Carr–Price reagent compared with Dragendorff reagent. The detection limit with Carr–Price reagent, defined as the concentration at which the signal-to-noise ratio is $\geq 2$, was comparable to that reported for optical brightners (OBs) [7], so it is the preferred detection reagent when the sensitivity is the main factor to be considered. The Dragendorff and Carr–Price reagents showed a good linear response ($r_1 = 0.9991$ and $r_2 = 0.9996$, respectively) in the 0.8–8.0 $\mu$g and 0.2–2.0 $\mu$g concentration ranges, and showed deviations from linearity only at relatively high concentrations.

Dragendorff reagent is more selective than the Carr–Price reagent, as can be seen by comparing Fig. 2a and b, so unless a lower detection limit and sensitivity are required, it is the reagent of choice.

*TLC scanning conditions*

To test the instrumental error, the same spot was measured 30 times. All the values were within the mean $\pm 1.6s$ range ($s$ = standard deviation) with a relative standard deviation (R.S.D.) of 3.3%.

The precision of the method was determined by applying the same GA concentration five times and measuring each three times. All the values were within the mean $\pm 1.5s$ range with an R.S.D. of 5.6%.

To determine the accuracy of the method, the values obtained with the standard solutions used above were interpolated on the calibration graph and the concentrations obtained were compared with the actual concentrations. The accuracy so determined was 6.2%.

*Extraction*

GA quaternary ammonium salts are soluble in both water and lower alcohols, but strong acids can hydrolyse the glycosidic linkages, reducing the recovery. Quantitative extraction has proved difficult, and the traditional extraction techniques [10] require the use of large volumes of solvents and several lengthy purification steps.

The proposed method is adequate for quantitative work with many samples, such as in breeding programmes, with good recoveries and simple operation. The overall recovery was measured by adding known concentrations of GAs to control samples, and was 82%. The technique gives "dirtier" extracts than the classical extraction procedures, but the chromatographic system used and the specificity of the detection reagent resolve the resulting mixtures.

ACKNOWLEDGEMENTS

The authors gratefully acknowledge the Instituto Nacional de Investigaciones Agrarias (Uruguay), the International Program in the Chemical Sciences (Uppsala, Sweden) and the CEE for grants that made this work possible. The help of D. Lorenzo and G. Gonzalez in graphic design is also acknowledged. A.V. also thanks the PEDECIBA program for a post-graduate fellowship.

REFERENCES

1 K. Schreiber, in R. Manske (Editor), *The Alkaloids*, Vol. 10, Academic Press, London, 1968, p. 1.
2 R.R. Dalvi and W.C. Bowie, *Vet. Hum. Toxicol.*, 23 (1983) 13.
3 W.M.J. Van Gelder, J. Vincke and J.J.C. Scheffer, *Euphytica*, 38 (1988) 147.
4 W.W. Bergers, *Potato Res.*, 23 (1980) 105.
5 R.J. Bushway, A.M. Wilson and A.A. Bushway, *Am. Potato J.*, 57 (1980) 561.
6 L.S. Cadle, D. Stelzig, K. Harper and R.J. Young, *J. Agric. Food Chem.*, 26 (1978) 1453.

7 R. Jellema, E.T. Elema and T.M. Malingre, *J. Chromatogr.*, 210 (1981) 121.
8 M.M.J. Van Gelder, H. Jonker, H. Huizing and J.J.C. Scheffer, *J. Chromatogr.*, 442 (1988) 133.
9 M.M.J. Van Gelder, L. Tuinstra, J. Van der Greef and J.J.C. Scheffer, *J. Chromatogr.*, 482 (1989) 13.
10 K. Saito, M. Horie, Y. Hoshino, N. Nose and M. Nakazawa, *J. Chromatogr.*, 508 (1990) 141.
11 *Dyeing Reageants for Thin Layer and Paper Chromatography*, Merck, Darmstadt, 1974.
12 M.J. Shih and J. Kuc, *Phytochemistry*, 13 (1974) 997.

*Journal of Chromatography A*, 653 (1993) 385–386
Elsevier Science Publishers B.V., Amsterdam

CHROM 25 474

# Book Review

*High Performance Liquid Chromatography in Food Control and Research*, edited by R. Matissek and R. Wittkowski, Technomic Publishing Co., Lancaster, Basel, 1993, 304 pp., price SFr. 143.00, ISBN 0-87762-999-4.

In this book the authors present a topical review of the possibilities of food quality control using high-performance liquid chromatography (HPLC).

The book is divided into four main sections. The first chapter, "High Performance Liquid Chromatography", by R. Matissek (I.1. Modern HPLC—Fundamentals and Developments), H. P. Nissen and H.W. Kreysel (I.2. Separation Systems and Instrumentation), familiarizes the reader with the chromatographically most important fundamental principles and with the essential equipment, the different stationary phases and the accompanying separation mechanisms in HPLC. The essential problems of peak identification and quantification are discussed and the latest methods such as micro-HPLC, supercritical fluid chromatography (SFC), column switching and automation, with their advantages and disadvantages, are demonstrated.

In the next chapter, "Separation Systems and Instrumentation", by H.P. Nissen and H.W. Kreysel, stationary phases are explained once more in detail with the help of some practical examples. Special demands on detector and pump types and their construction are considered. A subchapter on "troubleshooting" completes this chapter.

The second part deals with the analysis of food compounds. R. Galensa summarizes the scope and limitations of the analysis of carbohydrates using HPLC. On account of detection problems with sugars, pre- and postcolumn derivatization procedures are emphasized. In this chapter also a Chemical Abstracts literature search covering the period 1985–88 is published, which gives a review of the chromatographic separation of different sugars from complex matrices. Furthermore, separation methods for some plant phenols are classified into phenolic acids and flavonoids, with emphasis on different special detection possibilities, *e.g.*, photodiode-array and Fourier transform IR detectors and enzyme reactors.

Proteins are the subject of the following chapter, by H.-A. Mehrens and D. Reimerdes. Owing to the wide variations in protein compounds in food, the authors have chosen some typical examples (milk and milk products, meat, fish and soybean protein products). The analytical problems with milk and milk products are emphasized. The determinations of only the most important compounds are discussed in detail and for many other substances only the basic methods are outlined. Numerous literature references provide a comprehensive review.

The chapter on foods with high fat contents by U. Coors is divided into three parts. First the analysis of fat components is demonstrated by the determination of triglycerides, fatty acids, sterols, phospholipids and tocopherols. The determination of characteristic compounds is briefly described with the examples of sesame oil, cottonseed oil and butter in the second part. Finally, the determination of fat oxidation products is demonstrated, focusing mainly on cholesterol oxide. Numerous literature references and a table with HPLC conditions are provided.

The chapter on analytical methods for vitamins by C. Mladek is divided into fat- and water-soluble vitamins and outlines at least one HPLC method for each vitamin.

In the chapter "Ions and Ionic Compounds" by B. Rössner, ion-exchange chromatographic

and ion-pair chromatographic separation methods are explained. In an additional part the suitability of different detectors for this method is discussed. Finally, analytical procedures are demonstrated. The determination of ions in water and mineral water is described in detail. Similar compounds in products such as beverages, meat, milk, vegetables and also dental cream are briefly covered, with many literature references.

The chapter "Analysis of Food Additives", by H. Köbler, deals with common HPLC procedures for additives. Very detailed methods for the determination of preservatives, fungicides and sweeteners in different matrices are described, and analyses for antioxidants, food colorants and nitrite/nitrate are briefly discussed.

In the chapter "Analysis of Residues and Contaminants", by R. Malisch and G. Heusinger, numerous literature references are given for the determination of pharmacologically active compounds, pesticides, polycyclic hydrocarbons and a selection of toxins, clearly arranged in tabular form. The importance of different detection methods is shown once again by numerous chromatograms, also indicating the possibilities of derivatization in HPLC analysis.

Overall this book provides a wide and informative survey. However, in the opening chapters a concise description of the different eluent characteristics and their effects on the selectivity of chromatographic systems would have been desirable. The "troubleshooting" section offers valuable help to newcomers to HPLC.

Identification methods for food compounds and food additives are described in detail and numerous literature references are provided relating to the separation problems considered. However, with the current rapid developments in the field of chromatography it is difficult to give completely up-to-date versions. Therefore, it cannot be denied that today some of these separation problems could be resolved much more effectively than indicated by the chromatograms presented.

Owing to the intentions of the book to describe analytical systems and methods in detail, some repetition in the different chapters could not be avoided.

Despite the above comments, this book will provide valuable help for evaluating new analytical methods in food quality control.

C. Frank, V. Karl, A. Kaunzinger and K. Schumacher

*Universität Frankfurt/Main*
*Institut für Lebensmittelchemie*
*Robert-Mayer-Straße 7–9*
*D-60054 Frankfurt am Main II*

*Journal of Chromatography A*, 653 (1993) 387
Elsevier Science Publishers B.V., Amsterdam

CHROM. 25 475

# Book Review

*Advances in mass spectrometry* (*Proceedings of the 12th International Mass Spectrometry Conference, Amsterdam, August 26–30, 1992*), edited by P.J. Kistemaker and N.M.M. Nibbering, Elsevier, Amsterdam, London, New York, 1992, XXII + 950 pp., price US$ 281.50, Dfl. 450.00, ISBN 0-444-88871-3.

The *International Mass Spectrometry Conferences* take place every three years. This book presents 32 lectures (either plenary or keynote presentations) from the 12th conference, which took place in August of 1992 in Amsterdam. The book is a reprint of Vols. 118 and 199 from the *International Journal of Mass Spectrometry and Ion Processes*. It is impressive that some of the current leaders in mass spectrometry in both instrumentation and application aspects have contributed to this volume. Nevertheless, it is by no means a comprehensive coverage of current major topics in mass spectrometry. For example, none of the chapters completely focus on electrospray, matrix-assisted laser desorption MS, or carbohydrates. Some of the chapters are superb because the authors take into account the diversity of the audience and present the basic principles, recent developments (or a general review) and critical comments about the topic. Five examples of this are the chapters "Charge remote fragmentation: methods, mechanisms and applications" by M.L. Gross; "Plasma source mass spectrometry" by G.M. Hieftje and L.A. Norman; "Ion trap mass spectrometry" by R.E. March; "Analytical pyrolysis mass spectrometry (PYMS): new vistas opened up by temperatured-resolved in-source PYMS" by J.J. Boon; and "Unimolecular reaction mechanisms: the role of reactive intermediates" by H.-F. Grutzmacher. At the back of the book are 58 pages in which the titles and authors, without any abstracts, of the poster presentations are listed; this strikes me as a waste of ink and paper. The most disturbing feature of the volume is that it lacks a subject index, which compromises the usefulness of this publication. The publishers should do this now and provide it as a supplement.

*Boston, MA (USA)* Roger W. Giese

# Author Index

# Erratum

corrected 4 Apr. 94 /AP

*J. Chromatogr.*, 647 (1993) 219–234

Page 232, legend to Fig. 13, 4th line: "waste energy" should read "waste water".

Vol. 653, No. 2

Journal of Chromatography

# NEWS SECTION

## SYMPOSIUM PROGRAMME

3rd INTERNATIONAL SYMPOSIUM ON HYPHENATED TECHNIQUES IN CHROMATOGRAPHY (HTC 3): HYPHENATED CHROMATOGRAPHIC ANALYZERS, ANTWERP, BELGIUM, FEBRUARY 23–25, 1994

The fundamental aspects, instrumental developments and applications of the various hyphenated chromatographic techniques will be covered during this symposium (e.g. coupling of LC to LC, GC and SFC; MS, FTIR, AED and other techniques coupled with GC, (HP)LC, SFC and CZE; on-line air traps GC; purge-and-trap-GC, etc.). Emphasis will also be placed on the design of hyphenated, on-line and at-line chromatographic analyzers. The scientific programme includes oral presentations in plenary and parallel sessions, poster presentations and discussion sessions. A technical exhibition will give an overview of instruments, books and accessories. The latest developments in instrumentation will be presented during workshop type seminars.

A special volume of the **Journal of Chromatography** will be dedicated to the accepted and reviewed papers, which will be channelled through the usual refereeing system. Deadline for manuscripts: **February 25, 1994.**

Participants who wish to present a poster can still submit an abstract. The deadline for submission of abstracts of last-minute posters is **December 30, 1993.** Submission forms for contributed papers and all other information may be obtained from the Symposium Chairman: Dr. R. Smits, p/a BASF Antwerpen N.V., Central Laboratory, Scheldelaan 600, B-2040 Antwerp (Belgium), tel.: + 32-3/561.28.31, fax: + 32-3/561.32.50

### Preliminary Programme

(per September 15, 1993)

**Wednesday February 23, 1994**

Bartle K.D. (U.K.) – Unified microcolumn chromatography.

Blake E., Raynor M.W., Cornell D. (South Africa) – The determination of environmentally relevant organotin compounds by capillary SFC with ICP-MS.

Braumann U., Tseng L.-H, Albert K., Spraul M., Hofmann M., Dowl C. (Germany) – On-line coupling of SFC and $^1$H-NMR.

Hetem M., Steeman J., de Wit G. (The Netherlands) – TGA-FTIR: direct monitoring of polymer material thermal stability.

Just U., Mellor F., Keidel F. (Germany) – SFC/MS of cyclic siloxanes in technical silicone oils.

Okudan A., Kara H., Ayar A., Pehlivan E., Pehlivan M. (Turkey) – Examination of phenols in coals.

Rocca J.-L. (France) – Off-line and on-line coupling of chromatographic techniques and SFE.

Sandra P. (Belgium) – The future of pre-column hyphenation: on-line or off-line?

Schlegel D., Mattusch J., Dittrich K. (Germany) – Speciation of arsenic and selenium compounds by ion chromatography with ICP-AES detection using the hydride technique.

Taylor L.T. (USA) – Applications of bench top, on-line spectrometric detection in SFC.

Van der Velde E.G., Dietvorst M., Swart C.P., Ramlal M. (The Netherlands) – Optimisation of SFE of PCB's and pesticides from real soil samples.

Van der Velde E.G., Ramlal M., van Beuzekom A.C., Hoogerbrugge R. (The Netherlands) – Optimisation of parameters in SFE of triazines by use of multiple linear regression.

**Thursday, February 24, 1994**

Andrle C.M., van Espen P., Adams F., Broeckaert J.A.C. (Germany and Belgium) – Characterisation of different silicagel materials used as stationary phases in reversed-phase HPLC by various microanalytical techniques.

Boos K.-S. (Germany) – LC for on-line sample processing in hyphenated separation techniques: design and performance of novel column packings.

Brinkman U.A.Th., Ghijsen R.T., Lingeman H. (The Netherlands) – Hyphenated LC- and GC-based techniques for trace level environmental analysis.

Caboni M. F., Capella P., Lercker G. (Italy) – HPLC light-scattering evaporative detector analysis of natural phospholipids

Dittrich K. (Germany) – New and accurate tandem techniques of GC/LC-AES.

Ebdon L.C. (UK) – Adventures in coupling: ICP-MS as a detector for GC and HPLC.

Esmans E.L., Lemière F., Van Dongen W., Chauvaux N., Claeys M., Van Onckelen H., Van den Eeckhout E. (Belgium) – Analysis of polar biomolecules by combined LC-MS.

Galceran M.T., Moyano E. (Spain) – Analysis of hydroxy-PAHs by HPLC-MS with a pneumatically assisted electrospray as interface.

Games D.E. (UK) – Recent advances in LC-MS and CE-MS.

Gey M., Conrad B., Kaudewitz H., Wagner G., Unger K.K. (Germany) – Chromatographic analysis and structural characterisation of glycoprotein carbohydrates using 300 x 7.8 mm HPLC columns packed with styrene-divinylbenzene polymers and

coupled with on-line mass spectrometry (LC-MS/MS).

Goosens E.C., de Jong D., de Jong G.J., Brinkman U.A.Th. (The Netherlands) – Potential of on-line reversed-phase LC-GC.

Hetem M., Baars B., de Wit G. (The Netherlands) – LC-FTIR : a powerful combination for polymer blends and engineering plastics characterization.

Karlsson K.-E. (Sweden) – Deuterium oxide as mobile phase component in microcolumn LC-MS.

Lores M., Garcia M.C., Cela R. (Spain) – Improving phenolic aldehydes fluorimetric detection by means of post-column photochemical derivatization.

Massart D.L. (Belgium) – Evolving factor analysis and related methods applied to HPLC-DAD.

Planck C., Lorbeer E. (Austria) – On-line LC-GC for the analysis of free and esterified sterols in vegetable oil methyl esters used as diesel fuel substitutes.

Prokisch J., Kovacs B., Gyori Z., Loch J., Posta J. (Hungary) – Interfacing ion chromatography with ICP-AES for the determination of chromium(III) and chromium(VI).

Schütz S., Duhr A., Hummel H.E., Wollnik H. (Germany) – Trace analysis and structural elucidation with combined hyphenated chromatographic and MS methods.

Slobodnik J., Bagheri H., Jager M.E., Ghijsen R.T., Brinkman U.A.Th. (The Netherlands) – LC particle beam MS for identification of unknown pollutants in water.

Spanoghe B., Van Dongen W., Esmans E.L., Van Onckelen H. (Belgium) – Isolation and detection of some organochlor pesticides and herbicides with GC-MS and LC-MS.

Stradi R., Celentano G., Scigliuzzo M., Galli G., De Angelis L., Casetta B. (Italy and Germany) – Extractor-LC-MS and extractor-LC-Vis techniques for the quali-quantitative analysis of bird's plumage carotenoids.

Traore F., Merabet T., Caroff E., Fontan J.E., Arnaud D., Brion F. (France) – Diastereoisomers of leucovorin (folinic acid) and 5-N-methyltetrahydrofolate: a simultaneous HPLC analysis with postcolumn reactions.

Westerlund D. (Sweden) – Direct injection principles in coupled-column LC for the analysis of drugs and metabolites in biological fluids.

**Friday February 25, 1994**

André M., Shirey R.E. (Belgium and USA) – Analysis of volatile organic compounds by purge and trap GC/MS without a jet separator.

Auger J., Ferary S., Redor S. (France) – First results in trace identification of allelochemicals and pesticides by combining : GC/MS and GC/cryotrapping/FTIR.

Blazso M. (Hungary) – Pyrolysis-GC-MS of poly(dialkylsilylene)S.

Bortolomeazzi R., Pizzale L., Lercker G. (Italy) – Identification of degradation products of cholesterylacetate thermo-oxidation.

Carro M.A., Lorenzo R.A., Cela R. (Spain) – Speciation of organomercurials in biological and environmental samples by GC-MIP-AED.

Casabianca H., Graff J.B., Jame P., Perrucchietti C., Chastrette M. (France) – Development of hyphenated technics in chromatography. Application to authentification of flavors in food products and perfumes.

Casais Laino C., Cela R. (Spain) – Simultaneous determination of chlorobenzenes and chlorophenols in soil samples by hyphenated GC-AED.

Ceulemans M., Witte C., Szpunar-Lobinska J., Lobinski R., Adams F.C. (Belgium) – Speciation analysis for organotin and organolead in biological matrices by GC-MIP AES.

Cortes H.J. (USA) – Recent developments in coupled column separations.

Cramers C.A. (The Netherlands) – Analysis of large volumes of aqueous samples by capillary GC.

Donard O.F.X. (France) – Hyphenated techniques using cryogenic focussing, GC separation and detection by atomic spectrometry: Environmental applications.

Fell A.F. (UK) – Hyphenated detection systems in separation science.

Frank H. (Germany) – Automated repetitive air sampling and on-line high-speed GC of volatile organic air pollutants.

Geypens B., Ghoos Y., Hiele M., Rutgeerts P., Vantrappen G. (Belgium) – Quantitation of ethanol with stable isotope dilution and identification of some other volatile compounds in human faeces using CGC-ITD.

Goosens E.C., de Jong D., de Jong G.J., Rinkema F., Ghijsen R., Brinkman U.A.Th. (The Netherlands) – Large volume introduction into capillary GC with atomic emission detection.

Hajimiragha H., Dunemann L. (Germany) – Fully automated on-line purge and trap HRGC-MS for the determination of volatile organic compounds in body fluids.

Janssen H.-G. (The Netherlands) – High speed GC-MS : comparison of MS detection techniques.

Lobinski R., Adams F. (Belgium) – Ultrasensitivity in hyphenated analysis: organolead in the remote environment.

Louter A.J.H., Ghijsen R.T., Brinkman U.A.Th. (The Netherlands) – Enhanced sensitivity and selectivity in an automated SPE-GC-MS-based water analyser.

Louter A.J.H., van der Wagt R.A.C.A., Ghijsen R.T., Brinkman U.A.Th. (The Netherlands) – On-line coupling of an automated sample preparation device with capillary GC for the analysis of plasma samples.

Pakdel H., Roy C. (Canada) – Simultaneous GC-FTIR-MS analysis of synthetic fuel derived from used tire vacuum pyrolysis oil.

Pedersen-Bjergaard S., Greibrokk T. (Norway) – Recent developments and applications of on-column atomic emission detection in capillary GC.

Phillips J.B., Zhang L., Venkatramani C.J. (USA) – Comprehensive multidimensional GC: an orthogonal separation and analysis method.

Pico Y., Louter A.J.H., Goudriaan V.P., Ghijsen R.T., Brinkman U.A.Th. (The Netherlands) – Comparison of various drying agents for water free introduction desorption solvent into a GC after on-line SPE of aqueous samples.

Turnes M.I., Rodriguez I., Mejuto M.C., Cela R. (Spain) – Determination of chlorophenols in drinking water by GC-AED.

Tutschku S., Mothes S., Dittrich K. (Germany) – Determination and speciation of organotin compounds in environmental samples by capillary GC helium MIP AES.

Van Opstal L., Pascual Termens V., Gummersbach J., Smits R. (Belgium) – A GC method for the analysis of ethylene oxide.

Van Vyncht G., DePauw E., Gaspar P., Maghuin-Rogister G. (Belgium) – GC-MS/MS of anabolizing steroids in biological matrices.

Van Ysacker P.G., Janssen H.-G., Snijders H.M.J., Leclercq P.A., Wollnik H., Cramers C.A. (The Netherlands and Germany) – Evaluation of different MS detectors in combination with high-speed narrow-bore GC.

Vreuls J.J., Hankemaier Th., Ghijsen R.T., Brinkman U.A.Th. (The Netherlands) – A new water-resisting gap to prevent peak tailing during analysis of aqueous samples by SPE-GC.

Vreuls J.J., Louter A.J.H., Ghijsen R.T., Brinkman U.A.Th. (The Netherlands) – On-line solid-phase extraction-GC for the analysis of aqueous samples.

## PUBLICATION SCHEDULE FOR THE 1994 SUBSCRIPTION

*Journal of Chromatography A* and *Journal of Chromatography B: Biomedical Applications*

| MONTH | O 1993 | N 1993 | D 1993 | |
|---|---|---|---|---|
| Journal of Chromatography A | 652/1<br>652/2<br>653/1 | 653/2<br>654/1<br>654/2<br>655/1 | 655/2<br>656/1 + 2<br>657/1<br>657/2 | The publication schedule for further issues will be published later. |
| Bibliography Section | | | | |
| Journal of Chromatography B: Biomedical Applications | | | | |

## INFORMATION FOR AUTHORS

(Detailed *Instructions to Authors* were published in Vol. 609, pp. 437–443. A free reprint can be obtained by application to the publisher, Elsevier Science Publishers B.V., P.O. Box 330, 1000 AH Amsterdam, Netherlands.)

**Types of Contributions.** The following types of papers are published: Regular research papers (Full-length papers), Review articles, Short Communications and Discussions. Short Communications are usually descriptions of short investigations, or they can report minor technical improvements of previously published procedures; they reflect the same quality of research as Full-length papers, but should preferably not exceed five printed pages. Discussions (one or two pages) should explain, amplify, correct or otherwise comment substantively upon an article recently published in the journal. For Review articles, see inside front cover under Submission of Papers.

**Submission.** Every paper must be accompanied by a letter from the senior author, stating that he/she is submitting the paper for publication in the *Journal of Chromatography A* or *B*.

**Manuscripts.** Manuscripts should be typed in **double spacing** on consecutively numbered pages of uniform size. The manuscript should be preceded by a sheet of manuscript paper carrying the title of the paper and the name and full postal address of the person to whom the proofs are to be sent. As a rule, papers should be divided into sections, headed by a caption (*e.g.*, Abstract, Introduction, Experimental, Results, Discussion, etc.) All illustrations, photographs, tables, etc., should be on separate sheets.

**Abstract.** All articles should have an abstract of 50–100 words which clearly and briefly indicates what is new, different and significant. No references should be given.

**Introduction.** Every paper must have a concise introduction mentioning what has been done before on the topic described, and stating clearly what is new in the paper now submitted.

**Experimental conditions** should preferably be given on a *separate* sheet, headed "Conditions". These conditions will, if appropriate, be printed in a block, directly following the heading "Experimental".

**Illustrations.** The figures should be submitted in a form suitable for reproduction, drawn in Indian ink on drawing or tracing paper. Each illustration should have a legend, all the *legends* being typed (with double spacing) together on a *separate sheet*. If structures are given in the text, the original drawings should be supplied. Coloured illustrations are reproduced at the author's expense, the cost being determined by the number of pages and by the number of colours needed. The written permission of the author and publisher must be obtained for the use of any figure already published. Its source must be indicated in the legend.

**References.** References should be numbered in the order in which they are cited in the text, and listed in numerical sequence on a separate sheet at the end of the article. Please check a recent issue for the layout of the reference list. Abbreviations for the titles of journals should follow the system used by *Chemical Abstracts*. Articles not yet published should be given as "in press" (journal should be specified), "submitted for publication" (journal should be specified), "in preparation" or "personal communication".

Vols. 1–651 of the *Journal of Chromatography*; *Journal of Chromatography, Biomedical Applications* and *Journal of Chromatography, Symposium Volumes* should be cited as *J. Chromatogr.* From Vol. 652 on, *Journal of Chromatography A* (incl. Symposium Volumes) should be cited as *J. Chromatogr. A* and *Journal of Chromatography B: Biomedical Applications* as *J. Chromatogr. B.*

**Dispatch. Before sending the manuscript to the Editor please check that the envelope contains four copies of the paper complete with references, legends and figures. One of the sets of figures must be the originals suitable for direct reproduction. Please also ensure that permission to publish has been obtained from your institute.**

**Proofs.** One set of proofs will be sent to the author to be carefully checked for printer's errors. Corrections must be restricted to instances in which the proof is at variance with the manuscript. "Extra corrections" will be inserted at the author's expense.

**Reprints.** Fifty reprints will be supplied free of charge. Additional reprints can be ordered by the authors. An order form containing price quotations will be sent to the authors together with the proofs of their article.

**Advertisements.** The Editors of the journal accept no responsibility for the contents of the advertisements. Advertisement rates are available on request. Advertising orders and enquiries can be sent to the Advertising Manager, Elsevier Science Publishers B.V., Advertising Department, P.O. Box 211, 1000 AE Amsterdam, Netherlands; courier shipments to: Van de Sande Bakhuyzenstraat 4, 1061 AG Amsterdam, Netherlands; Tel. (+31-20) 515 3220/515 3222, Telefax (+31-20) 6833 041, Telex 16479 els vi nl. *UK*: T.G. Scott & Son Ltd., Tim Blake, Portland House, 21 Narborough Road, Cosby, Leics. LE9 5TA, UK; Tel. (+44-533) 753 333, Telefax (+44-533) 750 522. *USA and Canada*: Weston Media Associates, Daniel S. Lipner, P.O. Box 1110, Greens Farms, CT 06436-1110, USA; Tel. (+1-203) 261 2500, Telefax (+1-203) 261 0101.

# Capillary Electrophoresis

## Principles, Practice and Applications

NOW ALSO IN PAPERBACK

*by* **S.F.Y. Li**, *National University of Singapore, Singapore*

**Journal of Chromatography Library Volume 52**

Capillary Electrophoresis (CE) has had a very significant impact on the field of analytical chemistry in recent years as the technique is capable of very high resolution separations, requiring only small amounts of samples and reagents. Furthermore, it can be readily adapted to automatic sample handling and real time data processing. Many new methodologies based on CE have been reported. Rapid, reproducible separations of extremely small amounts of chemicals and biochemicals, including peptides, proteins, nucleotides, DNA, enantiomers, carbohydrates, vitamins, inorganic ions, pharmaceuticals and environmental pollutants have been demonstrated. A wide range of applications have been developed in greatly diverse fields, such as chemical, biotechnological, environmental and pharmaceutical analysis.

This book covers all aspects of CE, from the principles and technical aspects to the most important applications. It is intended to meet the growing need for a thorough and balanced treatment of CE. The book will serve as a comprehensive reference work and can also be used as a textbook for advanced undergraduate and graduate courses. Both the experienced analyst and the newcomer will find the text useful.

***Contents:***

**1. Introduction.** Historical Background. Overview of High Performance CE. Principles of Separations. Comparison with Other Separation Techniques. **2. Sample Injection Methods.** Introduction. Electrokinetic Injection. Hydrodynamic Injection. Electric Sample Splitter. Split Flow Syringe Injection System. Rotary Type Injector. Freeze Plug Injection. Sampling Device with Feeder. Microinjectors. Optical Gating. **3. Detection Techniques.** Introduction. UV-Visible Absorbance Detectors. Photodiode Array Detectors. Fluorescence Detectors. Laser-based Thermooptical and Refractive Index Detectors. Indirect Detection. Conductivity Detection. Electrochemical Detection. Mass Spectrometric Detection. **4. Column Technology.** Uncoated Capillary Columns. Coated Columns. Gel-filled Columns. Packed Columns. Combining Packed and Open-Tubular Column. **5. Electrophoretic Media.** Electrophoretic Buffer Systems. Micellar Electrokinetic Capillary Chromatography. Inclusion Pseudophases. Metal-complexing Pseudophases. Other Types of Electrophoretic Media. **6. Special Systems and Methods.** Buffer Programming. Fraction Collection. Hyphenated Techniques. Field Effect Electroosmosis. Systematic Optimization of Separation. **7. Applications of CE.** Biomolecules. Pharmaceutical and Clinical Analysis. Inorganic Ions. Hydrocarbons. Foods and Drinks. Environmental Pollutants. Carbohydrates. Toxins. Polymers and Particles. Natural Products. Fuel. Metal Chelates. Industrial Waste Water. Explosives. Miscellaneous Applications. **8. Recent Advances and Prospect for Growth.** Recent Reviews in CE. Advances in Injection Techniques. Novel Detection Techniques. Advances in Column Technology. Progress on Electrolyte Systems. New Systems and Methods. Additional Applications Based on CE. Future Trends. **References. Index.**

**1992 608 pages Hardbound**
**US$ 225.75 / Dfl. 395.00**
**ISBN 0-444-89433-0**
**1993 608 pages Paperback**
**Price: US$ 114.25 / Dfl. 200.00**
**ISBN 0-444-81590-2**

*"Everything seems to be there, any detection system you have ever dreamed of, any capillary coating, enough electrolyte systems to saturate your wits, and more..."*

*"...by far the most thorough and comprehensive book in the field yet to appear."*

**P.G. Righetti, Milan**

**ORDER INFORMATION**

*For USA and Canada*
**ELSEVIER SCIENCE PUBLISHERS**
Judy Weislogel,
P.O. Box 945
Madison Square Station,
New York, NY 10160-0757
Fax: (212) 633 3880

*In all other countries*
**ELSEVIER SCIENCE PUBLISHERS**
P.O. Box 211,
1000 AE Amsterdam
The Netherlands
Fax: (+31-20) 5803 705

*US$ prices are valid only for the USA & Canada and are subject to exchange rate fluctuations; in all other countries the Dutch guilder price (Dfl.) is definitive. Customers in the European Community should add the appropriate VAT rate applicable in their country to the price(s). Books are sent postfree if prepaid.*

ELSEVIER
SCIENCE PUBLISHERS

711/414/143/Li

0021-9673(19931105)653:2;1-#